



UNIVERSITY OF UDINE  
PhD COURSE IN BIOMEDICAL SCIENCES AND BIOTECHNOLOGY  
XXVI CICLE

PhD THESIS

***The Elastin MicrofibriL INterfacer1 (EMILIN1), is highly expressed in chronic lymphocytic leukemia (CLL)-involved tissues and promotes CLL cell adhesion and survival via CD49d***

TUTOR  
Prof. Carlo Pucillo

SUPERVISOR  
Dott. Valter Gattei  
Dott.ssa Antonella Zucchetto

PhD STUDENT  
Erika Tissino

ACADEMIC YEAR  
2013/2014

---

*The Elastin MicrofibriL Interfacer1 (EMILIN1), is highly expressed in chronic lymphocytic leukemia (CLL)-involved tissues and promotes CLL cell adhesion and survival via CD49d*

Abstract .....	4
1. Introduction.....	5
1.1. Chronic lymphocytic leukemia.....	6
1.2. Diagnosis, staging, prognosis, treatment of CLL.....	6
1.2.1. Diagnosis.....	6
1.2.2. Prognosis .....	6
1.2.3. Staging .....	7
1.2.4. Treatment .....	7
1.3. CLL cells immunophenotype .....	8
1.4. Prognostic factors in CLL.....	8
1.5. Lymphocyte doubling time (LDT) .....	8
1.6. Serum markers .....	8
1.7. Genetic abnormalities quantified by FISH and by molecular techniques .....	9
1.8. IGHV mutation status.....	9
1.9. Expression of specific proteins in or on CLL cells.....	10
1.9.1. ZAP-70 .....	10
1.9.2. CD38 .....	10
1.9.3. CD49d .....	11
1.10. Microenvironment in CLL .....	11
1.11. CD49d and microenvironment.....	12
1.12. Ligands of CD49d .....	14
1.12.1. VCAM-1 and fibronectin .....	15
1.12.2. EMILIN1 .....	15
1.13. <i>In vitro</i> and <i>in vivo</i> models .....	16
Aim of the study .....	18
2. Results.....	19
2.1. EMILIN1 is largely distributed in normal and CLL-involved tissues.....	20
2.2. CD49d is the sole ligand for EMILIN1 in CLL.....	23
2.3. EMILIN1 promotes CD49d-mediated cell adhesion.....	25
2.3.1. Set up of adhesion experiments on EMILIN1.....	25

---

2.3.2.	EMILIN1 promotes Mec-1 adhesion.....	26
2.3.3.	EMILIN1 promotes CLL cell adhesion .....	29
2.4.	EMILIN1 mediates survival signals .....	31
2.5.	EMILIN1 protects CLL cells from spontaneous apoptosis.....	35
2.6.	Mice wild type or knock-out for EMILIN1: work ongoing .....	36
3.	Discussion .....	38
4.	Materials and Methods .....	42
4.1.	CLL patients and cell lines.....	43
4.2.	Antibodies and other reagents .....	43
4.3.	Cytofluorimetric analysis.....	43
4.4.	Immunohistochemical analysis.....	44
4.5.	Preparation of C1q like domain, VCAM-1- or FN-coated culture dishes/coverslips .....	44
4.6.	Cell adhesion assays.....	44
4.7.	Immunofluorescence assay .....	45
4.8.	Immunoblot analysis.....	45
4.9.	Cell viability assays .....	45
4.10.	Mice models .....	46
4.11.	TCL1 leukemia cells .....	46
4.12.	Intraperitoneal injection of TCL1 leukemia cells in WT and <i>Emilin1</i> <sup>-/-</sup> mice .....	46
4.13.	Statistical analysis.....	46
	References .....	48

---

# Abstract

CD49d ( $\alpha 4$  integrin chain) is a negative prognosticator in chronic lymphocytic leukemia (CLL) with a key role in CLL cell microenvironmental interactions. CD49d triggering by its main ligands Vascular Cell Adhesion Molecule-1 (VCAM-1) and CS-1 fragment of fibronectin, activates signaling pathways delivering pro-survival signals, and promoting resistance to drug-induced apoptosis in CLL. Recently, the globular (g) C1q-like domain of Elastin Microfibril Interfacer1 (EMILIN1), an adhesive extracellular matrix constituent, was described as a new ligand for CD49d operating as a negative modulator of proliferation signals in substrate-adherent non-hematopoietic CD49d+ cells. Here we investigated the distribution of EMILIN1 in normal and CLL-involved tissues, and the effects of CD49d/EMILIN1 interaction in CLL in terms of adhesion and survival.

By taking advantage of a specific anti-human EMILIN1 monoclonal antibody, exploratory staining in reactive lymphoid tissues (tonsil) indicated a clear extracellular EMILIN1 specific reactivity in the outer zone of the mantle/marginal areas. When investigated in lymph node tissues from CLL cases (n=3) by both immunohistochemical and immunofluorescence (IF) analysis and in bone marrow biopsies from CLL cases (n=5) by immunohistochemistry, a clear EMILIN1 positive staining was detected intermingled with the neoplastic component and unexpectedly in the cytoplasm of some cells.

To verify whether EMILIN1 could promote CLL cells adhesion, *in-vitro* adhesion assays were performed. Both the CLL-derived CD49d+ Mec-1 cell line and primary CD49d+ CLL cells (n=12) were specifically able to adhere onto EMILIN1 substrates, and the adhesion efficiency was similar to that observed on VCAM-1 and CS-1 fragment as previously demonstrated. Adhesion was specifically blocked by pre-treatment with the anti-CD49d HP1/2 blocking antibody, and absent when a mutant gC1q domain was employed.

The effects of CD49d/EMILIN1 interactions in CLL were next investigated performing short-term adhesion onto EMILIN1 substrates. Western blot analysis documented an increased phosphorylation of AKT and ERK1/2, mediators of survival signals, similar to that observed upon CD49d engagement by VCAM-1 and CS-1 fragment. These results were corroborated by IF analysis showing pAKT and pERK up-regulation, and the concomitant increase of pVAV1 and F-actin reorganization, confirming the activation of the integrin signaling pathway.

Finally, we verified whether CD49d/EMILIN1 interaction was able to protect CLL cells from spontaneous apoptosis, by culturing purified cells from CLL cases (n=13) on gC1q domain, VCAM-1, or control substrate (1% BSA), and checking cell viability after 5 days by annexinV/7-AAD staining. Both VCAM-1 and EMILIN1 were able to protect CLL cells from spontaneous apoptosis (p=0.009 and p=0.002, respectively), the viability obtained on EMILIN1 was even significantly higher than that observed on VCAM-1 (p=0.004).

In conclusion for the first time we showed that EMILIN1 is present in normal and CLL-involved tissues, and it is able to efficiently bind to CD49d, as expressed by CLL cells. At variance of what demonstrated in non-hematopoietic models, EMILIN1 was able to deliver anti-apoptotic/pro-survival signals to circulating CLL cells. These evidences imply a role for CD49d/EMILIN1 interaction in the maintenance of the neoplastic clone in CD49d-expressing CLL.

---

# 1. Introduction

## 1.1. Chronic lymphocytic leukemia

Chronic lymphocytic leukemia (CLL) is the most common leukemia in Western countries and it mainly affects elderly individuals. Its course is extremely variable with survival ranging from months to decades. Disease remission can often be induced by available treatments (combination of chemoimmunotherapy regimens), however almost all patients relapse and CLL remains an incurable disease with conventional therapy. The current view defines CLL a proliferative disease with heterogeneity in the clinical behavior that accumulates small, homogeneous, mature-appearing CD5+ B lymphocytes in peripheral blood ( $>5 \times 10^9/L$ ), in the secondary lymphoid organs and in the bone marrow.<sup>2;3</sup> Morphologically, CLL lymphocytes appear small, mature lymphocytes with dense nucleus and scant cytoplasm with no prominent nucleoli.

The course of CLL is slow and protracts for most of the patients (indolent CLL) with an accumulation of CLL lymphocytes over many years after the initial diagnosis and never requires therapy. However, not negligible group of patients progresses rapidly with the median survival of 1-2 years (aggressive CLL) despite therapy.

A common clinical observation is that, although therapies are often effective at killing CLL cells in the peripheral blood, residual disease remains in the bone marrow and lymph nodes. It is likely that these malignant cells sequestered in the tissue receive protection from a wide variety of treatments through pro-survival signals and inhibition of apoptosis fostered by the stromal microenvironment. The complex biology underlying how these CLL cells are recruited, maintained, and released from the stroma is an area of active investigation.<sup>4</sup>

## 1.2. Diagnosis, staging, prognosis, treatment of CLL

### 1.2.1. Diagnosis

The diagnosis is often determined in asymptomatic individual based on a routine blood test, but certain signs and symptoms might suggest that a person suffers from CLL. Typical symptoms of CLL consist of weakness, fatigue, loss of weight, fever, night sweating, enlarged lymph nodes and a pressure in the abdomen caused by an enlarged spleen or liver.<sup>5</sup> More severe symptoms consist of progressive anemia, thrombocytopenia and neutropenia (decreased counts of red blood cells, thrombocytes and neutrophils), as a result of bone marrow infiltration by the CLL cells. Subsequently, the disruption of normal haematopoiesis in the infiltrated bone marrow of CLL patients leads to decreased immune response and thus occurrence of severe and repeated infections. The infections are the main complication and the most frequent cause of death in CLL patients.<sup>6</sup>

### 1.2.2. Prognosis

The first clinical prognostic systems to be developed and employed were those which consider clinical symptoms, physical signs and laboratory values. In the last years, however there has been considerable progress in the identification of molecular and cellular markers (deepened in the next chapter) that may predict the disease progression tendency in patients with CLL and may help in understanding the origin and the biology of this disease which can still be considered as incurable.<sup>7</sup>

### 1.2.3. Staging

In CLL the clinical staging system was based on disease burden. In 1975, a set of clinical staging criteria for CLL based on the presence of lymphadenopathy, organomegaly (spleen and liver), and cytopenias was developed by Rai et al.<sup>8</sup> They demonstrated a correlation between Rai stage and survival. The original Rai staging system was later revised from a 5-tier system (0-IV) to a 3-tier system that categorized patients into low-risk (original Rai stage 0), intermediate-risk (original Rai stages I-II), and high-risk (original Rai stages III-IV) groups. In 1978 Binet et al developed another staging system<sup>9</sup>, which was devised on the basis of a retrospective analysis that identified measures of disease burden, similar to those of Rai, as the most significant prognostic variables for survival.<sup>9</sup> These two systems have delineated the clinical presentation and natural history of CLL and have allowed stratification of patients into similar groups for clinical research. Over the past 30 years, there have been significant changes in the pattern of CLL diagnosis with a shift from patients presenting with bulky nodes and cytopenias, to the detection of asymptomatic individuals identified by an elevated lymphocyte count on automated differential blood counts. Moreover, it is now recognized that a subset of patients with early stage CLL have a disease that will rapidly evolve to a more advanced, refractory, and fatal disease. What Rai and Binet staging lack, is the ability to prospectively identify the rapidly evolving patient or not responding to therapy, from patients destined to remain with early stage for decades. For these reasons, during the last 10 years several biological variables, along with the classical prognostic factors, have been identified in order to refine prognosis and response to therapy in patients with CLL.

### 1.2.4. Treatment

Criteria for initiating treatment may vary depending on whether or not the patient is treated in a clinical trial. In general practice, newly diagnosed patients with asymptomatic early-stage disease (Rai 0, Binet A), should be monitored without therapy unless they have evidence of disease progression.<sup>10</sup>

Monotherapy with alkylating agents has served as initial, front-line therapy for CLL, and chlorambucil has been considered the “gold standard” for several decades.

Several new drugs have been approved such as fludarabine, bendamustine as well as three monoclonal antibodies, alemtuzumab, rituximab, and ofatumumab. Chemoimmunotherapies composed of fludarabine and rituximab (with or without cyclophosphamide), or composed of fludarabine and alemtuzumab have shown to improve overall survival when used as therapy for CLL patients. In addition, several specific inhibitors interrupting important pathways for CLL cell survival are currently in the final phases of clinical development. Among them there are agents targeting B-cell receptor signaling such as Fostamatinib (Spleen tyrosine kinase (Syk) inhibitor), Idelalisib (PI3K $\delta$ -isoform selective inhibitor), Ibrutinib (Bruton’s tyrosine kinase (BTK) inhibitor) and Dasatinib (Src- and Abl- kinase inhibitor) and agents targeting Bcl-2 inhibitor such as ABT-263 and ABT-199.<sup>10;11</sup> Indeed encouraging results came from the immunomodulatory drugs like lenalidomide.

### 1.3. CLL cells immunophenotype

Immunophenotypic analysis is routinely required to reach the correct diagnosis in the presence of any unknown lymphocytosis. Flow cytometry analysis, thus commonly follows the clinical and peripheral blood examination, shows a monoclonal expression of light surface immunoglobulin (sIg) chain (either kappa or lambda). CLL lymphocytes express mature B cell marker CD19, CD5 together with CD23 (expression of CD23 helps to distinguish CLL from another CD5+ hematopoietic disorder like mantle cell lymphoma (MCL)). CLL lymphocytes usually express reduced levels of membrane immunoglobulins (mostly IgM and IgD and sporadically IgG or IgA)<sup>12;13</sup>. CLL cells are typically negative for the expression of FMC7 and express CD79b, CD20 and CD22 with low density. From a diagnostic point of view, Matutes et al defined a scoring system using five markers and assigning 1 point when the marker is typical of CLL, 0 points when atypical, therefore ranging from 5 (typical immunophenotype) to 0 (atypical).<sup>12;13</sup> A typical immunophenotype of CLL is weak sIg expression, CD5+, CD23+, FMC7- and negative or weak CD22 expression. Most CLL cases have score 4 or 5 and rarely 3.

### 1.4. Prognostic factors in CLL.

The clinical course and outcome vary among CLL patients. CLL patients are currently categorized into risk groups based on the clinical staging systems developed by Rai et al.<sup>8</sup> and Binet et al. in the early 1980s.<sup>9</sup> As reported in the previous chapter these classifications are still helpful for dividing patients in regard to the expected overall survival (OS), however, both systems fail to indicate the higher risk of progression among patients in early stages of the disease. These clinical staging systems were complemented by prognostic markers based on peripheral blood or bone marrow examination, such as an identification of atypical morphology of CLL cells, high rate of prolymphocytes, or diffuse infiltration of bone marrow, which are associated with worse outcome.<sup>14;15</sup>

Among newer prognostic factors in CLL, there are lymphocyte doubling time (LDT), serum markers, cytogenetic abnormalities, biological prognostic factors (*IGHV*) mutational status, ZAP-70, CD38, and CD49d expression.<sup>15-17</sup>

### 1.5. Lymphocyte doubling time (LDT)

LDT longer than 12 months correlates with increased progression-free survival (PFS) and OS. An increase in the lymphocyte count of more than 50% in two months or LDT during less than 6 months is a recommended criterion of active disease and indication for treatment. The latter indication is relevant for patients with the baseline lymphocyte counts more than  $30 \times 10^9/L$  only.<sup>18</sup>

### 1.6. Serum markers

Serum prognostic factors, such as  $\beta$ 2-microglobulin ( $\beta$ -2M), soluble CD23 (sCD23), or serum thymidine kinase (TK), were indicated as an important prognostic factor for CLL patients. They are relevant markers of proliferative activity and a risk disease progression, correlating with other biological prognostic factors.<sup>14</sup>

### 1.7. Genetic abnormalities quantified by FISH and by molecular techniques

Fluorescent in situ hybridization (FISH) technique is an important part of the examination, probably the most frequently used and widely available for the clinical care of CLL patients. It allows detection of a set of specific defined chromosomal abnormalities in approximately 80% of patients. Most of the typical aberrations lead to loss or gain of genetic material, whereas translocations are not very common in CLL. The most frequent genomic lesions are listed below in order of increasing disease severity:

- a) deletion at 13q14.3 is detected in more than 50% of all cases. When it represents the only lesion it is associated with a good clinical outcome. The deleted region comprises a minimal region of 29kb located between exons 2 and 5 of DLEU2 (deleted in leukemia 2) which contains two microRNAs (mir-15a and mir-16-1) apparently involved in the regulation of antiapoptotic genes. The deleted region can also include the region coding for the retinoblastoma gene (RB1). More aggressive clinical courses are documented for del13q-only CLL carrying higher percentages of 13q deleted nuclei and involving the RB1 locus.<sup>19</sup>
- b) trisomy of the chromosome 12 (tri12), found in approximately 16-20% of CLL cases, bears an intermediate prognosis and is only marginally associated with an unmutated (UM) IGHV gene status.<sup>20</sup> Recently it was reported an association between tri12 and the presence of mutations in the NOTCH1 gene, where the cells may be more resistant to apoptosis-induced cell death, leading to a less favorable course,<sup>21;22</sup> and between tri12 and the expression of the adhesion molecule and negative prognostic marker CD49d.<sup>23</sup>
- c) deletions of 11q22-23, detected in 5-18% of all CLL cases, targets the gene ataxia telangiectasia mutated (ATM) a tumor suppressor gene crucial for the DNA repair. This abnormality is related to rapidly progressing disease, massive lymphadenopathy and bad prognosis.<sup>16;24;25</sup> These patients are often UM-CLL, which is consistent with their poor clinical outcome.<sup>17</sup>
- d) deletion in the region 17p13, in less than 10% of all CLL cases, removes p53 tumor suppressor gene and this genetic abnormality confers the worst prognosis among all the genetic lesions.<sup>26;27</sup>

Although FISH analyses of these and other chromosomal aberrations have been extremely helpful in predicting clinical course and indicating ongoing evolution of the leukemic clone, the FISH approach is limited by the fact that it can only detect lesions that have already been defined in other patients. New and sensitive techniques such as comparative genomic hybridization (CGH), genome-wide analyses of single nucleotide polymorphisms (SNPs), and whole-exome or whole genome sequencing (next-generation sequencing (NGS) or deep sequencing) defined new abnormalities.

New chromosomal loci apparently involved in the pathogenesis of the CLL have been defined (2q37.1, 6p25.3, 11q24.1, 15q23, 19q13.32 and 8p21.2-p12) and 18 recurrently mutated genes have been identified thus far: NOTCH1, Exportin 1 (XPO1), MYD88, Kelch-like 6 (KLH6), TP53, TGM, BIRC3, PLEKHG5, ATM, splicing factor 3, B1 unit (SF3B1), ZMYM3, MAPK1, FBXW7, and DDX3X. These mutations coexist with some of the genetic abnormalities analyzed by FISH: SF3B1 mutations with del(11q), NOTCH1 with tri(12), and MYD88 with del(13q).

### 1.8. IGHV mutation status

CLL cases are further divided into two groups according to the presence/absence of mutations in genes coding the variable region of immunoglobulin heavy chain (IGHV). Mature B lymphocytes express on the surface B cell receptor (BCR) which is coded by the immunoglobulin genes. Somatic hypermutations in the genes encoding IGHV are a result of a physiological process occurring in the

germinal centers of lymphoid organs after an antigen stimulation of B lymphocyte and provides a vast diversity in an antibody repertoire. Mutations in the IGHV genes are identified based on the comparison of a DNA sequence obtained from CLL lymphocytes to the corresponding genes in the germline composition. In the context of CLL, IGHV is considered as mutated (M-CLL) when the sequence differs from the germline by 2% or more. Mutated IGHV is present in more than 50% of CLL cases and strongly correlates with favorable prognosis of CLL. Therefore, the presence (favorable prognosis) or absence (poor prognosis) of IGHV gene mutations provide a prognostic value.<sup>17;28</sup>

## 1.9. Expression of specific proteins in or on CLL cells

### 1.9.1. ZAP-70

ZAP-70 encodes for T cell specific zeta-associated protein-70 belonging to the SYK family of tyrosine kinases, and associated with the  $\zeta$ -chain of the CD3 complex.<sup>29</sup>

Intracellular expression of the ZAP-70 protein above a certain threshold of cells by flow cytometry ( $\geq 20\%$ ) has proven to be an important indicator of time-to treatment and survival in CLL.<sup>30</sup> The cutoff to classify patients as ZAP-70 positive (negative prognostic factor, correlating with unmutated *IGHV* status) or ZAP-70 negative, as measured by flow cytometry, is widely proposed at 20% threshold. However, standardization of ZAP-70 estimation still remains a challenge.

Although the numbers of CLL cells expressing this protein are correlated with *IGHV* mutation status and CD38 expression<sup>18</sup>, ZAP-70 levels are an independent marker of clinical outcome.<sup>30</sup> Recent studies suggest that ZAP-70 retards internalization of smlgM (surface membrane immunoglobulin M) and CD79b from the cell membrane, leading to prolonged BCR pathway signaling.<sup>31;32</sup> In addition, ZAP-70 positive CLL cells are more likely to express adhesion molecules such as CD49d and chemokine receptors, in particular CCR7<sup>33</sup>, that promote migration toward a series of chemokines and inhibit apoptosis.

### 1.9.2. CD38

CD38 is a transmembrane glycoprotein widely expressed in humans within the hematopoietic system (e.g. bone marrow progenitor cells, monocytes, platelets, erythrocytes, discrete stages of T and B lymphocyte differentiation) and beyond, including brain, prostate, kidney, gut, heart and skeletal muscle.<sup>34;35</sup> CD38 is regulated by the tumor microenvironment and behaves simultaneously as a cell surface enzyme and as a receptor. As an ectoenzyme, CD38 presents multiple enzymatic activities, including the production of ADPR (from  $\text{NAD}^+$  or cADPR through hydrolysis) and NAADP (from  $\text{NADP}^+$ ), all of them involved in signal transduction through the regulation of cytoplasmic  $\text{Ca}^{++}$  levels.<sup>36</sup> As a receptor, CD38 binds CD31 that is expressed by a variety of immune cells including B and T cells subsets, and by vascular endothelial cells.<sup>37</sup>

CD38 positive patients (the threshold  $>30\%$  of CD38 positive CLL cells is proposed) were reported to have significantly worse prognosis regarding progression free survival (PFS) and overall survival (OS) than those who were CD38 negative. It was observed that CD38 expression on CLL cells correlates with the absence of *IGHV* mutations.<sup>14;15;38-40</sup>

### 1.9.3. CD49d

CD49d is a molecule belonging to the integrin superfamily, highly expressed in normal peripheral blood and bone marrow B lymphocytes. It is a surface molecule, the expression of which promotes microenvironment-mediated proliferation of CLL leukemic cells<sup>41,42</sup> and identifies a subgroup of about 40% of CLL patients characterized by a progressive course and short survival.<sup>43-48</sup>

Very recently, CD49d emerged as the strongest flow cytometry-based prognostic marker, with greater prognostic value than CD38 and ZAP-70, in a worldwide multicenter analysis (Bulian P et al, 2013 JCO, in press). In this study Bulian P et al established the 30% cut point as the most useful threshold for classification of CD49d positive CLL.

The prognostic relevance of CD49d in CLL may have therapeutic implications, envisioning the use for CLL patients of Natalizumab (TYSABRI, Biogen Idec, Cambridge, MA and Elan Pharmaceuticals, South San Francisco, CA, USA), a humanized anti-CD49d monoclonal antibody already available and currently employed in autoimmune diseases such as multiple sclerosis and Crohn's disease.<sup>49</sup>

### 1.10. Microenvironment in CLL

Normal B cells are programmed to rapidly respond to the environment, while causing little damage to normal tissues. They have the ability to recognize, process, and present foreign antigens to other components of the immune system, and to undergo maturation and eventually secrete antibodies directed at a specific antigen. It is not surprising that CLL cells, the malignant counterpart of normal B cells, retain the ability to interact with their surrounding environment, where the finely tuned orchestration and normal compartmentalization of the immune response is altered. Invasion of the primary and secondary lymphoid tissues by CLL cells disrupts the normal tissue architecture and physiology. The spleen and lymph nodes are diffusely infiltrated by CLL cells, whereas the bone marrow is involved in an interstitial, nodular, and/or diffuse pattern. CLL cells retain the capacity to react to a variety of external stimuli and the tissue microenvironment provides supporting signals that may differ within the various anatomic sites.<sup>50</sup>

In the tissue microenvironment, CLL cells reside in close contact with T lymphocytes, stromal cells, endothelial cells, follicular dendritic cells, and macrophages. Interactions between these components regulate CLL cell trafficking, survival, and proliferation in a manner that may be partly dependent on direct physical cell-to-cell contact or mediated through the exchange of soluble factors.

Effectively, CLL cells typically undergo apoptosis when cultured *in vitro*, indicating that the *in vivo* accumulation of leukemic lymphocytes is favored by factors originating from the microenvironment.<sup>51</sup> *In vitro* apoptosis of CLL cells can be prevented by co-culture with different accessory cells that are part of the CLL microenvironment, such as monocyte-derived nurse-like cells (NLC)<sup>52-54</sup>, mesenchymal marrow stromal cells (MSC)<sup>52</sup>, or follicular dendritic cells (FDC)<sup>55</sup> that provide survival signals to CLL cells. Thereby CLL cells interact with different accessory cells according to the lymphoid system they are travelling.

Several molecules involved in the cross talk between CLL cells and their microenvironment have been identified: those secreted by CLL cells and those secreted by stromal cells.<sup>4</sup> While chemokine secretion by CLL cells may play an important role in recruitment of accessory cells, chemokines secreted by stromal cells are also critical for homing and tissue retention of CLL cells.

The main chemokines secreted by CLL cells are CCL3, CCL4, CCL22 and CCL17. CCL3/4 provide survival signals to CLL cells through the recruitment of CCR5+ regulatory T cells<sup>56</sup> and the recruitment of monocyte or NLC. Link to this point, Zucchetto and colleagues showed that CD38 and CD49d may

play a key role in stimulating CCL3/4 production, and ultimately to improving survival of CLL cells, involving the CD38/CD31 pair, and the CD49d/VCAM-1 axes.<sup>57</sup> CCL22 and CCL17 recruit activated T lymphocytes that will ensure provision of pro-survival signals (IL-4 or CD40 ligand).<sup>58</sup>

CXCL12 (SDF-1), a chemokine secreted by MSC and NLC, acts as a chemotactic and anti-apoptotic factor for CLL through its cognate receptor CXCR4 expressed on CLL cells.<sup>59-61</sup> NLC express another chemokine, called CXCL13, that binds to CXCR5 CLL cells receptor, and recruits circulating B-cells to follicles.<sup>62</sup> CCL19 and CCL21 are two additional chemokines secreted by stromal cells, and they serve as ligands for the CCR7 receptor on the CLL cell surface and lead to migration of CLL cells across the vascular endothelium.

In the tissues microenvironment, CLL cells are surrounded by a supportive microenvironment that includes cells expressing CD40L, fibronectin, and VCAM-1, all of which provide additional survival and anti-apoptotic signals to the CLL cells. In this context adhesion molecules such as integrins play an important role in regulating cell growth and function in the stromal microenvironment. A key integrin in CLL is CD49d, which plays an important role in the homing and retention of CLL cells in the microenvironment<sup>63</sup>, as described in the following chapter.

### 1.11. CD49d and microenvironment

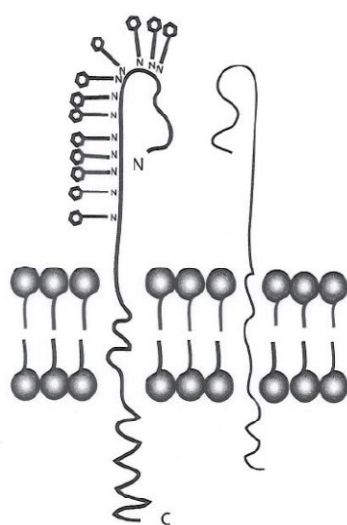


**Figure 1: Schematic representation of the integrin CD49d (left chain) and CD29 (right chain)**

CD49d, a.k.a.  $\alpha 4$  integrin, forms a heterodimeric integrin by the non-covalent association of the CD29 subunit ( $\beta 1$ )<sup>64</sup> and acts primarily as an adhesion molecule capable of mediating both cell-to-cell interactions, via binding to vascular-cell adhesion molecule-1 (VCAM-1), and interactions with extracellular matrix components by binding to non-RGD sites (a.k.a. CS-1 fragments) of fibronectin (FN), as well as the globular C1q-like domain of elastin microfibril interfacier-1 (EMILIN1).<sup>65-68</sup>

CD49d has a strong prognostic relevance that can be explained by considering the specific roles of this molecule in the context of the CLL microenvironment. In this regard, CD49d has been demonstrated to play a central role in the migration/infiltration processes, orchestrating the activities of several molecules including chemokine receptors and metalloproteases (MMPs).

In particular, chemokine-induced transmigration of CLL cells across high endothelial venules (HEV) into lymph nodes are known to depend on cell adhesion of CLL cells via the CD49d/VCAM-1 pair, and the subsequent response of adherent CLL cells to specific chemokines, mainly CCL21 and CCL19, produced by HEV themselves or by the surrounding lymph node stroma, through the chemokine receptor CCR7.<sup>69</sup> Moreover, the combined stimulation of CLL cells by vascular endothelial cell growth factor (VEGF) and CD49d engagement was shown to be critical for chemokine induced transendothelial migration (TEM).<sup>70</sup>

TEM and organ invasion of malignant cells require proteolytic degradation of the vascular basement membrane and the extracellular matrix of lymphoid tissues.<sup>70</sup> In the context of CLL, MMP-9 is the

predominant MMP expressed<sup>71</sup>, and its intracellular levels correlated with advanced stage disease and poor patient survival.<sup>72</sup> Recent data have demonstrated that adhesion of CLL cells via CD49d up-regulates MMP-9 production, and that the MMP-9 proteolytic activity may be enhanced by its localization at the CLL cell surface.<sup>73</sup> In particular, CLL cells bind soluble and immobilized proMMP-9 and active MMP-9 through a novel cell surface docking complex for MMP-9, composed by CD49d and a splice variant of CD44, that has been described to confer a metastatic phenotype to locally growing tumor cells, and whose expression is associated to tumor progression.<sup>74</sup>

CD49d is also functionally linked to CXCR4, the receptor for the CXCL12 chemokine<sup>75</sup>, as demonstrated in multiple myeloma or in bone marrow hematopoietic progenitors, where CXCR4 triggering by CXCL12 is able to up-regulate CD49d-mediated adhesion to VCAM-1 and FN.<sup>76;77</sup> Of note, as for CD49d, also CXCR4 engagement was shown to up-regulate MMP-9 production by CLL cells.<sup>73</sup>

Recently, it has been shown that MMP-9 not only regulates the migration/arrest of CLL cells, but it is also a functional ligand for CD49d, able to provide survival signals independently of its proteolytic activity.<sup>74;78</sup> Interestingly, the pro-survival effect of MMP-9 derives from activation of the Lyn kinase, thus following a distinct and BCR-independent mechanism.<sup>78</sup> Moreover, the Lyn/STAT3/Mcl-1 pathway, which is elicited by MMP-9 ligation to the CD49d/CD44v docking receptor, is not shared by the CD49d-VCAM-1 axis, suggesting that CD49d may trigger distinct intracellular events depending on the ligand.<sup>78</sup>

Integrin ligation enhances cell survival through several mechanisms. In the context of CLL, ligation of CD49d by FN was demonstrated to prevent CLL *in vitro* onset of apoptosis, likely due to an increase in the BCL-2/BAX ratio.<sup>79</sup> Moreover, the same molecular interactions were found to be able to protect CLL cells from fludarabine-induced apoptosis, this effect correlated with an increased expression of BCL<sub>XL</sub>.<sup>68;80</sup> CD49d triggering is also able to induce SYK phosphorylation and SYK-dependent AKT phosphorylation, through mechanisms distinct from the BCR signaling.<sup>81</sup> The SYK-dependent AKT/MCL-1 pathway is known to contribute to CLL cell survival.<sup>82-85</sup>

CD49d and CD38 are both involved in the continuous interactions taking place between CLL cells and tumor microenvironment, being part of a complex network sustaining growth and survival of CLL cells.<sup>37;57;79</sup> A functional link between CD49d and CD38 has been reported moving from the observation of a distinct over-expression of transcripts for the chemokines CCL3 and CCL4 in CD49d<sup>+</sup>/CD38<sup>+</sup> CLL, and an up-regulation of their production by CD49d<sup>+</sup>/CD38<sup>+</sup> CLL cells upon CD38 triggering.<sup>57</sup> CCL3 and CCL4 have overlapping effects and are known to act as potent chemoattractants for monocyte macrophage<sup>57</sup> or T cell<sup>86</sup> lineages in the context of CLL-involved bone marrow microenvironmental sites and this is supported by the following lines of evidence: i) CCR1 and CCR5, i.e. the receptors for CCL3 and CCL4, are strongly expressed, the former more than the latter, by PB monocytes and macrophages from healthy and CLL samples; ii) PB monocytes from CLL samples are uniquely sensitive to CCL3-mediated migratory signals *in vitro*; iii) a higher number of infiltrating CD68<sup>+</sup> in the context of CLL-involved areas of bone marrow biopsies from CD49d<sup>+</sup>/CD38<sup>+</sup> CLL CCL3-producing cases have been observed when compared to CD49d<sup>-</sup>/CD38<sup>-</sup> CLL cases.<sup>57;87;88</sup> Besides, compelling evidences indicate a strong correlation among the CD49d<sup>+</sup>/CD38<sup>+</sup> phenotype, infiltration of CD68<sup>+</sup> macrophages, and presence of a stromal/endothelial component highly expressing VCAM-1 in the context of lymphoid aggregates in bone marrow biopsies of CD49d/CD38-expressing CLL. VCAM-1 upregulation has been demonstrated to be due to an overproduction by the

infiltrating CD68<sup>+</sup> macrophage component of TNF $\alpha$  and other cytokines. VCAM-1/CD49d interactions resulted in an increased survival of CD49d-expressing CLL cells.<sup>57</sup> This circuitry may contribute to explain the aggressive clinical course of CLL coexpressing CD49d and CD38 (figure 2). Notably, triggering of BCR of UM CLL, as well as co-cultures of CLL cells with specialized CD68<sup>+</sup> macrophages known as nurse-like cells<sup>54;86</sup>, again result in an overproduction by CLL cells of CCL3 and CCL4, thus strengthening the functional link between UM and/or CD49d-expressing CLL cells, the production of specific chemokines and infiltration of macrophages and/or T cells of CLL-involved tissues. These T cells may express the membrane bound TNF superfamily member CD40L/CD154, that, through the binding with CD40<sup>+</sup> CLL cells, exert a key role preserving CLL cells from apoptosis in the context of the so-called lymph nodes proliferation centers.<sup>58</sup>

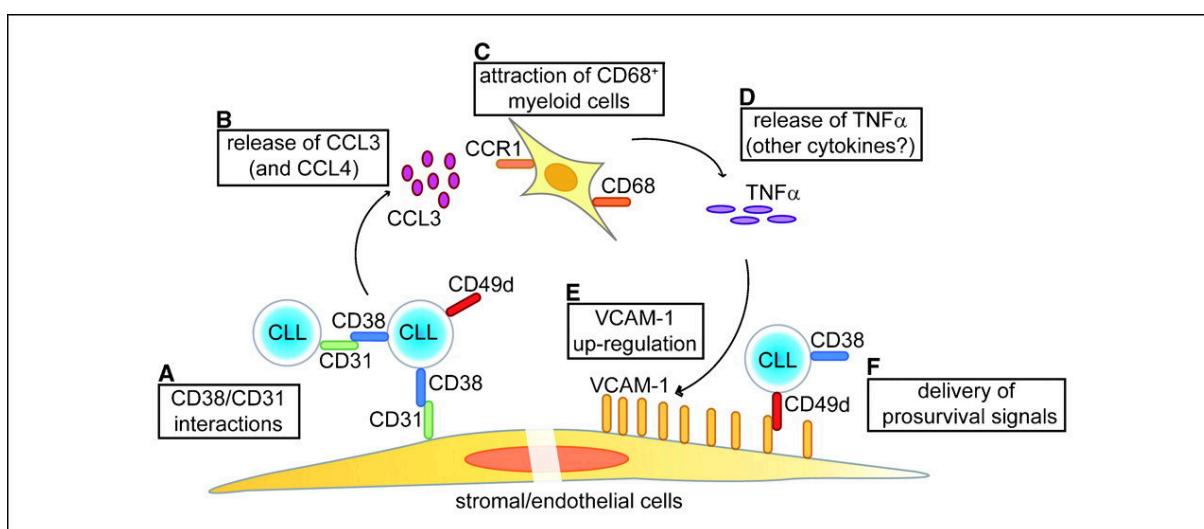


**Figure 2: Model for a prosurvival circuitry operating in CD38<sup>+</sup>CD49d<sup>+</sup> CLL, from Zucchetto et al<sup>57</sup>**

In addition to the above described functional interplay connecting CD49d and CD38 in CLL through soluble factors, the two molecules have been recently described to be part of a cell surface macromolecular complex which includes, along with CD49d and CD38, also CD44 and MMP9, altogether characterizing poor prognosis CLL. Functionally, the co-expression of CD38 was demonstrated to enhance CD49d-mediated activities; in particular: i) CD49d<sup>+</sup>CD38<sup>+</sup> cells have higher propensity to adhere to the CD49d specific substrates VCAM-1 and FN compared to CD49d<sup>+</sup>CD38<sup>-</sup> cells; ii) CD49d/VCAM-1 interactions exert a more marked anti-apoptotic effect in CD49d<sup>+</sup>CD38<sup>+</sup> cells as compared to CD49d<sup>+</sup>CD38<sup>-</sup>. The more efficient adhesive properties characterizing CD49d<sup>+</sup>CD38<sup>+</sup> CLL cells can be explained on the basis of a cooperation between the two molecules. In particular, it has been hypothesized that a possible role of CD38 in CD49d mediated adhesion can be the recruitment of proteins involved in the downstream integrin signaling leading to enforced actin polymerization and cell adhesion.<sup>41</sup>

### 1.12. Ligands of CD49d

The two main well-known ligands for CD49d are VCAM-1 and fibronectin. As described in the previous chapter both molecules activate signaling pathways delivering pro-survival signals, and promoting resistance to drug-induced apoptosis in CLL expressing CD49d.

Recently, the globular (g) C1q-like domain of Elastin Microfibril Interfacier1 (EMILIN1), an adhesive extracellular matrix constituent, was described as a new ligand for CD49d, where it operates as a negative modulator of proliferation signals in substrate-adherent non-hematopoietic CD49d+ cells.<sup>89</sup>

### 1.12.1. VCAM-1 and fibronectin

VCAM-1 is a transmembrane glycoprotein and is a member of the immunoglobulin superfamily, consisting of six or seven C2-type immunoglobulin domains. It is expressed by endothelial cells in response to inflammatory cytokines, by activated neurons, smooth muscle cells, fibroblasts, macrophages (Kupffer cells), dendritic cells, oocytes and Sertoli cells. Soluble forms of VCAM-1 have been identified in tissue culture supernatants and in blood. Blood levels appear elevated in disease as CLL<sup>90</sup>, acute myelomonocytic leukemia<sup>91</sup>, bronchial asthma<sup>92</sup>, and acute phase multiple sclerosis.<sup>93</sup> Primarily, the VCAM-1 protein is an endothelial ligand for CD49d ( $\alpha 4\beta 1$ ) and for integrin  $\alpha 4\beta 7$ .

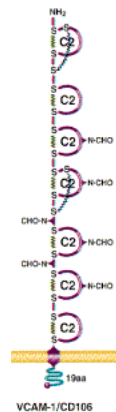


Figure 3: VCAM-1 structure

Fibronectin is a prototype cell adhesion protein, widely distributed in the tissues of all vertebrates and a potential ligand for most cell types. It is present as a polymeric fibrillar network in the ECM and as soluble protomers in body fluids. Fibronectin is a glycoprotein consisting of repeating units of amino acids, which form domains that enable the molecule to interact with a variety of cells through both integrin and non-integrin receptors. It is encoded by a single gene, but alternative splicing of pre-mRNA allows formation of multiple isoforms that have critical roles in cell adhesion, migration and proliferation.

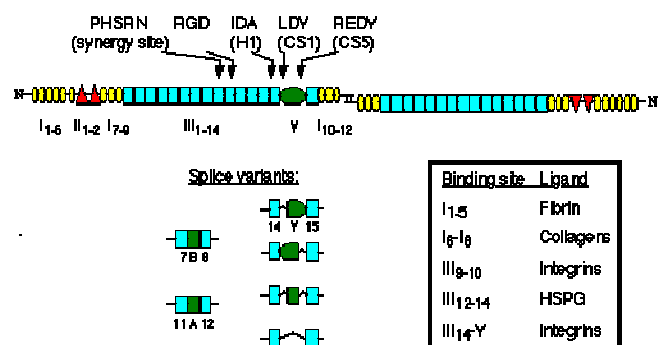


Figure 4: Schematic model of a plasma fibronectin protomer. The protein is a dimer of two subunits which are identical except for the inclusion of the V-segment in one of the chains. Integrin binding sites are indicated in one of the subunits by arrows.<sup>1</sup>

The III14-V region is recognized by the same integrin that recognized VCAM-1 and three binding sites have been identified within this region (figure 4). The so called CS1 site has approximately 20-fold higher affinity for the integrins than the other two sites, namely CS5 and H1.<sup>94</sup>

### 1.12.2. EMILIN1

EMILIN1, the prototype of the EMILIN family, is an adhesive extracellular matrix constituent associated with elastic fibers, detected also in the proximity of cell surfaces and it is particularly abundant in the walls of large blood vessels<sup>95</sup>, in intestine, lung, lymph nodes, skin, and lymphatic capillaries.<sup>96</sup> The structure of EMILIN1 consists of a cysteine-rich domain (EMI domain) at the N terminal, an extended region with a high potential coiled-coil structure, a short collagenous stalk, and a self-interacting globular gC1q domain at the C-terminal, a region homologous to the globular domain of complement that represent a structurally unique component. EMILIN1 has been implicated in multiple functions, linking to the functional domain. The coiled coil structure is

responsible of elastogenesis, maintenance of blood vascular cell morphology<sup>95</sup>, and regulation of the growth and integrity of lymphatic vessels.<sup>96</sup> The elastin microfibril interface domain at the N-terminal<sup>97</sup>, interacts with pro-TGF- $\beta$  and regulates the blood pressure homeostasis.<sup>98</sup> The gC1q domain is necessary for the non covalent formation of homotrimers that are then linked by disulfide bonds giving rise to very large extracellular aggregates.<sup>99</sup> The gC1q domain is particularly important for the protein polymerization, for the interaction with cellular adhesion molecules<sup>100</sup>, for the migration, and for the trophoblast invasion via interaction with the CD49d/CD29 ( $\alpha 4\beta 1$ ) integrin.<sup>65;101</sup> Indeed recently Danussi et al reported the involvement of gC1q domain in the regulation of skin homeostasis  $\alpha 4/\alpha 9\beta 1$ -integrin mediated<sup>89</sup>, in the regulation of skin carcinogenesis<sup>102</sup> and in lymphatic valve formation and maintenance after engagement of  $\alpha 9\beta 1$ -integrin.<sup>103</sup>

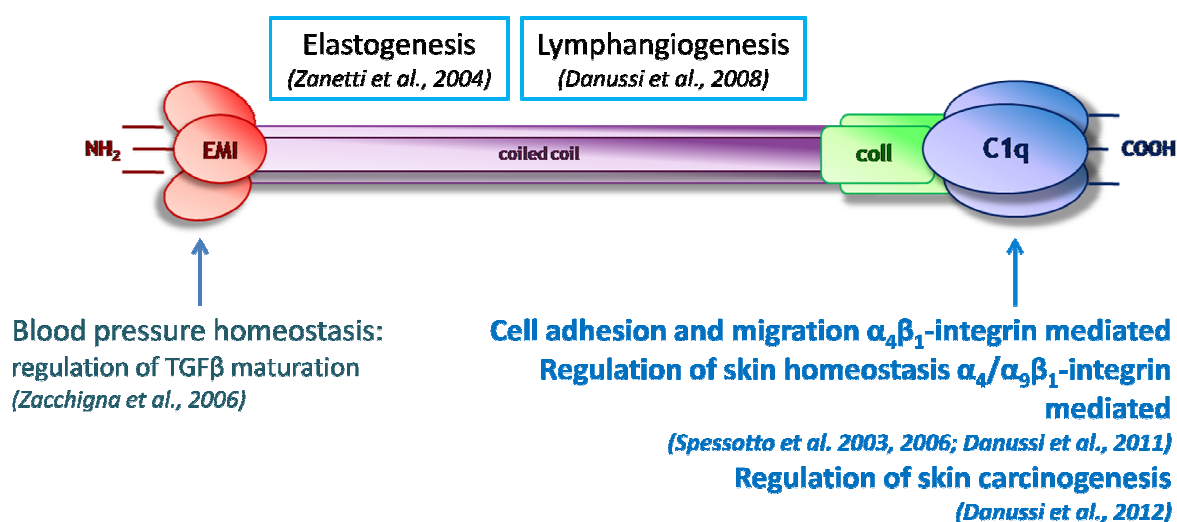


Figure 5: Schematic representation of EMILIN1 and its functions

In skin homeostasis the lack of direct engagement between EMILIN1 and  $\alpha 4\beta 1$ -integrin induce activation of PI3K/AKT and ERK1/2 pathways as a result of the reduction of PTEN. The downregulation of PTEN empowered ERK1/2 phosphorylation that in turn inhibited Smad2 signaling. These results highlight the activation of proliferative pathway of dermal fibroblast and keratinocyte. The ability of CD49d integrin to recognize the trimeric EMILIN1 gC1q domain mainly depends on a single glutamic acid residue (E933).<sup>104</sup> The substitution of the glutamic acid at position 933 with an alanine residue makes the gC1q domain no longer functional in cell adhesion assay and it is not recognized by CD49d. This E933A mutant was employed in the experiment presented in this thesis as a negative control of adhesion.

### 1.13. *In vitro* and *in vivo* models

The *in vitro* model for chronic lymphocytic leukaemia is the MEC-1 cell line that derive from a patient with B-chronic lymphocytic leukemia. They express mature B cell markers CD19, CD20, CD22, CD23 and, are CD18+, CD11+, CD44+, CD54+ and CD49d+. CD5 and FMC7 are negative in MEC1 cells.<sup>105</sup> The *in vivo* models are mice wild type and knock out for EMILIN1, that are inoculated with leukemia cells derived from mice TCL-1.

The genetic background of both mice is the same: C57BL/6.

EMILIN1 deficient mice (*Emi*<sup>-/-</sup>) are fertile, have a normal life span and do not exhibit gross morphological abnormalities. However, they present alteration of the fine structure of elastic fibers

and of cell morphology in elastic arteries;<sup>95</sup> they display elevated blood pressure as a result of increased TGF- $\beta$  signaling in the vasculature<sup>98</sup> and have an abnormal lymphatic phenotype with a significant reduction of anchoring filaments and lymphatic vessel hyperplasia, leading to a mild lymphatic dysfunction.<sup>96</sup> Indeed the phenotype of the *Emi*<sup>-/-</sup> mouse skin revealed increased thickness of epidermis and dermis.

The *E $\mu$ -TCL1* were established with *TCL1* under the control of a VH promoter-IgH-E $\mu$  enhancer to target TCL1 expression to immature and mature B cells. Flow cytometric analysis reveals a markedly expanded CD5+ population in the peritoneal cavity of *E $\mu$ -TCL1* mice starting at 2 months of age that becomes evident in the spleen by 3–5 months and in the bone marrow by 5–8 months. Analysis of Ig gene rearrangements indicates monoclonality or oligoclonality in these populations, suggesting a preneoplastic expansion of CD5+ B cell clones, with the elder mice eventually developing a chronic lymphocytic leukemia (CLL)-like disorder resembling human B-CLL.

Thereby, *E $\mu$ -TCL1* transgenic mice develop a disease resembling human CLL. The mice develop at first a preleukemic state evident in blood, spleen, bone marrow, peritoneal cavity, and peripheral lymphoid tissue, developing later a frank leukemia with all characteristics of CLL.<sup>106</sup>

---

# Aim of the study

Chronic lymphocytic leukemia (CLL) is a heterogeneous disease with highly variable clinical courses with survivals ranging from months to decades. In this context, CD49d expression represents a strong negative prognosticator marking a subset of about 40% of CLL patients characterized by aggressive disease and accelerated clinical course. Functionally, CD49d ( $\alpha 4$  integrin) acts as an adhesion molecule, mediating both cell-to-cell interactions, via binding to vascular-cell adhesion molecule-1 (VCAM-1), and interactions with extracellular matrix components by binding to CS-1 fragments of fibronectin (FN). In CLL, the CD49d/VCAM-1/fibronectin axis regulates recirculation of leukemic cells from the blood stream to bone marrow and lymphoid organs, delivers pro-survival signals, and promotes resistance to drug-induced apoptosis.<sup>57;68</sup> CD49d is deeply involved in the continuous interactions between CLL cells and microenvironmental cells in bone marrow and secondary lymphoid organs, being responsible for CLL cell growth advantages and extended survival.

Recently, the globular (g) C1q-like domain of Elastin microfibril interfacer-1 (EMILIN1) has been identified as a new ligand for CD49d, although its putative role in CLL is completely unknown. EMILIN1 is an adhesive extracellular matrix constituent associated with elastic fibres and it is particularly abundant in the walls of large blood vessels, intestine, lung, skin, lymph nodes and lymphatic capillaries. CD49d/EMILIN1 interactions have been mainly studied in non-hematopoietic cell models; in this context, EMILIN1 was shown to operate as negative modulator of proliferation signals when interacting with CD49d-expressing fibroblasts and keratinocytes. To date, no studies have addressed the role of CD49d/EMILIN1 interaction in CLL.

In the present thesis we focused on the distribution of EMILIN1 in CLL-lymphoid tissues and on the capacity of CLL cells to interact with EMILIN1 via CD49d. The interplay between CD49d and gC1q-like domain of EMILIN1 was investigated, compared with VCAM-1 and fibronectin, focusing on the modulation of phosphoproteins involved in cell adhesion and survival. Then, the role of CD49d/EMILIN1 interaction was studied in terms of protection from spontaneous apoptosis.

The results included in the present thesis have defined for the first time the important role of CD49d/EMILIN1 interaction in CLL which consists in the maintenance of the neoplastic clone.

---

## 2. Results

### 2.1. EMILIN1 is largely distributed in normal and CLL-involved tissues

The protein Elastin Microfibril Interface Located proteIN (EMILIN1) is so called for its peculiarly fine distribution on the surface of amorphous elastin.<sup>107</sup> EMILIN1 forms a fibrillar network *in vitro* and *in vivo* in the extracellular matrix (ECM) of several tissues including lymphatic and blood vessels, skin, heart, lung, kidney, and cornea. This glycoprotein codistributes with elastin in most sites and likely constitutes an associated component of elastic fibers. EMILIN1 is localized mainly at the interface between amorphous elastin and the surrounding microfibrils, and it has been implicated in the correct deposition of elastin *in vitro*.<sup>65</sup>

Regarding its distribution in the secondary lymphatic organs really little information is reported in literature and these organs are frequently involved by CLL disease. Therefore an investigation on this context was performed by immunohistochemistry (IHC) using a specific anti-human EMILIN1 monoclonal antibody.<sup>65</sup>

The first exploratory staining was performed in human reactive lymphoid tissues, such as spleen, tonsil and lymph node, considered as a model for “normal tissues”. As reported in figure 6, in these organs EMILIN1 appeared well distributed and with defined fibrillar structures organized as a mesh in particular in the white pulp, in the capsule and around the veins of the spleen. In the white pulp of the spleen EMILIN1 was observed also in the germinal center, in the mantle and marginal zone. We observed an extracellular EMILIN1 specific reactivity mainly in the outer zone of the mantle/marginal areas and in the germinal center both in the tonsil and lymph node (figure 6).

#### SPLEEN

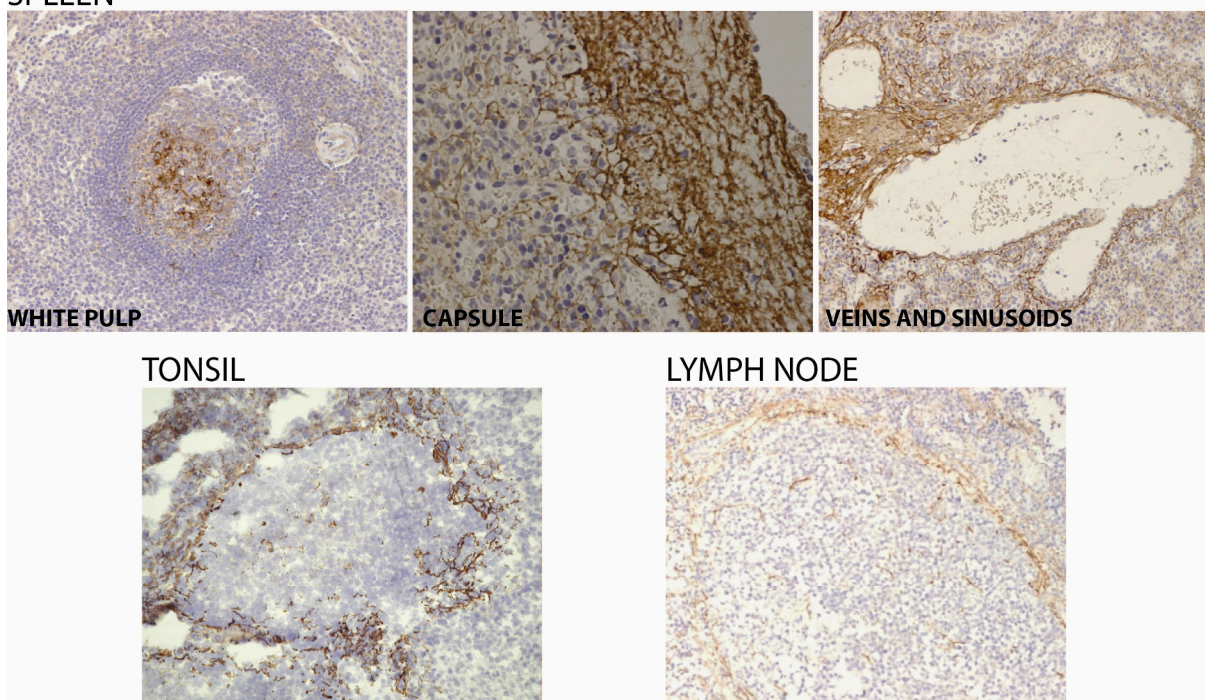


**Figure 6:** Panels represent examples of human reactive lymphoid tissues stained with EMILIN1 (brown). Spleen tissues were from paraffined block and are those on the top of the figure: left panel shows the white pulp, central panel shows the capsule and right panel shows veins and sinusoids. At the bottom of the figure the left panel shows a tonsil and the right panel a lymph node, both from frozen block. Original magnification, 400X.

Having defined the EMILIN1 distribution in non-CLL lymphoid tissues, afterwards IHC analysis was performed in CLL-involved tissues: lymph node tissues from three CLL cases and bone marrow biopsies from five CLL cases were analyzed.

In CLL lymph nodes an unexpected EMILIN1 positive staining was observed in the cytoplasm of some cells in close proximity of high endothelium vessel (figure 7, panel 1). These cells seemed to be typical CLL cells as indicated from the aspect of the shape and the nucleus. Interestingly, the expression of EMILIN1 in these malignant cells was really intense. This pattern of EMILIN1 expression was observed mainly in perivascular area, and this evidence could be linked to the role of EMILIN1 in favoring the cell migration.

EMILIN1 positive staining cells were observed also in the proliferation center and in the marginal sinus where the staining presented an extracellular pattern, and even here some cells positive for EMILIN1 were observed. Of note, these cells seemed to be osteocyte or accessory cells from morphology and bean shape of the nucleus (figure 7, panel 2 and 3).

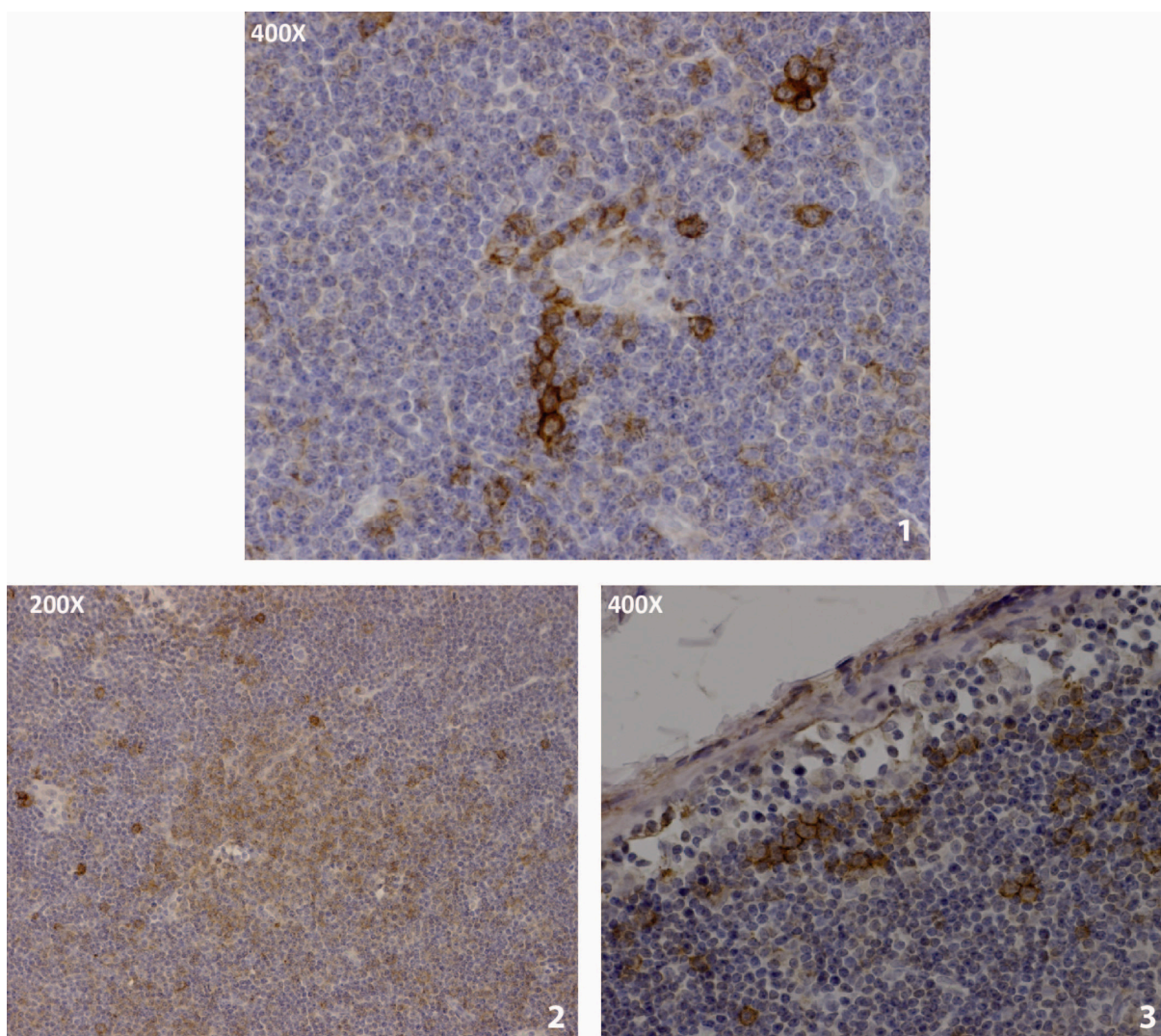


**Figure 7: CLL lymph node tissues stained with EMILIN1 (brown). Panel 1 shows a lymph node high endothelium vessel with unexpected EMILIN1 positive staining in the cytoplasm of some particular CLL cells; panel 2 shows lymph node germinal center with EMILIN1 extracellular staining pattern and some staining accessory cells or osteocyte and panel 3 shows lymph node marginal sinus with EMILIN1 staining intermingled the pathological cells and in the cytoplasm of accessory cells or osteocyte. Original magnification is reported in each panel.**

Moreover, when CLL-bone marrow biopsies were considered, the positive EMILIN1 staining in interstitial reticular cells formed a meshwork among the CLL cells (figure 8).

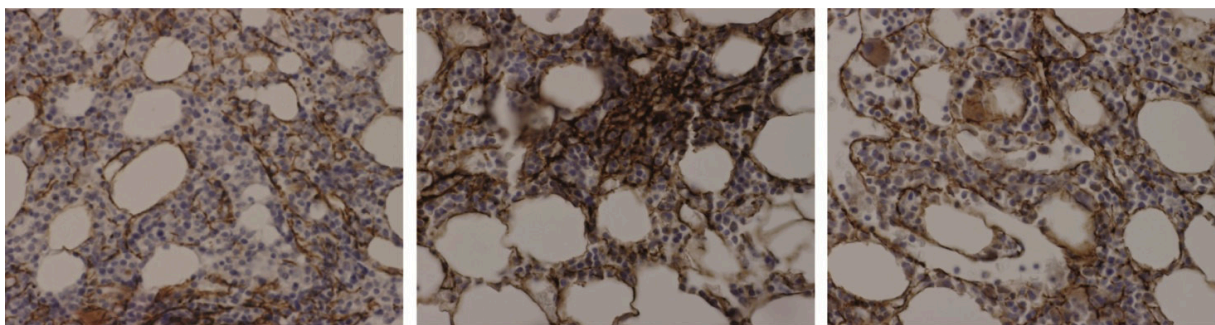


**Figure 8: CLL-bone marrow biopsies stained with EMILIN1 (brown). The three panels show three representative staining from a CLL case. EMILIN1 is well distributed forming a network among the CLL cells. Original magnification, 400 X.**

Finally, we performed immunofluorescence staining for EMILIN1 and fibronectin in cryostat sections of CLL lymph node (figure 9). To this purpose an antibody directed against the gC1q domain of EMILIN1 and against fibronectin were used, followed by a FITC-conjugated anti-rabbit IgG. The staining showed a clear network of EMILIN1 positive staining (figure 9) intermingled with the neoplastic component and closely adjacent to the surface of cells, as described by Daga Gordini et al.<sup>108;109</sup> They described *in vivo* EMILIN1 reactive structures near the surface of cells suggesting the capacity of EMILIN1 to directly interact with cell membrane receptor. Comparing the EMILIN1 staining with the fibronectin staining, it was evident not only a different network pattern, but also a higher expression (more density of stained fibrils) of EMILIN1 respect the fibronectin.

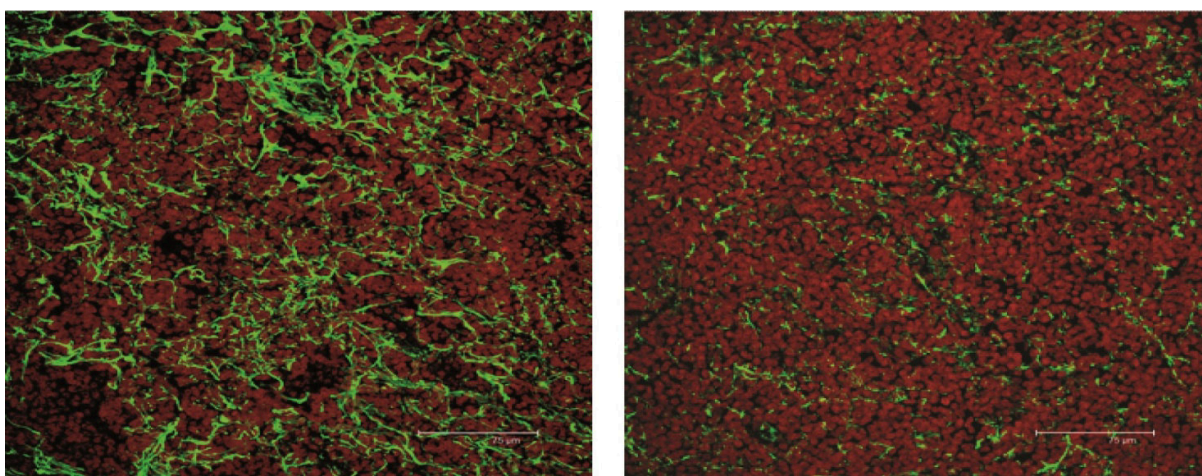


**Figure 9: Two representative CLL lymph node immunofluorescence images stained with EMILIN1 (left panel) and fibronectin (right panel); CLL cells are in red and EMILIN1/fibronectin in green. Scale bars panel, 75μm.**

This evidence suggested a possible involvement of EMILIN1 in CLL disease and it is also supported by the fact that EMILIN1 is a ligand of the integrin CD49d, which is a negative prognostic marker in CLL. Due to this preliminary result we decided to proceed with the study of the role of EMILIN1, in parallel to the other already characterized two ligands of CD49d, VCAM-1 and fibronectin.<sup>41</sup>

## 2.2. CD49d is the sole ligand for EMILIN1 in CLL

EMILIN1 is one of the ligands of two integrins: the CD49d (alpha4) integrin and the alpha9 integrin, both associated with the CD29 (beta1 subunit). Whereas the CD49d integrin is well-known in the CLL context, nothing is known about integrin alpha9-beta1 ( $\alpha_9\beta_1$ ) expression in CLL. Thus, in order to verify if alpha 9 is expressed by CLL cells and by the CLL-derived CD49d+ Mec-1 cell line (Mec-1) cytofluorimetric assays were performed. As reported in figure 10, both CLL cases and Mec-1 cells did not express alpha 9 integrin and, consistently, the expression of alpha 9 was not detectable at mRNA level when investigated in 41 CLL cases in the context of a gene expression profile analysis (data not shown).

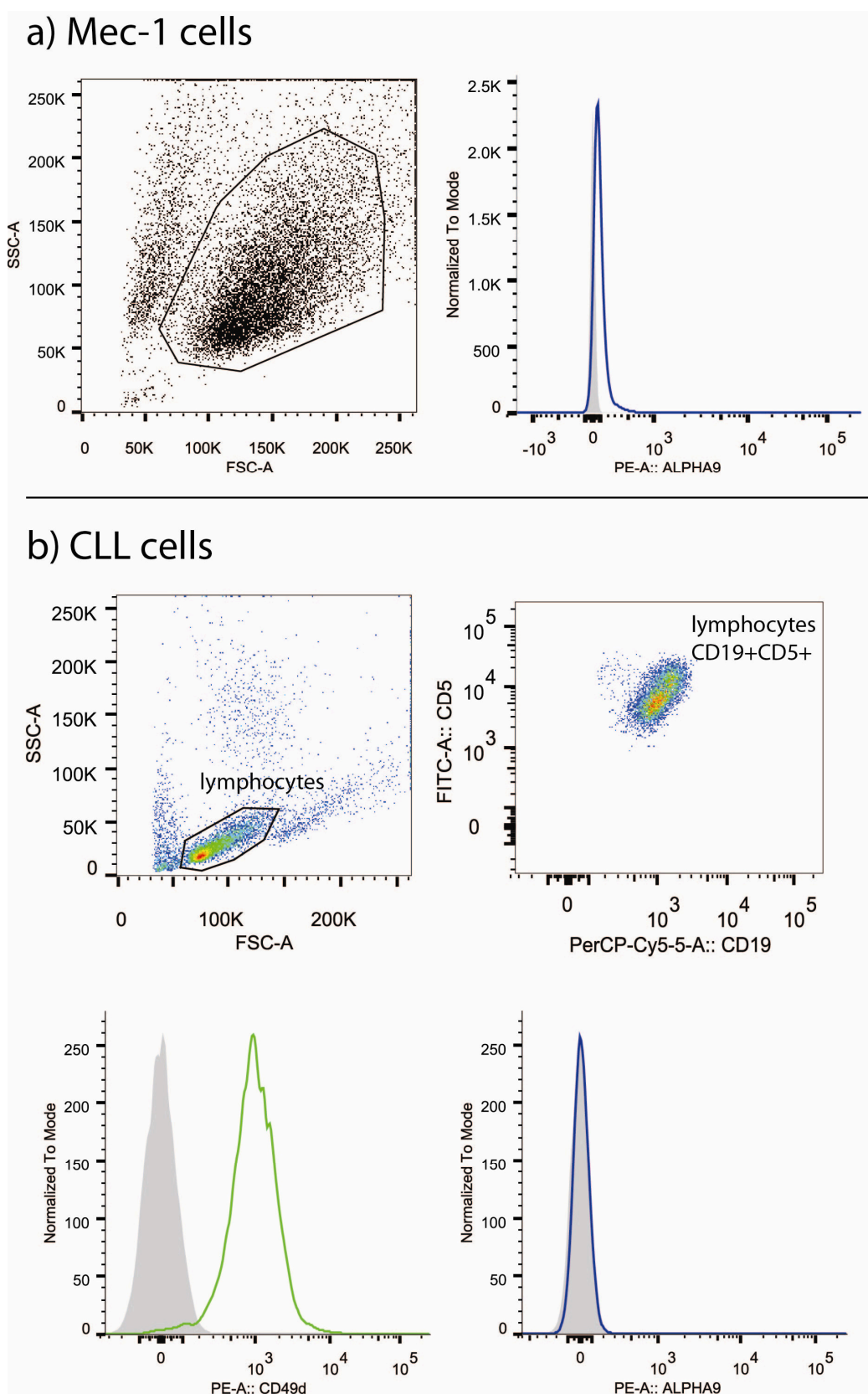


**Figure 10: Cytofluorimetric analysis with FlowJo software illustrates that Mec-1 cell line and CLL cases do not express alpha 9 integrin. a) Mec-1 cells: the first plot shows the cell line physical parameter and the second plot shows the histogram with a grey peak for the negative control staining and a blue peak of the Mec-1 cells, positive for CD19 (not shown), that do not express alpha 9. b) CLL cells: the left plot at the top shows the physical parameter of the entire lymphocyte population and the right plot shows the pathological population, CD19+CD5+. The histograms at the bottom show at the left the expression level of CD49d (green line peak) and at the right the expression of alpha9 integrin (blue line peak) in comparison to the negative control staining (grey peak) of the pathological population.**

## 2.3. EMILIN1 promotes CD49d-mediated cell adhesion

### 2.3.1. Set up of adhesion experiments on EMILIN1

In the research group where this thesis was carried out, it was studied the CD49d engagement by its two main ligands, VCAM-1 and fibronectin<sup>41</sup>, thereby the protocol for the adhesion assay was already validated as reported in the materials and methods chapter.

To set up the adhesion assay for EMILIN1 protein, we took the advantage of the presence of purified globular C1q-like domain (gC1q domain), the portion of EMILIN1 directly involved in the interaction with CD49d (kindly provided by R. Doliana). We firstly defined the optimal dilution for the gC1q domain preparing a scalar dilution of the gC1q domain, from 10 µg/mL, to 0,1 µg/mL. For each dilution we performed three independent adhesion experiments using our cell line model, Mec-1 cell line (figure 11, line blue). The specificity of the interaction between gC1q domain and CD49d was verified performing in parallel adhesion assays utilizing the same concentration dilutions of a mutated ligand called gC1q-like domain mutant (gC1q mutant) (figure 11, line red). The gC1q mutant is devoid of Leu932–Gly945 segment, that contain the Glu933 responsible for integrin interaction. Results suggested that all the concentration dilutions of gC1q domain induced Mec-1 cell adhesion, and the adhesion was significantly reduced on the gC1q mutant ( $p=0.0001$ ), whereas no significant differences were found between concentrations ( $p=0.986$ ). Therefore, we decided to use also for gC1q domain the concentration of 10 µg/mL, as well as the other ligands of CD49d (VCAM-1 and CS-1 fragment).

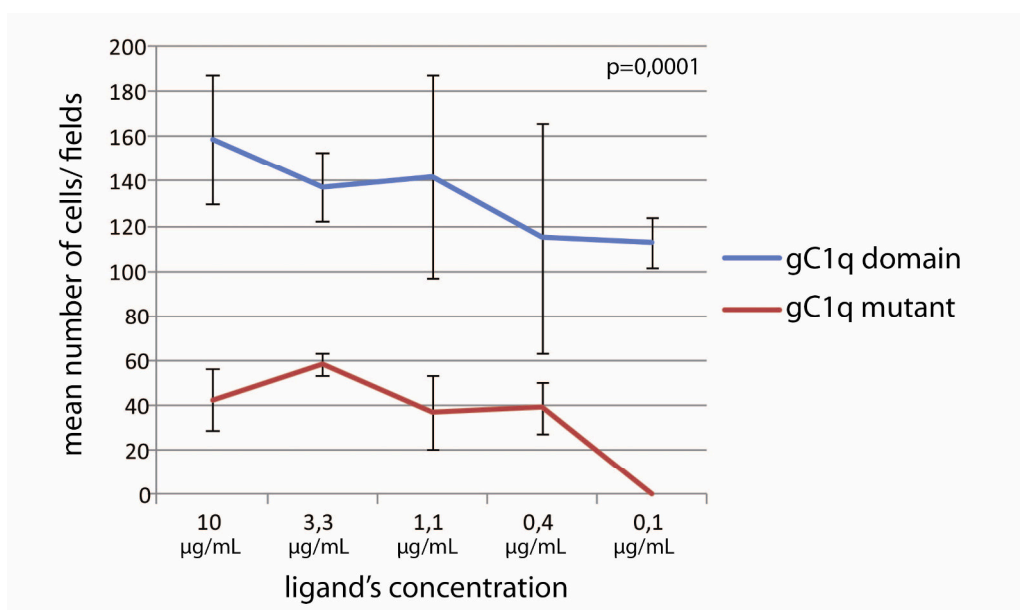


**Figure 11: Adhesion assays using scalar dilution of gC1q domain (blue line) and gC1q mutant (red line) concentration. In the graph are reported for each dilution the cell count mean per fields  $\pm$  standard deviation (sd) of independent experiments run in triplicate. Differences between gC1q domain and its mutant were analysed by paired T test (0,0001) and differences between concentration by one-way Anova (no significant).**

### 2.3.2. EMILIN1 promotes Mec-1 adhesion

Two different methods were employed to evaluate the Mec-1 cell adhesion onto substrate. The first adhesion assay applied to study whether EMILIN1 promotes Mec-1 adhesion consisted on counting the adherent cells, post washing, after 15 minutes of adhesion on substrates. The adhesion assay was performed in triplicate, using the gC1q mutant as negative adhesion control and the CS-1 fragment of fibronectin (FN) and VCAM-1 as positive controls. As described in material and methods, the ligand coating was made only in the center of the glass coverslips, to have in the same coverslip a negative adhesion control on BSA. After cell adhesion, the cells were fixed, labeled and manually counted (at least 8 fields per slide). Adherent cells were counted both on ligand and on BSA, and the latter was subtracted to the first one as constitutive adhesion. Results, expressed as number of adherent cells, demonstrated adhesion levels of Mec-1 cells on gC1q-like domain completely overlapping to those obtained on CS-1 fragment and on VCAM-1 ( $p > 0.05$  for both ligands), the two main ligands of CD49d ( $161 \pm 69$ ,  $159 \pm 127$  and  $135 \pm 43$ , respectively; figure 12). Instead the number of adherent cells per field on gC1q mutant ( $61 \pm 32$ ) indicated a significant ( $p = 0.0056$ ) decrease of the adhesion levels (figure 12, orange histogram).

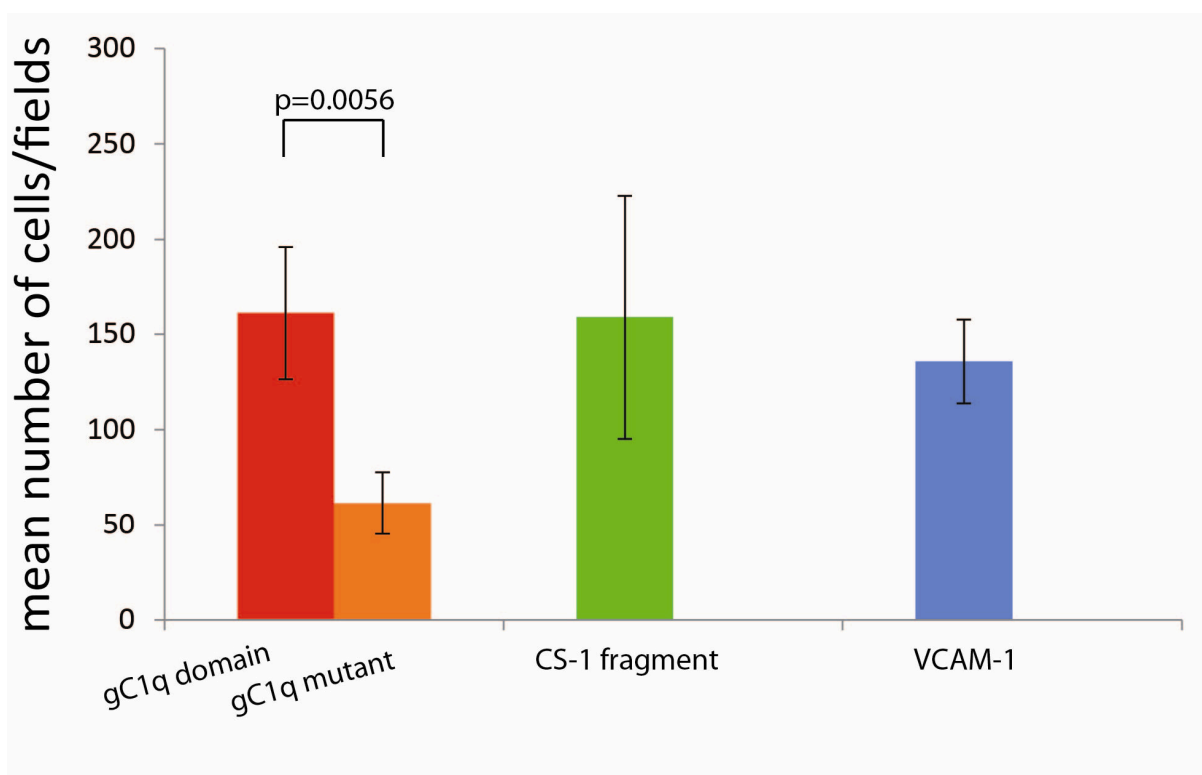
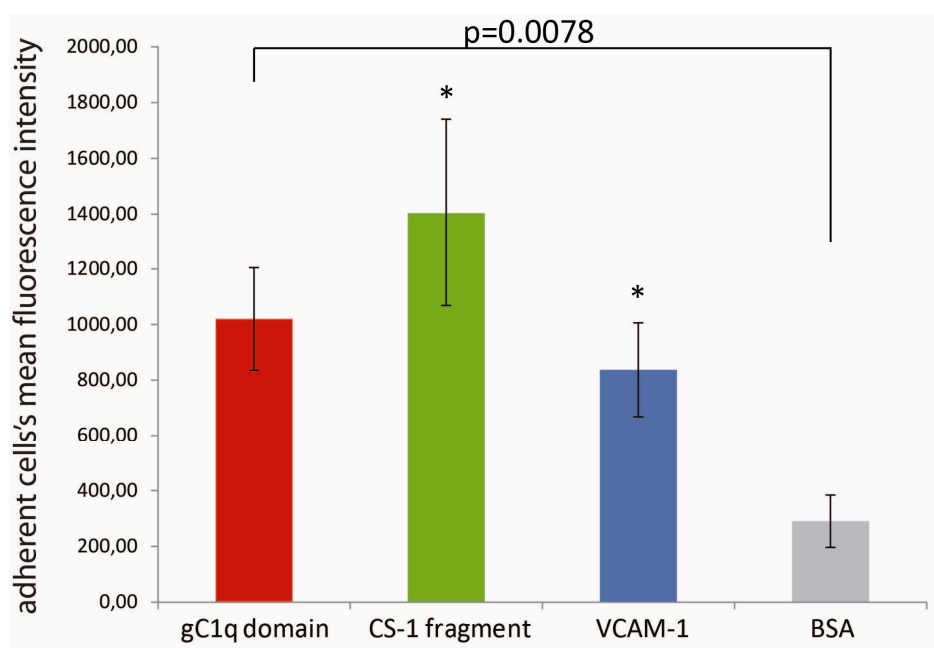


Figure 12: Mec-1 cell adhesion on CD49d's ligands. The histograms represented the mean count of adherent cells per fields minus the mean count of aspecific adherent cells on BSA  $\pm$  s.e.m. (showed by black error bars). The comparison between the adhesion levels on gC1q domain and on its mutant is significant by Mann-Whitney test (independent samples) ( $p = 0.0056$ ).

The second assay applied to study whether EMILIN1 promotes Mec-1 adhesion consisted on labelling Mec-1 cells with the vital fluorochrome calcein AM. The cells were seeded on 96-well coated plates (with gC1q domain, CS-1 fragment and VCAM-1) and incubated for 15 minutes at 37°C in RPMI. The non adherent cells were washed using  $\text{Ca}^{2+}/\text{Mg}^{2+}$  buffer and the fluorescence of adherent cells were detected in a computer-interfaced microplate fluorometer (TECAN). The experiment was run in triplicate. The mean fluorescence quantification of adherent cells on gC1q domain, on CS-1 fragment, on VCAM-1 and on BSA were respectively,  $1020 \pm 370$ ;  $1404 \pm 672$ ;  $836 \pm 338$ ;  $290 \pm 187$  (figure 13). These data indicated a significantly higher adhesion on gC1q domain respect to the BSA control ( $p=0.0078$ ), not dissimilar to those obtained for VCAM-1 and CS-1 fragment respect to the BSA control ( $p=0.0033$  and  $p=0.0109$ , respectively).



**Figure 13:** Calcein labelled-Mec-1 cells adhesion on gC1q domain, CS-1 fragment, VCAM-1 and BSA. Results of fluorescence detection were expressed as mean fluorescence intensity  $\pm$  s.e.m (showed by black error bars) of four independent experiments run in triplicate. Data were compared using Mann-Whitney test.

\*  $p<0.05$  in comparison to BSA

Consistently, cell morphology of Mec-1 cells after adhesion on substrates, changed respect to cell morphology of Mec-1 cells in suspension, suggesting an adhesion pattern. Specifically, in phase contrast microscopy images the adherent cells displayed a pattern of filopodia-like protrusions in which each cell presented several cellular projections and most of them seemed spread on the substrate (figure 14).

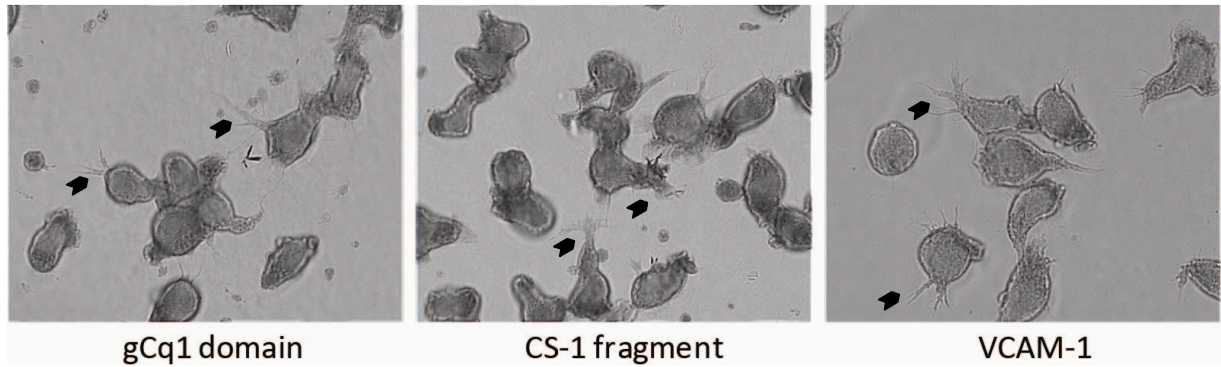


**Figure 14:** Representative phase-contrast microscopy images of adherent Mec-1 cells on gC1q domain, CS-1 fragment and VCAM-1. Black arrows indicate the filopodia-like protrusions. Original magnification 100x.

### 2.3.3. EMILIN1 promotes CLL cell adhesion

Having demonstrated the capacity of Mec-1 cell line model to adhere on EMILIN1, we proceeded with primary CLL cells *in vitro*. The adhesion experiments were performed on EMILIN1 together with CS-1 fragment and VCAM-1 using purified CLL cells from 12 cases characterized by high and homogeneous CD49d expression, evaluated by cytofluorimetric analysis on the pathological pure population identified as CD5+ and CD19+ (data not shown).

The adhesion assays were performed as previously described for Mec-1 cell adhesion experiments, where the ligand coating was in the center of the slide with all around the BSA coating. After cell adhesion and fix, at least 8 fields per slide were acquired with the microscope. Adherent cells were counted both on ligand and on BSA, and the latter was subtracted to the first one. Results demonstrated that also primary CLL cells are able to adhere on EMILIN1 and the levels of adhesion were similar to those obtained on CS-1 fragment and on VCAM-1. The mean values of adherent cells minus the non-adherent cells on BSA were  $346 \pm 127$ ,  $318 \pm 97$  and  $309 \pm 87$ , respectively on gC1q domain, CS-1 fragment and VCAM-1 (figure 15).

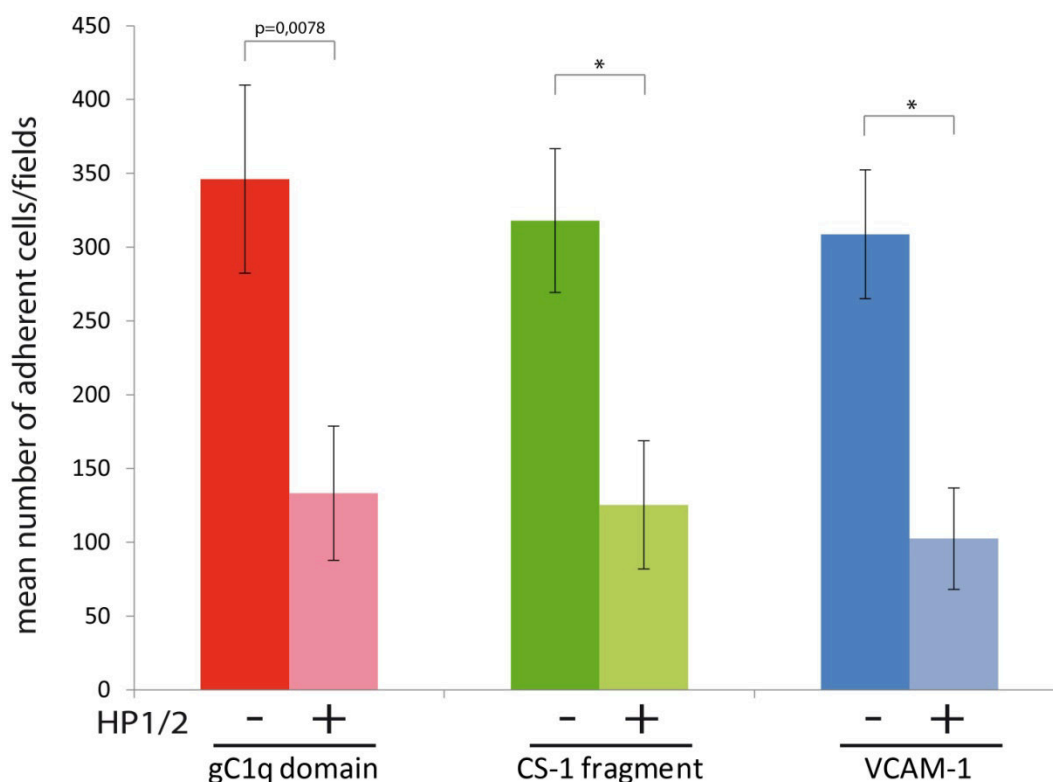


Figure 15: Adhesion experiments using 12 CLL cases on gC1q domain, CS-1 fragment and on VCAM-1. The histograms in dark color indicate the adhesion on ligands, while those in light color indicate the treatment with the blocking anti-CD49d mAb HP2/1. The histograms report the mean number of adherent cell for field minus the mean number of aspecific adherent cells on BSA  $\pm$  s.e.m. (showed by black error bars). The p-value was calculated with Wilcoxon test (paired samples).

\* p-value are significant, in accordance with the literature ( $p < 0.05$ )

The adhesion specificity was verified through CLL cell pre-incubation with the function-blocking anti-CD49d monoclonal antibody HP2/1. The mean count on ligands minus the count on BSA were  $133 \pm 91$ ,  $125 \pm 87$  and  $102 \pm 69$ , on gC1q domain, on CS-1 fragment and on VCAM-1, respectively.

The adhesion levels on gC1q domain were significantly reduced ( $p=0.0078$ ), as well as on CS-1 fragment and VCAM-1 ( $p=0.01$  and  $p=0.0078$ , respectively), indicating the involvement of CD49d in the interaction with EMILIN1 (figure 15, light color histograms). Altogether these results confirmed that the adhesion between CD49d-expressing cells and EMILIN1 is due to a specific interaction, as previously demonstrated for fibronectin and VCAM-1.<sup>41</sup>

Evidence that CLL cells adhered on the substrates derived from the observation of the cell morphology after labeling with phalloidin. In fact, normally circulating CLL cells present a round shape and when they get in contact with the microenvironment they could change their shape, as described in the article of Zucchetto et al.<sup>41</sup> Here we observed a similar behavior of CLL cells adhering on EMILIN1, that presented a more complex pattern of actin-rich structures mainly clustering at the adhesion site (figure 16).

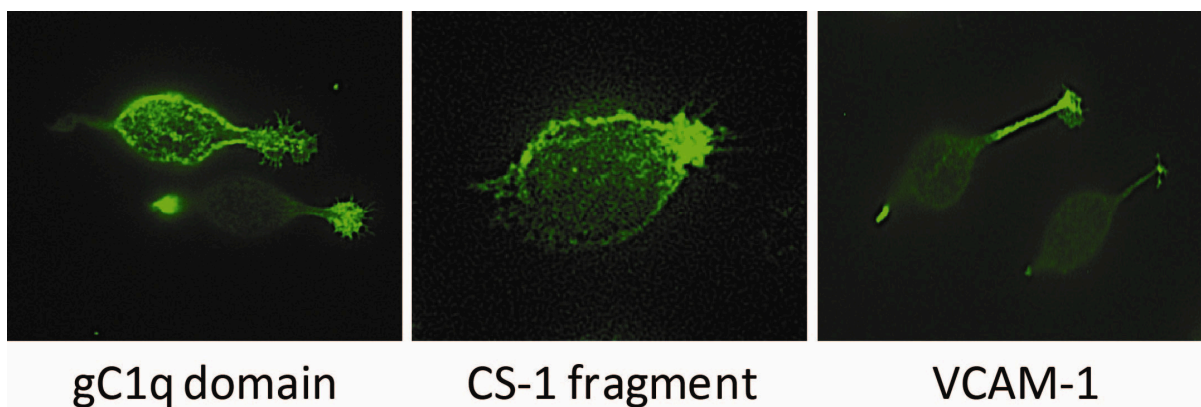


Figure 16: Representative images of CLL cells on CD49d's ligands. F-actin labelled with fluorescein phalloidin highlights the adhesion pattern (green). Original magnification 100x.

#### 2.4. EMILIN1 mediates survival signals

Once demonstrated that the CLL cells adhere on EMILIN1 we next studied the effect of the interaction between EMILIN1 and CD49d.

In the laboratory where I performed the thesis it was demonstrated that the interaction between CLL cells expressing CD49d and VCAM-1 or fibronectin, induces survival and inhibits apoptosis mechanism in CLL cells.<sup>41</sup> Instead in a skin homeostasis context, EMILIN1/CD49d interaction inhibits dermal fibroblast and keratinocyte proliferation.<sup>89</sup>

Given these premises, it was interesting to explore the role of EMILIN1 in CLL, and for this reason we focused the experiments mainly on the expression of two proteins AKT and ERK1/2, that are key mediators of survival signals, evaluating their phosphorylation levels. Their phosphorylation levels were evaluated first by western blot analysis, and then by immunofluorescence analysis.

As shown in figure 17, 14 purified CLL cases were analysed by western blot analysis. The results were expressed as the mean intensity of the ratio between phosphorylate signal and total signal and compared to the control, the signal on polylysine, as summerized by the histograms in figure 17. As reported, adhesion on gC1q domain showed an activation of pAKT and pERK after CD49d engagement in CLL cells, as well as on VCAM-1 and CS-1 fragment, suggesting the activation of survival pathways.

For each CLL case, we also evaluated the phosphorylation of VAV1, which is a protein involved in the integrin pathway, as further evidence of the occurred interaction between CD49d and EMILIN1. Results showed, also in this case, a significant increase in VAV1 phosphorylation after the adhesion on substrates respect to polylysine control (figure 17).

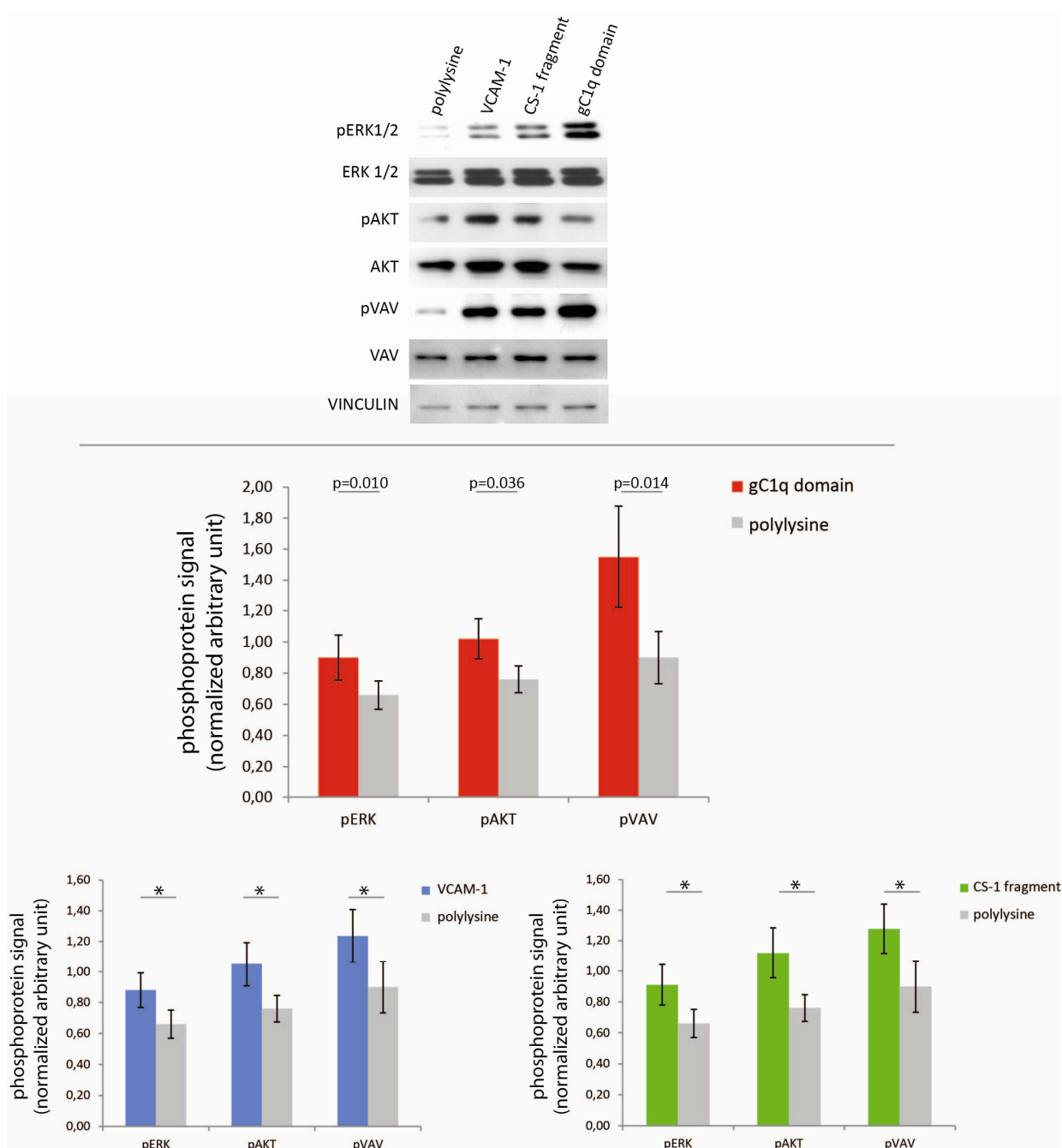


**Figure 17: Representative western blot image of a CLL case and histograms summarizing the results of all patients. At the top of the figure western blot images show the phosphorylated proteins with their equivalent total protein; vinculin was used as loading control.**

The histogram graph with red histograms represent the value on gC1q domain, with blue histograms on VCAM-1 and with green histograms on CS-1 fragment. A histogram represents the mean fold increase of the ratio between phosphoprotein and total protein compared to the polylysine. The p-value upon each histogram were calculated with paired T-test and black error bars indicate the s.e.m.

\* p-value are significant (p<0.05)

Another proof that EMILIN1 is able to activate the survival pathway derived from immunofluorescence analysis on 9 CLL cases.

As first proof of activation due to CD49d engagement from different substrates was the phosphorylation's signal better rendered on ligands than on polylysine as shown in figure 18.

Moreover, results showed the pAKT, pERK and pVAV mean fluorescence intensity, after the CD49d engagement on substrates, that was higher than the control on polylysine.

Altogether these results suggested that EMILIN1 activates the survival pathway and the integrin pathway in CLL cells, as well as VCAM-1 and fibronectin.

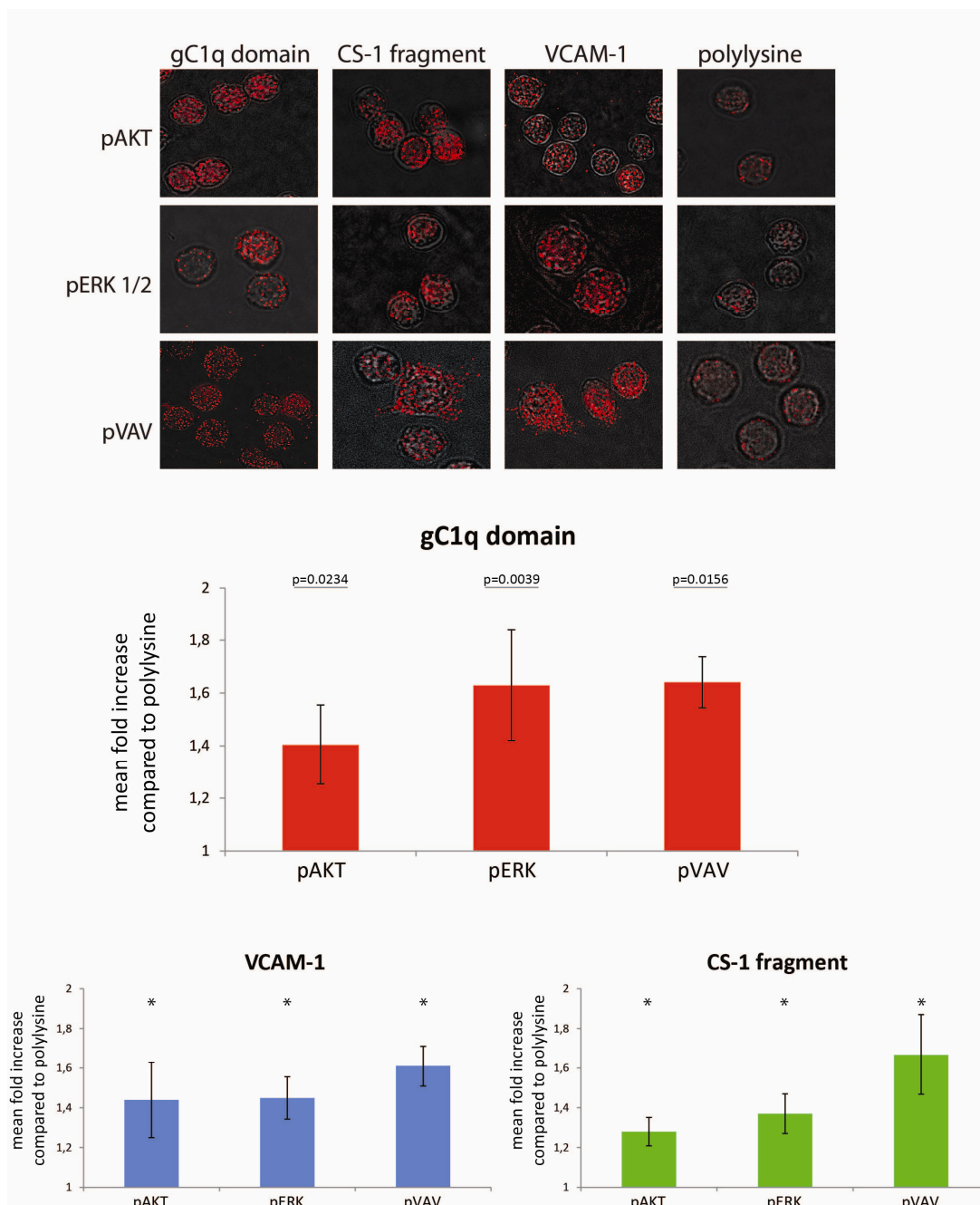


**Figure 18: Representative immunofluorescence images and histogram graphs of the mean intensity quantification for each CD49d's ligand.**

At the top of the figure an immunofluorescence image for each phosphoprotein on each CD49d's ligand is reported.

The histograms below represent the mean ratio of the mean fluorescence intensity for each protein compared to polylysine. In red are the histograms for gC1q domain, in blue for VCAM-1 and in green for CS-1 fragment. The statistical significance of the fluorescence intensity ratio between ligand and polylysine (fixed ratio of 1) was tested by Wilcoxon test (paired sample).

\* p-value are significant (p<0.05)

## 2.5. EMILIN1 protects CLL cells from spontaneous apoptosis

The simple observation that CLL cells progressively accumulate *in vivo*, but more or less rapidly undergo apoptosis when cultured *in vitro*, draws attention to the microenvironment and its ability to deliver signals that may ensure the survival of malignant cells.<sup>110</sup> In fact in the article where I gave a contribution, it was demonstrated that the engagement of CD49d by VCAM-1 was able to delay the spontaneous apoptosis observed in cultured CLL cells.<sup>41</sup>

Since EMILIN1 was shown to induce the survival pathway in CLL cell expressing CD49d, the next step was to evaluate whether it has a capacity to protect CLL cell from spontaneous apoptosis *in vitro* using purified CLL cells from 13 cases.

Results showed that gC1q domain of EMILIN1 was able to rescue CLL cells from spontaneous apoptosis, as well as VCAM-1 ( $p=0.002$  and  $p=0.009$ , respectively) and also with a significantly higher viability on EMILIN1 than on VCAM-1 ( $p=0.004$ ) (figure 19).

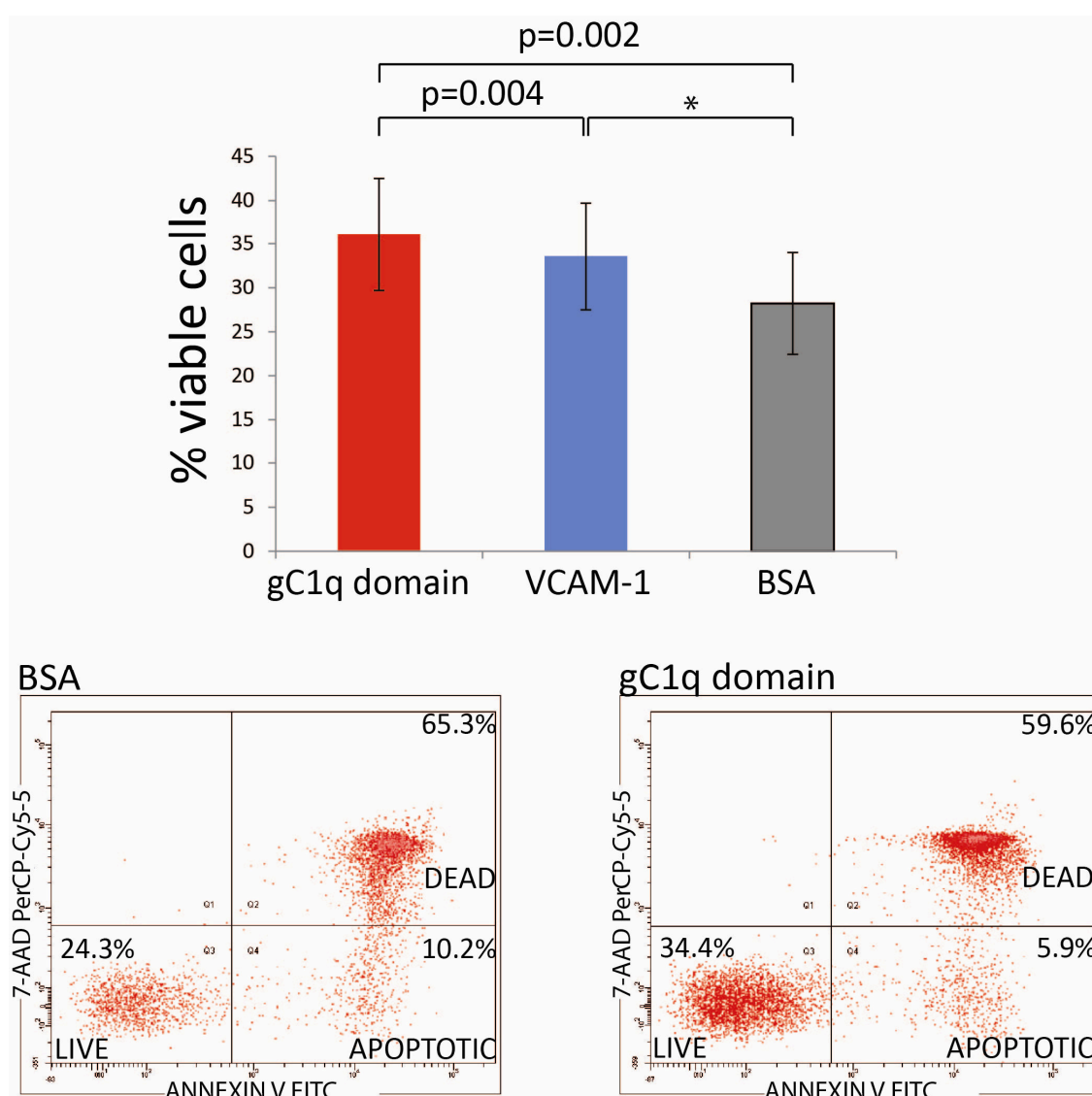


**Figure 19: Apoptosis assay.** In the histogram graph at the top of the figure is reported the percentage of viable CLL cells after five day in culture on gC1q domain, on VCAM-1 and on BSA. The two plots in the middle of the figure show the cytofluorimetric analysis of two representative CLL cases. The p-values were calculated by Wilcoxon test (paired sample) and asterisk (\*) indicates a significant difference ( $p<0.05$ ).

## 2.6. Mice wild type or knock-out for EMILIN1: work ongoing

Since we demonstrated that EMILIN1: a) is a ligand for CD49d in CLL, b) induces the activation of survival pathways, c) protects CLL cells from spontaneous apoptosis *in vitro*, we decided to explore the role of EMILIN1 *in vivo*. To fulfill this aim we planned to use mice wild type (EMILIN1<sup>+/+</sup>) and knock out (EMILIN1<sup>-/-</sup>) and CLL leukemic cells from TCL1 mice with the same genetic background of wild type or knock-out mice.

The immunophenotype of murine leukemic cells is reported in figure 20: essential for the project was the CD49d expression by the leukemic population identified by B220 and CD5 expression.

The basic phenotype of EMILIN1<sup>+/+</sup> and EMILIN1<sup>-/-</sup> mice is reported in figure 21 (panel a and b): T cells and B cells are distinguished by the expression of CD5 and CD19 respectively; indeed B cells express, more light chain kappa than lambda, as expected.<sup>111</sup>

To date we have treated 6 mice EMILIN1<sup>+/+</sup> and 6 mice EMILIN1<sup>-/-</sup> with six different cases of murine CLL leukemia expressing CD49d. Mice were monitored for the development of CLL every month, checking lymph nodes and spleen enlargement and taking blood sample to perform an immunophenotype. The immunophenotype consisted in evaluating the expression of CD19, CD5 and light chain kappa.

After five months from injection, mice have not develop leukemia, as reported in figure 21 (panel c and d); the immunophenotype did not differ from the ones of not inoculated mice, not presenting onset of CD5 positive B cells and changes in the percentage of kappa positive cells.

This delay in leukemia development was not unexpected because, TCL1 mice, from which derived the injected leukemic cells, develop delayed disease.

### TCL1 leukemic cells

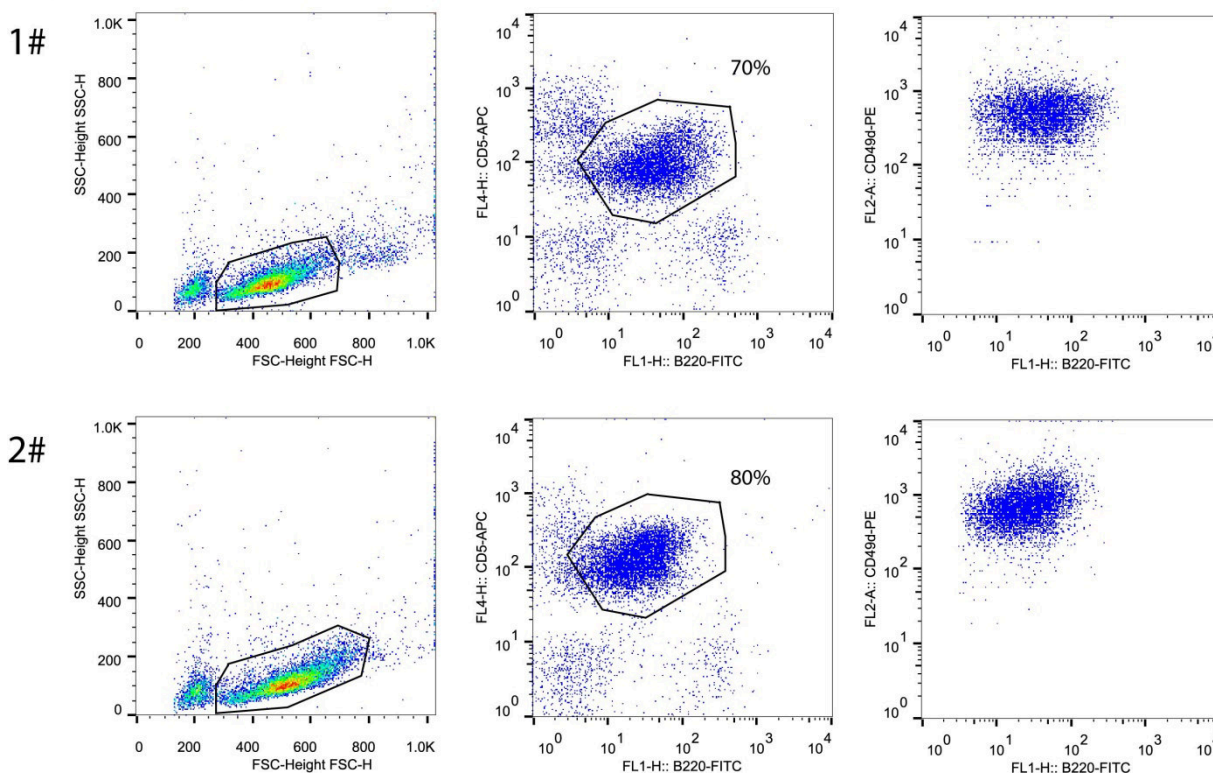
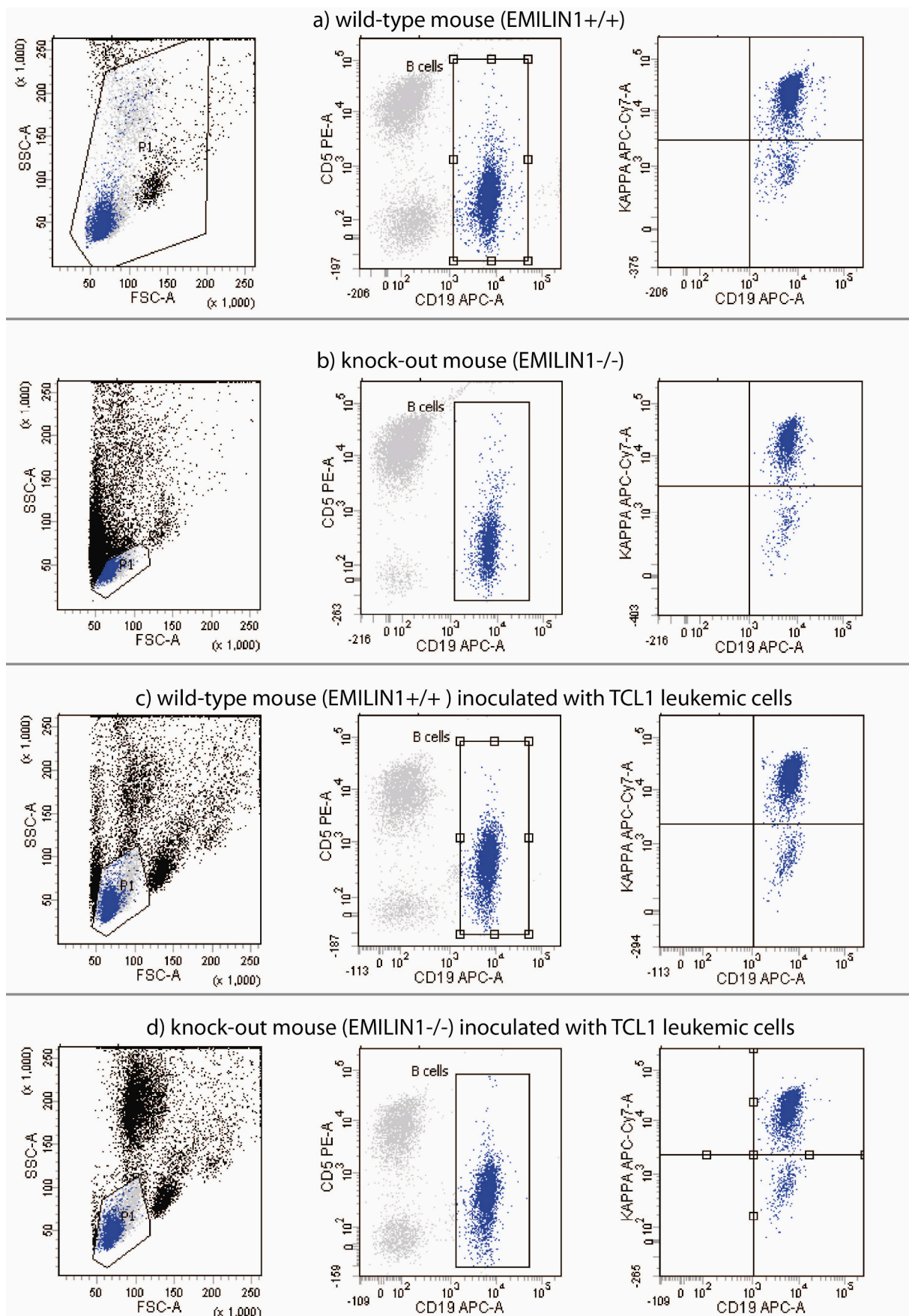


**Figure 20: Representative immunophenotype of CLL cells from two TCL1 mice (1# and 2#). Both for 1# and for 2# the plot on the left represent the physical parameter of the entire lymphocyte population. In the central plot is identified the leukemic population by the expression of B220 and CD5 and this population also expresses CD49d (plot on the right). Samples run in FACScalibur and analysed by FlowJo software.**



---

## 3. Discussion

Chronic lymphocytic leukemia (CLL) is a heterogeneous disease whose clinical course and outcome vary among CLL patients. The clinical staging systems are complemented by prognostic markers and among them stands out the CD49d, the alpha4 subunit of the VLA-4 integrin ( $\alpha4\beta1$ ). High CD49d expression predicts reduced overall survival and time to first treatment in a subset of CLL patients. Its strong prognostic relevance can be explained by considering the specific roles of this molecule in the context of CLL microenvironment. In this regard CD49d is directly involved in the microenvironmental interaction through the engagement of its main ligands: VCAM-1, expressed on endothelial cells and bone marrow stromal cells, and the extracellular matrix molecule fibronectin, promoting CLL cell survival, proliferation and migration/infiltration.

Recently, the globular (g) C1q-like domain of Elastin Microfibril Interfacier1 (EMILIN1), an adhesive extracellular matrix (ECM) constituent, was described as a new ligand for CD49d<sup>65</sup>, and this interaction was mainly studied in the context of skin homeostasis and carcinogenesis and of blood pressure homeostasis. On the contrary, the role of CD49d/EMILIN1 interaction is still unknown in the context of CLL and thereby this thesis was aimed to investigate on it.

The starting observation of the present thesis was the intermingled distribution of EMILIN1 between CLL cells in CLL-involved tissues. In particular, EMILIN1 was expressed in these tissues with an extracellular pattern, as previously reported for several other tissues such as blood vessels, skin, heart, lung, kidney, and cornea where EMILIN1 forms a fibrillar network in the ECM.<sup>65</sup> Indeed EMILIN1 was observed closely adjacent to the surface of CLL cells, as described by Daga Gordini<sup>108;109</sup> suggesting that EMILIN1 interacts directly with cell membrane receptors.

Surprisingly, in CLL-lymph node cases an unexpected EMILIN1 positive staining was observed in the cytoplasm of some cells (figure 7 panel 1). Some of them were accessory cells or osteocyte, whereas other were CLL cells. This suggested the presence in the microenvironment of cells able to produce EMILIN1. In this context, an interesting point is that, the distribution in term of quantity of EMILIN1 was higher than that of fibronectin in CLL-lymph node (figure 9). Altogether these results suggest that EMILIN1 could act a relevant role in the cross-talk between CLL cells and the tissue microenvironment.

Moving from these preliminary observations and from the previously published observation in which the gC1q domain of EMILIN1 is recognized by CD49d<sup>65</sup>, the capacity to adhere on EMILIN1 of CD49d positive CLL cells was firstly investigated in the Mec-1 "CLL-like" cell line model, and then, the obtained results were verified using primary CLL samples.

In particular, the results presented in this thesis reveal that Mec-1 cell line can adhere on EMILIN1 and that this adhesion is specifically dependent from the gC1q domain. Decreased adhesion levels are shown in presence of the gC1q mutant (figure 12), in which there is a single mutation (E933A), directly responsible for the interaction.<sup>104</sup> Moreover, evidences were provided that in CLL cells the adhesion on EMILIN1 is CD49d-dependent given that the interaction is impaired by the anti-CD49d monoclonal antibody HP2/1 (figure 15) and that the adhesion on EMILIN1 does not occur in CD49d negative CLL cells (data not shown). In particular, results revealed that the interaction between CD49d and EMILIN1 induces the activation of the integrin pathway with adhered CLL cells changing from a round to a more stretched shape (figure 16), evidenced by high level of phosphorylation of VAV, a molecule involved in cytoskeletal remodelling (figure 17-18). Finally, further evidences

indicated that adhesion levels on EMILIN1 are similar to those on VCAM-1 and fibronectin, as well as the increment of VAV phosphorylation, as previously reported by Zucchetto et al.<sup>41</sup>

The effects of CD49d/EMILIN1 interaction were studied *in vitro*, taking into account a recent article of Danussi et al, in which EMILIN1 operates as a negative modulator of proliferation signals in substrate-adherent non-hematopoietic CD49d positive cells.<sup>89</sup> To this purpose, pAKT and pERK, key mediators of survival signal, were evaluated after the CD49d/EMILIN1 interaction by western blot and immunofluorescence analyses. After short term adhesion experiments an increased phosphorylation level of pAKT and pERK was observed (figure 17-18). These results were discordant with the previous studies in dermal fibroblast and keratinocyte<sup>89</sup>, but were in concordance with the previous studies on CD49d positive CLL cells engaged by VCAM-1 and fibronectin.<sup>57</sup>

CLL cells typically undergo apoptosis when cultured *in vitro*, and this can be prevented by co-culture with different accessory cells that are part of the CLL microenvironment<sup>51</sup> or with CD49d ligands, VCAM-1 or fibronectin, as previously reported.<sup>41</sup> Since EMILIN1 was present in the lymphoid microenvironment, as observed in the germinal centre of CLL-involved lymph node (figure 7 panel 3), it was evaluated whether also CD49d positive CLL cells were rescued from spontaneous apoptosis by EMILIN1. Results showed that EMILIN1 protects CLL cells from spontaneous apoptosis, even in a higher fashion than VCAM-1 (figure 19).

Further details on the effects of the interaction between CD49d and EMILIN1 could be obtained by *in vivo* experiments. In this context, it was previously demonstrated that VCAM-1 and fibronectin knock-out mice give embryonic lethality<sup>112</sup> while EMILIN1 deficiency is compatible with murine life.<sup>95</sup> Therefore *in vivo* experiments are currently running, in which engraftment of CD49d positive CLL cells from TCL1 mice is evaluated in wild-type (EMILIN1<sup>+/+</sup>) and knock-out (EMILIN1<sup>-/-</sup>) for EMILIN1 recipients after intraperitoneal injection. Expected results will include an early development of leukemia in EMILIN1<sup>+/+</sup> mice and a minor infiltration and homing of CLL cells in EMILIN1<sup>-/-</sup> mice.

In conclusion, the present thesis describes the role of EMILIN1 as a new ligand for CD49d integrin in CLL. In particular, for the first time we showed that EMILIN1 is present in normal and CLL-involved tissues, and it is able to efficiently bind to CD49d, as expressed by CLL cells. At variance with what demonstrated in non-hematopoietic models, EMILIN1 was able to deliver anti-apoptotic/pro-survival signals to circulating CLL cells. Thus, the CD49d/EMILIN1 interactions showed a role in the maintenance of the neoplastic clone in CD49d-expressing CLL, as well as CD49d/VCAM-1 and CD49d/fibronectin interactions, previously defined as the two main ligands for CD49d<sup>41,57</sup> (figure 22).

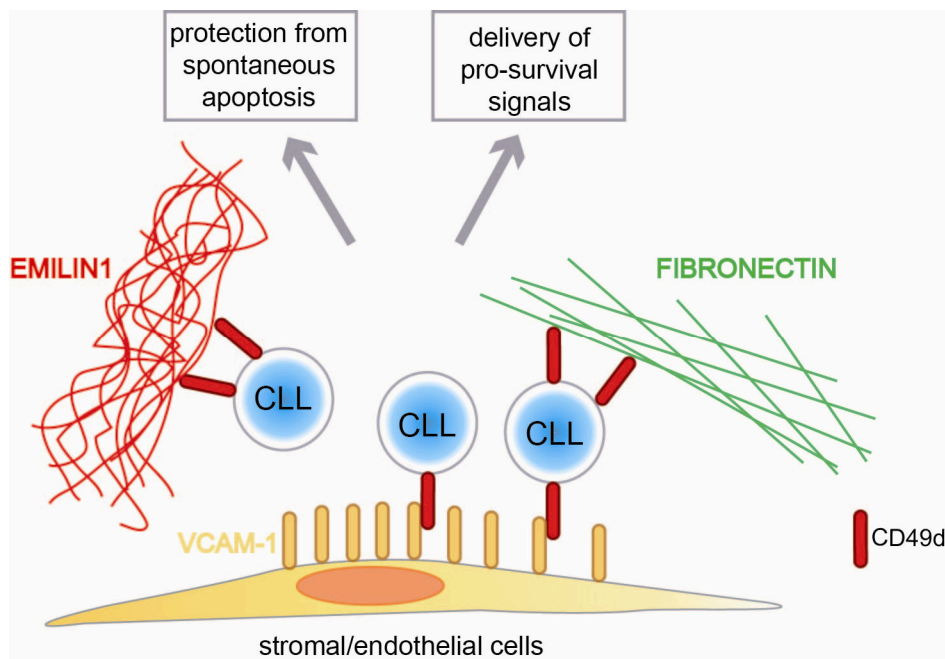


Figure 22: Schematic representation of CD49d positive CLL cells interacting with the main ligands of CD49d and the main signals delivered after the CD49d engagement.

Altogether considered, results from the present thesis and previously published data<sup>41;68</sup> provide further relevance to therapy based on impairing the CLL cells/microenvironment interactions via CD49d, such as immunotherapy with Natalizumab, a monoclonal humanized anti-CD49d antibody currently employed in autoimmune diseases such as multiple sclerosis and Crohn's disease.<sup>49</sup> In this context, it is noteworthy that CD49d blocking therapy also causes CD34+ progenitor cell mobilization from the bone marrow (BM)<sup>113</sup> and this is generally associated with functional inactivation or down-regulation of CD49d interactions within the BM niches, in particular with VCAM-1 as reported.<sup>114;115</sup> Therefore, CD49d blocking therapy could be highly effective in releasing CD49d positive CLL from the BM and in preventing their re-entry into the BM<sup>116</sup>, eventually making CLL cells more susceptible to chemotherapeutic agents.

---

## 4. Materials and Methods

#### 4.1. CLL patients and cell lines

The CLL-derived cell line Mec-1 (Mec-1) were used as a model for chronic lymphocytic leukemia<sup>105</sup> and were cultured in Roswell Park Memorial Institute medium (RPMI) with 10% of fetal bovine serum (FBS).

The study includes peripheral blood (PB) samples from chronic lymphocytic leukemia cases whose diagnosis was made according to IWCLL-NCI criteria<sup>38</sup>, collected after informed consent for routine diagnostic and follow-up procedures. All cases were characterized for CD49d, CD38 and ZAP-70 expression, IGHV mutational status, and fluorescence *in situ* hybridization (FISH) karyotype.<sup>117</sup> The list of all CLL cases employed for the experiments is reported in Table 1.

Functional and biochemical experiments (see below) were carried out on CLL cases with a high and homogeneous CD49d expression. In these cases, CLL cells were purified from the peripheral blood by density gradient centrifugation on Ficoll-Hypaque (Pharmacia), followed in some cases by negative selection using a mixture of anti-CD3, anti-CD16 and anti-CD14 monoclonal antibodies (mAbs, Laboratory of Immunogenetics, Turin) and separation by immunomagnetic beads. In all cases B-cell purity was  $\geq 95\%$ , as assessed by flow cytometry.

#### 4.2. Antibodies and other reagents

Mouse anti-human gC1q (clone 1H2) antibodies were produced in the laboratory of Prof. Colombatti as previously described.<sup>65,96</sup> Rabbit anti-phospho-p44/42 MAPK (ERK 1/2; Thr202/Tyr204) and anti-phospho-AKT (Thr308 and Ser 473) antibodies were obtained from Cell Signaling Technology. Rabbit anti-phospho-VAV1 (Tyr-174) was purchased from Abcam. Goat anti-AKT and anti-vinculin, rabbit anti-ERK1/2 and mouse anti-Vav-1 antibodies were obtained from Santa Cruz Biotechnology, Inc. HRP-donkey anti-rabbit and HRP-sheep anti-mouse IgG antibodies were used from Amersham GE Healthcare. HRP-rabbit anti-goat IgG were obtained from Invitrogen.

Anti-CD49d (clone HP2/1, Serotec) blocking monoclonal antibody was used.

The C-terminal domain of EMILIN1 (gC1q domain), the recombinant mutant of the integrin-binding sequence of gC1q (gC1q mutant) and the CS-1 fragment of fibronectin were produced as previously described<sup>65,104</sup> and were provided by R. Doliana and A. Capuano (Centro di Riferimento Oncologico, CRO). The human recombinant VCAM-1 was from R&D Systems.

#### 4.3. Cytofluorimetric analysis

The diagnosis of CLL cases was made according to IWCLL-NCI criteria<sup>38</sup>, that included the expression of CD19, CD5, CD23 and low expression levels of clonally restricted surface immunoglobulins (Igs).<sup>118</sup> CD49d and alpha 9 expression were evaluated using a combination of anti-CD5- fluorescein isothiocyanate (FITC), anti-CD19- peridinin chlorophyll protein cyanin 5.5 (PerCP-Cy5.5) and anti-CD49d- phycoerythrin (PE) (BD Bioscience) or anti alpha9-PE (BioLegend) mAbs. For the purposes of the present study, a CLL sample was judged to express CD49d (CD49d<sup>+</sup>) when the molecule was found in at least 30% of the CD5<sup>+</sup>/CD19<sup>+</sup> CLL cell population as previously described.<sup>43,119</sup> Data were acquired on a FACSCanto flow cytometer and analysed by Diva software (BD Bioscience) or FlowJo software (Miltenyi Biotec).

#### 4.4. Immunohistochemical analysis

Reactive lymphoid tissues and CLL-involved lymph nodes and bone marrow biopsies (BMB) sections were stained for EMILIN1.

Staining was performed on 4 µm formalin-fixed paraffin-embedded tissue sections. Deparaffinization was obtained by a 20 minutes wash in xylene and hydration by sequential washes in 100% (10 minutes), 85%, and 70% ethanol solutions (5 minutes), distilled water (5 minutes) and twice in PBS (5 minutes each). Sections were bathed in ER2 solution (pH 8, Leica Biosystems) at 90°C for 30 minutes for antigen retrieval and then cooled 15 minutes at room temperature and 15 minutes in water. Next, the slides were rinsed with distilled water for two minutes, and then with PBS. Antibody incubation was preceded by 20 minutes protein block (DAKO). Slides were then incubated with EMILIN1 primary antibody (AS556, 1:50; antiserum rabbit polyclonal antibody was a kind gift of Prof. Colombatti's group) in dilution solution (Leica Biosystems) for 1 hour at room temperature in a humid chamber. DAB staining was obtained by Novolink Polymer Detection System (Leica Biosystems) according to manufacturer's instructions.

#### 4.5. Preparation of C1q like domain, VCAM-1- or FN-coated culture dishes/coverslips

The coating was performed at 4°C overnight either onto ethanol-washed coverslips (6mm Ø, Menzel-Glaeser or 12mm Ø, Knittel Galss ) or µ-dishes (35mm high, IBIDI) using gC1q domain of EMILIN1, CS-1 fragment of fibronectin (FN), VCAM-1 (final concentration 10 µg/ml ) or polylysine (final concentration 10 µg/ml) in bicarbonate buffer. Subsequently, the ligand in excess was removed with two washes in phosphate-buffered saline (PBS) and the coverslips or dishes were saturated for two hours at room temperature with 1% bovine serum albumin (BSA) in PBS. BSA was used as internal control of non-specific adhesion.

#### 4.6. Cell adhesion assays

Two different adhesion assays were performed: i) Mec-1 cells were labeled for 10 minutes at 37°C with the vital fluorochrome calcein AM (Molecular Probes, Eugene, OR, USA). The cells were then seeded ( $2 \times 10^5$  cells/well) onto 96-well plates coated with the appropriate substrate, and incubated for 15 minutes at 37°C. Adherent cells were evaluated by fluorescence detection in a computer-interfaced microplate GENios Plus microplate reader (Tecan Group Ltd.), after several washes with  $\text{Ca}^{2+}/\text{Mg}^{2+}$  buffer. Results were expressed as mean fluorescence intensity  $\pm$  standard error mean (s.e.m.); ii) MEC-1 cell lines ( $5 \times 10^5$  cells/well) and primary CLL cells ( $1 \times 10^6$  purified cells/well) were seeded onto coverslips coated with the appropriate substrate for 15' min at 37°C in RPMI. The non-adherent cells were washed away with  $\text{Ca}^{2+}/\text{Mg}^{2+}$  buffer, while adherent cells were fixed (4% paraformaldehyde), stained with May-Gruenwald/Giemsa and coverslips mounted on slides and microscopically analyzed using a 20x objective. In parallel the cells were preincubated 10 minutes at 37°C with the anti-CD49d HP1/2 blocking antibody (final concentration 30 µg/mL) to verify the specificity of the interaction between CD49d and its ligands. After acquiring at least 8 fields per slide, adherent cells were counted, and results reported as the mean number of adherent cells per field on each specific ligand minus the mean number of cells on BSA  $\pm$  standard error mean (s.e.m.).

#### 4.7. Immunofluorescence assay

Mec-1 ( $5 \times 10^5$  cells /well) or primary CLL cells ( $1 \times 10^6$  purified cells /well) resuspended in RPMI were plated onto coverslips coated with the appropriate substrate. Coverslips were placed in 24-well plates, centrifuged for 5 minutes at 100 RCF, and incubated for 5' at 37°C to promote cell adhesion. For Perk 1/2, pAKT and pVAV detection, adherent cells were fixed with 4% paraformaldehyde, permeabilized with 0.1% Tween-20/0.1% BSA/PBS buffer for 5 minutes, blocked 30 minutes with 10% FBS/PBS and incubated for 1 hour with pERK 1/2 (1:500), pAKT (1:200), pVAV (1:400) primary antibodies, followed by 45 minutes incubation with 1:150 TRITC-conjugated anti-rabbit secondary antibody in the dark at room temperature. All the antibodies dilution were made in 10% FBS/PBS. Coverslips were mounted on slides and the fluorescence intensity were analyzed through Nikon Eclipse 90i microscope and the ND2 software (Nikon). The ND2 software allowed to select manually the area of each cell and to detect the mean fluorescence intensity of each cell. For each coverslip data from at least 100 cells were recorded and results were reported as the phosphoprotein mean fluorescence intensity obtained from the ligands versus the mean fluorescence intensity obtained from polylysine used as control.

The images of CLL cells with F-actin filaments were obtained labeling the cells 40 minutes with 1:100 fluorescein-labeled Phalloidin (Sigma).

#### 4.8. Immunoblot analysis

Primary CLL cells ( $5 \times 10^6$  cells/dish) were allowed to adhere on  $\mu$ -dishes coated with gC1q domain (10  $\mu$ g/ml), CS-1 fragment (10  $\mu$ g/ml), VCAM-1 (10  $\mu$ g/ml) or polylysine (10  $\mu$ g/ml) for 5 minutes at 37°C in RPMI without serum. Non adherent cells were washed away and adherent cells were directly lysed in ice-cold RIPA buffer (Santa Cruz Biotechnology) containing protease inhibitor cocktail, PMSF, Sodium Orthovanadate and NaF for 30 minutes at 4°C. Cell lysates were centrifuged at  $10,000 \times g$  for 20 minutes at 4°C. The protein quantification of each sample was determined using Bradford protein assay reagent (Bio-Rad Laboratories). Fifteen  $\mu$ g of total protein were resuspended in sample buffer with 2-beta-mercaptoethanol, boiled for 5 minutes, resolved in 4-20% Criterion precast gels (Bio-Rad Laboratories), and transferred onto Hybond-ECL nitrocellulose membranes (Amersham, GE Healthcare). Membranes were blocked for 1 hour at room temperature with 5% dry milk in TBS-T (Tris Buffer Saline-0.1% Tween) and probed overnight at 4°C with the appropriate antibodies: p-p44/42 MAPK (ERK 1/2), pAKT, pVAV, AKT, ERK 1/2, VAV-1 and vinculin. The antibodies against the phosphorylated protein were diluted 1:1000 in 5%BSA/TBS-T, whereas the antibodies against the total protein were diluted 1:1000 in 5% dry milk/TBS-T. All the washes were made in TBS-T. The incubation with the secondary antibody (see Antibodies and other reagents) was performed for 1 hour at room temperature in 5% dry milk/TBS-T.

Immunoreactivity was revealed using Immobilon western chemiluminescent HRP substrate (Millipore Corporation). Densitometric quantification of western blots was determined with the Quantity One 4.1.0 software (Bio-Rad).

#### 4.9. Cell viability assays

Primary CLL cells ( $2 \times 10^5$  cells/well) were seeded on gC1q domain-, VCAM-1- and BSA-coated 96-well plates in RPMI with 0.1% FBS. Cell viability was evaluated after 5 days of culture, staining cells with AnnexinV (BD Bioscience) and 7-amino-actinomycin-D (7-AAD, BD Bioscience) in 1X Annexin buffer

(BD Bioscience) for 15 minutes in the dark at room temperature. The cells were then run in a FACSCanto flow cytometer and analyzed by the Diva software (BD Bioscience).

#### 4.10. Mice models

C57BL/6 WT and *Emilin1*<sup>-/-</sup> mice were kindly obtained from the laboratory of Prof. Colombatti. All the procedures involved in the animal experiments were performed according to approved protocols and in accordance to institutional guidelines in compliance with national laws (D.Lgs. n° 116/92).

#### 4.11. TCL1 leukemia cells

TCL1 leukemia cells from E $\mu$ -TCL1 transgenic mice on C57BL6 background were kindly provided by Dr. Efremov (ICGEB, Monterotondo). Overt leukemia was defined as at least 50% monoclonal CD5+ B cells in the peripheral blood and WBC above normal range ( $> 10.7 \times 10^6$ /mL). Mononuclear cells were separated from the spleens of leukemic mice by Ficoll gradient centrifugation (Amersham Biosciences) and not purified because they represented more than 90% of cells. The purity of the selected populations was evaluated by staining with anti-CD5 allophycocyanin (APC) – conjugated and anti-B220 FITC–conjugated antibodies, followed by flow cytometric analysis on a FACSCalibur flow cytometer (BD Biosciences). The TCL1 leukemias were also evaluated by flow cytometry for the expression of CD49d, using an anti-CD49d PE (BD Biosciences).

#### 4.12. Intraperitoneal injection of TCL1 leukemia cells in WT and *Emilin1*<sup>-/-</sup> mice

Before the intraperitoneal injection, TCL1 leukemia cells were cultured at 37°C for 1 hours in RPMI with 10% FBS, then washed in PBS and resuspended in 500  $\mu$ l of PBS. WT and *Emilin1*<sup>-/-</sup> mice were 5 weeks older and in one mouse  $50 \times 10^7$  cells were injected with an insulin syringe. Every month after the injection, a blood sample was taken from the orbital sinus using a fine Pasteur pipette.

#### 4.13. Statistical analysis

Data were compared using either the non-parametric Mann–Whitney test (independent samples) or Wilcoxon test (paired samples). All statistical analyses were performed using the MedCalc software (MedCalc) and a value of  $p < 0.05$  was considered significant.

Table 1: Clinical characteristics of CLL patients selected for biochemical and functional studies

Patient ID	sex	CD19	CD49d	CD38	IGHV	risultato	Studies
CCL#1	m	97.6	<b>93.6</b>	3.6	UM	del13	Adh/WB/Apo
CCL#2	m	96.8	<b>80.8</b>	49.1	UM	del11	Adh/WB/Apo
CCL#3	m	92.1	<b>99.9</b>	81.2	M	norm	Adh/WB/IF/Apo
CCL#4	m	92.8	<b>99.0</b>	99.3	na	tri12	Adh/WB/Apo
CCL#5	m	93.5	<b>100.0</b>	99.9	M	del13, tri12	Adh/WB/Apo
CCL#6	f	92.7	<b>83.2</b>	1.2	M	del13	WB
CCL#7	m	95.0	<b>99.7</b>	17.5	UM	del13	WB
CCL#8	m	92.5	<b>93.0</b>	27.0	na	tri12	WB
CCL#9	f	87.4	<b>98.8</b>	33.2	M	del13, tri12	WB
CCL#10	m	85.7	<b>94.8</b>	47.2	UM	tri12	WB
CCL#11	f	88.0	<b>98.0</b>	49.0	UM	norm	WB/Apo
CCL#12	m	88.3	<b>97.9</b>	61.4	UM	del13, del11	WB
CCL#13	m	94.4	<b>84.8</b>	79.1	na	del13	WB
CCL#14	f	90.7	<b>98.7</b>	93.4	M	tri12	WB/IF/Apo
CCL#15	f	96.0	<b>99.8</b>	98.0	UM	del13, del11	WB
CCL#16	m	89.9	<b>81.3</b>	2.3	M	norm	Adh
CCL#17	m	93.6	<b>94.9</b>	11.0	UM	tri12	Adh/Apo
CCL#18	m	88.1	<b>94.7</b>	28.7	M	del13 omo	Adh/Apo
CCL#19	f	89.0	<b>92.4</b>	31.4	UM	norm	Adh/Apo
CCL#20	f	93.0	<b>84.5</b>	82.6	UM	del17	Adh
CCL#21	f	93.7	<b>99.1</b>	86.8	UM	norm	Adh
CCL#22	m	95.0	<b>97.3</b>	95.9	UM	norm	Adh/Apo
CCL#23	m	88.0	<b>100.0</b>	3.3	M	norm	IF
CCL#24	m	97.6	<b>96.7</b>	4.6	UM	tri12	IF
CCL#25	m	86.5	<b>91.8</b>	41.8	UM	del13	IF
CCL#26	f	90.3	<b>81.5</b>	70.8	UM	norm	IF
CCL#27	f	94.5	<b>99.9</b>	75.8	M	del13	IF
CCL#28	f	92.9	<b>97.9</b>	89.4	UM	norm	IF
CCL#29	m	97.1	<b>99.7</b>	99.8	M	tri12	IF
CCL#30	f	82.6	<b>98.5</b>	98.5	UM	tri12, del11	Apo
CCL#31	f	85.7	<b>99.9</b>	4.0	M	tri12	Apo

m, male; f, female; M, mutated IGHV; UM, unmutated IGHV; Adh, adhesion assay; WB, western blot assay; IF, immunofluorescence assay; Apo, apoptosis assay; na, not available

# References

1. Johansson S, Svineng G, Wennerberg K, Armulik A, Lohikangas L. Fibronectin-integrin interactions. *Front Biosci.* 1997;2:d126-d146.
2. Caligaris-Cappio F, Hamblin TJ. B-cell chronic lymphocytic leukemia: a bird of a different feather. *J.Clin.Oncol.* 1999;17:399-408.
3. Chiorazzi N, Rai KR, Ferrarini M. Chronic Lymphocytic Leukemia. *N Engl J Med* 2005;352:804-815.
4. Davids MS, Burger JA. Cell Trafficking in Chronic Lymphocytic Leukemia. *Open.J.Hematol.* 2012;3:
5. Oscier DG. Cytogenetic and molecular abnormalities in chronic lymphocytic leukaemia. *Blood Rev.* 1994;8:88-97.
6. Molica S, Levato D, Cascavilla N, Levato L, Musto P. Clinico-prognostic implications of simultaneous increased serum levels of soluble CD23 and beta2-microglobulin in B-cell chronic lymphocytic leukemia. *Eur.J.Haematol.* 1999;62:117-122.
7. Shanafelt TD, Geyer SM, Kay NE. Prognosis at diagnosis: integrating molecular biologic insights into clinical practice for patients with CLL. *Blood* 2004;103:1202-1210.
8. Rai KR, Sawitsky A, Cronkite EP et al. Clinical staging of chronic lymphocytic leukemia. *Blood* 1975;46:219-234.
9. Binet JL, Auquier A, Dighiero G et al. A new prognostic classification of chronic lymphocytic leukemia derived from a multivariate survival analysis. *Cancer* 1981;48:198-206.
10. Hallek M. Chronic lymphocytic leukemia: 2013 update on diagnosis, risk stratification and treatment. *Am.J.Hematol.* 2013;88:803-816.
11. Wiestner A. Emerging role of kinase-targeted strategies in chronic lymphocytic leukemia. *Blood* 2012;120:4684-4691.
12. Matutes E, Catovsky D. The value of scoring systems for the diagnosis of biphenotypic leukemia and mature B-cell disorders. *Leuk.Lymphoma* 1994;13 Suppl 1:11-14.
13. Moreau EJ, Matutes E, A'Hern RP et al. Improvement of the chronic lymphocytic leukemia scoring system with the monoclonal antibody SN8 (CD79b). *Am J Clin Pathol* 1997;108:378-382.
14. Cramer P, Hallek M. Prognostic factors in chronic lymphocytic leukemia-what do we need to know? *Nat.Rev.Clin.Oncol.* 2011;8:38-47.
15. Weinberg JB, Volkheimer AD, Chen Y et al. Clinical and molecular predictors of disease severity and survival in chronic lymphocytic leukemia. *Am.J.Hematol.* 2007;82:1063-1070.

16. Dohner H, Stilgenbauer S, Benner A et al. Genomic aberrations and survival in chronic lymphocytic leukemia. *N.Engl.J.Med.* 2000;343:1910-1916.
17. Hamblin TJ, Davis Z, Gardiner A, Oscier DG, Stevenson FK. Unmutated Ig V(H) genes are associated with a more aggressive form of chronic lymphocytic leukemia. *Blood* 1999;94:1848-1854.
18. Crespo M, Bosch F, Villamor N et al. ZAP-70 expression as a surrogate for immunoglobulin-variable-region mutations in chronic lymphocytic leukemia. *N Engl J Med* 2003;348:1764-1775.
19. Dal Bo M, Rossi FM, Rossi D et al. 13q14 deletion size and number of deleted cells both influence prognosis in chronic lymphocytic leukemia. *Genes Chromosomes.Cancer* 2011;50:633-643.
20. Haferlach C, Dicker F, Schnittger S, Kern W, Haferlach T. Comprehensive genetic characterization of CLL: a study on 506 cases analysed with chromosome banding analysis, interphase FISH, IgV(H) status and immunophenotyping. *Leukemia* 2007;21:2442-2451.
21. Balatti V, Bottoni A, Palamarchuk A et al. NOTCH1 mutations in CLL associated with trisomy 12. *Blood* 2012;119:329-331.
22. Del Giudice I, Rossi D, Chiaretti S et al. NOTCH1 mutations in +12 chronic lymphocytic leukemia (CLL) confer an unfavorable prognosis, induce a distinctive transcriptional profiling and refine the intermediate prognosis of +12 CLL. *Haematologica* 2012;97:437-441.
23. Zucchetto A, Caldana C, Benedetti D et al. CD49d is overexpressed by trisomy 12 chronic lymphocytic leukemia cells: evidence for a methylation-dependent regulation mechanism. *Blood* 2013;122:3317-3321.
24. Schaffner C, Stilgenbauer S, Rappold GA, Dohner H, Lichter P. Somatic ATM mutations indicate a pathogenic role of ATM in B-cell chronic lymphocytic leukemia. *Blood* 1999;94:748-753.
25. Stankovic T, Weber P, Stewart G et al. Inactivation of ataxia telangiectasia mutated gene in B-cell chronic lymphocytic leukaemia. *Lancet* 1999;353:26-29.
26. el RS, Thomas A, Costin D et al. p53 gene mutation in B-cell chronic lymphocytic leukemia is associated with drug resistance and is independent of MDR1/MDR3 gene expression. *Blood* 1993;82:3452-3459.
27. Gaidano G, Ballerini P, Gong JZ et al. p53 mutations in human lymphoid malignancies: association with Burkitt lymphoma and chronic lymphocytic leukemia. *Proc.Natl.Acad.Sci.U.S.A* 1991;88:5413-5417.
28. Damle RN, Wasil T, Fais F et al. Ig V gene mutation status and CD38 expression as novel prognostic indicators in chronic lymphocytic leukemia. *Blood* 1999;94:1840-1847.
29. Chan AC, Iwashima M, Turck CW, Weiss A. ZAP-70: a 70 kd protein-tyrosine kinase that associates with the TCR zeta chain. *Cell* 1992;71:649-662.
30. Rassenti LZ, Jain S, Keating MJ et al. Relative value of ZAP-70, CD38, and immunoglobulin mutation status in predicting aggressive disease in chronic lymphocytic leukemia. *Blood* 2008;112:1923-1930.

31. Gobessi S, Laurenti L, Longo PG et al. ZAP-70 enhances B-cell-receptor signaling despite absent or inefficient tyrosine kinase activation in chronic lymphocytic leukemia and lymphoma B cells. *Blood* 2007;109:2032-2039.
32. Chen L, Huynh L, Apgar J et al. ZAP-70 enhances IgM signaling independent of its kinase activity in chronic lymphocytic leukemia. *Blood* 2008;111:2685-2692.
33. Calpe E, Codony C, Baptista MJ et al. ZAP-70 enhances migration of malignant B lymphocytes toward CCL21 by inducing CCR7 expression via IgM-ERK1/2 activation. *Blood* 2011;118:4401-4410.
34. Deaglio S, Aydin S, Vaisitti T, Bergui L, Malavasi F. CD38 at the junction between prognostic marker and therapeutic target. *Trends Mol Med* 2008;14:210-218.
35. Ferrero E, Malavasi F. Human CD38, a leukocyte receptor and ectoenzyme, is a member of a novel eukaryotic gene family of nicotinamide adenine dinucleotide+-converting enzymes: extensive structural homology with the genes for murine bone marrow stromal cell antigen 1 and aplysian ADP-ribosyl cyclase. *J Immunol* 1997;159:3858-3865.
36. Howard M, Grimaldi JC, Bazan JF et al. Formation and hydrolysis of cyclic ADP-ribose catalyzed by lymphocyte antigen CD38. *Science* 1993;262:1056-1059.
37. Deaglio S, Aydin S, Grand MM et al. CD38/CD31 interactions activate genetic pathways leading to proliferation and migration in chronic lymphocytic leukemia cells. *Mol.Med.* 2010;16:87-91.
38. Hallek M, Cheson BD, Catovsky D et al. Guidelines for the diagnosis and treatment of chronic lymphocytic leukemia: a report from the International Workshop on Chronic Lymphocytic Leukemia updating the National Cancer Institute-Working Group 1996 guidelines. *Blood* 2008;111:5446-5456.
39. Mauro FR, Foa R, Giannarelli D et al. Clinical characteristics and outcome of young chronic lymphocytic leukemia patients: a single institution study of 204 cases. *Blood* 1999;94:448-454.
40. Wang YH, Zou ZJ, Liu L et al. Quantification of ZAP-70 mRNA by real-time PCR is a prognostic factor in chronic lymphocytic leukemia. *J.Cancer Res.Clin.Oncol.* 2012;138:1011-1017.
41. Zucchetto A, Vaisitti T, Benedetti D et al. The CD49d/CD29 complex is physically and functionally associated with CD38 in B-cell chronic lymphocytic leukemia cells. *Leukemia* 2012;26:1301-1312.
42. Burger JA. Targeting the microenvironment in chronic lymphocytic leukemia is changing the therapeutic landscape. *Curr.Opin.Oncol.* 2012;24:643-649.
43. Gattei V, Bulian P, Del Principe MI et al. Relevance of CD49d protein expression as overall survival and progressive disease prognosticator in chronic lymphocytic leukemia. *Blood* 2008;111:865-873.
44. Rossi D, Zucchetto A, Rossi FM et al. CD49d expression is an independent risk factor of progressive disease in early stage chronic lymphocytic leukemia. *Haematologica* 2008;93:1575-1579.

45. Shanafelt TD, Geyer SM, Bone ND et al. CD49d expression is an independent predictor of overall survival in patients with chronic lymphocytic leukaemia: a prognostic parameter with therapeutic potential. *Br J Haematol* 2008;140:537-546.
46. Nuckel H, Switala M, Collins CH et al. High CD49d protein and mRNA expression predicts poor outcome in chronic lymphocytic leukemia. *Clin.Immunol.* 2009;131:472-480.
47. Cro L, Ferrario A, Lionetti M et al. The clinical and biological features of a series of immunophenotypic variant of B-CLL. *Eur.J.Haematol.* 2010;85:120-129.
48. Shanafelt TD, Drake MT, Maurer MJ et al. Vitamin D insufficiency and prognosis in chronic lymphocytic leukemia. *Blood* 2011;117:1492-1498.
49. Leger OJ, Yednock TA, Tanner L et al. Humanization of a mouse antibody against human alpha-4 integrin: a potential therapeutic for the treatment of multiple sclerosis. *Hum.Antibodies* 1997;8:3-16.
50. Herishanu Y, Katz BZ, Lipsky A, Wiestner A. Biology of chronic lymphocytic leukemia in different microenvironments: clinical and therapeutic implications. *Hematol.Oncol.Clin.North Am.* 2013;27:173-206.
51. Ghia P, Chiorazzi N, Stamatopoulos K. Microenvironmental influences in chronic lymphocytic leukaemia: the role of antigen stimulation. *J.Intern.Med.* 2008;264:549-562.
52. Burger JA, Tsukada N, Burger M et al. Blood-derived nurse-like cells protect chronic lymphocytic leukemia B cells from spontaneous apoptosis through stromal cell-derived factor-1. *Blood* 2000;96:2655-2663.
53. Deaglio S, Vaisitti T, Bergui L et al. CD38 and CD100 lead a network of surface receptors relaying positive signals for B-CLL growth and survival. *Blood* 2005;105:3042-3050.
54. Tsukada N, Burger JA, Zvaifler NJ, Kipps TJ. Distinctive features of "nurselike" cells that differentiate in the context of chronic lymphocytic leukemia. *Blood* 2002;99:1030-1037.
55. Pedersen IM, Kitada S, Leoni LM et al. Protection of CLL B cells by a follicular dendritic cell line is dependent on induction of Mcl-1. *Blood* 2002;100:1795-1801.
56. Bystry RS, Aluvihare V, Welch KA, Kallikourdis M, Betz AG. B cells and professional APCs recruit regulatory T cells via CCL4. *Nat.Immunol.* 2001;2:1126-1132.
57. Zucchetto A, Benedetti D, Tripodo C et al. CD38/CD31, the CCL3 and CCL4 chemokines, and CD49d/vascular cell adhesion molecule-1 are interchained by sequential events sustaining chronic lymphocytic leukemia cell survival. *Cancer Res* 2009;69:4001-4009.
58. Ghia P, Strola G, Granziero L et al. Chronic lymphocytic leukemia B cells are endowed with the capacity to attract CD4+, CD40L+ T cells by producing CCL22. *Eur.J.Immunol.* 2002;32:1403-1413.
59. Burger JA, Peled A. CXCR4 antagonists: targeting the microenvironment in leukemia and other cancers. *Leukemia* 2009;23:43-52.
60. Burger JA, Burger M, Kipps TJ. Chronic lymphocytic leukemia B cells express functional CXCR4 chemokine receptors that mediate spontaneous migration beneath bone marrow stromal cells. *Blood* 1999;94:3658-3667.

61. Mohle R, Failenschmid C, Bautz F, Kanz L. Overexpression of the chemokine receptor CXCR4 in B cell chronic lymphocytic leukemia is associated with increased functional response to stromal cell-derived factor-1 (SDF-1). *Leukemia* 1999;13:1954-1959.
62. Burkle A, Niedermeier M, Schmitt-Graff A et al. Overexpression of the CXCR5 chemokine receptor, and its ligand, CXCL13 in B-cell chronic lymphocytic leukemia. *Blood* 2007;110:3316-3325.
63. Burger JA, Zvaifler NJ, Tsukada N, Firestein GS, Kipps TJ. Fibroblast-like synoviocytes support B-cell pseudoemperipolesis via a stromal cell-derived factor-1- and CD106 (VCAM-1)-dependent mechanism. *J.Clin.Invest* 2001;107:305-315.
64. Hemler ME, Elices MJ, Parker C, Takada Y. Structure of the integrin VLA-4 and its cell-cell and cell-matrix adhesion functions. *Immunol.Rev.* 1990;114:45-65.
65. Spessotto P, Cervi M, Mucignat MT et al. beta 1 Integrin-dependent Cell Adhesion to EMILIN-1 Is Mediated by the gC1q Domain. *J.Biol.Chem.* 2003;278:6160-6167.
66. Ruoslahti E. Integrins. *J Clin Invest* 1991;87:1-5.
67. Rose DM, Han J, Ginsberg MH. Alpha4 integrins and the immune response. *Immunol.Rev.* 2002;186:118-124.
68. de la Fuente MT, Casanova B, Moyano JV et al. Engagement of alpha4beta1 integrin by fibronectin induces in vitro resistance of B chronic lymphocytic leukemia cells to fludarabine. *J Leukoc.Biol.* 2002;71:495-502.
69. Till KJ, Lin K, Zuzel M, Cawley JC. The chemokine receptor CCR7 and alpha4 integrin are important for migration of chronic lymphocytic leukemia cells into lymph nodes. *Blood* 2002;99:2977-2984.
70. Till KJ, Spiller DG, Harris RJ et al. CLL, but not normal, B cells are dependent on autocrine VEGF and alpha4beta1 integrin for chemokine-induced motility on and through endothelium. *Blood* 2005;105:4813-4819.
71. Bauvois B, Dumont J, Mathiot C, Kolb JP. Production of matrix metalloproteinase-9 in early stage B-CLL: suppression by interferons. *Leukemia* 2002;16:791-798.
72. Kamiguti AS, Lee ES, Till KJ et al. The role of matrix metalloproteinase 9 in the pathogenesis of chronic lymphocytic leukaemia. *Br.J.Haematol.* 2004;125:128-140.
73. Redondo-Munoz J, Escobar-Diaz E, Samaniego R et al. MMP-9 in B-cell chronic lymphocytic leukemia is up-regulated by alpha4beta1 integrin or CXCR4 engagement via distinct signaling pathways, localizes to podosomes, and is involved in cell invasion and migration. *Blood* 2006;108:3143-3151.
74. Redondo-Munoz J, Ugarte-Berzal E, Garcia-Marco JA et al. Alpha4beta1 integrin and 190-kDa CD44v constitute a cell surface docking complex for gelatinase B/MMP-9 in chronic leukemic but not in normal B cells. *Blood* 2008;112:169-178.
75. Majid A, Lin TT, Best G et al. CD49d is an independent prognostic marker that is associated with CXCR4 expression in CLL. *Leuk.Res.* 2011;35:750-756.

76. Sanz-Rodriguez F, Hidalgo A, Teixido J. Chemokine stromal cell-derived factor-1alpha modulates VLA-4 integrin-mediated multiple myeloma cell adhesion to CS-1/fibronectin and VCAM-1. *Blood* 2001;97:346-351.
77. Hidalgo A, Sanz-Rodriguez F, Rodriguez-Fernandez JL et al. Chemokine stromal cell-derived factor-1alpha modulates VLA-4 integrin-dependent adhesion to fibronectin and VCAM-1 on bone marrow hematopoietic progenitor cells. *Exp.Hematol.* 2001;29:345-355.
78. Redondo-Munoz J, Ugarte-Berzal E, Terol MJ et al. Matrix metalloproteinase-9 promotes chronic lymphocytic leukemia b cell survival through its hemopexin domain. *Cancer Cell* 2010;17:160-172.
79. de la Fuente MT, Casanova B, Garcia-Gila M, Silva A, Garcia-Pardo A. Fibronectin interaction with alpha4beta1 integrin prevents apoptosis in B cell chronic lymphocytic leukemia: correlation with Bcl-2 and Bax. *Leukemia* 1999;13:266-274.
80. de la Fuente MT, Casanova B, Cantero E et al. Involvement of p53 in alpha4beta1 integrin-mediated resistance of B-CLL cells to fludarabine. *Biochem.Biophys.Res.Commun.* 2003;311:708-712.
81. Buchner M, Baer C, Prinz G et al. Spleen tyrosine kinase inhibition prevents chemokine- and integrin-mediated stromal protective effects in chronic lymphocytic leukemia. *Blood* 2010;115:4497-4506.
82. Petlickovski A, Laurenti L, Li X et al. Sustained signaling through the B-cell receptor induces Mcl-1 and promotes survival of chronic lymphocytic leukemia B cells. *Blood* 2005;105:4820-4827.
83. Matsusaka S, Tohyama Y, He J et al. Protein-tyrosine kinase, Syk, is required for CXCL12-induced polarization of B cells. *Biochem.Biophys.Res.Commun.* 2005;328:1163-1169.
84. Longo PG, Laurenti L, Gobessi S et al. The Akt/Mcl-1 pathway plays a prominent role in mediating antiapoptotic signals downstream of the B-cell receptor in chronic lymphocytic leukemia B cells. *Blood* 2008;111:846-855.
85. Baudot AD, Jeandel PY, Mouska X et al. The tyrosine kinase Syk regulates the survival of chronic lymphocytic leukemia B cells through PKCdelta and proteasome-dependent regulation of Mcl-1 expression. *Oncogene* 2009;28:3261-3273.
86. Burger JA, Quiroga MP, Hartmann E et al. High-level expression of the T-cell chemokines CCL3 and CCL4 by chronic lymphocytic leukemia B cells in nurselike cell cocultures and after BCR stimulation. *Blood* 2009;113:3050-3058.
87. Menten P, Wuyts A, Van DJ. Macrophage inflammatory protein-1. *Cytokine Growth Factor Rev.* 2002;13:455-481.
88. Kaufmann A, Salentin R, Gemsa D, Sprenger H. Increase of CCR1 and CCR5 expression and enhanced functional response to MIP-1 alpha during differentiation of human monocytes to macrophages. *J.Leukoc.Biol.* 2001;69:248-252.
89. Danussi C, Petrucco A, Wassermann B et al. EMILIN1-alpha4/alpha9 integrin interaction inhibits dermal fibroblast and keratinocyte proliferation. *J.Cell Biol.* 2011;195:131-145.

90. Christiansen I, Sundstrom C, Totterman TH. Elevated serum levels of soluble vascular cell adhesion molecule-1 (sVCAM-1) closely reflect tumour burden in chronic B-lymphocytic leukaemia. *Br.J.Haematol.* 1998;103:1129-1137.
91. Sudhoff T, Wehmeier A, Kliche KO et al. Levels of circulating endothelial adhesion molecules (sE-selectin and sVCAM-1) in adult patients with acute leukemia. *Leukemia* 1996;10:682-686.
92. Koizumi A, Hashimoto S, Kobayashi T et al. Elevation of serum soluble vascular cell adhesion molecule-1 (sVCAM-1) levels in bronchial asthma. *Clin.Exp.Immunol.* 1995;101:468-473.
93. Matsuda M, Tsukada N, Miyagi K, Yanagisawa N. Increased levels of soluble vascular cell adhesion molecule-1 (VCAM-1) in the cerebrospinal fluid and sera of patients with multiple sclerosis and human T lymphotropic virus type-1-associated myelopathy. *J.Neuroimmunol.* 1995;59:35-40.
94. Mould AP, Askari JA, Craig SE et al. Integrin alpha 4 beta 1-mediated melanoma cell adhesion and migration on vascular cell adhesion molecule-1 (VCAM-1) and the alternatively spliced IIICS region of fibronectin. *J.Biol.Chem.* 1994;269:27224-27230.
95. Zanetti M, Braghetta P, Sabatelli P et al. EMILIN-1 deficiency induces elastogenesis and vascular cell defects. *Mol.Cell Biol.* 2004;24:638-650.
96. Danussi C, Spessotto P, Petrucco A et al. Emilin1 deficiency causes structural and functional defects of lymphatic vasculature. *Mol.Cell Biol.* 2008;28:4026-4039.
97. Doliana R, Bot S, Bonaldo P, Colombatti A. EMI, a novel cysteine-rich domain of EMILINs and other extracellular proteins, interacts with the gC1q domains and participates in multimerization. *FEBS Lett.* 2000;484:164-168.
98. Zacchigna L, Vecchione C, Notte A et al. Emilin1 links TGF-beta maturation to blood pressure homeostasis. *Cell* 2006;124:929-942.
99. Colombatti A, Bonaldo P, Volpin D, Bressan GM. The elastin associated glycoprotein gp115. Synthesis and secretion by chick cells in culture. *J.Biol.Chem.* 1988;263:17534-17540.
100. Mongiat M, Mungiguerra G, Bot S et al. Self-assembly and supramolecular organization of EMILIN. *J.Biol.Chem.* 2000;275:25471-25480.
101. Spessotto P, Bulla R, Danussi C et al. EMILIN1 represents a major stromal element determining human trophoblast invasion of the uterine wall. *J.Cell Sci.* 2006;119:4574-4584.
102. Danussi C, Petrucco A, Wassermann B et al. An EMILIN1-negative microenvironment promotes tumor cell proliferation and lymph node invasion. *Cancer Prev.Res.(Phila)* 2012;5:1131-1143.
103. Danussi C, Del Bel BL, Pivetta E et al. EMILIN1/alpha9beta1 integrin interaction is crucial in lymphatic valve formation and maintenance. *Mol.Cell Biol.* 2013;33:4381-4394.
104. Verdone G, Doliana R, Corazza A et al. The solution structure of EMILIN1 globular C1q domain reveals a disordered insertion necessary for interaction with the alpha4beta1 integrin. *J.Biol.Chem.* 2008;283:18947-18956.

105. Stacchini A, Aragno M, Vallario A et al. MEC1 and MEC2: two new cell lines derived from B-chronic lymphocytic leukaemia in prolymphocytoid transformation. *Leuk.Res.* 1999;23:127-136.
106. Bichi R, Shinton SA, Martin ES et al. Human chronic lymphocytic leukemia modeled in mouse by targeted TCL1 expression. *Proc.Natl.Acad.Sci.U.S.A* 2002;99:6955-6960.
107. Bressan GM, Daga-Gordini D, Colombatti A et al. Emilin, a component of elastic fibers preferentially located at the elastin-microfibrils interface. *J.Cell Biol.* 1993;121:201-212.
108. Daga GD, Castellani I, Volpin D, Bressan GM. Ultrastructural immuno-localization of tropoelastin in the chick eye. *Cell Tissue Res.* 1990;260:137-146.
109. Daga-Gordini D, Bressan GM, Castellani I, Volpin D. Detection of elastin by immunoelectronmicroscopy. A comparison of different procedures. *Histochemistry* 1987;87:573-578.
110. Caligaris-Cappio F. Role of the microenvironment in chronic lymphocytic leukaemia. *Br J Haematol* 2003;123:380-388.
111. Ehlich A, Schaal S, Gu H et al. Immunoglobulin heavy and light chain genes rearrange independently at early stages of B cell development. *Cell* 1993;72:695-704.
112. Koni PA, Joshi SK, Temann UA et al. Conditional vascular cell adhesion molecule 1 deletion in mice: impaired lymphocyte migration to bone marrow. *J.Exp.Med.* 2001;193:741-754.
113. Zohren F, Toutzaris D, Klarner V et al. The monoclonal anti-VLA-4 antibody natalizumab mobilizes CD34+ hematopoietic progenitor cells in humans. *Blood* 2008;111:3893-3895.
114. Lichterfeld M, Martin S, Burkly L, Haas R, Kronenwett R. Mobilization of CD34+ haematopoietic stem cells is associated with a functional inactivation of the integrin very late antigen 4. *Br.J.Haematol.* 2000;110:71-81.
115. Rossi FM, Zucchetto A, Tissino E et al. CD49d expression identifies a chronic-lymphocytic leukemia subset with high levels of mobilized circulating CD34 hemopoietic progenitors cells. *Leukemia* 2013
116. Hartmann TN, Grabovsky V, Wang W et al. Circulating B-cell chronic lymphocytic leukemia cells display impaired migration to lymph nodes and bone marrow. *Cancer Res.* 2009;69:3121-3130.
117. Chiorazzi N. Implications of new prognostic markers in chronic lymphocytic leukemia. *Hematology.Am.Soc.Hematol.Educ.Program.* 2012;2012:76-87.
118. Matutes E, Owusu-Ankomah K, Morilla R et al. The immunological profile of B-cell disorders and proposal of a scoring system for the diagnosis of CLL. *Leukemia* 1994;8:1640-1645.
119. Del Poeta G, Maurillo L, Venditti A et al. Clinical significance of CD38 expression in chronic lymphocytic leukemia. *Blood* 2001;98:2633-2639.

# blood

2013 122: 3317-3321  
Prepublished online September 25, 2013;  
doi:10.1182/blood-2013-06-507335

## **CD49d is overexpressed by trisomy 12 chronic lymphocytic leukemia cells: evidence for a methylation-dependent regulation mechanism**

Antonella Zucchetto, Chiara Caldana, Dania Benedetti, Erika Tissino, Francesca Maria Rossi, Evelyn Hutterer, Federico Pozzo, Riccardo Bomben, Michele Dal Bo, Giovanni D'Arena, Francesco Zaja, Gabriele Pozzato, Francesco Di Raimondo, Tanja N. Hartmann, Davide Rossi, Gianluca Gaidano, Giovanni Del Poeta and Valter Gattei

---

Updated information and services can be found at:  
<http://bloodjournal.hematologylibrary.org/content/122/19/3317.full.html>

Articles on similar topics can be found in the following Blood collections  
[Brief Reports](#) (1702 articles)  
[Lymphoid Neoplasia](#) (1594 articles)

---

Information about reproducing this article in parts or in its entirety may be found online at:  
[http://bloodjournal.hematologylibrary.org/site/misc/rights.xhtml#repub\\_requests](http://bloodjournal.hematologylibrary.org/site/misc/rights.xhtml#repub_requests)

Information about ordering reprints may be found online at:  
<http://bloodjournal.hematologylibrary.org/site/misc/rights.xhtml#reprints>

Information about subscriptions and ASH membership may be found online at:  
<http://bloodjournal.hematologylibrary.org/site/subscriptions/index.xhtml>



## LYMPHOID NEOPLASIA

### CD49d is overexpressed by trisomy 12 chronic lymphocytic leukemia cells: evidence for a methylation-dependent regulation mechanism

Antonella Zucchetto,<sup>1</sup> Chiara Caldana,<sup>1</sup> Dania Benedetti,<sup>1</sup> Erika Tissino,<sup>1</sup> Francesca Maria Rossi,<sup>1</sup> Evelyn Hutterer,<sup>2</sup> Federico Pozzo,<sup>1</sup> Riccardo Bomben,<sup>1</sup> Michele Dal Bo,<sup>1</sup> Giovanni D'Arena,<sup>3</sup> Francesco Zaja,<sup>4</sup> Gabriele Pozzato,<sup>5</sup> Francesco Di Raimondo,<sup>6</sup> Tanja N. Hartmann,<sup>2</sup> Davide Rossi,<sup>7</sup> Gianluca Gaidano,<sup>7</sup> Giovanni Del Poeta,<sup>8</sup> and Valter Gattei<sup>1</sup>

<sup>1</sup>Clinical and Experimental Onco-Hematology Unit, Centro di Riferimento Oncologico, I.R.C.C.S., Aviano (PN), Italy; <sup>2</sup>Laboratory for Immunological and Molecular Cancer Research, 3rd Medical Department, Paracelsus Medical University, Salzburg, Austria; <sup>3</sup>Onco-Hematology Department, Centro di Riferimento Oncologico della Basilicata, IRCCS, Rionero in Vulture, Italy; <sup>4</sup>Clinica Ematologica, Centro Trapianti e Terapie Cellulari Carlo Melzi, DISM, Azienda Ospedaliero-Universitaria S. M. Misericordia, Udine, Italy; <sup>5</sup>Department of Internal Medicine and Hematology, Maggiore General Hospital, University of Trieste, Trieste, Italy; <sup>6</sup>Division of Hematology, Ferrarotto Hospital, University of Catania, Catania, Italy; <sup>7</sup>Division of Hematology, Department of Translational Medicine, Amedeo Avogadro University of Eastern Piedmont, Novara, Italy; and <sup>8</sup>Division of Hematology, S. Eugenio Hospital and University of Tor Vergata, Rome, Italy

#### Key Points

- CD49d, a negative prognosticator with a key role for microenvironmental interactions in CLL, is near universally expressed in trisomy 12 CLL.
- CD49d overexpression in trisomy 12 CLL is regulated by a methylation-dependent mechanism.

**CD49d is a negative prognosticator in chronic lymphocytic leukemia (CLL), expressed by ~40% of CLL cases and associated with aggressive, accelerated clinical courses. In this study, analyzing CD49d expression in a wide CLL cohort (n = 1200) belonging to different cytogenetic groups, we report that trisomy 12 CLL almost universally expressed CD49d and were characterized by the highest CD49d expression levels among all CD49d<sup>+</sup> CLL. Through bisulfite genomic sequencing, we demonstrated that, although CD49d<sup>+</sup>/trisomy 12 CLL almost completely lacked methylation of the CD49d gene, CD49d<sup>-</sup>/no trisomy 12 CLL were overall methylated, the methylation levels correlating inversely to CD49d expression (P = .0001). Consistently, CD49d expression was recovered in CD49d<sup>-</sup> hypermethylated CLL cells upon in vitro treatment with the hypomethylating agent 5-aza-2'-deoxycytidine. This may help explain the clinicobiological features of trisomy 12 CLL, including the high rates of cell proliferation and disease progression, lymph node involvement, and predisposition to Richter syndrome transformation. (Blood. 2013;122(19):3317-3321)**

#### Introduction

CD49d recently emerged as a negative prognosticator in chronic lymphocytic leukemia (CLL), marking a subset of ~30% to 40% of CLL characterized by a more aggressive clinical course.<sup>1,2</sup> CD49d, the  $\alpha 4$  subunit of the  $\alpha 4\beta 1$  integrin heterodimer, has a role in CLL cell migration and retention in lymph node (LN) and bone marrow (BM) microenvironments, where they receive growth- and survival-supporting signals.<sup>3</sup>

Among the recurrent chromosomal abnormalities detectable in CLL,<sup>4</sup> trisomy 12 marks a disease subset (~15% of cases) characterized by high rates of cell proliferation and disease progression, and Richter syndrome (RS) transformation.<sup>5,6</sup> Despite the recent demonstration of a relative enrichment in *NOTCH1* mutations in CLL carrying trisomy 12,<sup>7-9</sup> no specific genetic and/or biological features have so far been identified in trisomy 12 CLL to explain the peculiar clinical behavior of this CLL subset.<sup>10,11</sup>

Medical University (Approval n. 415-E/1287/4-2011), included peripheral blood samples from 1200 patients with typical CLL according to the current guidelines.<sup>12</sup> Informed consent was obtained from the participants in accordance with the Declaration of Helsinki. CLL was characterized for the main cytogenetic abnormalities, flow cytometry-based prognosticators, *IGHV* mutations (all cases), and *NOTCH1* mutations (944/1200 cases), as described.<sup>1,13</sup> Treatment-free-survival (TFS) and RS transformation data were available for 601 and 324 cases, respectively.

Procedures for cell sorting, quantitative real-time polymerase chain reaction (qRT-PCR), bisulfite sequencing, and in vitro 5-aza-2'-deoxycytidine (DAC) experiments are reported in the supplemental Methods. All studies were performed on highly purified (>95%) CLL cells.<sup>14</sup>

#### Patients and methods

This study, approved by the Internal Review Boards of the Centro di Riferimento Oncologico di Aviano (Approval n. IRB-05-2010) and Salzburg

#### Results and discussion

##### CD49d is expressed by a vast majority of trisomy 12 CLL

CD49d expression was investigated by flow cytometry in the neoplastic component of 1200 CLL patients. Using the 30% cutoff,<sup>1</sup> 735 cases (61%) were classified as CD49d<sup>-</sup>, whereas

Submitted June 6, 2013; accepted September 21, 2013. Prepublished online as *Blood* First Edition paper, September 25, 2013; DOI 10.1182/blood-2013-06-507335.

The online version of this article contains a data supplement.

The publication costs of this article were defrayed in part by page charge payment. Therefore, and solely to indicate this fact, this article is hereby marked "advertisement" in accordance with 18 USC section 1734.

© 2013 by The American Society of Hematology

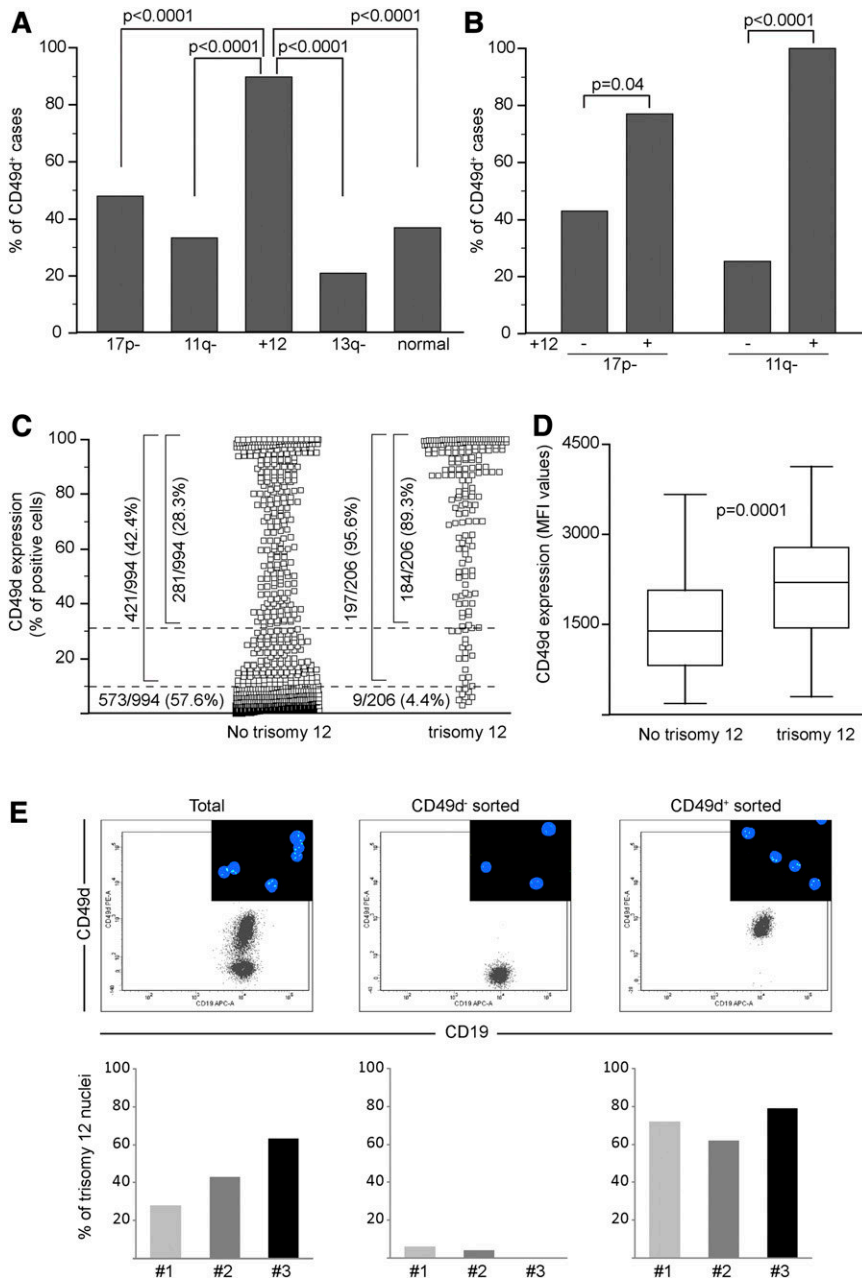


**Figure 1. CD49d is almost universally expressed by trisomy 12 CLL.** The percent of CD49d<sup>+</sup> cases among 1200 CLL split according to the cytogenetic groups defined by Döhner et al<sup>4</sup> (A) and in the context of the 17p- and 11q- groups, split according to the presence or not of trisomy 12 (B). 17p-, 17p13.1 deletion; 11q-, 11q22-q23 deletion; +12, trisomy 12; 13q-, 13q14.3 deletion; normal, none of the above. All *P* values refer to the  $\chi^2$  test. (C) CD49d expression in CLL cases split into 2 groups according to the presence of trisomy 12. Dotted lines were set at 30% and 10% cutoffs, and the number and percentages of cases expressing different CD49d levels are reported. (D) CD49d MFI values in CD49d<sup>+</sup> CLL bearing or not bearing trisomy 12. Boxes represent the interquartile range (25-75%), with the middle line indicating the median and the horizontal lines indicating the minimum and maximum values. (E) FISH analysis in the total and in the CD49d<sup>-</sup> and CD49d<sup>+</sup> sorted components from 3 CLL cases characterized by CD49d bimodal expression. The upper panels represent dot plots of CD19 vs CD49d expression from 1 representative case (case 2). The insets show representative fields of FISH analysis performed with an  $\alpha$  satellite DNA probe CEP12, directly labeled with SpectrumGreen to detect aneuploidy of chromosome 12. Histograms represent the percent of trisomy 12 nuclei in the total CD5<sup>+</sup>CD19<sup>+</sup> (left), CD5<sup>+</sup>CD19<sup>+</sup>CD49d<sup>-</sup> (middle), and the CD5<sup>+</sup>CD19<sup>+</sup>CD49d<sup>+</sup> sorted components from 3 CLL cases.

465 (39%) were CD49d<sup>+</sup>. Analysis within the major cytogenetic groups<sup>4</sup> showed a significantly higher percentage of CD49d<sup>+</sup> cases (89.4%) in the trisomy 12 group compared with the other cytogenetic groups (*P* < .0001 for all pairwise comparisons, supplemental Table 1 and Figure 1A). This also held true by comparing the percentages of CD49d<sup>+</sup> cases in CLL bearing or not bearing trisomy 12 in the context of the del17p13.1 and del11q22-q23 cytogenetic groups (Figure 1B).<sup>4</sup> Altogether, in trisomy 12 CLL, 89% (184/206) of cases expressed CD49d in >30% of CLL cells; 6% (13/206) in 10% to 27% of cells, mostly with a bimodal pattern (not shown); and 4% (9/206) in <10% of cells (Figure 1C). In the context of trisomy 12 CLL, no differences were found between CD49d<sup>+</sup> and CD49d<sup>-</sup> cases for the main cytogenetic abnormalities, as well as for *IGHV* or *NOTCH1* mutations (data not shown), but, as expected,<sup>7-9</sup> *NOTCH1* mutations were significantly over-represented (*P* < .0001; supplemental Table 1).

Among CD49d<sup>+</sup> CLL, trisomy 12 CLL expressed CD49d at higher mean fluorescence intensity (MFI) levels (median MFI = 2200; 95% confidence interval [CI], 1810-2546; n = 54) compared with no trisomy 12 CLL (median MFI = 1386; 95% CI, 1050-1673; n = 55; *P* = .0001; Figure 1D).

Fluorescence in situ hybridization (FISH) analysis of flow cytometry-sorted CD49d<sup>-</sup> and CD49d<sup>+</sup> subpopulations in the context of CLL with bimodal CD49d expression (n = 3) documented that trisomy 12 was restricted to the CD49d<sup>+</sup> fraction and was virtually absent in CD49d<sup>-</sup> cells (Figure 1E).

Overall, these data indicate the almost universal expression of CD49d in trisomy 12 CLL, corroborating the notion that this chromosomal aberration marks a CLL entity with distinct clinicobiological features.<sup>10,15</sup>

The impact of CD49d and trisomy 12 as TFS predictors and of CD49d in RS transformation are reported in the supplemental Results and supplemental Figures 1-3.

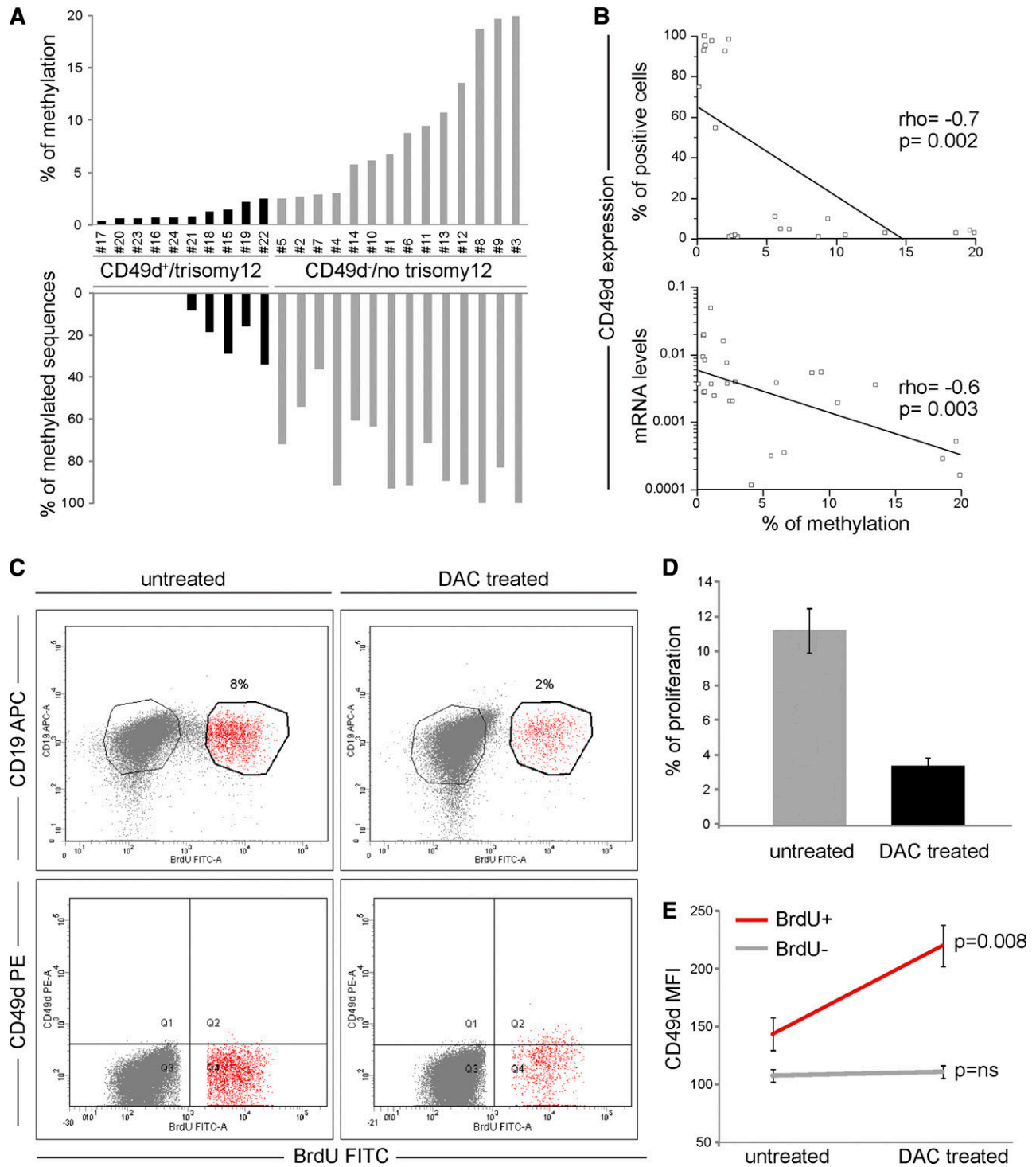


**Figure 2. CD49d expression is correlated with DNA methylation levels.** (A) DNA methylation was studied within the CpG island of the *ITGA4* gene (reported in supplemental Figure 5). The upper graph reports the percentage of methylation calculated as the number of methylated CpG over the total number of CpGs. The lower graph reports the percentage of sequences with at least 2 methylated CpGs. At least 10 clones for each of 10 CD49d<sup>+</sup>/trisomy 12 (black histograms) and 14 CD49d<sup>-</sup>/no trisomy 12 (gray histograms) CLL cases were analyzed. (B) Correlation between the percentage of methylation and CD49d protein expression, as detected by flow cytometry (upper panel) and mRNA as detected by qRT-PCR (lower panel).  $\rho$  and  $P$  values refer to the Spearman's rank correlation test. (C-E) Primary CLL cells from 7 cases were cultured for 96 hours using CpG-ODN/interleukin-2 in the presence or not of 5  $\mu$ mol/L DAC and analyzed by flow cytometry for the surface expression of CD49d. (C) Dot plots of CD19-APC vs BrdU-FITC (upper panels) and CD49d-PE vs BrdU-FITC (lower panels) in untreated and DAC-treated CLL cells from a representative case (case 13). The proliferative/BrdU<sup>+</sup> and nonproliferative/BrdU<sup>-</sup> fractions are noted in red and gray, respectively. (D) Proliferation levels (mean percent  $\pm$  SEM) of untreated (gray bar) and DAC-treated (black bar) CLL cells after 96 hours in culture with CpG-ODN/interleukin-2. (E) CD49d MFI (mean expression  $\pm$  SEM) by proliferative/BrdU<sup>+</sup> (red line) and nonproliferative/BrdU<sup>-</sup> (gray line) fractions in untreated and DAC-treated CLL cells;  $P$  values refer to the Student  $t$  test.

### CD49d overexpression in trisomy 12 CLL is associated with ITGA4 hypomethylation

As investigated by qRT-PCR in 74 CLL (31 CD49d<sup>-</sup>/no trisomy 12 and 43 CD49d<sup>+</sup>/trisomy 12), CD49d mRNA expression positively correlated with CD49d protein levels ( $r = 0.6$ ,  $P < .0001$ , supplemental Figure 4), implying a transcriptional regulation of CD49d protein expression. Therefore, we decided to study whether DNA hypomethylation, a well-known epigenetic mechanism regulating gene transcription in tumors including CLL,<sup>16</sup> could explain the CD49d overexpression found in trisomy 12 CLL.

DNA methylation was studied within a 5'-UTR CpG island (77 CpGs) of the CD49d gene (*ITGA4*) (supplemental Figure 5 and supplemental Methods). CD49d<sup>-</sup>/no trisomy 12 CLL ( $n = 14$ ) showed a higher degree of *ITGA4* methylation compared with CD49d<sup>+</sup>/trisomy 12 cases ( $n = 10$ ), which almost completely lacked methylated CpGs (average amount of methylated CpGs = 9.2% vs 0.9%,  $P < .0001$ , Figure 2A). Moreover, the number of methylated clones in at least 2 CpG sites was higher in CD49d<sup>-</sup>/no trisomy 12 (mean, 78%; range, 36-100%) than in CD49d<sup>+</sup>/trisomy 12 CLL cases (mean, 10%; range, 0-33%;  $P < .0001$ ; Figure 2A).

Although *ITGA4* methylation in the CD49d<sup>+</sup>/trisomy 12 CLL group was homogeneously low, 4/14 CD49d<sup>-</sup>/no trisomy 12 cases displayed <3% methylation. These cases, and 4 CD49d<sup>+</sup>/trisomy 12 cases for comparison, were therefore analyzed for methylation levels within an additional *ITGA4* CpG island (44 CpGs), spanning exons 1 and 2 (supplemental Figure 5). Despite the overall lower methylation levels characterizing this CpG island, CD49d<sup>-</sup> CLL displayed higher percentages of methylated CpG than CD49d<sup>+</sup> cases (average amount of methylated CpG = 4.0% vs 0.5%,  $P < .0001$ ).

Similar levels of *ITGA4* hypomethylation were found in 10 CD49d<sup>+</sup> CLL with a normal karyotype (data not shown).

To further corroborate the direct role of DNA methylation in regulating CD49d expression, a significant inverse correlation was observed between the percentage of methylated CpGs and CD49d expression at both mRNA ( $r = -0.6$ ,  $P = .003$ ) and protein levels ( $r = -0.7$ ,  $P = .002$ ; Figure 2B).

Hypomethylating agents are known regulators of gene expression. Among them, DAC operates by inhibiting DNA methyltransferase activity, thus preventing methylation of newly replicated DNA, leading to DNA demethylation and subsequent gene activation.<sup>17</sup> According to this notion, highly purified CLL cells from 7 CD49d<sup>-</sup> cases (supplemental Table 2) were exposed to DAC in the presence of CpG-ODN/interleukin-2 as proliferative stimulus.<sup>18,19</sup> Although DAC-treated CLL cells displayed lower levels of proliferation compared with untreated cells (mean % proliferation levels =  $11.2 \pm 1.3$  vs  $3.4 \pm 0.5$ , respectively; Figure 2C-D), the proliferative fraction of DAC-treated CLL cells significantly upregulated CD49d protein levels (mean MFI,  $220 \pm 18$  vs  $144 \pm 14$ ;  $P = .008$ ; Figure 2E). Consistently, analysis of *ITGA4* methylation in these DAC-treated proliferating cells ( $n = 2$ ) highlighted lower levels of methylation (% methylated CpGs = 4.0 and 5.3) compared with proliferating cells of untreated cultures (% methylated CpGs = 12.3 and 10.0).

In CLL, the close dependency of CD49d expression on DNA methylation, as demonstrated here also outside the trisomy 12

subset, was similar to that reported for other CLL bad prognosticators and key regulators of CLL cells, such as ZAP-70, lipoprotein lipase, *CLU1*, and *NOTCH1*.<sup>19-21</sup>

Although a functional relation between trisomy 12 and hypomethylation of the CD49d gene remains to be established, preliminary gene expression profiling data generated by us suggest that trisomy 12 CLL cells differentially express genes involved in the regulation of methyltransferase activity and chromatin modification processes (A.Z., unpublished observation).

The role of trisomy 12 in the pathogenesis of CLL has always been elusive. Previous reports showed that the proportion of trisomy 12 CLL cells is higher in LN than in peripheral blood or BM, thus reflecting a specific tropism toward LN of trisomy 12 CLL cells.<sup>22</sup> The overexpression of CD49d may provide the molecular basis to explain the peculiar biological behavior of trisomy 12 CLL and may predict for the development of additional cytogenetic lesions, as reported.<sup>23</sup>

In light of a recent demonstration that the use of Bruton tyrosine kinase inhibitors in CLL is able to impair the integrin-mediated retention of CLL cells in the LN and BM microenvironments,<sup>24</sup> trisomy 12 CLL may represent a CLL subset that can particularly benefit of Bruton tyrosine kinase inhibitor treatment.

---

## Acknowledgments

This work was supported in part by Ministero della Salute Ricerca Finalizzata I.R.C.C.S., Progetto Giovani Ricercatori (GR-2010-2317594, GR-2009-1475467, GR-2008-1138053), Rome, Italy; Fondazione Internazionale di Ricerca in Medicina Sperimentale (FIRMS); Associazione Italiana contro le Leucemie, linfomi e mielomi (AIL), Venezia Section; Pramaggiore Group, Italy; Ricerca Scientifica Applicata, Regione Friuli Venezia Giulia ("Linfonet" Project), Trieste, Italy; Associazione Italiana Ricerca Cancro (AIRC; IG-13227, MFAG-10327), Milan, Italy; and "5x1000 Intramural Program," Centro di Riferimento Oncologico, Aviano, Italy.

---

## Authorship

Contribution: A.Z. and V.G. designed the study, coordinated the experiments, and wrote the manuscript; C.C., D.B., E.T., F.M.R., E.H., F.P., R.B., M.D.B., and T.N.H. performed the experiments and contributed to characterize samples and to data analysis; G.D.A., F.Z., G.P., F.D.R., G.D.P., D.R., and G.G. provided well-characterized biological samples and clinical data; and all authors commented and contributed to writing the manuscript.

Conflict-of-interest disclosure: The authors declare no competing financial interests.

Correspondence: Antonella Zucchetto, PhD, Clinical and Experimental Onco-Hematology Unit, Centro di Riferimento Oncologico, I.R.C.C.S., Via Franco Gallini 2, Aviano (PN), Italy; e-mail: zucchetto.soecs@cro.it.

## References

1. Gattei V, Bulian P, Del Principe MI, et al. Relevance of CD49d protein expression as overall survival and progressive disease prognosticator in chronic lymphocytic leukemia. *Blood*. 2008; 111(2):865-873.
2. Shanafelt TD, Geyer SM, Bone ND, et al. CD49d expression is an independent predictor of overall survival in patients with chronic lymphocytic leukaemia: a prognostic parameter with therapeutic potential. *Br J Haematol*. 2008;140(5): 537-546.
3. Dal Bo M, Bomben R, Zucchetto A, et al. Microenvironmental interactions in chronic lymphocytic leukemia: hints for pathogenesis and identification of targets for rational therapy. *Curr Pharm Des*. 2012;18(23):3323-3334.
4. Döhner H, Stilgenbauer S, Benner A, et al. Genomic aberrations and survival in chronic lymphocytic leukemia. *N Engl J Med*. 2000; 343(26):1910-1916.
5. Tsimberidou AM, Keating MJ. Richter syndrome: biology, incidence, and therapeutic strategies. *Cancer*. 2005;103(2):216-228.
6. Rossi D, Spina V, Bomben R, et al. Association between molecular lesions and specific B-cell receptor subsets in chronic lymphocytic leukemia. *Blood*. 2013;121(24):4902-4905.
7. López C, Delgado J, Costa D, et al. Different distribution of NOTCH1 mutations in chronic lymphocytic leukemia with isolated trisomy 12 or associated with other chromosomal alterations. *Genes Chromosomes Cancer*. 2012;51(9): 881-889.
8. Del Giudice I, Rossi D, Chiaretti S, et al. NOTCH1 mutations in +12 chronic lymphocytic leukemia (CLL) confer an unfavorable prognosis, induce a distinctive transcriptional profiling and refine the intermediate prognosis of +12 CLL. *Haematologica*. 2012;97(3):437-441.
9. Balatti V, Bottoni A, Palamarchuk A, et al. NOTCH1 mutations in CLL associated with trisomy 12. *Blood*. 2012;119(2):329-331.
10. Buhl AM, Jurlander J, Jørgensen FS, et al. Identification of a gene on chromosome 12q22 uniquely overexpressed in chronic lymphocytic leukemia. *Blood*. 2006;107(7):2904-2911.
11. Winkler D, Schneider C, Kröber A, et al. Protein expression analysis of chromosome 12 candidate genes in chronic lymphocytic leukemia (CLL). *Leukemia*. 2005;19(7):1211-1215.
12. Matutes E, Owusu-Ankomah K, Morilla R, et al. The immunological profile of B-cell disorders and proposal of a scoring system for the diagnosis of CLL. *Leukemia*. 1994;8(10):1640-1645.
13. Rossi D, Rasi S, Fabbri G, et al. Mutations of NOTCH1 are an independent predictor of survival in chronic lymphocytic leukemia. *Blood*. 2012; 119(2):521-529.
14. Zucchetto A, Vaisitti T, Benedetti D, et al. The CD49d/CD29 complex is physically and functionally associated with CD38 in B-cell chronic lymphocytic leukemia cells. *Leukemia*. 2012;26(6):1301-1312.
15. Tsimberidou AM, Wen S, O'Brien S, et al. Assessment of chronic lymphocytic leukemia and small lymphocytic lymphoma by absolute lymphocyte counts in 2,126 patients: 20 years of experience at the University of Texas M.D. Anderson Cancer Center. *J Clin Oncol*. 2007;25(29):4648-4656.
16. Cahill N, Rosenquist R. Uncovering the DNA methylome in chronic lymphocytic leukemia. *Epigenetics*. 2013;8(2):138-148.
17. Stressemann C, Lyko F. Modes of action of the DNA methyltransferase inhibitors azacytidine and decitabine. *Int J Cancer*. 2008;123(1):8-13.
18. Bomben R, Gobessi S, Dal Bo M, et al. The miR-17~92 family regulates the response to Toll-like receptor 9 triggering of CLL cells with unmutated IGHV genes. *Leukemia*. 2012;26(7):1584-1593.
19. Moreno P, Abreu C, Borge M, et al. Lipoprotein lipase expression in unmutated CLL patients is the consequence of a demethylation process induced by the microenvironment. *Leukemia*. 2013;27(3):721-725.
20. Cahill N, Bergh AC, Kanduri M, et al. 450K-array analysis of chronic lymphocytic leukemia cells reveals global DNA methylation to be relatively stable over time and similar in resting and proliferative compartments. *Leukemia*. 2013; 27(1):150-158.
21. Claus R, Lucas DM, Stilgenbauer S, et al. Quantitative DNA methylation analysis identifies a single CpG dinucleotide important for ZAP-70 expression and predictive of prognosis in chronic lymphocytic leukemia. *J Clin Oncol*. 2012;30(20): 2483-2491.
22. Liso V, Capalbo S, Lapietra A, Pavone V, Guarini A, Specchia G. Evaluation of trisomy 12 by fluorescence in situ hybridization in peripheral blood, bone marrow and lymph nodes of patients with B-cell chronic lymphocytic leukemia. *Haematologica*. 1999;84(3):212-217.
23. Shanafelt TD, Hanson C, Dewald GW, et al. Karyotype evolution on fluorescent in situ hybridization analysis is associated with short survival in patients with chronic lymphocytic leukemia and is related to CD49d expression. *J Clin Oncol*. 2008;26(14):e5-e6.
24. de Rooij MF, Kuil A, Geest CR, et al. The clinically active BTK inhibitor PCI-32765 targets B-cell receptor- and chemokine-controlled adhesion and migration in chronic lymphocytic leukemia. *Blood*. 2012;119(11):2590-2594.

## LETTER TO THE EDITOR

# CD49d expression identifies a chronic-lymphocytic leukemia subset with high levels of mobilized circulating CD34<sup>+</sup> hemopoietic progenitors cells

Leukemia advance online publication, 29 November 2013;  
doi:10.1038/leu.2013.331

CD49d is a strong negative prognosticator in chronic lymphocytic leukemia (CLL), marking a subset of ~40% of CLL patients characterized by aggressive and accelerated clinical course.<sup>1,2</sup> Functionally, CD49d, the  $\alpha 4$  integrin subunit, has a key role in CLL microenvironmental interactions by binding to fibronectin (FN) and vascular-cell adhesion molecule-1 (VCAM-1).<sup>3,4</sup> CD49d is known to be associated with another CLL-negative prognosticator, CD38, which acts both as a receptor for the endothelial cell marker CD31 and as an enhancer of CD49d-mediated adhesion to FN and VCAM-1 substrates.<sup>1,2,5,6</sup> The role of CD49d as a key adhesion molecule involved in disease pathogenesis has also been described in auto-immune diseases, such as multiple sclerosis (MS) where CD49d is responsible for migration of leukocytes through the blood–brain barrier to sites of inflammation. The use of the humanized anti-CD49d monoclonal antibody, natalizumab, has been successfully employed in MS clinical trials to prevent CD49d-mediated leukocyte transmigration.<sup>7</sup> Notably, an increased number of circulating CD34<sup>+</sup> hemopoietic progenitor cells (HPC) has been documented upon natalizumab treatment of MS patients, in keeping with the notion of high CD49d expression by HPC, and of the relevance of CD49d-mediated

microenvironmental interactions to maintain HPC in the context of the hemopoietic niche.<sup>8,9</sup>

Here, we focused on the amount of circulating HPC in peripheral blood (PB) samples of CLL cases with different CD49d expression levels.

PB samples from 145 untreated CLL patients were collected in different cooperating institutions, and informed consents were obtained from the participants in accordance with the Declaration of Helsinki. All CLL samples were purposely selected with a white blood count (WBC) >25 000/ $\mu$ l, thus assuming massive bone-marrow infiltration. CLL cell characterization included the main cytogenetic abnormalities, expression of flow cytometry-based prognosticators CD49d, CD38 and ZAP-70, and *IGHV* and *NOTCH1* gene mutations (Supplementary Table 1).<sup>1,4,10</sup> PB samples from 20 cases of B-cell non-Hodgkin lymphoma (B-NHL) enrolled as candidates to high dose chemotherapy with autologous CD34<sup>+</sup> HPC rescue and monitored for PB CD34<sup>+</sup> cell count at the beginning of the mobilization procedure were used as reference controls.

Enumeration of the circulating HPC was performed according to a single platform strategy, utilizing a combination of anti-CD45-FITC and anti-CD34-PE conjugated monoclonal antibodies, and 7-aminoactinomycin D (BD Biosciences, San Jose, CA, USA), acquiring at least 200 HPC events per sample (Supplementary Figure 1).<sup>11</sup> Immunophenotypic characterization of HPC was performed by investigating the expression of lineage-specific

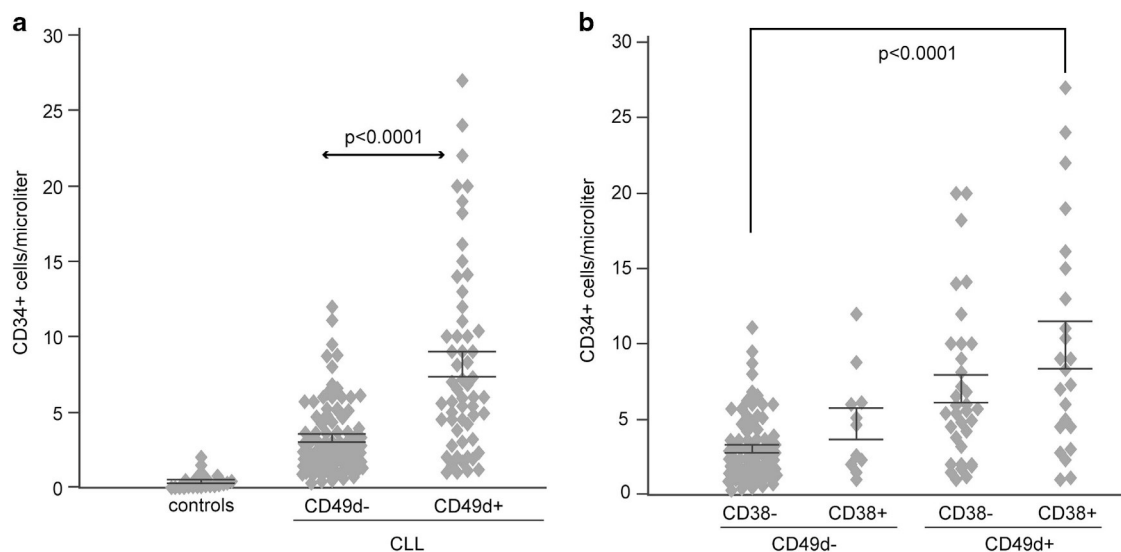


**Figure 1.** Mobilized circulating CD34<sup>+</sup> hemopoietic progenitors cells in CLL. Enumeration of CD34<sup>+</sup> cells was performed on fresh PB samples from 145 CLL cases and from 20 B-NHL cases before pre-transplant mobilization procedures (controls), according to the single platform strategy reported in text and in Supplementary Figure 1A. Graphs represent enumeration of CD34<sup>+</sup> cells in CLL samples split according to CD49d expression (a) or CD49d and CD38 co-expression (b). *P*-values refer to the *t*-test.

antigens and surface molecules mediating cell–cell and cell–matrix interactions. All data, acquired on a FACSCanto flow cytometer and analyzed by Diva software (BD Biosciences), were evaluated as percent of positive cells. Cell sorting of HPC CD34<sup>+</sup> cells and their CLL counterpart was performed using a FACSriaIII (BD Biosciences), using the same strategy adopted for CD34<sup>+</sup> cell absolute counts and a CD5-FITC/CD19-APC antibody combination, respectively. Colony-forming unit (CFU) assays were performed by plating 1000 purified HPC CD34<sup>+</sup> cells ( $n=3$ ) on Methocult GF H84444 (StemCell Technologies, Grenoble, France) according to the standard protocol, and colonies of different hemopoietic composition were counted (CFU-GEMM, CFU-GM, CFU-M, BFU-E) after 14 days.<sup>12</sup>

Enumeration of CD34<sup>+</sup> cells on fresh PB samples (mean WBC/ $\mu\text{l}$   $59.2 \times 10^3$ , range  $25.0\text{--}300.0 \times 10^3$ ) from 145 CLL cases resulted in a mean absolute count of 5.2 cells/ $\mu\text{l}$  (range 0.3–27.0). CD34<sup>+</sup> cell absolute counts were significantly higher when compared with those obtained in PB from B-NHL cases before pre-transplant mobilization procedures (0.4/ $\mu\text{l}$ , range 0–2.0, mean WBC  $5.0 \times 10^3$ ;  $P<0.0001$ ).

When CLL samples were split in two subsets according to CD49d expression by CLL cells, a higher number of CD34<sup>+</sup> cell absolute counts was found in CD49d<sup>+</sup> ( $n=57$ ) as compared with CD49d<sup>-</sup> ( $n=88$ ) CLL ( $8.2 \pm 0.8$  versus  $3.3 \pm 0.3$  mean  $\pm$  s.e.m. cells/ $\mu\text{l}$ ,  $P<0.0001$ ; Figure 1a).

A further stratification of samples according to the co expression of CD49d and CD38 resulted in a higher number of CD34<sup>+</sup> cell absolute counts in CD49d<sup>+</sup>CD38<sup>+</sup> ( $n=23$ ) as compared with CD49d<sup>-</sup>CD38<sup>-</sup> ( $n=77$ ) CLL ( $9.9 \pm 1.5$  versus  $3.1 \pm 0.2$  mean  $\pm$  s.e.m. cells/ $\mu\text{l}$ ,  $P<0.0001$ ; Figure 1b). These data are in line with the known capability of CD38 to potentiate the CD49d-mediated adhesive properties of CLL cells,<sup>6</sup> suggesting that the copresence of the two molecules has a role in determining the levels of circulating HPC in CLL. These differences in the number of circulating CD34<sup>+</sup> cells were not found by comparing CLL cases bearing or not bearing unmutated *IGHV* genes ( $P=0.05$ ), 11q22-q23/17p13.1 deletion ( $P=0.1$ ), *NOTCH1* mutations ( $P=0.09$ ), ZAP-70 ( $P=0.3$ ), or expressing or not expressing CD38 in the absence of CD49d ( $P=0.04$ ).

Previous studies in B-cell lymphoproliferative disorders described an increased number of circulating CD34<sup>+</sup> cells with phenotypic features of endothelial progenitors bona fide clonally related to the neoplastic B-cell component.<sup>13,14</sup> To verify the possibility of a common origin between CLL cells and CD34<sup>+</sup> HPC cells in our series, we identified the CD19<sup>+</sup>CD5<sup>+</sup> and CD34<sup>+</sup> components in five CLL cases characterized by a clonal trisomy 12 chromosomal abnormality ( $n=3$ ), or by the presence of clonal *NOTCH1* mutations ( $n=2$ );<sup>10</sup> in these cases the CD19<sup>+</sup>CD5<sup>+</sup> and CD34<sup>+</sup> components were flow cytometrically sorted (>99% purity) and subjected to FISH and molecular analyses for trisomy 12 and *NOTCH1* mutation detection. As shown in Figure 2, the sorted CD34<sup>+</sup> components from all the cases failed to display trisomy 12-bearing nuclei or *NOTCH1* mutations, indicating that these circulating HPC were not clonally related to the neoplastic component.

Immunophenotypic analysis of CD34<sup>+</sup>CD45<sup>low</sup> cell population in 58/148 samples displaying a cluster of at least 100 HPC CD34<sup>+</sup> by flow cytometry showed that most HPC were of myeloid origin (that is, CD13<sup>+</sup>/CD33<sup>+</sup>/CD19<sup>-</sup>/CD7<sup>-</sup>) and characterized by the expression of the stem markers CD133, CD90 and CD117 (mean percent of positive cells, 95% confidence interval, CI: 64%, 58–68%; 63%, 56–70%; 77%, 66–89%, respectively), as well as of CD31, CD38, CD49d, CD62L, and CXCR4 (mean percent of positive cells, 95% CI: 94%, 92–96%; 79%, 73–84%; 94%, 91–97%; 64%, 54–73%; and 26%, 18–33%, respectively), all markers of micro-environment interaction that are known to be also expressed by CLL cells.<sup>15</sup> Conversely, the endothelial cell markers CD144/VE-cadherin and CD146/MCAM were either not expressed (CD146,

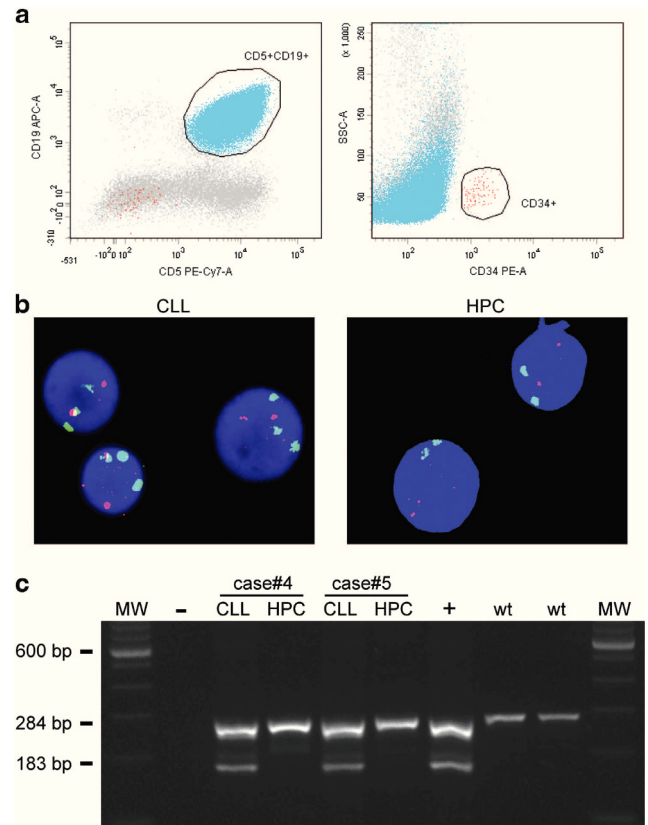


**Figure 2.** Molecular analyses of CD19<sup>+</sup>CD5<sup>+</sup> and CD34<sup>+</sup> sorted cells. (a) Dot plots of CD5 versus CD19 expression (left panel) and CD34 versus side scatter (right panel) used for cell-sorting experiments. (b) Representative fields of FISH analysis performed with an alpha-satellite DNA-probe CEP12, directly labeled with SpectrumGreen to detect aneuploidy of chromosome 12, in the sorted CD5<sup>+</sup>CD19<sup>+</sup> (left panel) and CD34<sup>+</sup> (right panel) cell populations from one representative case; in both images, red signals refer to the 13q FISH probe locus-specific identifier (LSI)-D13S319, utilized as internal control. (c) Results of the ARMS PCR assay for delCT *NOTCH1* mutation in the CD5<sup>+</sup>CD19<sup>+</sup> (CLL) and CD34<sup>+</sup> (HPC) populations from two CLL cases. Negative samples show a normal band of 284 bp. Samples bearing the delCT *NOTCH1* mutation show an additional mutant band of 183 bp. PCR controls are represented by a negative control (–), one mutated (+) and two wild-type (wt) samples. MW, molecular weight (100 bp ladder). Camera: Gel Doc EZ, Bio-Rad; image acquisition software: Image Lab 3.0, BioRad.

mean percent of positive cells 3, 95% CI 1–4) or expressed at very low levels (CD144, mean percent of positive cells 8, 95% CI 6–11).

Finally, *in-vitro* colony assay showed that CLL-derived circulating HPC maintained a full hemopoietic potential, with CFU-GEMM (13%), CFU-GM (29%), CFU-M (1%) and BFU-E (56%) all represented (Supplementary Figure 1b). The skewing toward a higher frequency of BFU-E was similar to that observed by investigating the hematopoietic potential of PB CD34<sup>+</sup> cells mobilized either from B-NHL patients (not shown) or upon natalizumab treatment of MS patients.<sup>9</sup>

In conclusion, the presence of CD49d, in association or not with CD38, on the surface of CLL cells identifies a disease subset with significantly higher number of mobilized circulating HPC. This phenomenon might be explained considering the sharing of common phenotypic traits between CD49d<sup>+</sup>/CD38<sup>+</sup> CLL cells and CD34<sup>+</sup> HPC that could be responsible for a displacement of CD34<sup>+</sup> cells from the microenvironmental niche.<sup>15</sup> Altogether, data presented here represent an unusual indirect *in-vivo* proof of the actual engagement of CD49d, as expressed by CLL cells, by its

specific ligands in the context of the bone marrow microenvironment. This observation should be considered when searching for CLL-specific stem cells within the CD34 component of PB CLL samples.<sup>14</sup>

## CONFLICT OF INTEREST

The authors declare no conflict of interest.

## ACKNOWLEDGEMENTS

This work was supported in part by: Ministero della Salute, Ricerca Finalizzata IRCCS, Progetto Giovani Ricercatori no GR-2010-2317594, no GR-2009-1475467 and no GR-2008-1138053, Rome, Italy; Fondazione Internazionale di Ricerca in Medicina Sperimentale; Associazione Italiana contro le Leucemie, linfomi e mielomi, Venezia Section, Pramaggiore Group, Italy; Ricerca Scientifica Applicata, Regione Friuli Venezia Giulia ('Linfonet' Project), Trieste, Italy; the Associazione Italiana Ricerca Cancro, Special Program Molecular Clinical Oncology, 5 × 1000, no 10007; Investigator Grant IG-13227, and MFAG-10327, Milan, Italy; '5 × 1000 Intramural Program', Centro di Riferimento Oncologico, Aviano, Italy.

FM Rossi<sup>1</sup>, A Zucchetto<sup>1</sup>, E Tissino<sup>1</sup>, M Dal Bo<sup>1</sup>, R Bomben<sup>1</sup>,  
C Caldana<sup>1</sup>, F Pozzo<sup>1</sup>, G Del Poeta<sup>2</sup>, D Rossi<sup>3</sup>, G Gaidano<sup>3</sup>  
and V Gattei<sup>1</sup>

<sup>1</sup>Clinical and Experimental Onco-Hematology Unit, Centro di  
Riferimento Oncologico, I.R.C.C.S., Aviano, Italy;

<sup>2</sup>Division of Hematology, S.Eugenio Hospital and University of Tor  
Vergata, Rome, Italy and

<sup>3</sup>Division of Hematology, Department of Translational Medicine,  
Amedeo Avogadro University of Eastern Piedmont, Novara, Italy  
E-mail: frossi@cro.it

## REFERENCES

- Gattei V, Bulian P, Del Principe MI, Zucchetto A, Maurillo L, Buccisano F *et al.* Relevance of CD49d protein expression as overall survival and progressive disease prognosticator in chronic lymphocytic leukemia. *Blood* 2008; **111**: 865–873.
- Shanafelt TD, Geyer SM, Bone ND, Tschumper RC, Witzig TE, Nowakowski GS *et al.* CD49d expression is an independent predictor of overall survival in patients with chronic lymphocytic leukaemia: a prognostic parameter with therapeutic potential. *Br J Haematol* 2008; **140**: 537–546.
- Vincent AM, Cawley JC, Burthem J. Integrin function in chronic lymphocytic leukemia. *Blood* 1996; **87**: 4780–4788.
- Dal-Bo M, Bertoni F, Forconi F, Zucchetto A, Bomben R, Marasca R *et al.* Intrinsic and extrinsic factors influencing the clinical course of B-cell chronic lymphocytic leukemia: prognostic markers with pathogenetic relevance. *J Transl Med* 2009; **7**: 76.
- Damle RN, Wasil T, Fais F, Ghiotto F, Valetto A, Allen SL *et al.* Ig V gene mutation status and CD38 expression as novel prognostic indicators in chronic lymphocytic leukemia. *Blood* 1999; **94**: 1840–1847.
- Zucchetto A, Vaisitti T, Benedetti D, Tissino E, Bertagnolo V, Rossi D *et al.* The CD49d/CD29 complex is physically and functionally associated with CD38 in B-cell chronic lymphocytic leukemia cells. *Leukemia* 2012; **26**: 1301–1312.
- Engelhardt B, Kappos L. Natalizumab: targeting alpha4-integrins in multiple sclerosis. *Neurodegener Dis* 2008; **5**: 16–22.
- Bonig H, Wundes A, Chang KH, Lucas S, Papayannopoulou T. Increased numbers of circulating hematopoietic stem/progenitor cells are chronically maintained in patients treated with the CD49d blocking antibody natalizumab. *Blood* 2008; **111**: 3439–3441.
- Zohren F, Toutzaris D, Klarner V, Hartung HP, Kieseier B, Haas R. The monoclonal anti-VLA-4 antibody natalizumab mobilizes CD34+ hematopoietic progenitor cells in humans. *Blood* 2008; **111**: 3893–3895.
- Del Poeta G, Dal Bo M, Del Principe MI, Pozzo F, Rossi FM, Zucchetto A *et al.* Clinical significance of c.7544-7545 delCT NOTCH1 mutation in chronic lymphocytic leukaemia. *Br J Haematol* 2013; **160**: 415–418.
- Brocklebank AM, Sparrow RL. Enumeration of CD34+ cells in cord blood: a variation on a single-platform flow cytometric method based on the ISHAGE gating strategy. *Cytometry* 2001; **46**: 254–261.
- Bonig H, Priestley GV, Oehler V, Papayannopoulou T. Hematopoietic progenitor cells (HPC) from mobilized peripheral blood display enhanced migration and marrow homing compared to steady-state bone marrow HPC. *Exp Hematol* 2007; **35**: 326–334.
- Rigolin GM, Fraulini C, Ciccone M, Mauro E, Bugli AM, De AC *et al.* Neoplastic circulating endothelial cells in multiple myeloma with 13q14 deletion. *Blood* 2006; **107**: 2531–2535.
- Rigolin GM, Maffei R, Rizzotto L, Ciccone M, Sofritti O, Daghia G *et al.* Circulating endothelial cells in patients with chronic lymphocytic leukemia: clinical-prognostic and biologic significance. *Cancer* 2010; **116**: 1926–1937.
- Zucchetto A, Sonogo P, Degan M, Bomben R, Dal Bo M, Russo S *et al.* Signature of B-CLL with different prognosis by shrunken centroids of surface antigen expression profiling. *J Cell Physiol* 2005; **204**: 113–123.

Supplementary Information accompanies this paper on the Leukemia website (<http://www.nature.com/leu>)

ORIGINAL ARTICLE

# The CD49d/CD29 complex is physically and functionally associated with CD38 in B-cell chronic lymphocytic leukemia cells

A Zucchetto<sup>1,9</sup>, T Vaisitti<sup>2,9</sup>, D Benedetti<sup>1</sup>, E Tissino<sup>1</sup>, V Bertagnolo<sup>3</sup>, D Rossi<sup>4</sup>, R Bomben<sup>1</sup>, M Dal Bo<sup>1</sup>, MI Del Principe<sup>5</sup>, A Gorgone<sup>6</sup>, G Pozzato<sup>7</sup>, G Gaidano<sup>4</sup>, G Del Poeta<sup>5</sup>, F Malavasi<sup>8</sup>, S Deaglio<sup>2,10</sup> and V Gattei<sup>1,10</sup>

CD49d and CD38 are independent negative prognostic markers in chronic lymphocytic leukemia (CLL). Their associated expression marks a disease subset with a highly aggressive clinical course. Here, we demonstrate a constitutive physical association between the CD49d/CD29 integrin complex and CD38 in primary CLL cells and B-cell lines by (i) cocapping, (ii) coimmunoprecipitation and (iii) cell adhesion experiments using CD49d-specific substrates (vascular-cell adhesion molecule-1 or CS-1/H89 fibronectin fragments). The role of CD38 in CD49d-mediated cell adhesion was studied in CD49d<sup>+</sup>CD38<sup>+</sup> and CD49d<sup>+</sup>CD38<sup>-</sup> primary CLL cells, and confirmed using CD38 transfectants of the originally CD49d<sup>+</sup>CD38<sup>-</sup> CLL-derived cell line Mec-1. Results indicate that CD49d<sup>+</sup>CD38<sup>+</sup> cells adhered more efficiently onto CD49d-specific substrates than CD49d<sup>+</sup>CD38<sup>-</sup> cells ( $P < 0.001$ ). Upon adhesion, CD49d<sup>+</sup>CD38<sup>+</sup> cells underwent distinctive changes in cell shape and morphology, with higher levels of phosphorylated Vav-1 than CD49d<sup>+</sup>CD38<sup>-</sup> cells ( $P = 0.0006$ ) and a more complex distribution of F-actin to the adhesion sites. Lastly, adherent CD49d<sup>+</sup>CD38<sup>+</sup> cells were more resistant to serum-deprivation-induced ( $P < 0.001$ ) and spontaneous ( $P = 0.03$ ) apoptosis than the CD49d<sup>+</sup>CD38<sup>-</sup> counterpart. Altogether, our results point to a direct role for CD38 in enhancing CD49d-mediated adhesion processes in CLL, thus providing an explanation for the negative clinical impact exerted by these molecules when coexpressed in neoplastic cells.

*Leukemia* (2012) 26, 1301–1312; doi:10.1038/leu.2011.369; published online 6 January 2012

**Keywords:** CLL; CD49d; CD38; integrins; chronic lymphocytic leukemia

## INTRODUCTION

The role of microenvironment in tumor cell maintenance and expansion has been described for different B-cell malignancies, including chronic lymphocytic leukemia (CLL). CLL cells, like other small B-cell lymphoma cells, develop in specialized niches present in the bone marrow and in secondary lymphoid organs, where interactions with different populations of accessory stromal/endothelial cells and T cells through different receptor–ligand pairs convey proliferation and survival signals to malignant cells.<sup>1–5</sup>

A key role in the interactions of CLL cells with other microenvironmental cell populations has been described for CD49d and CD38, two molecules whose expression by CLL cells is generally correlated,<sup>6–8</sup> and is known to mark disease subsets with particularly unfavorable clinical outcomes.<sup>6–12</sup> CD49d, also known as the  $\alpha 4$  integrin subunit, is usually complexed with CD29 (the  $\beta 1$  subunit) and mediates interactions with extracellular matrix components, including fibronectin (FN)<sup>13,14</sup> or with opposing cells through the binding with vascular-cell adhesion molecule-1 (VCAM-1).<sup>15</sup> CD38 is a cell surface glycoprotein acting as an enzyme and a receptor for CD31, this interaction regulating

lymphocyte adhesion to endothelial cells and promoting lymphocyte activation.<sup>16–18</sup> In CLL cells, CD49d and CD38 are functionally linked, through the production of specific soluble factors, in a circuitry regulating adhesion and survival of CD49d<sup>+</sup>CD38<sup>+</sup> CLL.<sup>5</sup>

Several studies demonstrated the propensity of CD38 to form supra-molecular complexes in various hematopoietic cell types.<sup>19–24</sup> The reason of such physical interactions of CD38 is at least twofold. First, given the lack of signaling motifs in the cytoplasmic tail of CD38, CD38-mediated intracellular signal transduction is strongly influenced by lateral associations, usually occurring in the context of membrane lipid rafts, with other cell surface molecules and/or membrane adaptors specialized in signal transduction, for example, CD19 and CD81.<sup>22,25</sup> Second, CD38, through its lateral interactions, may enhance the activity of other molecules. In particular, CD38 was demonstrated to have an active role in synergizing with the CXCR4 signaling pathway, by controlling CXCL12-driven chemotaxis/homing processes of CLL cells to growth-favorable niches.<sup>26</sup> Moreover, lateral associations on the plasma membrane of the CD49d/CD29 complex, with the tetraspanins CD81 and CD9, have been demonstrated to have a

<sup>1</sup>Clinical and Experimental Onco-Hematology Unit, Centro di Riferimento Oncologico, I.R.C.C.S., Aviano, Italy; <sup>2</sup>Human Genetics Foundation, Department of Genetics, Biology and Biochemistry, University of Turin, Turin, Italy; <sup>3</sup>Signal Transduction Unit, Section of Human Anatomy, Department of Morphology and Embryology, University of Ferrara, Ferrara, Italy; <sup>4</sup>Department of Clinical and Experimental Medicine and IRCAD, Division of Hematology, Amedeo Avogadro University of Eastern Piedmont, Novara, Italy; <sup>5</sup>Division of Hematology, S.Eugenio Hospital and University of Tor Vergata, Rome, Italy; <sup>6</sup>Division of Hematology, Ferrarotto Hospital, University of Catania, Catania, Italy; <sup>7</sup>Department of Internal Medicine and Hematology, Maggiore General Hospital, University of Trieste, Trieste, Italy and <sup>8</sup>Laboratory of Immunogenetics, Department of Genetics, Biology and Biochemistry, University of Turin, Turin, Italy. Correspondence: Dr V Gattei, Clinical and Experimental Onco-Hematology Unit, Centro di Riferimento Oncologico, I.R.C.C.S., Via Franco Gallini 2, Aviano (PN), Italy.

E-mail: vgattei@cro.it

<sup>9</sup>Co-first authors.

<sup>10</sup>Co-last authors.

Received 22 July 2011; revised 27 October 2011; accepted 24 November 2011; published online 6 January 2012

role in enhancing the phosphorylation cascade triggered by the integrin–ligand association.<sup>27</sup>

Recently, a cell surface macromolecular complex which includes CD38, CD49d, CD44 and MMP-9 has been found in poor prognosis CLL.<sup>28</sup> Here we investigated in detail the physical relationship between the CD49d/CD29 heterodimer and CD38 in CLL, and provided evidence that the resulting molecular complex enhances CD49d-mediated activities.

## MATERIALS AND METHODS

### CLL patients and cell lines

This study was approved by the Internal Review Board of the Centro di Riferimento Oncologico di Aviano (Approval no. IRB-05-2010). It includes peripheral blood samples collected after informed consent for diagnostic/prognostic purposes from 488 CLL patients diagnosed according to standard criteria,<sup>29</sup> and characterized for CD49d, CD38 and ZAP-70 expression, IGHV mutational status, and fluorescence *in situ* hybridization karyotype (Supplementary Table S1).<sup>6,30</sup> This series was employed to extend our previous observations on correlated expression and clinical impact of CD49d and CD38 in CLL.<sup>6,31,32</sup>

For CD49d and CD38 simultaneous detection, a combination of anti-CD5-FITC, anti-CD49d-PE, anti-CD19-PerCP and anti-CD38-APC monoclonal antibodies (mAbs; Becton Dickinson, San Jose, CA, USA) was used. A CLL case was judged CD49d<sup>+</sup> and/or CD38<sup>+</sup> when the marker was expressed in at least 30% of the CD5<sup>+</sup>CD19<sup>+</sup> CLL cell population, as described.<sup>6,10</sup> To correlate the fluorescence intensity of CD38 and CD49d, mean fluorescence intensity data were also recorded.

Functional and biochemical experiments (see below) were carried out on CLL cases expressing either a CD49d<sup>+</sup>CD38<sup>+</sup> or a CD49d<sup>+</sup>CD38<sup>-</sup> phenotype (Supplementary Table S2). In these cases, CLL cells were purified from the peripheral blood by density gradient centrifugation followed by negative selection using a mixture of anti-CD3, anti-CD16 and anti-CD14 mAbs (Laboratory of Immunogenetics, Turin, Italy) and separation by immunomagnetic beads, as described.<sup>33</sup> In all cases B-cell purity was  $\geq 95\%$ , as assessed by flow cytometry.

The Burkitt's lymphoma cell line Raji (CD49d<sup>+</sup>CD38<sup>+</sup>), the myeloma-like cell line RPMI-8226 (CD49d<sup>+</sup>CD38<sup>+</sup>) and the CLL-derived cell line Mec-1 (Mec-1 WT; CD49d<sup>+</sup>CD38<sup>-</sup>) were cultured as described.<sup>33</sup> CD49d<sup>+</sup>CD38<sup>+</sup> Mec-1 (Mec-1 S38W or Mec-1 CD38 EP) and CD49d<sup>+</sup>CD38<sup>-</sup> Mec-1 (Mec-1 SEW or Mec-1 EP) transfectants were generated by infection with lentiviral particles or electroporation of expression vectors containing or not the genetic material for CD38, as described.<sup>26</sup>

### Cocapping experiments and cell treatment with methyl- $\beta$ -cyclodextrin

Cocapping experiments were carried out on primary CLL cells and cell lines exactly as previously reported utilizing anti-CD38 (SUN-4B7, Laboratory of Immunogenetics), anti-CD49d (clone HP2/1, Serotec, Oxford, UK) mAbs and TRITC-labeled G $\alpha$ Mlg (Dako, Glostrup, Denmark) for capping, and anti-CD38-FITC, CD81-FITC, HLA Class I-FITC (Laboratory of Immunogenetics), CD29-FITC (clone K20, Immunotech, Marseille, France) and CD49d-FITC (clone 44H6, Serotec) for counterstaining.<sup>33</sup> When indicated, CLL cells were pre-incubated (30 min, 37 °C) with 10 mM methyl- $\beta$ -cyclodextrin (M $\beta$ CD, Sigma, St Louis, MO, USA). Cells were fixed (4% paraformaldehyde), settled on poly-L-lysine-coated coverslips, and analyzed either with an Olympus 1  $\times$  70 microscope, using the FluoView software (Olympus, Milan, Italy), or with a Nikon Eclipse 90i microscope and the ND2 software (Nikon, Tokyo, Japan).

### Lipid raft isolation, immunoprecipitation and western blotting

Lysates from purified CLL, Mec-1 SEW or Mec-1 S38W cells were separated into supernatant (S; cytosolic and soluble membrane proteins) and pellet (P; cholesterol-enriched membrane areas and cytoskeletal proteins) fractions in the presence or not of 60 mM octyl- $\beta$ -glucopyranoside, as described.<sup>22</sup> Immunoprecipitations were performed with anti-CD49d (Serotec), anti-CD29 (clone Moon-4), anti-CD38 (clones OKT-10 and AT13/5) and X63 (irrelevant, isotype-matched mAb, all produced in the

Laboratory of Immunogenetics) mAbs and analyzed by western blot using anti-CD38 (SUN-4B7), anti-CD49d (Abcam, Cambridge, UK), anti-CD29 (Moon-4) or anti-Vav-1 (Santa Cruz Biotechnology, Santa Cruz, CA, USA) mAbs, as described.<sup>22,26</sup>

Selected western blotting was performed using cell lysates from Mec-1 incubated or not with anti-CD38 mAbs and left to adhere onto culture coverslips for 2 and 5 min, hybridized with antibodies recognizing Vav-1 (Santa Cruz), Vav-1 pTyr-174 (Abcam), and Beta actin (Sigma). Densitometric quantitation of western blots was determined with the ImageJ 1.43u software (<http://rsbweb.nih.gov/ij/>).

### Preparation of VCAM-1- or FN-coated culture dishes/coverslips

The H89 FN fragment, containing several binding sites for CD49d, was a kind gift of Angeles Garcia-Pardo (Centro de Investigaciones Biológicas, Madrid, Spain). Purified FN CS-1 fragments were a kind gift of Alfonso Colombatti (Centro di Riferimento Oncologico, Aviano, Italy). The human recombinant VCAM-1 was from R&D Systems (Minneapolis, MN, USA).

For adhesion assays, 96-well flat-bottomed culture dishes were coated with 10  $\mu$ g/ml FN (H89 or CS-1 fragments) or VCAM-1 in bicarbonate buffer (4 °C, overnight), followed by phosphate-buffered saline supplemented with 1.0% bovine serum albumin (2 h, room temperature). For immunofluorescence studies, ethanol-washed coverslips were placed into 24-well plates and coated with either VCAM-1 or FN as described above.

### Cell adhesion assay

Mec-1 cells were labeled with the vital fluorochrome calcein AM (Molecular Probes, Eugene, OR, USA), seeded ( $2 \times 10^5$  cells/well) onto 96-well plates coated with the appropriate substrate, and incubated for 15 or 30 min at 37 °C. Adherent cells were evaluated by fluorescence detection in a computer-interfaced microplate fluorometer. Results were expressed as relative fold change in fluorescence intensity compared to relative controls.

For adhesion assays with primary CLL cells,  $1 \times 10^6$  purified cells were seeded onto coverslips coated with the appropriate substrate for 15 min. Adherent cells were fixed (4% paraformaldehyde), and coverslips mounted on slides and microscopically analyzed using a  $\times 20$  objective. After acquiring at least 10 fields per slide, adherent cells were counted, and results reported as mean number of adherent cells per field.

### Immunofluorescence

Mec-1 ( $0.2 \times 10^6$ /well) or primary CLL cells ( $1 \times 10^6$ /well) were plated onto coverslips coated with the appropriate substrate and incubated for different time points at 37 °C to promote adhesion. Adherent cells were sequentially incubated with unconjugated anti-CD49d mAbs (clone 44H6, Serotec), TRITC-labeled G $\alpha$ Mlg secondary antibody (Millipore, Billerica, MA, USA) and anti-CD38-FITC. Cells were fixed, and coverslips were mounted on slides and microscopically analyzed as above.

For Vav1 pTyr-174 detection, adherent fixed cells on coverslips were permeabilized with 0.1% Tween-20, blocked with 10% fetal bovine serum, and stained with anti-Vav-1 pTyr-174 (Abcam) followed by TRITC-conjugated secondary antibody and fluorescein-labeled Phalloidin (Sigma) to visualize F-actin filaments. Coverslips were mounted on slides and microscopically analyzed as above. Staining quantification was performed using ImageJ software by acquiring at least 10 high-power fields for analysis.

### Cell viability assays

Mec-1 cells ( $0.5 \times 10^5$ /well) or primary CLL cells ( $0.5 \times 10^6$ /well) were, respectively, seeded on VCAM-1-coated 96-well or 24-well plates in Roswell Park Memorial Institute medium without fetal bovine serum. Cell viability was evaluated by sequentially staining cells with AnnexinV (Becton-Dickinson) and 7-amino-actinomycin-D (7-AAD, Becton-Dickinson). For Mec-1 cells absolute counts, 20  $\mu$ l of Perfect-Count Microspheres (Cytognos, Salamanca, Spain) containing a known number of beads per unit volume were added to 100  $\mu$ l of the cell suspension. Data were

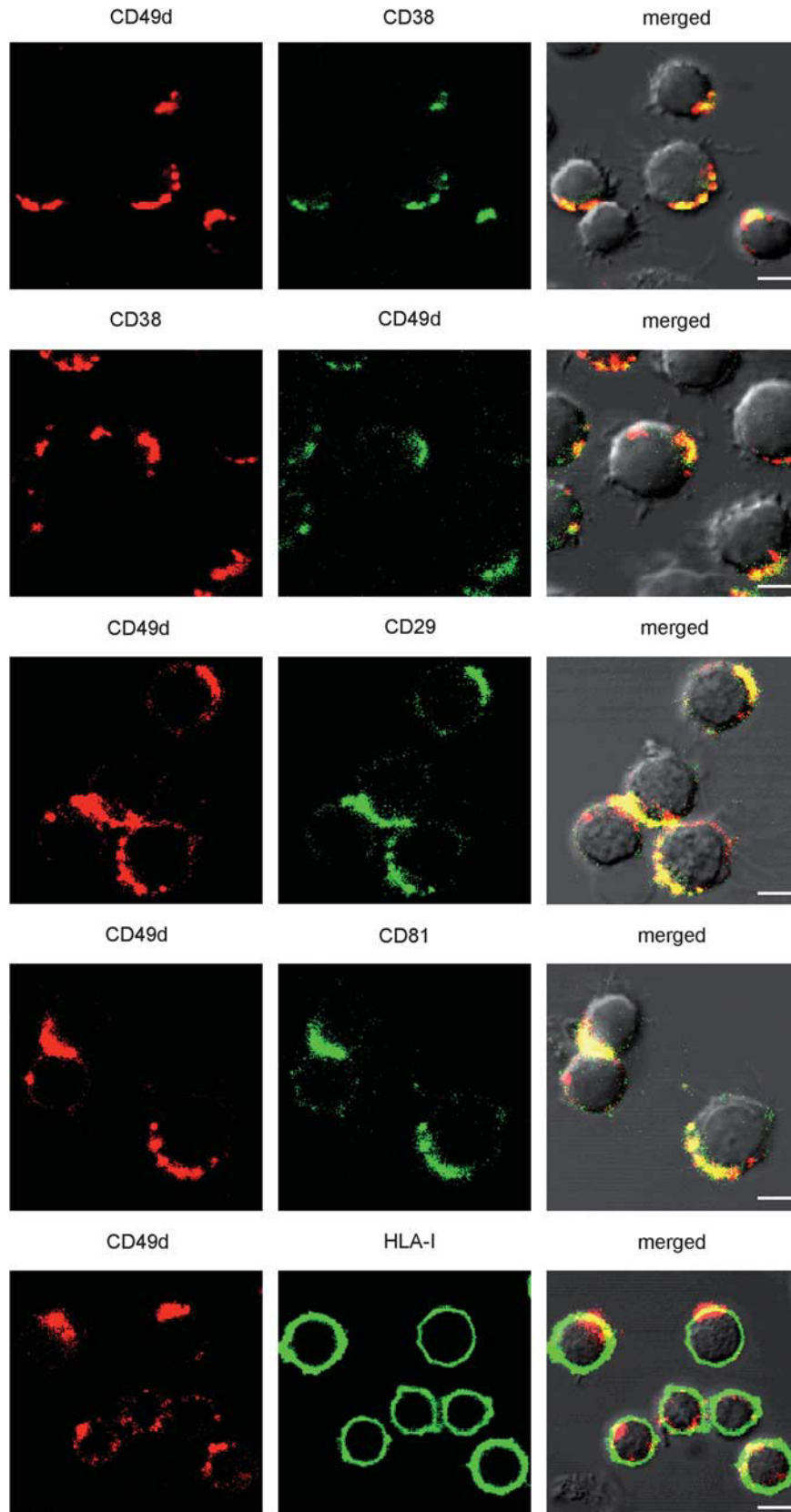


**Figure 1.** CD38 and CD49d are laterally associated on the CLL cell membrane. Purified B cells from CD38<sup>+</sup>CD49d<sup>+</sup> CLL cases were incubated with either the anti-CD38 or the anti-CD49d mAbs, next followed by TRITC-labeled G $\alpha$ Mlg (red), and incubated for 30 min at 37 °C to promote capping. Counterstaining was performed with FITC-labeled mAbs to CD38, CD49d, CD29, CD81 or HLA-I (green). The panels on the right show the merging of the two images and the differential interference contrast field. Images refer to one representative case (CLL#1). Original magnification  $\times 60$ . Scale bars, 5  $\mu$ m.

acquired on a FACSCanto flow cytometer and analyzed by Diva software (Becton-Dickinson).

### Statistical analysis

Data were compared using either the non-parametric Mann-Whitney test or the Student's *t*-test for independent samples. Association between CD49d and CD38 expression and time-to-treatment (time from diagnosis to treatment or end of follow-up) was calculated as reported.<sup>6</sup> All statistical analyses were performed using the MedCalc software (MedCalc, Mariakerke, Belgium).

## RESULTS

Expression of CD49d and CD38 is correlated and marks a CLL subset with very poor prognosis

Expression of CD49d and CD38 was investigated by flow cytometry in the neoplastic component of 488 CLL patients (Supplementary Figure S1). Using the 30% positive cut-off value for both the antigens,<sup>9,31,32</sup> 273/488 cases (55.9%) were concordantly negative (CD49d<sup>-</sup>CD38<sup>-</sup>), whereas 96 cases (19.7%) were CD49d<sup>+</sup>CD38<sup>+</sup> ( $P < 0.0001$ ,  $\chi^2$ -test). Discordant CD49d<sup>+</sup>CD38<sup>-</sup> or CD49d<sup>-</sup>CD38<sup>+</sup> phenotypes were documented in 75 (15.4%) and 44 (9.0%) out of 488 cases, respectively (Supplementary Figure S1A and B). CD38 and CD49d expression intensities, evaluated as mean fluorescence intensity, were significantly correlated (Pearson's correlation coefficient  $r = 0.81$ ,  $P < 0.0001$ ,  $n = 75$ , Supplementary Figure S1C). Moreover, the simultaneous analysis of CD49d and CD38 mean fluorescence intensity performed in the CD49d<sup>+</sup>CD38<sup>+</sup> cohort used for functional experiments (Supplementary Table S2), demonstrated a high correlation between the molecules also at the cell level (in all cases  $r > 0.80$ ,  $P < 0.005$ ,  $n = 11$ , Supplementary Figure S1D).

An updating of the previously published clinical data<sup>6</sup> confirmed a worse clinical behavior for CD49d<sup>+</sup>CD38<sup>+</sup> CLL, as compared with CD49d<sup>-</sup>CD38<sup>-</sup> cases, or cases expressing either molecule (Supplementary Figure S1E).

CD49d and CD38 are laterally associated both inside and outside lipid rafts

The membrane relationship between CD49d and CD38 in CD49d<sup>+</sup>CD38<sup>+</sup> CLL cells (Supplementary Table S2) was analyzed by cocapping experiments. Antibody-mediated cross-linking of CD49d led to its redistribution in a polar aggregate at the cell surface, where a clear colocalization of CD38 was observed (Figure 1). As summarized in Table 1, anti-CD49d mAbs induced capping in about 75% of CLL cells; of these, 80% displayed a redistribution of CD38 in the context of the capping area. Similarly, a redistribution of CD49d molecules was obtained when capping was induced by anti-CD38 mAbs (Figure 1). Further cocapping experiments revealed the presence of the integrin  $\beta 1$  subunits (CD29) in CD49d caps, indicating that the  $\alpha 4$  integrin subunit (CD49d) is part of the  $\alpha 4\beta 1$  (CD49d/CD29) heterodimer. The overlapping of CD81 staining in CD49d caps confirmed the association between this tetraspanin with  $\alpha 4$  integrins,<sup>27</sup> whereas the lack of redistribution of HLA Class I molecules when caps were induced by anti-CD49d mAbs, indicated the specificity in the molecular associations revealed by this technique (Figure 1).

Association between CD49d and CD38 was also confirmed in CD49d<sup>+</sup>CD38<sup>+</sup> B-cell lines (Raji and RPMI-8226; Supplementary Figure S2A). In both the cell lines, cocaps of CD38 scored 60% of CD49d-induced caps, and CD49d molecules were observed in 70% of caps induced by anti-CD38 mAbs. Also in these cellular models, CD49d was laterally associated with CD29 and CD81 but not with HLA-I molecules (Table 1 and Supplementary Figure S2B).

The lateral association between CD49d and CD38 was next confirmed in primary CLL cells ( $n = 6$ ) at the biochemical level by immunoprecipitation of CD49d followed by western blotting with

**Table 1.** Cocapping experiment results

Cap/cocap	Total cells, number	Caps, number	Cocaps, number (%)
<b>CLL</b>			
CD49d/CD38	108	75	60 (80)
CD49d/CD29	82	64	59 (92)
CD49d/CD81	100	63	50 (79)
CD49d/HLA-I	110	72	2 (3)
<b>B-cell lines</b>			
CD49d/CD38	218	114	69 (61)
CD49d/CD29	108	51	38 (74)
CD49d/CD81	245	127	83 (66)
CD49d/HLA-I	254	115	20 (17)
CD38/CD49d	167	104	72 (69)
CD38/CD29	101	45	27 (60)
<b>CLL (M<math>\beta</math>CD treatment)</b>			
CD49d/CD38	144	98	91 (93)
CD49d/CD29	109	71	65 (92)
CD49d/CD81	150	79	60 (76)

Abbreviation: CLL, chronic lymphocytic leukemia. Cumulative data from different experiments performed with CLL cells, B-cell lines (Raji and RPMI-8226) and CLL cells after M $\beta$ CD treatment. The number of total counted cells and the number of caps is presented as an absolute value, while cocaps are presented both as an absolute value and as a percentage of capped cells. Cells exhibiting partial redistribution of the surface molecule detected by the primary capping antibody were excluded from the analysis.

anti-CD38 mAb. These experiments were performed after separating cell membranes on the basis of cholesterol content, into S and P fractions.<sup>22</sup> This approach demonstrated that CD38 coimmunoprecipitated with CD49d, and that CD49d/CD38 complexes could be found both inside and outside the cholesterol-enriched raft domains. Although no preferential association was observed when anti-CD38 immunoprecipitates were blotted with anti-CD49d mAbs (data not shown), CD38 immunoprecipitates contained significant amounts of CD29, and CD29 immunoprecipitates were associated with both CD38 and CD49d (Figure 2a). Collectively, these results suggest that the association between CD49d and CD38 mainly occurred via the CD29 subunit.

The maintenance of CD49d/CD38 and CD38/CD29 complexes, and their partial redistribution to the S fraction upon treatment of the cells with octyl-D-glucopyranoside (Figure 2a), which solubilizes raft-associated proteins, suggest that these molecular interactions are independent of the integrity of lipid rafts, in line with the participation of cytoskeletal proteins stabilizing the association. A further confirmation of these observations was provided by cocapping experiments upon pretreatment of CLL cells with M $\beta$ CD, a chemical that disrupts lipid rafts by extracting cholesterol from plasma membranes. Results clearly showed that the CD49d/CD38 association was largely unaffected by lipid rafts disruption; the same was observed for other associations, including CD49d/CD29, CD49d/CD81 and CD38/CD29 (Table 1, Figure 2b and data not shown).

CD38 localizes in CD49d-specific adhesion sites

The molecular interaction between CD49d and CD38 may be of functional relevance in the context of CD49d-mediated activities. To test this hypothesis, CLL cells were allowed to adhere to CD49d-specific substrates (VCAM-1 or H89/CS-1 FN fragments), and double stained with mAbs against CD49d and CD38. Confocal microscopy clearly showed a colocalization of CD49d and CD38 in the cell uropods during the stages of cell spreading onto both VCAM-1 and CS-1/H89 FN fragments (Figure 3).

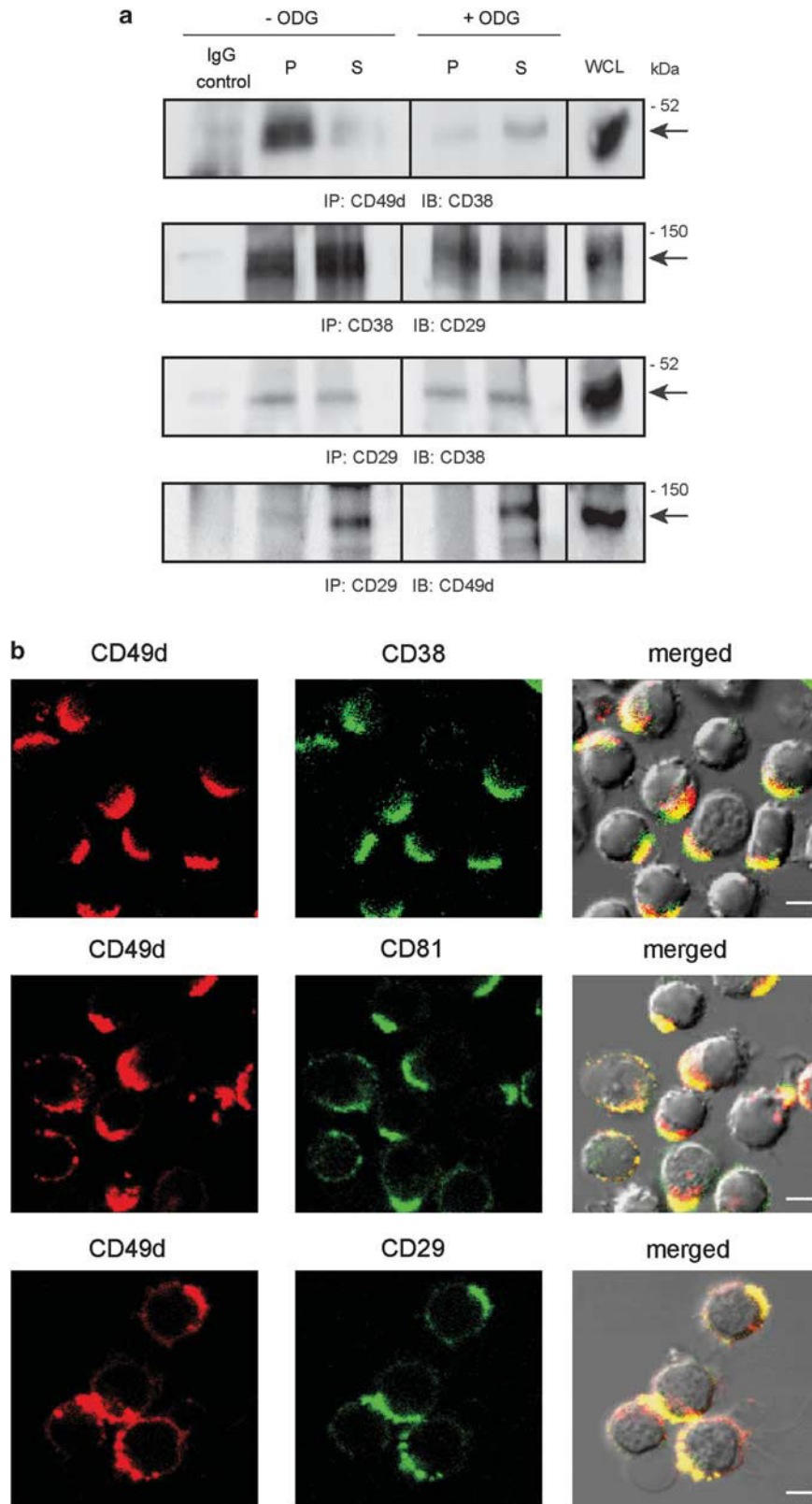


**Figure 2.** CD38 coimmunoprecipitates with the CD49d/CD29 complex and their lateral association is independent of lipid rafts. **(a)** CLL cells lysates, fractionated into a supernatant (S) and a pellet (P) fraction, were subjected to immunoprecipitation with anti-CD49d, anti-CD38 or anti-CD29 mAbs and then incubated with either anti-CD38, anti-CD29 or anti-CD49d mAbs. Where indicated, ODG (octyl- $\beta$ -glucopyranoside) was added to the lysis buffer. Immunoprecipitation with irrelevant IgG was performed as control. The blots refer to one representative case (CLL#6) out of six. WCL, whole cell lysate. **(b)** Purified B cells from CD38<sup>+</sup>CD49d<sup>+</sup> CLL cases were incubated with 10 mM methyl- $\beta$ -cyclodextrin (M $\beta$ CD) in order to extract cholesterol from the plasma membranes. CD49d capping (red) and counterstaining with FITC-labeled CD38, CD81 and CD29 (green) were then performed. The panels on the right show the merging of the two images and the differential interference contrast field. Images refer to one representative case (CLL#5). Original magnification  $\times 60$ . Scale bar, 5  $\mu$ m.

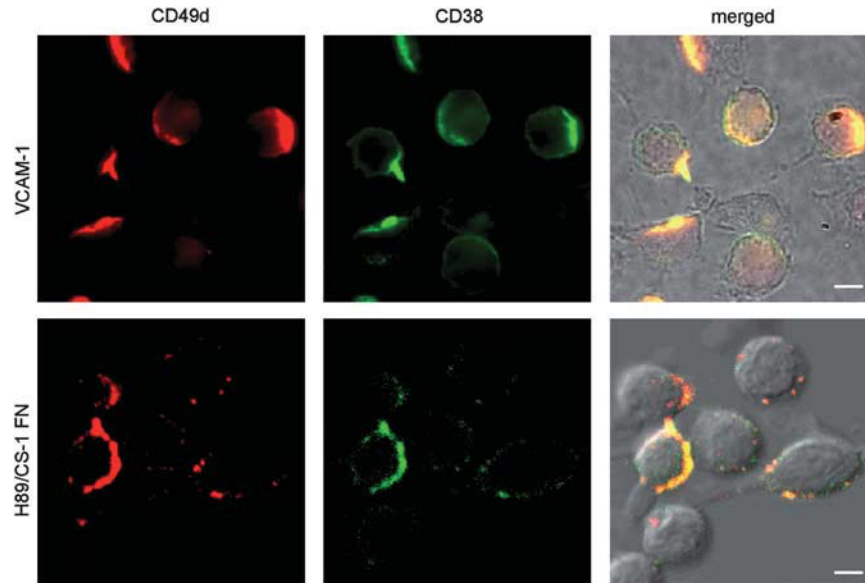


**Figure 3.** CD38 localizes in the cell adhesion sites. CLL cells were plated onto either VCAM-1-coated or FN-coated (H89/CS-1 FN fragment) coverslips and allowed to adhere for 30 min at 37 °C. Adherent cells were incubated with the anti-CD49d mAb, next reacted with TRITC-labeled G $\alpha$ Mlg (red) and finally stained with CD38-FITC (green). Coverslips were mounted on slides and analyzed. The panels on the right show the merging of the two images and the differential interference contrast field. Images refer to two representative cases (CLL #3, upper panel; CLL#4, lower panel). Original magnification  $\times 60$ . Scale bar, 5  $\mu$ m.

#### CD38 influences CD49d-mediated cell adhesion

To investigate whether CD38 had a role in CD49d-mediated adhesion processes, we took advantage of the CD49d<sup>+</sup>CD38<sup>-</sup> CLL-derived cell line model Mec-1, in which CD38 expression was induced by viral infection (Mec-1 S38W).<sup>26</sup> Mec-1 S38W cells maintained the original phenotype in terms of CD49d, CD19 and CD5 expression (Supplementary Figure S3A and data not shown), and membrane localization of CD38 was similar to that observed in primary CLL cells, being distributed both inside and outside the lipid rafts (Supplementary Figure S3B). Cocapping experiments confirmed the CD49d/CD38 physical association also in Mec-1 S38W cells (Supplementary Figure S3C). The preferential association between CD38 and the CD49d/CD29 complex was confirmed by showing that CD38 is present in CD49d immunoprecipitates. In line with data obtained in CLL cells, also in Mec-1 transfectants CD38 immunoprecipitates contained CD29, in turn complexed with CD49d (Supplementary Figure S3D).

The adhesive properties of Mec-1 transfectants were investigated by adhesion experiments onto VCAM-1 substrates. A marked increase in the number of Mec-1 S38W cells adherent to VCAM-1 as compared with both Mec-1 SEW (Figures 4a and b) and Mec-1 WT (Supplementary Figure S3E) was observed. A quantification of adherent cells revealed  $4.7 \pm 0.8$  vs  $2.0 \pm 0.5$  vs  $2.0 \pm 0.2$  fold increase of adherent cells as compared with controls after 15 min and  $5.9 \pm 0.9$  vs  $2.2 \pm 0.4$  vs  $2.0 \pm 0.3$  after 30 min ( $P < 0.05$  in all comparisons) for Mec-1 S38W, Mec-1 SEW and Mec-1 WT, respectively. Cell pre-incubation with the function-blocking anti-CD49d mAb HP2/1 completely abolished cell adhesion to VCAM-1 (Figure 4b). The increased adhesion onto VCAM-1 substrates of Mec-1 S38W cells was due to CD38 expression and not to lentiviral infection, as demonstrated by additional adhesion assays performed with Mec-1 CD38 EP cells (Supplementary Figure S3E) in which CD38-expressing vectors were introduced by electroporation (Supplementary Figure S3E).

Besides an increased adhesion (Figures 4a and b), phase-contrast microscopy images highlighted a different cell morphology characterizing VCAM-1 adherent Mec-1 S38W cells. As shown in Figure 4a (lower panels), Mec-1 S38W cells displayed a more

complex pattern of filopodia-like protrusions than Mec-1 SEW, with a colocalization of CD49d and CD38 in these adhesion sites.

Pre-incubation of Mec-1 S38W with the anti-CD38 mAb SUN-4B7 resulted in a significant reduction of cell adhesion onto VCAM-1, whereas no alteration was observed when using the isotype-matched anti-CD38 mAb OKT-10 (Figures 4c and d). Moreover, Mec-1 S38W adherent cells pre-treated with the anti-CD38 mAb SUN-4B7 lost their complex pattern of cell morphology, being instead characterized by a cell shape comparable to that of Mec-1 SEW (Figure 4c, lower panels).

Similar results, both in terms of increased adhesion and modified cell morphology of adherent cells, were obtained using FN, either as H89 or CS-1 fragments, as alternative CD49d-dependent substrate (data not shown). Collectively, these data indicate a contribution of CD38 in enhancing CD49d-mediated adhesion and cell spreading.

#### CD38 promotes different patterns of CD49d-mediated signaling protein phosphorylation

Phosphorylation of Vav-1 at tyrosine-174 (Vav-1 pTyr-174), an early event in the downstream pathway leading to integrin-induced actin polymerization,<sup>34,35</sup> was investigated in the early phases of adhesion of Mec-1 cells to CD49d-specific substrates.

After 5 min of VCAM-1 adhesion, Mec-1 S38W cells exhibited stronger phosphorylation of Vav-1 compared with Mec-1 SEW ( $P < 0.001$ ), mainly localized to the periphery of the cells, near the actin-rich structures (Figures 5a and b). Consistently, western blot analysis demonstrated that adhesion onto VCAM-1 substrates for 2 and 5 min yielded a stronger upregulation of Vav-1 pTyr-174 in Mec-1 S38W than Mec-1 SEW cells (Figure 5c), both the cell lines displaying comparable levels of total Vav-1 (data not shown). Moreover, slightly higher constitutive levels of Vav-1 pTyr-174 were observed in Mec-1 S38W ( $P = 0.02$ ), suggesting a basal activation of the integrin signaling pathway in CD38-expressing cells. Overlapping results were obtained in experiments carried out by utilizing other CD49d-specific adhesive substrates (that is, CS-1 or H89 FN fragments; data not shown).

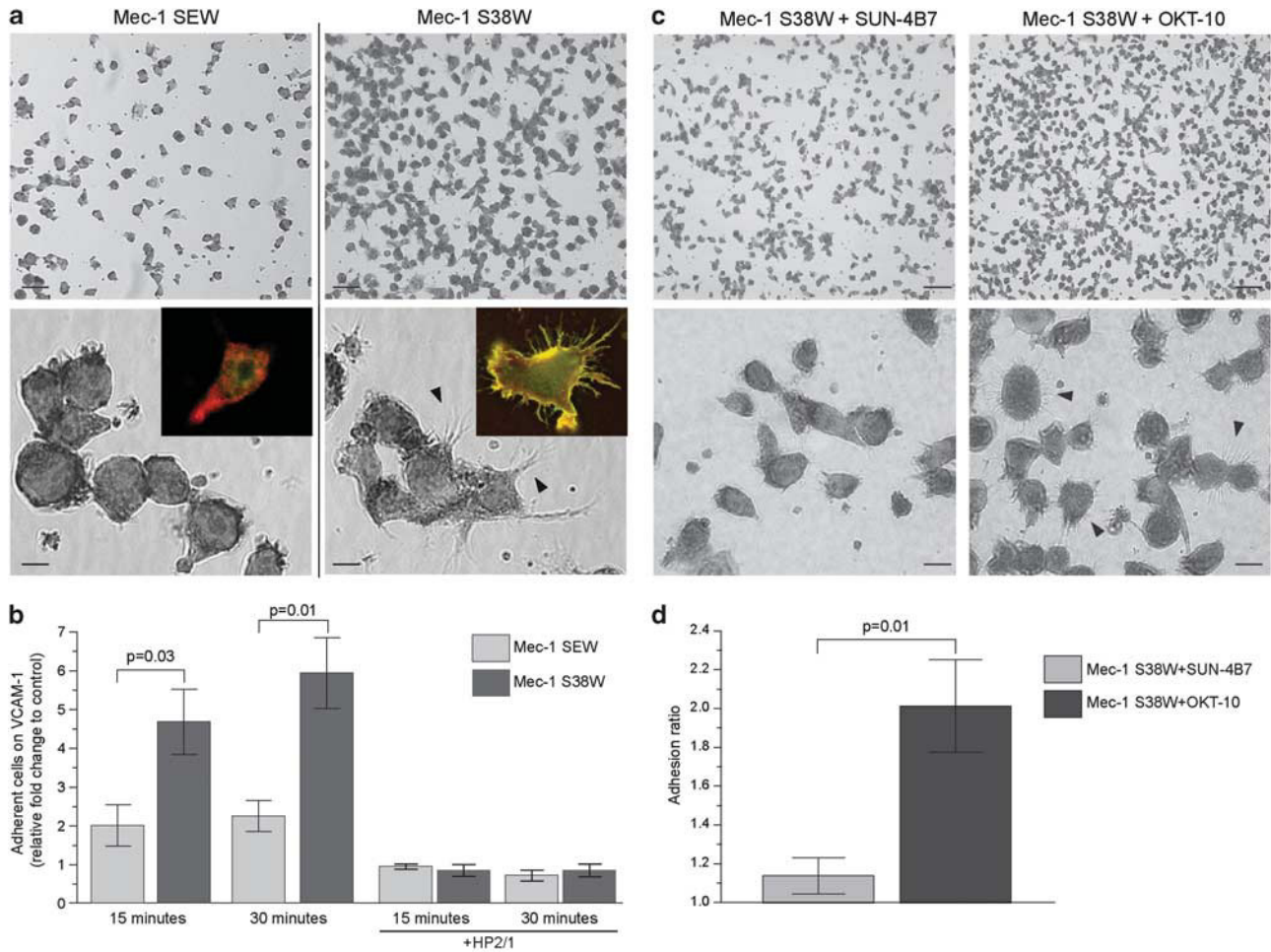


**Figure 4.** Influence of CD38 in CD49d-mediated cell adhesion using the Mec-1 cell line model. **(a)** Representative phase-contrast microscopy fields are reported for Mec-1 SEW (left panels) and Mec-1 S38W (right panels) adhesion on VCAM-1. Insets show double staining with anti-CD38 (green) and anti-CD49d (red). Arrows indicate the filopodia-like protrusions characterizing Mec-1 S38W adherent cells. Original magnification of the upper panels  $\times 20$ , of lower panels and insets  $\times 100$ . Scale bars upper panel,  $25 \mu\text{m}$ ; lower panel,  $6 \mu\text{m}$ . **(b)** Mec-1 SEW and Mec-1 S38W cells, labeled with the vital fluorochrome calcein AM, were seeded onto 96-well VCAM-1-coated plates and incubated for 15 or 30 min at  $37^\circ\text{C}$ . The specificity of the adhesions was verified through cell pre-incubation with the function-blocking anti-CD49d mAb HP2/1. Results were expressed as relative fold change in fluorescence intensity compared with controls carried out by seeding cells onto bovine serum albumin. Adhesion values refer to the mean  $\pm$  s.e.m. of four independent experiments run in triplicate. **(c)** Representative phase-contrast microscopy fields of Mec-1 S38W adhesion on VCAM-1 after pre-incubation with anti-CD38 SUN-4B7 (left) or OKT-10 (right) mAbs. Arrows indicate the filopodia-like protrusions specifically characterizing Mec-1 S38W adhesion. Original magnification upper panels  $\times 20$ , lower panels  $\times 100$ . Scale bars upper panel,  $40 \mu\text{m}$ ; lower panel,  $10 \mu\text{m}$ . **(d)** Mec-1 S38W cells pretreated with either SUN-4B7 or OKT-10 anti-CD38 mAbs and Mec-1 SEW cells were labeled with the vital fluorochrome calcein AM, seeded onto 96-well VCAM-1-coated plates, and incubated for 30 min at  $37^\circ\text{C}$ . The relative number of adherent cells was evaluated by fluorescence detection and results were expressed as adhesion ratio, that is, the number of adherent Mec-1 S38W cells pre-incubated with anti-CD38 OKT-10 (black) or SUN-4B7 (gray) divided by the number of adherent Mec-1 SEW cells. Adhesion values refer to the mean  $\pm$  s.e.m. of four independent experiments run in triplicate.

To test whether CD38 could be directly responsible for the recruitment of Vav-1 molecules in close contact with CD49d and the integrin signaling machinery, we immunoprecipitated Mec-1 S38W cell lysates with antibodies against CD38 or CD49d. Vav-1 was present in the CD38-immunoprecipitates both inside and outside the lipid rafts, but not in immunoprecipitates formed with anti-CD49d antibodies (Figure 5d).

We next checked whether the reduction in cell adhesion observed after pretreatment of Mec-1 S38W with the anti-CD38 mAb SUN-4B7 could be explained by a reduction of Vav-1 activation. For this purpose, cells were pre-incubated with SUN-4B7 or with control OKT-10 anti-CD38 mAbs and left to adhere onto VCAM-1 substrates. Results revealed a significant reduction in Vav-1 phosphorylation levels in cells pre-treated with the SUN-4B7 blocking mAb, compared with the ones incubated with the

control binding mAb. The effect was apparent both after 2 ( $P = 0.01$ ) and 5 min ( $P = 0.001$ ; Figure 5e).

CD49d engagement prevents cell apoptosis triggered by serum deprivation

The final issue concerned the functional effects determined by the CD38/CD49d/CD29 axis in CLL cell homeostasis. We first noticed that the growth curves of Mec-1 SEW and Mec-1 S38W overlapped in the presence of 10% fetal bovine serum or under serum deprivation, the latter a condition that blocked cell growth and dramatically affected viability starting from 3–4 days of culture (Figure 5f).<sup>36</sup> Culture of Mec-1 SEW and Mec-1 S38W on VCAM-1-coated wells exerted protective effects from cell apoptosis after 4 and 5 days of culture in serum-free conditions (Figure 5f).

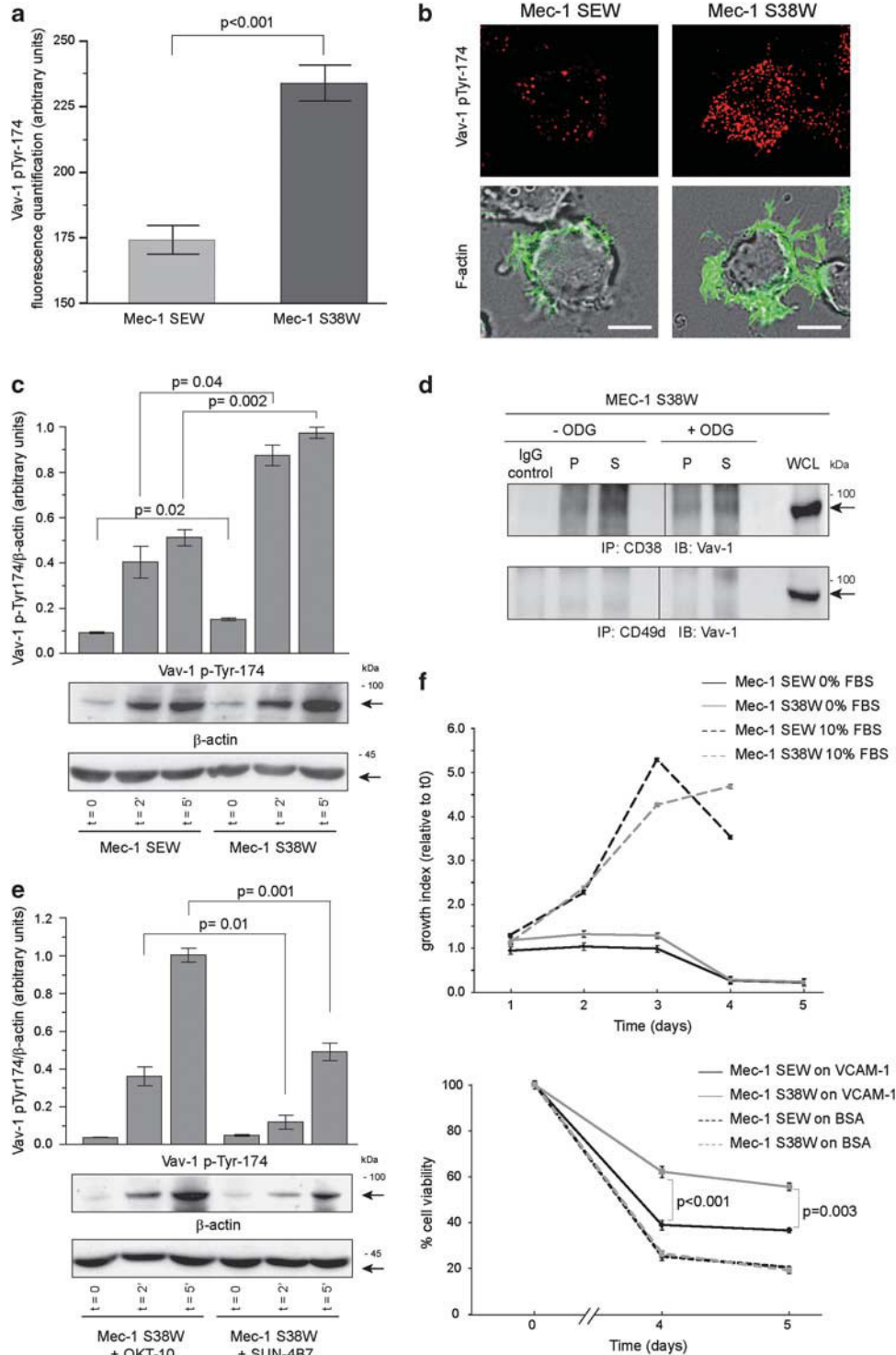
The protective effect of VCAM-1 was more pronounced in the CD49d<sup>+</sup>CD38<sup>+</sup> cell line than in the CD49d<sup>+</sup>CD38<sup>-</sup> counterpart, with 62% ± 4.8 and 55% ± 3.2 viable Mec-1 S38W cells compared with 38% ± 4.2 and 36% ± 2.2 viable Mec-1 SEW ( $P < 0.001$  and  $P = 0.003$  after 4 and 5 days respectively, Figure 5f).

CD38 influences CD49d-mediated cell adhesion in primary CLL cells

The results obtained with the Mec-1 cell line model were confirmed upon adhesion to CD49d-specific ligands of purified

CLL cells from 10 CD49d<sup>+</sup>CD38<sup>-</sup> and 10 CD49d<sup>+</sup>CD38<sup>+</sup> cases characterized by high and homogeneous CD49d expression (Supplementary Table S2).

After 15-min adhesion, CD49d<sup>+</sup>CD38<sup>+</sup> CLL cases displayed higher numbers of adherent cells compared with CD49d<sup>+</sup>CD38<sup>-</sup> cases with a median number of adherent cells per field of 290 (range 185–510) vs 100 (range 34–161,  $P = 0.0001$ , Figures 6a and b). Adherent cells from CD49d<sup>+</sup>CD38<sup>+</sup> CLL displayed changes in cell shape associated with a more complex pattern of actin-rich structures mainly clustering at the adhesion sites,



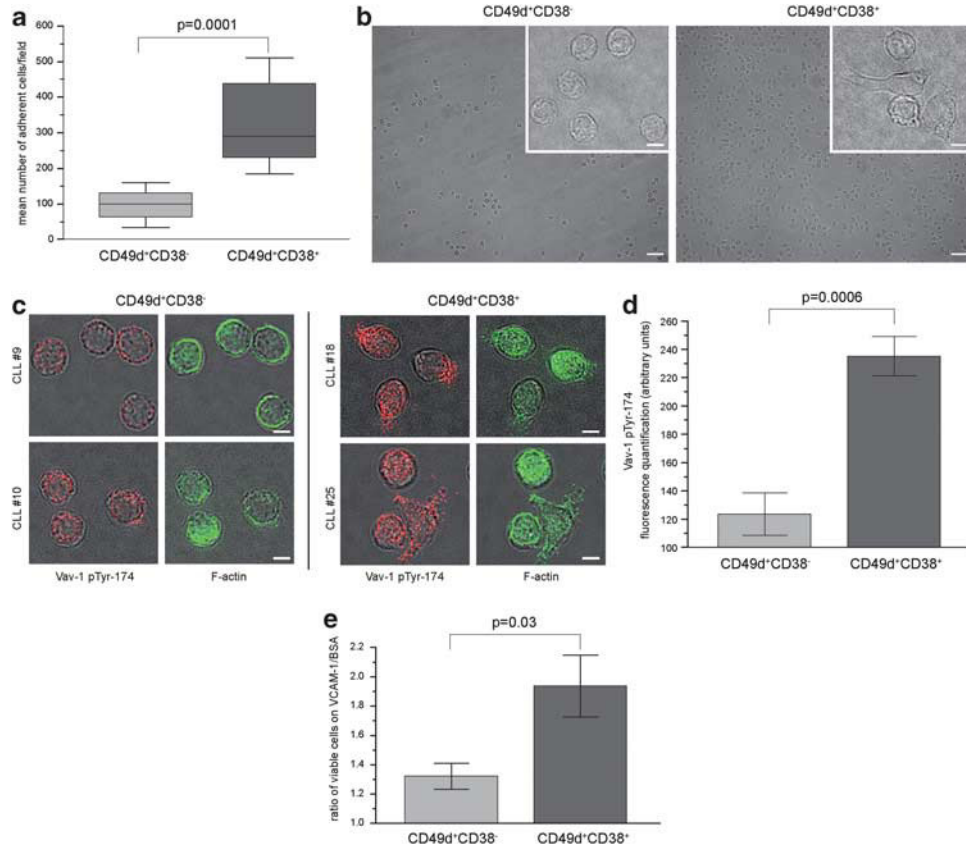


**Figure 6.** CD38 influences CD49d-mediated cell adhesion in primary CLL cells. **(a)** Adhesion assays were performed with purified CLL cells from 10 CD49d<sup>+</sup>CD38<sup>-</sup> and 10 CD49d<sup>+</sup>CD38<sup>+</sup> cases. After 15 min adhesion on VCAM-1-coated coverslips, non adherent cells were washed away, adherent cells were fixed, and coverslips were mounted on slides. At least ten fields were acquired for each slide, adherent cells were counted, and results were reported as mean number of adherent cells for field. The comparison of adhesion levels between CD49d<sup>+</sup>CD38<sup>-</sup> and CD49d<sup>+</sup>CD38<sup>+</sup> CLL is reported as box and whiskers plot, displaying the median and range values for each group. **(b)** Representative phase-contrast microscopy fields are reported for one representative CD49d<sup>+</sup>CD38<sup>-</sup> case (CLL#16, left) and one representative CD49d<sup>+</sup>CD38<sup>+</sup> case (CLL#29, right). Original magnification larger panels  $\times 20$ , insets  $\times 100$ . Scale bars larger panels, 30  $\mu$ m, insets, 5  $\mu$ m. **(c)** Vav-1 pTyr-174 (red) and F-actin (green) staining of CLL cells after adhesion on VCAM-1 from two representative CD49d<sup>+</sup>CD38<sup>-</sup> cases (CLL#14 and #15, left panels) and two representative CD49d<sup>+</sup>CD38<sup>+</sup> cases (CLL #23 and #31, right panels). Original magnification  $\times 100$ . **(d)** Quantification of Vav1 pTyr-174 fluorescence was assessed with ImageJ software using stained images from at least ten high-power fields from each experiment. **(e)** Purified CLL cells from 5 CD49d<sup>+</sup>CD38<sup>-</sup> and 5 CD49d<sup>+</sup>CD38<sup>+</sup> cases (see Supplementary Table S2) were cultured on VCAM-1 or BSA (bovine serum albumin), used as control condition, and cell viability was determined after 7 days of culture, staining cells with AnnexinV and 7-amino-actinomycin-D. Values refer to viable cells cultured onto VCAM-1 vs BSA. Error bars indicate s.e.m.

**Figure 5.** CD38 promotes different patterns of CD49d-mediated signaling protein phosphorylation. **(a)** Vav1 phosphorylation (Vav-1 pTyr-174) was evaluated in Mec-1 SEW and Mec-1 S38W after 5 min adhesion on VCAM-1. Quantification of Vav1 pTyr-174 fluorescence was assessed with ImageJ software using stained images from at least 10 high-power fields from each experiment. **(b)** Representative adherent Mec-1 SEW cell (left) and Mec-1 S38W cell (right) stained for Vav-1 pTyr-174 (upper panels) and F-actin (lower panels). Original magnification  $\times 100$ . Scale bars, 5  $\mu$ m. **(c)** Western blot analysis of Vav-1 pTyr-174 in cell lysates from Mec-1 SEW and Mec-1 S38W in resting conditions ( $t = 0$ ) and after 2 ( $t = 2'$ ) and 5 min ( $t = 5'$ ) of adhesion on VCAM-1. One representative blot is reported. Vav-1 p-Tyr174 was quantified using ImageJ software and normalized to  $\beta$ -actin. Bars represent the average results of three independent experiments. Error bars indicate s.e.m. **(d)** Cell lysates from Mec-1 S38W cells, fractionated into a supernatant (S) and a pellet (P), were subjected to immunoprecipitation with anti-CD38 (upper blot) or anti-CD49d (lower blot) mAb, and incubated with anti-Vav-1 mAb. Immunoprecipitation with irrelevant IgG was performed as negative control. Where indicated, ODG (octyl-D-glucopyranoside) was added to the lysis buffer. WCL, whole cell lysate. **(e)** Western blot analysis of Vav-1 pTyr-174 in cell lysates from Mec-1 S38W pretreated with either OKT-10 or SUN-4B7 anti-CD38 mAbs in resting conditions ( $t = 0$ ) and after 2 ( $t = 2'$ ) and 5 min ( $t = 5'$ ) of adhesion on VCAM-1. Vav-1 p-Tyr174 quantification was performed as reported above. Bars represent the average results of three independent experiments. Error bars indicate s.e.m. **(f)** A total of 50 000 Mec-1 SEW (black lines) and Mec-1 S38W (gray lines) cells were seeded on 96-well plates coated (solid lines lower panel) or not (upper panel and dashed lines lower panel) with VCAM-1, in Roswell Park Memorial Institute medium in the presence of 10% fetal bovine serum (FBS; dashed lines, upper panel) or in the absence of FBS (lower panel and solid lines upper panel). At the indicated time points, cell number (number of viable cells over the number of seeded cells) and viability were evaluated by flow cytometry. Values refer to the average from three different experiments performed in triplicate. *P*-values obtained by comparing the percentage of Mec-1 SEW and Mec-1 S38W viable cells upon 4 and 5 days of culture on VCAM-1 are reported (lower panel). Comparisons of values of Mec-1 SEW and Mec-1 S38W viable cells cultured onto VCAM-1 vs BSA (bovine serum albumin) also yielded significant *P*-values ( $P < 0.05$ ).

whereas CLL cells from CD49d<sup>+</sup>CD38<sup>-</sup> cases maintained an almost uniform round shape, even in the adherent component (Figures 6b and c).

The higher adhesive properties characterizing CD49d<sup>+</sup>CD38<sup>+</sup> CLL cells were paralleled by a more activated integrin signaling pathway, as witnessed by a significantly higher degree of Vav-1 phosphorylation signals in CD49d<sup>+</sup>CD38<sup>+</sup> compared with CD49d<sup>+</sup>CD38<sup>-</sup> CLL cells ( $P=0.0006$ ), the signal being mainly distributed at the cell adhesion sites (Figures 6c and d).

In line with the results obtained in the Mec-1 model, we checked whether CD38 expression impacted on the amount of protection from spontaneous apoptosis known to be induced by CD49d engagement by the VCAM-1 substrate.<sup>5</sup> Purified CLL cells from five CD49d<sup>+</sup>CD38<sup>-</sup> and five CD49d<sup>+</sup>CD38<sup>+</sup> cases (Supplementary Table S2) were cultured on VCAM-1, and cell viability determined at day 7. As expected, CD49d/VCAM-1 interaction protected from spontaneous apoptosis both CD49d<sup>+</sup>CD38<sup>+</sup> ( $P=0.004$ ) and CD49d<sup>+</sup>CD38<sup>-</sup> ( $P=0.001$ ) CLL cells (data not shown). However, the viability of CD49d<sup>+</sup>CD38<sup>+</sup> subgroup after VCAM-1 cultures was significantly higher than that of CD49d<sup>+</sup>CD38<sup>-</sup> subgroup ( $P=0.03$ , Figure 6e), in line with the notion of a functional synergy between these molecules.

## DISCUSSION

Clinically, the combined analysis of CD49d and CD38 expression in CLL was demonstrated to worsen the negative prognostic information provided by any of the factors alone (see also this study), thus supporting the idea of a functional cooperation between these molecules usually coexpressed in CLL cell membranes.<sup>6-10,28,37</sup> In this regard, we have previously described a pro-survival circuitry operating in the context of CD49d<sup>+</sup>CD38<sup>+</sup> CLL bone marrow milieu, sequentially involving the CD38/CD31 pair, CCL3 and CCL4 with their receptors, and eventually pro-survival signals delivered through the CD49d/VCAM-1 axis.<sup>5</sup> Moreover, CD49d and CD38 have been linked together in a recent study demonstrating that coculture of CLL cells with endothelial cells determines a significant increase of CD49d and CD38 expression, and enhances CLL cell viability, these effects being mediated by activation of the NF- $\kappa$ B transcription factor Rel A.<sup>38</sup>

The starting observation of the present study was that CD49d and CD38 along with CD44 and MMP-9 are physically associated on the membrane of CLL cells as part of a macromolecular complex.<sup>28</sup> Moving from these observations, here we investigated in detail the relationship between CD38 and the CD49d/CD29 integrin by: (i) cocapping experiments, a validated experimental procedure for disclosing membrane molecular complexes,<sup>33</sup> demonstrating a colocalization of CD38 in polar aggregates containing CD49d molecules; (ii) bidirectional immunoprecipitation experiments, providing evidence for an association between CD38 and the CD49d/CD29 integrin heterodimer, both inside and outside the cell membrane lipid rafts. The last finding suggests that the CD49d/CD29/CD38 complexes are free to shuttle in and out of these specialized cholesterol-enriched membrane microdomains, where signaling transduction is organized.<sup>22,39</sup> At variance with what observed for CD38/CD19 association,<sup>22</sup> CD49d/CD29/CD38 complexes were not dependent on integrity of the membrane structure, as the association was unaffected by cholesterol depletion. It is therefore likely that these molecules are joined together by other cellular structures, including cytoskeletal proteins, known to directly or indirectly associate with integrins.<sup>40</sup>

Once bound by specific ligands, integrins deliver outside-in signals that control cell proliferation, survival, gene induction, differentiation and cell motility. To achieve these diverse biological outcomes, integrins are recruited into complexes containing numerous cytoskeletal proteins and signaling molecules that can determine conformational changes leading to

higher affinity forms of the integrin itself.<sup>40,41</sup> In addition, ligand-binding avidity can be increased by lateral associations with other transmembrane molecules (for example, the tetraspanin CD81), independently of ligand engagement.<sup>42</sup>

In this context, the presence of CD38 at sites of CD49d binding to its natural ligands may represent an intriguing suggestion for a functional role of CD38 in the adhesion processes mediated by CD49d. The strategy used to test this working hypothesis was to challenge CD49d<sup>+</sup>CD38<sup>+</sup> and CD49d<sup>+</sup>CD38<sup>-</sup> cells in comparative adhesion assays, using transfectants from the CLL-derived cell line Mec-1, as well as primary CLL samples. The results from these experiments indicate that: (i) CD49d<sup>+</sup>CD38<sup>+</sup> cells had higher propensity to adhere to CD49d-specific substrates (either VCAM-1 or FN) compared to CD49d<sup>+</sup>CD38<sup>-</sup> cells; (ii) adherent CD49d<sup>+</sup>CD38<sup>+</sup> cells displayed a distinctive morphology, characterized by a more complex pattern of filopodia-like protrusions compared with cells expressing a CD49d<sup>+</sup>CD38<sup>-</sup> phenotype.

Both the phenomena were reverted by pre-exposure of cells to selected anti-CD38 mAbs, suggesting that mAb binding to specific domains of CD38 would reduce the accessibility of the CD49d/CD29 heterodimer to its ligands or, more intriguingly, CD38 blocking might affect CD49d conformational changes. Notably, the anti-CD38 mAb that was effective in hampering CD49d-mediated adhesion was also capable to inhibit migration of CLL cells induced by CXCL12 through its receptor CXCR4, another surface structure operating in close contact with CD38.<sup>26</sup>

The more efficient adhesive properties characterizing CD49d<sup>+</sup>CD38<sup>+</sup> CLL cells could be explained on the basis of a cooperation between the two molecules. In particular, we hypothesized that a possible role of CD38 in CD49d-mediated adhesion could be the recruitment of proteins involved in the downstream integrin signaling leading to actin polymerization and cell adhesion. In this context, attention was focused on Vav-1, a key molecule that operates as guanine exchange factor for Rac and Cdc42, two Rho GTPases involved in lamellipodia/filopodia generation in various cell models.<sup>34,35,43</sup> Upon integrin engagement, Vav-1 can become phosphorylated on tyrosine-174, as part of an intracellular signaling cascade leading to adhesion and cytoskeleton rearrangement. The higher levels of Vav-1 phosphorylation upon adhesion onto CD49d-specific substrates, described in Mec-1 S38W and in primary CD49d<sup>+</sup>CD38<sup>+</sup> CLL cells, can be the result of a more robust integrin signaling pathway characterizing CD49d<sup>+</sup>CD38<sup>+</sup> cells. In this regard, CD38 could contribute by increasing the recruitment of either key signaling molecules responsible for Vav-1 phosphorylation,<sup>34,44</sup> or of Vav-1 itself. To corroborate the latter hypothesis, the presence of Vav-1 was demonstrated in the Mec-1 S38W cell lysates immunoprecipitated with anti-CD38, but not in immunoprecipitates of the same cells formed with anti-CD49d antibodies. Moreover, pre-exposure of Mec-1 S38W cells with the same anti-CD38 mAbs affecting cell adhesion, resulted in a significant reduction of Vav-1 phosphorylation. This finding indicates that CD38 can operate by recruiting Vav-1 in close contact to the CD49d/CD29 complexes, potentiating its phosphorylation and the activation of the integrin signaling pathway. Notably, a similar association between CD38 and Vav-1 has been reported to promote cell growth and differentiation in a human myeloblastic leukemia cell model.<sup>45</sup>

Microenvironmental interactions in bone marrow and secondary lymphoid organs confer growth advantages and extend CLL cell survival. For these reasons they are deemed to be critical in disease progression and resistance to therapy.<sup>1,46</sup> The CD49d/VCAM-1/FN axes regulate recirculation of leukemic cells from the bloodstream to bone marrow and lymphoid organs, deliver pro-survival signals and promote resistance to drug-induced apoptosis.<sup>5,11,47</sup> In the present study, a more marked anti-apoptotic effect was exerted upon CD49d/VCAM-1 interactions in CD49d<sup>+</sup>CD38<sup>+</sup> cells, as compared with CD49d<sup>+</sup>CD38<sup>-</sup> cells. This observation can be explained by a more efficient adhesion of

CD49d<sup>+</sup>CD38<sup>+</sup> cells, and a consequent more pronounced activation of the anti-apoptotic machinery,<sup>5,11</sup> also thanks to the contribution to the survival process of specific signaling proteins, including Vav-1,<sup>48</sup> already recruited to the adhesion site.

Although further studies are needed to fully disclose the mechanism(s) behind the role of CD38 in CD49d-mediated adhesion in CLL, the present work provides evidence of a functional interaction between these molecules, which could explain at least in part the negative clinical outcome characterizing patients with a CD49d<sup>+</sup>CD38<sup>+</sup> CLL clone. This finding may also have a therapeutic relevance by envisioning the combined use of anti-CD49d and anti-CD38 mAbs, as well as of bi-specific antibodies simultaneously recognizing CD49d or the CD49d/CD29 heterodimer and CD38, to target the neoplastic component of this poor prognosis CLL subset.

## CONFLICT OF INTEREST

The authors declare no conflict of interest.

## ACKNOWLEDGEMENTS

This study is supported in part by: the Ministero della Salute (Ricerca Finalizzata IRCCS, 'Alleanza Contro il Cancro', Rete Nazionale Bio-Informatica Oncologica/RN-BIO and 'Giovani Ricercatori' project, grant GR-2008-1138053), Rome, Italy; the Ministero dell'Istruzione (Bando FIRB Giovani 2008, grant # RBF08ATLH and Bando PRIN 2009, LMEEH\_002), Rome, Italy; the Associazione Italiana contro le Leucemie, linfomi e mielomi (AIL), Venezia Section, Pramaggiore (VE) Group; the Associazione Italiana Ricerca Cancro (AIRC, Investigator Grant IG-8701 and IG-8590; MFAG 10327; Special Program Molecular Clinical Oncology, 5 × 1000, N. 10007 and N. 9980, 2010/15), the Milan, Italy; '5 × 1000 program' of the Centro di Riferimento Oncologico, Aviano, Italy; Ricerca Scientifica Applicata, Regione Friuli Venezia Giulia, ('Linfonet' Project), Trieste, Italy and the Human Genetics Foundation, Turin, Italy. The Fondazione Internazionale di Ricerca in Medicina Sperimentale (Turin, Italy) provided valuable administrative assistance. We thank Drs Francesca Cottino and Katuscia Gizzi for excellent technical assistance.

## REFERENCES

- Caligaris-Cappio F. Role of the microenvironment in chronic lymphocytic leukaemia. *Br J Haematol* 2003; **123**: 380–388.
- Scielzo C, Ten HE, Bertilaccio MT, Muzio M, Calissano C, Ghia P *et al*. How the microenvironment shapes chronic lymphocytic leukemia: the cytoskeleton connection. *Leuk Lymphoma* 2010; **51**: 1371–1374.
- Deaglio S, Vaisitti T, Bergui L, Bonello L, Horenstein AL, Tamagnone L *et al*. CD38 and CD100 lead a network of surface receptors relaying positive signals for B-CLL growth and survival. *Blood* 2005; **105**: 3042–3050.
- Deaglio S, Vaisitti T, Zucchetto A, Gattei V, Malavasi F. CD38 as a molecular compass guiding topographical decisions of chronic lymphocytic leukemia cells. *Semin Cancer Biol* 2010; **20**: 416–423.
- Zucchetto A, Benedetti D, Tripodo C, Bomben R, Dal BM, Marconi D *et al*. CD38/CD31, the CCL3 and CCL4 chemokines, and CD49d/vascular cell adhesion molecule-1 are interchained by sequential events sustaining chronic lymphocytic leukemia cell survival. *Cancer Res* 2009; **69**: 4001–4009.
- Gattei V, Bulian P, Del Principe MI, Zucchetto A, Maurillo L, Buccisano F *et al*. Relevance of CD49d protein expression as overall survival and progressive disease prognosticator in chronic lymphocytic leukemia. *Blood* 2008; **111**: 865–873.
- Rossi D, Zucchetto A, Rossi FM, Capello D, Cerri M, Deambrogi C *et al*. CD49d expression is an independent risk factor of progressive disease in early stage chronic lymphocytic leukemia. *Haematologica* 2008; **93**: 1575–1579.
- Shanafelt TD, Geyer SM, Bone ND, Tschumper RC, Witzig TE, Nowakowski GS *et al*. CD49d expression is an independent predictor of overall survival in patients with chronic lymphocytic leukaemia: a prognostic parameter with therapeutic potential. *Br J Haematol* 2008; **140**: 537–546.
- Damle RN, Wasil T, Fais F, Ghiotto F, Valetto A, Allen SL *et al*. Ig V gene mutation status and CD38 expression as novel prognostic indicators in chronic lymphocytic leukemia. *Blood* 1999; **94**: 1840–1847.
- Del Poeta G, Maurillo L, Venditti A, Buccisano F, Epiceno AM, Capelli G *et al*. Clinical significance of CD38 expression in chronic lymphocytic leukemia. *Blood* 2001; **98**: 2633–2639.
- de la Fuente MT, Casanova B, Moyano JV, Garcia-Gila M, Sanz L, Garcia-Marco J *et al*. Engagement of {alpha}4{beta}1 integrin by fibronectin induces *in vitro* resistance of B chronic lymphocytic leukemia cells to fludarabine. *J Leukoc Biol* 2002; **71**: 495–502.
- Eksioglu-Demiralp E, Alpdogan O, Aktan M, Firatli T, Ozturk A, Budak T *et al*. Variable expression of CD49d antigen in B cell chronic lymphocytic leukemia is related to disease stages. *Leukemia* 1996; **10**: 1331–1339.
- Ruoslahti E. Integrins. *J Clin Invest* 1991; **87**: 1–5.
- Verdone G, Doliana R, Corazza A, Colebrooke SA, Spessotto P, Bot S *et al*. The solution structure of EMILIN1 globular C1q domain reveals a disordered insertion necessary for interaction with the alpha4beta1 integrin 2. *J Biol Chem* 2008; **283**: 18947–18956.
- Rose DM, Han J, Ginsberg MH. Alpha4 integrins and the immune response. *Immunol Rev* 2002; **186**: 118–124.
- Malavasi F, Deaglio S, Funaro A, Ferrero E, Horenstein AL, Ortolan E *et al*. Evolution and function of the ADP ribosyl cyclase/CD38 gene family in physiology and pathology. *Physiol Rev* 2008; **88**: 841–886.
- Deaglio S, Mallone R, Baj G, Arnulfo A, Surico N, Dianzani U *et al*. CD38/CD31, a receptor/ligand system ruling adhesion and signaling in human leukocytes. *Chem Immunol* 2000; **75**: 99–120.
- Deaglio S, Morra M, Mallone R, Ausiello CM, Prager E, Garbarino G *et al*. Human CD38 (ADP-ribosyl cyclase) is a counter-receptor of CD31, an Ig superfamily member. *J Immunol* 1998; **160**: 395–402.
- Frasca L, Fedele G, Deaglio S, Capuano C, Palazzo R, Vaisitti T *et al*. CD38 orchestrates migration, survival, and Th1 immune response of human mature dendritic cells. *Blood* 2006; **107**: 2392–2399.
- Zubiaur M, Fernandez O, Ferrero E, Salmeron J, Malissen B, Malavasi F *et al*. CD38 is associated with lipid rafts and upon receptor stimulation leads to Akt/protein kinase B and Erk activation in the absence of the CD3-zeta immune receptor tyrosine-based activation motifs. *J Biol Chem* 2002; **277**: 13–22.
- Morra M, Zubiaur M, Terhorst C, Sancho J, Malavasi F. CD38 is functionally dependent on the TCR/CD3 complex in human T cells. *FASEB J* 1998; **12**: 581–592.
- Deaglio S, Vaisitti T, Billington R, Bergui L, Omede P, Genazzani AA *et al*. CD38/CD19: a lipid raft-dependent signaling complex in human B cells. *Blood* 2007; **109**: 5390–5398.
- Deaglio S, Zubiaur M, Gregorini A, Bottarel F, Ausiello CM, Dianzani U *et al*. Human CD38 and CD16 are functionally dependent and physically associated in natural killer cells. *Blood* 2002; **99**: 2490–2498.
- Zilber MT, Setterblad N, Vasselon T, Doliger C, Charron D, Mooney N *et al*. MHC class II/CD38/CD9: a lipid-raft-dependent signaling complex in human monocytes. *Blood* 2005; **106**: 3074–3081.
- Deaglio S, Vaisitti T, Aydin S, Ferrero E, Malavasi F. In-tandem insight from basic science combined with clinical research: CD38 as both marker and key component of the pathogenetic network underlying chronic lymphocytic leukemia. *Blood* 2006; **108**: 1135–1144.
- Vaisitti T, Aydin S, Rossi D, Cottino F, Bergui L, D'Arena G *et al*. CD38 increases CXCL12-mediated signals and homing of chronic lymphocytic leukemia cells. *Leukemia* 2010; **24**: 958–969.
- Berditchevski F. Complexes of tetraspanins with integrins: more than meets the eye. *J Cell Sci* 2001; **114**: 4143–4151.
- Buggins AG, Levi A, Gohil S, Fishlock K, Patten PE, Calle Y *et al*. Evidence for a macromolecular complex in poor prognosis CLL that contains CD38, CD49d, CD44 and MMP-9. *Br J Haematol* 2011; **154**: 216–222.
- Matutes E, Owusu-Ankomah K, Morilla R, Garcia MJ, Houlihan A, Que TH *et al*. The immunological profile of B-cell disorders and proposal of a scoring system for the diagnosis of CLL. *Leukemia* 1994; **8**: 1640–1645.
- Bomben R, Dal Bo M, Capello D, Benedetti D, Marconi D, Zucchetto A *et al*. Comprehensive characterization of IGHV3-21-expressing B-cell chronic lymphocytic leukemia: an Italian multicenter study. *Blood* 2007; **109**: 2989–2998.
- Zucchetto A, Sonogo P, Degan M, Bomben R, Dal Bo M, Russo S *et al*. Signature of B-CLL with different prognosis by Shrunken centroids of surface antigen expression profiling. *J Cell Physiol* 2005; **204**: 113–123.
- Zucchetto A, Bomben R, Dal Bo M, Bulian P, Benedetti D, Nanni P *et al*. CD49d in B-cell chronic lymphocytic leukemia: correlated expression with CD38 and prognostic relevance. *Leukemia* 2006; **20**: 523–525.
- Deaglio S, Capobianco A, Bergui L, Durig J, Morabito F, Duhrsen U *et al*. CD38 is a signaling molecule in B-cell chronic lymphocytic leukemia cells. *Blood* 2003; **102**: 2146–2155.
- Bustelo XR. Vav proteins, adaptors and cell signaling. *Oncogene* 2001; **20**: 6372–6381.
- Nobes CD, Hall A, Rho, Rac, and Cdc42 GTPases regulate the assembly of multimolecular focal complexes associated with actin stress fibers, lamellipodia, and filopodia. *Cell* 1995; **81**: 53–62.
- Koopman G, Keehnen RM, Lindhout E, Newman W, Shimizu Y, van Seventer GA *et al*. Adhesion through the LFA-1 (CD11a/CD18)-ICAM-1 (CD54) and the VLA-4 (CD49d)-VCAM-1 (CD106) pathways prevents apoptosis of germinal center B cells. *J Immunol* 1994; **152**: 3760–3767.

- 37 Nuckel H, Switala M, Collins CH, Sellmann L, Grosse-Wilde H, Dührsen U *et al*. High CD49d protein and mRNA expression predicts poor outcome in chronic lymphocytic leukemia. *Clin Immunol* 2009; **131**: 472-480.
- 38 Buggins AG, Pepper C, Patten PE, Hewamana S, Gohil S, Moorhead J *et al*. Interaction with vascular endothelium enhances survival in primary chronic lymphocytic leukemia cells via NF-kappaB activation and *de novo* gene transcription. *Cancer Res* 2010; **70**: 7523-7533.
- 39 Jacobson K, Mouritsen OG, Anderson RG. Lipid rafts: at a crossroad between cell biology and physics. *Nat Cell Biol* 2007; **9**: 7-14.
- 40 Hemler ME. Integrin associated proteins. *Curr Opin Cell Biol* 1998; **10**: 578-585.
- 41 Takagi J, Petre BM, Walz T, Springer TA. Global conformational rearrangements in integrin extracellular domains in outside-in and inside-out signaling. *Cell* 2002; **110**: 599-611.
- 42 Feigelson SW, Grabovsky V, Shamri R, Levy S, Alon R. The CD81 tetraspanin facilitates instantaneous leukocyte VLA-4 adhesion strengthening to vascular cell adhesion molecule 1 (VCAM-1) under shear flow. *J Biol Chem* 2003; **278**: 51203-51212.
- 43 Bertagnolo V, Brugnoli F, Mischiati C, Sereni A, Bavelloni A, Carini C *et al*. Vav promotes differentiation of human tumoral myeloid precursors. *Exp Cell Res* 2005; **306**: 56-63.
- 44 Deaglio S, Vaisitti T, Aydin S, Bergui L, D'Arena G, Bonello L *et al*. CD38 and ZAP-70 are functionally linked and mark CLL cells with high migratory potential. *Blood* 2007; **110**: 4012-4021.
- 45 Congleton J, Jiang H, Malavasi F, Lin H, Yen A. ATRA-induced HL-60 myeloid leukemia cell differentiation depends on the CD38 cytosolic tail needed for membrane localization, but CD38 enzymatic activity is unnecessary. *Exp Cell Res* 2010; **317**: 910-919.
- 46 Ferrarini M, Chiorazzi N. Recent advances in the molecular biology and immunobiology of chronic lymphocytic leukemia. *Semin Hematol* 2004; **41**: 207-223.
- 47 Till KJ, Lin K, Zuzel M, Cawley JC. The chemokine receptor CCR7 and alpha4 integrin are important for migration of chronic lymphocytic leukemia cells into lymph nodes. *Blood* 2002; **99**: 2977-2984.
- 48 Vigorito E, Gambardella L, Colucci F, McAdam S, Turner M. Vav proteins regulate peripheral B-cell survival. *Blood* 2005; **106**: 2391-2398.

Supplementary Information accompanies the paper on the Leukemia website (<http://www.nature.com/leu>)

## ORIGINAL ARTICLE

The *miR-17~92* family regulates the response to Toll-like receptor 9 triggering of CLL cells with unmutated *IGHV* genesR Bomben<sup>1</sup>, S Gobessi<sup>2</sup>, M Dal Bo<sup>1</sup>, S Volinia<sup>3,4,5</sup>, D Marconi<sup>1</sup>, E Tissino<sup>1</sup>, D Benedetti<sup>1</sup>, A Zucchetto<sup>1</sup>, D Rossi<sup>6</sup>, G Gaidano<sup>6</sup>, G Del Poeta<sup>7</sup>, L Laurenti<sup>8</sup>, DG Efremov<sup>2,9</sup> and V Gattei<sup>1,9</sup>

Chronic lymphocytic leukemia (CLL) cells from clinically aggressive cases have a greater capacity to respond to external microenvironmental stimuli, including those transduced through Toll-like-receptor-9 (TLR9). Concomitant microRNA and gene expression profiling in purified CLL cells ( $n = 17$ ) expressing either unmutated (UM) or mutated (M) *IGHV* genes selected microRNAs from the *miR-17~92* family as significantly upregulated and in part responsible for modifications in the gene expression profile of UM CLL cells stimulated with the TLR9 agonist CpG. Notably, the stable and sustained upregulation of *miR-17~92* microRNAs by CpG was preceded by a transient induction of the proto-oncogene *MYC*. The enforced expression of *miR-17*, a major member from this family, reduced the expression of the tumor suppressor genes *E2F5*, *TP53INP1*, *TRIM8* and *ZBTB4*, and protected cells from serum-free-induced apoptosis ( $P \leq 0.05$ ). Consistently, transfection with *miR-17~92* family antagonists reduced Bromo-deoxy-uridine incorporation in CpG-stimulated UM CLL cells. Finally, *miR-17* expression levels, evaluated in 83 CLL samples, were significantly higher in UM ( $P = 0.03$ ) and ZAP-70<sup>high</sup> ( $P = 0.02$ ) cases. Altogether, these data reveal a role for microRNAs of the *miR-17~92* family in regulating pro-survival and growth-promoting responses of CLL cells to TLR9 triggering. Overall, targeting of this pathway may represent a novel therapeutic option for management of aggressive CLL.

Leukemia (2012) 26, 1584–1593; doi:10.1038/leu.2012.44

**Keywords:** chronic lymphocytic leukemia; microRNAs; Toll-like receptor

## INTRODUCTION

Chronic lymphocytic leukemia (CLL) is characterized by a highly variable clinical course, with an unfavorable prognosis being strongly associated with the expression of unmutated (UM) immunoglobulin heavy variable (*IGHV*) genes.<sup>1</sup> Such a clinical behavior has been associated with a greater capacity of UM CLL cells to signal through the B-cell receptor (BCR) upon antigen stimulation, suggesting that this feature could contribute to disease progression. In fact, UM BCRs are known to operate as polyreactive receptors that bind to various foreign and self antigens, although often with low affinity.<sup>2,3</sup>

Besides antigen stimulation, the development and progression of CLL could also be affected by other external signals, synergistically cooperating to regulate the proliferation and survival of the malignant clone. In this regard, UM CLL cells have been recently found to respond more efficiently to microenvironmental pro-survival signals than mutated (M) CLL cells, being on the other hand more susceptible to spontaneous apoptosis when these signals are absent.<sup>4</sup> Moreover, UM CLL cells frequently have high levels of the enzyme activation-induced cytidine deaminase and present evidence of ongoing class-switch recombination, both hallmarks of recent activation by microenvironmental signals.<sup>5</sup>

Signals that are transmitted through Toll-like-receptor-9 (TLR9) may also have a role in CLL, as they could drive the expansion of

CLL cells that express BCRs reactive with DNA or DNA-containing complexes.<sup>6,7</sup> Notably, CLL cells from patients with aggressive disease, mainly those expressing UM BCRs, respond more effectively to TLR9 stimulation than CLL cells from patients with less aggressive diseases, mainly expressing M *IGHV* genes,<sup>8,9</sup> suggesting that the capacity to respond to TLR9 signals could have prognostic relevance in CLL.<sup>9</sup>

MicroRNAs represent a class of small non-coding RNAs that act as master regulators of protein expression by inhibiting the translation or inducing the degradation of target messenger RNAs (mRNAs) with partially complementary sites in the 3'-untranslated regions.<sup>10</sup> MicroRNAs orchestrate various cellular functions and have been shown to have critical roles in many biological processes, including cell differentiation, apoptosis, proliferation and cancer development by acting either as tumor suppressors or oncogenes.<sup>11</sup>

In the case of CLL, several studies have identified certain microRNAs (for example, *miR-15a*, *miR-16-1*, *miR-21*, *miR-24*, *miR-34*, *miR-155* and *let-7* family) as either implicated in CLL pathogenesis or as part of a microRNA signature predicting clinical outcome or drug resistance.<sup>12,13</sup> However, little is known regarding the capacity of external stimuli to modulate the expression of specific microRNAs and/or microRNA families in CLL. In this regard, studies by our group have recently demonstrated a close correlation between the expression of a particular BCR

<sup>1</sup>Clinical and Experimental Onco-Hematology Unit, Centro di Riferimento Oncologico, I.R.C.C.S., Aviano (PN), Italy; <sup>2</sup>Department of Molecular Hematology, ICGEB Outstation-Monterotondo, Rome, Italy; <sup>3</sup>DAMA, Data Mining for Analysis of Microarrays, Department of Morphology and Embryology, University of Ferrara, Ferrara, Italy; <sup>4</sup>Department of Biomedical Informatics, Ohio State University, Columbus, OH, USA; <sup>5</sup>Comprehensive Cancer Center, Ohio State University, Columbus, OH, USA; <sup>6</sup>Division of Hematology, Department of Clinical and Experimental Medicine, Amedeo Avogadro University of Eastern Piedmont, Novara, Italy; <sup>7</sup>Division of Hematology, S.Eugenio Hospital and University of Tor Vergata, Rome, Italy and <sup>8</sup>Department of Hematology, Catholic University Hospital A. Gemelli, Rome, Italy. Correspondence: Dr V Gattei, Clinical and Experimental Onco-Hematology Unit, Centro di Riferimento Oncologico, I.R.C.C.S., Via Franco Gallini 2, Aviano (PN) 33081, Italy. E-mail: vgattei@cro.it

<sup>9</sup>These authors contributed equally to this work.

Received 5 October 2011; revised 7 February 2012; accepted 8 February 2012; accepted article preview online 20 February 2012; advance online publication, 16 March 2012

(that is, *IGHV3-23*) with relatively higher levels of two key microRNAs (that is, *miR-15a* and *miR-16-1*),<sup>14</sup> indicating that the expression of certain microRNAs could be modulated by BCR signals.

In the present study, we provide evidence that TLR9 elicits its response in UM CLL cells through the upregulation, MYC-dependent, of microRNAs from the *miR-17~92* family, with the subsequent downregulation of specific *miR-17~92* targets. MicroRNAs from the *miR-17~92* family are at least in part responsible for the increased proliferation/survival induced by TLR9 triggering in UM CLL cells.

## MATERIALS AND METHODS

### CLL patients

The study included peripheral blood samples from 117 CLL patients, divided as follows: (i) a discovery panel of 17 CLL utilized for global microRNA profile (miRome) and gene expression profiling (GEP) analyses; (ii) a validation panel of additional 17 CLL cases utilized for transfection/functional assays; and (iii) a further additional panel of 83 CLL utilized for correlation studies. All patients provided informed consent in accordance with the local Institutional Review Board requirements (IRB-04-2010, Centro di Riferimento Oncologico, Aviano, Italy) and declaration of Helsinki. Peripheral blood mononuclear cells were separated by Ficoll gradient centrifugation (Amersham Biosciences, Uppsala, Sweden). Detection of *IGHV* mutational status was performed as previously reported.<sup>14</sup> The 2% cutoff was chosen to discriminate UM versus M CLL cases. Additional biological features of CLL cases entering this study, including expression of ZAP-70 and CD38, interphase fluorescence *in-situ* hybridization for the main chromosomal abnormalities and the experiments for which each sample has been used are listed in Supplementary Table S1.<sup>14,15</sup>

In all cases, CLL cells were purified by negative selection using anti-CD3, anti-CD14 and anti-CD16 mouse monoclonal antibodies and Dynabeads coated with a pan anti-mouse IgG antibody (DynaL Biotech, Oslo, Norway).<sup>8</sup> The purity of the CLL cells after negative selection was monitored by flow cytometry, and the percentage of CD5<sup>+</sup>/CD19<sup>+</sup> cells exceeded 98% for all the CLL samples from the patients entering the study.

### Cell culture conditions

Freshly isolated negatively selected CLL cells ( $n=17$ ) were cultured ( $1 \times 10^7$  cells/ml) in RPMI-1640 supplemented with 10% heat-inactivated fetal bovine serum, 100 U/ml penicillin, 0.1 mg/ml streptomycin, 2 mM L-glutamine and 1 mM sodium pyruvate (Invitrogen, Carlsbad, CA, USA) in the presence or not of 7.5  $\mu$ g/ml complete phosphorothioate CpG-ODN oligonucleotide 2006 (5-TCGTCGTTTTGTCGTTTTGTCGTT-3; Microsynth, Balgach, Switzerland; hereafter CpG) for 18 h, as previously reported.<sup>8,9</sup> To amplify the proliferative effect of CpG, selected experiments were carried out in the presence of 100 U/ml interleukin-2 (IL-2; R&D Systems, Minneapolis, MN, USA), as previously reported.<sup>16</sup>

In time-course experiments, purified primary CLL cells ( $n=3$ ) were stimulated for 3 h with CpG, washed and subsequently resuspended in complete medium to evaluate MYC and *miR-17* expression levels at various time points (1–24 h), as detailed below.

### miRome, GEP and data mining tools

Total RNA was extracted from purified CLL cells and normal peripheral blood B cells of healthy donors using the TRIZOL Reagent (Invitrogen) and validated for integrity and purity using the Agilent 2100 Bioanalyzer (Agilent Technologies, Santa Clara, CA, USA).

Single-color hybridization microarray experiments for miRome were performed with 100-ng total RNA/sample labeled with Cyanine(Cy)-3 dye using the microRNA Complete Labeling System & Hyb Kit (Agilent Technologies). Cy3-labeled RNA was hybridized to the Human microRNA microarray Version 3 from the Sanger database v12.0 (Agilent Technologies).

GEP was performed using the whole-human genome (4  $\times$  44 K) oligo microarray platform (Agilent Technologies) as previously described.<sup>14</sup>

Microarray slides were analyzed with an Agilent Microarray Scanner (Agilent Technologies). The hybridization signal values for the multiple probes for each microRNA were obtained with the use of Agilent Feature Extraction Software 10.7.3 (Agilent Technologies). Microarray data are available in Gene Expression Omnibus (GEO; <http://www.ncbi.nlm.nih.gov/geo/>) under accession number GSE30107.

Bioinformatics analyses were performed integrating three different methods for supervised analysis: the LIMMA algorithm, Partek software (Partek Incorporated, St Louis, MO, USA) and GeneSpringGX (Agilent Technologies). Results were visualized by hierarchical clustering applying Ward's method with Euclidean distance.<sup>17</sup> The biological functions of genes were investigated using Onto-Express.<sup>18</sup> Significant Gene Ontology (GO) categories were selected for having a *P*-value of at least 0.05 and containing at least seven genes per category. To identify the putative microRNAs involved in gene deregulation, GEP data were investigated using the open-source applications 'Targets' Reverse Expression' (T-REX), available at <http://aqua.unife.it>, and 'Gene Set Enrichment Analysis' (GSEA).<sup>14,19</sup>

Further details are provided in Supplementary Materials and Methods.

### Transfection

Three micrograms of microRNA precursor for *miR-17* (Ambion, Life Technologies, Carlsbad, CA, USA) or an anti-microRNA mixture comprising anti-microRNAs specific for *miR-17*, *miR-18a*, *miR-20a* and *miR-20b* (Ambion) were transfected into  $7.5 \times 10^6$  primary CLL cells with the Amaxa Nucleofector system (Lonza, Basel, Switzerland) according to the manufacturer's guidelines. As negative control, cells were transfected with equal amounts of pre-miR-negative control1 or anti-miR-negative control 1 (Ambion), as applicable.

### Quantitative real-time PCR (qRT-PCR)

Expression of selected microRNAs and of the control *RNU6B* was assessed using a standard TaqMan MicroRNA assay kit (Applied Biosystems, Life Technologies, Carlsbad, CA, USA) according to the manufacturer's instructions and as previously described.<sup>14</sup> Briefly, microRNA was reverse transcribed to complementary DNA using gene-specific primers, and the relative amount of each microRNAs was computed using the equation  $2^{-\Delta Ct}$  where  $\Delta Ct = (Ct_{\text{microRNA}} - Ct_{\text{RNU6B}})$ .

Expression of specific genes of interest (that is, *E2F5*, *TP53INP1*, *TRIM8*, *ZBTB4*, *MYC*, *CAD*, *PGK1*, *TFAM* and  $\beta_2$ -microglobulin,  $\beta_2M$ ) was evaluated with the TaqMan Gene Expression assay kit (Applied Biosystems); the relative amount of each gene was calculated as above but using the expression of  $\beta_2M$  as internal control. Fold change between classes was calculated as reported.<sup>14</sup> All qRT-PCR experiments were performed on an Applied Biosystem 7700 Sequence Detection System (Applied Biosystems).

### Western blot

Total proteins were extracted from CLL cells ( $n=3$ ) collected 18 h after *miR-17* transfection, loaded and run in 10% SDS-PAGE gels before transfer to nitrocellulose membranes (GE Healthcare, Little Chalfont, UK) for western analysis and detection by ECL (GE Healthcare) or Immobilon (Millipore Corporation, Billerica, MA, USA). 1:500 rabbit-anti-TP53INP1 (Abcam, Cambridge, MA, USA), 1:1000 rabbit-anti-TRIM8 (Abcam) and 1:1000 rabbit-anti-ZBTB4 (Abcam) were used for protein detection. 1:2000 mouse-anti- $\alpha$ -tubulin antibody (Sigma-Aldrich, St Louis, MO, USA) was used as an internal control. Densitometric quantitation of western blots was determined with the Quantity One 4.1.0 software (Bio-Rad, Hercules, CA, USA).

### Functional studies

MicroRNA-transfected primary CLL cells were cultured in RPMI-1640 without serum addition for 24–96 h. The percentage of viable cells was determined by AnnexinV and 7-amino-actinomycin-D (Becton-Dickinson, San Jose, CA, USA) staining. In selected experiments, primary CLL cells were transfected with the anti-microRNA mixture and cultured in the presence of CpG/IL-2 as above. To determine the percentage of proliferating CLL cells, Bromo-deoxy-uridine (BrdU) 10  $\mu$ M was added after stimulation of 48 h with CpG-ODN/IL-2 and the cells were cultured for additional

18 h before harvesting. After washing and overnight fixation, cells were permeabilized (2N HCl and 0.5% Triton X-100 for 30 min), neutralized (0.1 M Na<sub>2</sub>B<sub>4</sub>O<sub>7</sub> × 10H<sub>2</sub>O, pH 8.5) and incorporated BrdU was detected with an anti-BrdU-FITC antibody (Becton-Dickinson, Franklin Lakes, NJ, USA). Data were acquired on a FACSCalibur flow cytometer and analyzed by the CellQuest software (Becton-Dickinson).

## RESULTS

### miRome of CpG-stimulated CLL cells

Purified CLL cells were either left unstimulated or stimulated with CpG for 18 h, and analyzed for changes in the microRNA expression profile. Bioinformatics analysis of UM and M CLL samples was performed separately, given their distinct responses to CpG stimulation.<sup>8,9</sup>

Supervised analysis of UM CLL cells yielded a list of 24 differentially expressed microRNAs, of which 21 were upregulated (*miR-1260*, *miR-1274a*, *miR-1274b*, *miR-1280*, *miR-155*, *miR-155\**, *miR-17*, *miR-17\**, *miR-18a*, *miR-19b-1\**, *miR-20a*, *miR-20b*, *miR-221*, *miR-221\**, *miR-222*, *miR-29b-1\**, *miR-30b\**, *miR-30d\**, *miR-720*, *miR-886-3p* and *miR-92a-1\**) and 3 were downregulated (*miR-125a-3p*, *miR-135a\** and *miR-150\**) upon CpG stimulation (Supplementary Table S2). A hierarchical clustering generated using these 24 microRNAs clearly split CpG-stimulated samples from their respective unstimulated counterparts in all the analyzed UM CLL cases (Figure 1a).

When the same algorithms for supervised analyses and the same *P*-value were applied to M CLL, we failed to identify any differences in the miRome by comparing CpG-stimulated and unstimulated M CLL cells. Consistently, in a hierarchical cluster driven by the 24 microRNA differentially expressed in UM CLL, CpG-stimulated M CLL either directly clustered along with unstimulated CLL (4/8 cases; Supplementary Figure S1), or

displayed changes in microRNA expression only in part resembling those occurring in UM CLL cells (4/8 cases; Supplementary Figure S1). However, additional supervised analyses carried out by solely considering the latter cases again failed to identify differentially expressed microRNAs (not shown). These data are overall in keeping with our previous findings that the capability to respond to TLR9 stimulation is frequently reduced in M CLL.<sup>8,9</sup>

### GEP of CpG-stimulated CLL cells

A parallel GEP comparing CpG-stimulated and unstimulated CLL cells was performed utilizing the same RNAs considered for miRome. Again, bioinformatics analyses were separately performed in UM and M CLL, in agreement with previous results.<sup>8,9</sup>

In the case of UM CLL, 1585 highly differentially expressed genes, 826 upregulated and 759 downregulated upon CpG stimulation, were identified (Supplementary Table S3). A hierarchical clustering using these genes correctly separated CLL cells exposed to CpG from those left unstimulated (Figure 1b). According to bioinformatics tools for global analysis of gene function, among the 50 top-ranked GO categories that were selected as containing differentially expressed genes, 20 (40%) were GO categories related to proliferation and cell cycle control (for example, cell division, DNA replication, mitosis and G1/S transition of cell cycle), apoptosis (for example, regulation of apoptosis, induction of apoptosis and anti-apoptosis) and activation of the NF- $\kappa$ B cascade (Supplementary Table S4).<sup>8,20</sup>

When performed on M CLL cells, GEP analysis found a set of 379 differentially expressed genes between CpG-stimulated and unstimulated M CLL cells (Supplementary Figure S2 and Supplementary Table S5). Among these genes, only a minority (13 genes) was in common with the genes differentially expressed between CpG-stimulated and unstimulated UM CLL cells (Supplementary Tables S3–S5). More important, bioinformatic analyses revealed

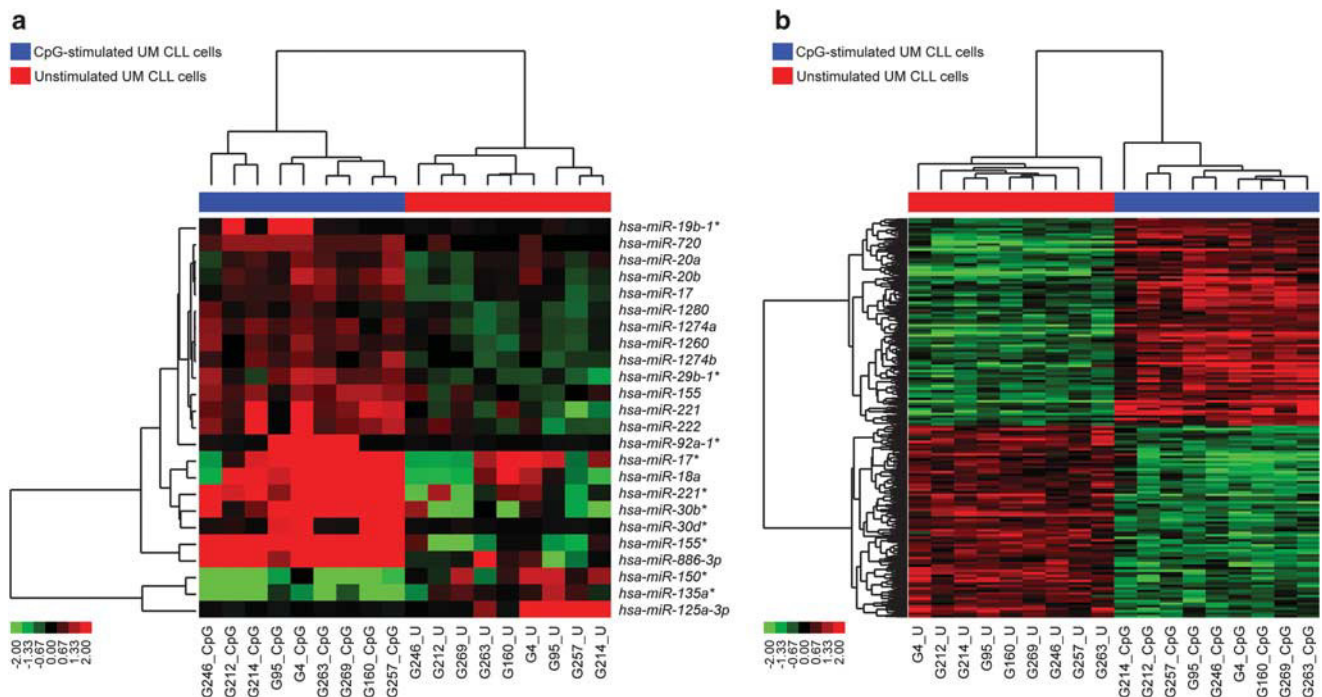


**Figure 1.** miRome and GEP of CpG-stimulated and unstimulated UM CLL cells. **(a)** miRome: hierarchical clustering of CpG-stimulated (blue bar under the horizontal dendrogram) and unstimulated (red bar under the horizontal dendrogram) UM CLL cell samples using the 24 differentially expressed microRNAs upon CpG stimulation. Color codes for microRNA expression values refer to mean centered log-ratio values. **(b)** GEP: hierarchical clustering of CpG-stimulated (blue bar under the horizontal dendrogram) and unstimulated (red bar under the horizontal dendrogram) UM CLL cell samples using the 1585 differentially expressed genes upon CpG stimulation. Color codes for gene expression values refer to mean centered log-ratio values.

that, at variance with UM CLL cells (Supplementary Table S4), only 1 out of 15 (6.7%) GO categories selected as containing genes representing the differential expression signature of M CLL was related to cell proliferation (Supplementary Table S6), again in agreement with previous studies.<sup>8,9</sup>

CpG stimulation induces changes in mRNA levels of miR-17~92 targets

The dramatic changes in miRome and GEP of UM CLL cells upon CpG stimulation prompted us to integrate these data with the aim to identify those microRNAs whose modulated expression could

mostly affect gene expression.<sup>19</sup> To do this, the gene expression signature of UM CLL cells was analyzed by taking advantage of the T-REX algorithm,<sup>19</sup> and results were combined with those derived from miRome.

Results of T-REX analysis (complete data available at the website <http://aqua.unife.it/Bomben/>; password: odraccir) identified 30 microRNAs whose putative mRNA targets were significantly downregulated by TLR9 triggering (Supplementary Figure S3). Four of these microRNAs, that is, *miR-17*, *miR-20a*, *miR-20b* and *miR-1260*, were also identified by miRome as upregulated in CpG-stimulated UM CLL cells (Figure 1a and Supplementary Figure S3). Three of these microRNAs (*miR-17*, *miR-20a* and

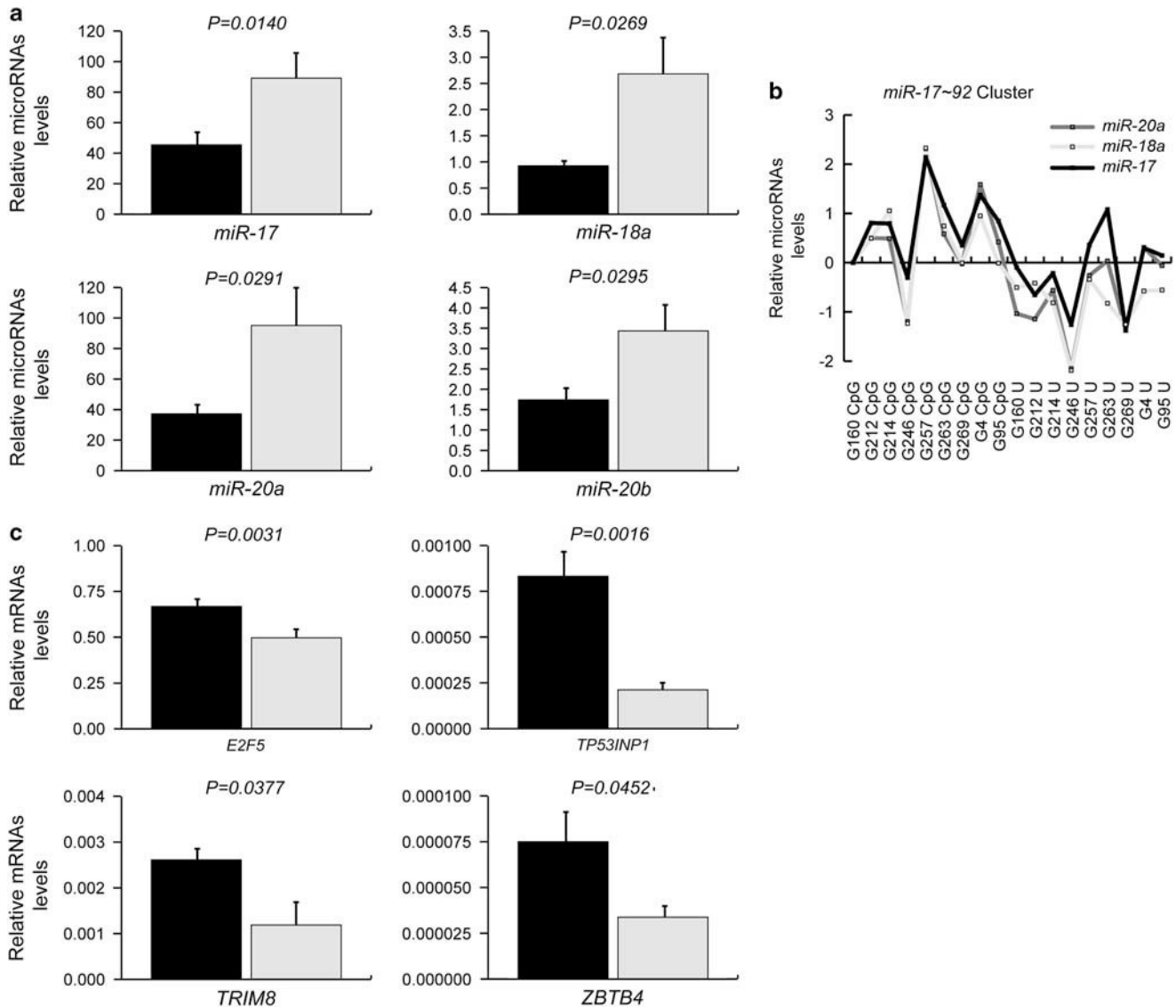


**Figure 2.** qRT-PCR analysis of selected differentially expressed microRNAs and genes in CpG-stimulated or unstimulated UM CLL cells. (a) MicroRNA expression. Expression of members of the *miR-17~92* family (i.e., *miR-17*, *miR-18*, *miR-20a* and *miR-20b*) in UM CLL cells stimulated with CpG or left unstimulated for 18 h. For qRT-PCR amplification of mature miRNAs, RNA was reverse transcribed to complementary DNA using gene-specific primers and the relative amount of each microRNA was computed using the equation  $2^{-\Delta Ct}$ , where  $\Delta Ct = (Ct_{\text{microRNAs}} - Ct_{\text{RNUB6}})$ ; Ct values were defined as the fractional cycle number in which the fluorescence crossed the fixed threshold. (b) Expression pattern of members from the *miR-17~92* cluster. Members of *miR-17~92* family belonging to the same polycistronic element (i.e., *miR-17*, *miR-18* and *miR-20a*) are overexpressed in CpG-stimulated UM CLL cells and follow similar profiles of expression across the different UM CLL samples. Relative microRNA levels refer to log-ratio values. (c) Gene expression. Four target genes for microRNAs of the *miR-17~92* family that were found differentially expressed between CpG-stimulated and unstimulated CLL samples were assayed by qRT-PCR using the equation  $2^{-\Delta Ct}$ , where  $\Delta Ct = (Ct_{\text{mRNAs}} - Ct_{\beta 2M})$ . In all graphs, data represent mean  $\pm$  s.e.m.; gray histograms indicate the average expression levels of CpG-stimulated UM CLL cells (nine cases); black histograms indicate the average expression levels of the nine UM CLL cells left unstimulated (nine cases); P-values (Student's t-test) for each microRNAs/genes are shown.

*miR-20b*), together with four additional microRNAs (*miR-17\**, *miR-18a*, *miR-19b-1\** and *miR-92a-1\**) that were also upregulated in miRome of CpG-stimulated UM CLL cells (Figure 1a), belonged to the *miR-17~92* family of microRNA clusters.<sup>21</sup>

Data obtained by applying the T-REX algorithm were confirmed by GSEA. By focusing on the gene set grouping the genes sharing the same DNA-binding motifs, including the binding motifs of microRNAs, the gene set containing genes under control of *miR-17* presented the lowest nominal *P*-value (nominal *P*-value < 0.0001, false discovery rate *q*-value = 0.236). In the context of this gene set, CpG-stimulated UM CLL cells were characterized by a significant enrichment in downregulated genes under control of the *miR-17~92* cluster (Supplementary Figure S4).

Collectively, both miRome and in-silico analyses of GEP data revealed that CpG stimulation upregulated expression of microRNAs from the *miR-17~92* family and downregulated their putative mRNA targets in UM CLL. To further validate these findings, the expression levels of four microRNAs from the *miR-17~92* family, that is, *miR-17*, *miR-18a*, *miR-20a* and *miR-20b*, were quantified by real-time RT-PCR. As shown in Figure 2a, all four microRNAs were expressed at significantly higher levels in CpG-stimulated UM CLL cells than in their unstimulated counterparts. Moreover, given the notion that members of the same microRNA cluster are transcribed as a single pri-microRNA and frequently exhibit similar expression patterns,<sup>22</sup> *miR-17*, *miR-18a* and *miR-20a* followed a similar expression profile across the different CLL samples (Figure 2b). Finally, for all these microRNAs, results of qRT-PCR experiments and miRome were strongly correlated ( $P < 0.001$ ) (Supplementary Figure S5a).

#### Effects of miR-17~92 microRNAs on expression of candidate target genes

According to the T-REX analysis, 57 out of the 759 genes that were downregulated in CpG-stimulated UM CLL cells (7.5%) were putative mRNA targets of the *miR-17~92* family (Supplementary Table S7). Of these genes, we selected *TP53INP1*, *E2F5*, *ZBTB4* and *TRIM8* for further studies, given their potential activity as tumor suppressors and their roles in regulating cell cycle and apoptosis.<sup>23-26</sup> As shown in Figure 2c, qRT-PCR experiments confirmed the downregulation of these genes upon CpG stimulation, consistent with GEP results (Supplementary Figure S5b).

Expression of *TP53INP1*, *E2F5*, *ZBTB4* and *TRIM8* was also significantly downregulated in primary CLL cells transiently transfected with *miR-17* (mean fold change of *miR-17* levels after 18 h =  $477.57 \pm 202.57$ ), both at mRNA (Figure 3a) and protein (Figures 3b and c) levels, suggesting a regulation of their expression by *miR-17~92* family members, as reported previously in other cell systems.<sup>27-34</sup>

#### MYC regulates miR-17~92 expression in UM CLL cells

UM CLL cells upregulated the proto-oncogene *MYC* after CpG stimulation both in GEP (Supplementary Figure S6 and Supplementary Table S3) and qRT-PCR experiments (Figure 4a). Moreover, transcripts for three established *MYC* target genes (that is, *CAD*, *PGK1* and *TFAM*), selected for being functionally related to cell metabolism functions but unconnected to known biological activities in lymphoproliferative disorders,<sup>35</sup> resulted in upregulation of CpG-stimulated UM CLL in comparison with their respective unstimulated counterparts both in GEP ( $P < 0.001$  in all cases; data not shown) and in qRT-PCR experiments (Figure 4a). Conversely, in the context of M CLL, neither *MYC* nor the three *MYC* targets were found among the differentially expressed genes characterizing CpG-stimulated cells (Supplementary Table S5).

In keeping with these data, time-course experiments showed that CpG stimulation of primary UM CLL cells resulted in transient induction of *MYC*, peaking at 3 h from the end of CpG exposure, followed by a slower but sustained induction of *miR-17* levels that

reached a peak at 6 h, and were maintained at least until 24 h from the removal of CpG from the culture media (Figure 4b). A similar kinetic profile was observed when expression levels of other members of the *miR-17~92* family (that is, *miR18a* and *miR20a*) were investigated (not shown). These findings, along with the known activity of *MYC* as a master regulator of *miR-17~92* cluster in other cell systems,<sup>35-39</sup> strongly suggest an associative interaction between *MYC* and *miR-17~92* also in CLL.

#### MicroRNAs from the miR-17~92 family regulate apoptosis and proliferation in primary UM CLL cells

Negatively purified UM CLL cells were transfected either with pri-miR-17 or scrambled control, and evaluated for apoptosis and

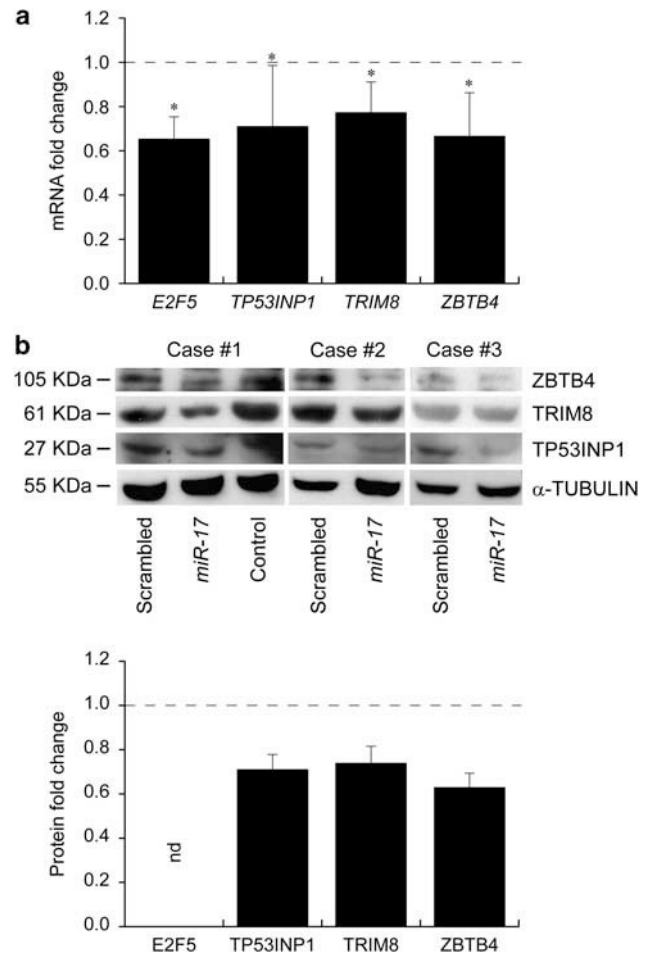


**Figure 3.** Effect of *miR-17* overexpression on mRNA and protein levels of selected genes. **(a)** *miR-17* overexpression and mRNA levels. Effects of *miR-17* overexpression on mRNA levels of *E2F5*, *TP53INP1*, *TRIM8* and *ZBTB4* in six primary CLL samples. Gene expression levels were measured by qRT-PCR using TaqMan Gene Expression Assays (Applied Biosystems) at 18 h after transfection. **(b)** *miR-17* overexpression and protein levels—upper panel. Relative TP53INP1, TRIM8 and ZBTB4 protein expression levels of three primary CLL cases transfected with a scrambled control versus a precursor for *miR-17*, assessed by western blot. Control refers to protein levels in untreated condition.  $\alpha$ -Tubulin levels were used as loading control in all cases. Lower panel: effects of *miR-17* overexpression on protein levels of *E2F5*, *TP53INP1*, *TRIM8* and *ZBTB4* in three primary CLL samples. Protein expression levels were measured by western blot experiment at 18 h after transfection. In all graphs, values are represented as mean fold expression with respect to transfection of the same CLL cells with scrambled control. Asterisk indicate  $P$ -value < 0.05 (Student's *t*-test). A dashed line indicates the reference level of gene expression (1.0). nd, not done.

viability after 24–96 h of culture in serum-deprived culture medium. qRT-PCR analysis of *miR-17* levels showed that transfection was successful in all cases, with an increase in *miR-17* expression levels ranging from 24- to 800-fold compared with cells transfected with scrambled control ( $P < 0.0034$ ; Figure 5a). Both *miR-17*- and scrambled control-transfected UM CLL cells underwent apoptosis throughout the culture period. However, *miR-17*-transfected UM CLL cells always showed a slightly greater viability, compared with cells transfected with scrambled control. These differences in the percentage of viable cells were already evident at 24 h ( $P = 0.021$ ) and peaked at 48 h ( $P = 0.010$ ) of culture (Figure 5b).

In complementary experiments, purified UM CLL cells were transfected with a mixture of antagomiRs against *miR-17*, *miR-18a*, *miR-20a* and *miR-20b* or an anti-miR-negative control (Figure 5c). In samples transfected with the negative control, CpG stimulation increased the levels of *miR-17~92* microRNAs and induced leukemic cell proliferation, as evidenced by BrdU incorporation. The antagomiR mixture inhibited the CpG-induced rise in microRNA levels and concomitantly reduced the percentage of BrdU-positive cells (Figure 5d and Supplementary Figure S7).

#### Association between miR-17, IGHV mutational status and ZAP-70

The expression level of *miR-17* was analyzed by qRT-PCR in a series of 83 CLL cases for which information regarding different biological parameters was available (Supplementary Table S1). As shown in Figure 6, the levels of *miR-17* were significantly higher in UM CLL and in ZAP-70-positive samples compared with their relative counterparts ( $P = 0.0324$  and  $P = 0.0264$ , respectively). This difference was even more evident when CLL cells expressing UM *IGHV* genes and high ZAP-70 levels were compared with cells with M *IGHV* genes and low/absent ZAP-70 ( $P = 0.0156$ ; Figure 6). Finally, no significant correlation was found between *miR-17* and *MYC* baseline levels in the same CLL series (Supplementary Figure S8), and *MYC* was not differentially expressed between the different prognostic groups (data not shown).

#### DISCUSSION

The capability of the malignant cells to respond to microenvironmental stimuli has recently emerged as an important determinant of the clinical course in CLL. In particular, CLL cells from patients with aggressive disease typically respond with increased survival

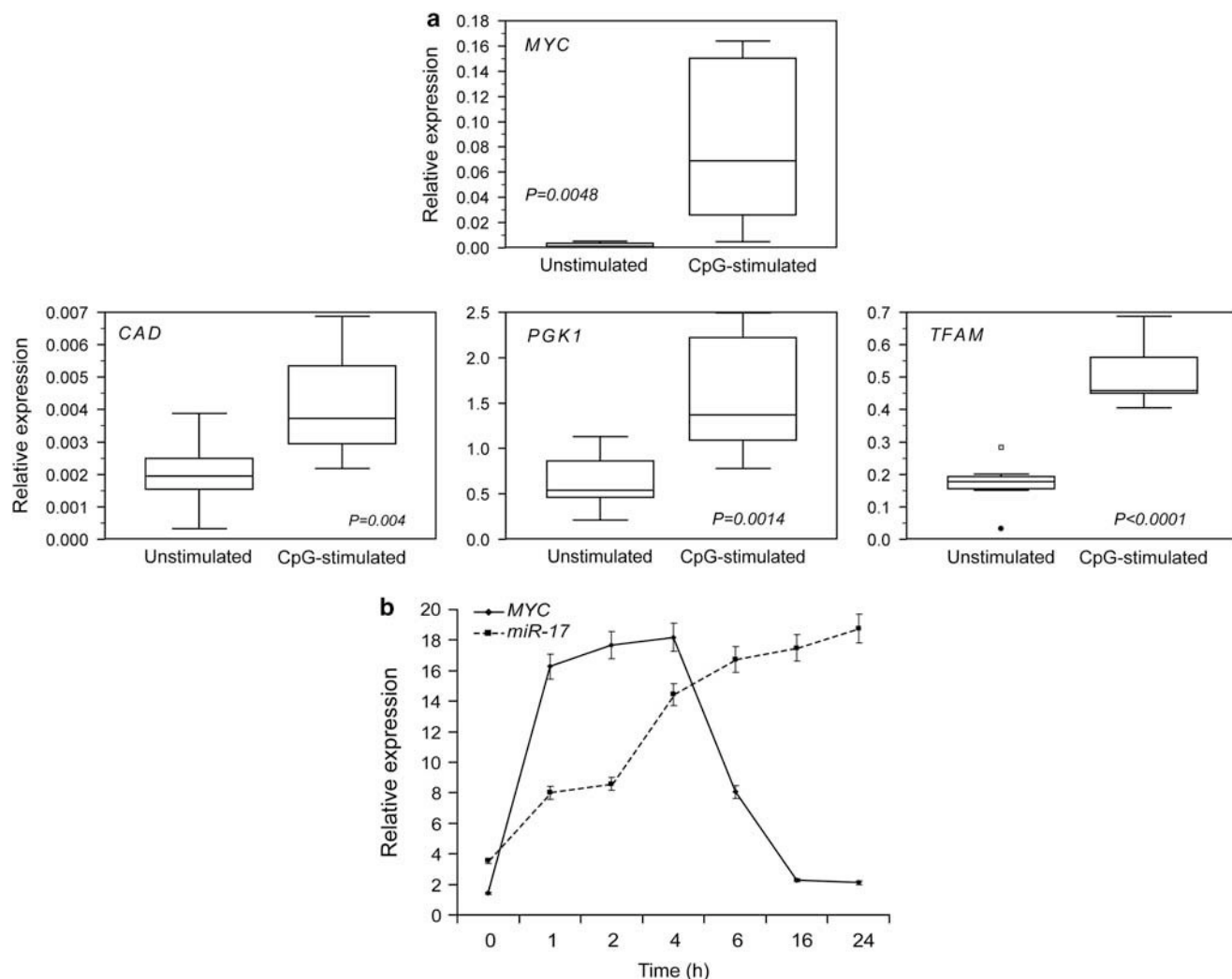


**Figure 4.** Expression of *MYC* and *MYC* target genes in CpG-stimulated and unstimulated UM CLL cells. **(a)** Expression of *MYC* and *MYC* target genes. Box plots display results from qRT-PCR analyses of *MYC* and three independent *MYC* target genes, *CAD* (carbamoyl-phosphate synthetase 2, aspartate transcarbamylase and dihydroorotase), *PGK1* (phosphoglycerate kinase 1) and *TFAM* (transcription factor A, mitochondrial) in CpG-stimulated and unstimulated UM CLL cells (nine samples). *P*-values indicate Student's *t*-test. **(b)** Time-course expression of *MYC* and *miR-17*. qRT-PCR analysis of *MYC* and *miR-17* expression levels following CpG stimulation of three primary UM CLL samples. Data represent mean values  $\pm$  s.e.m.

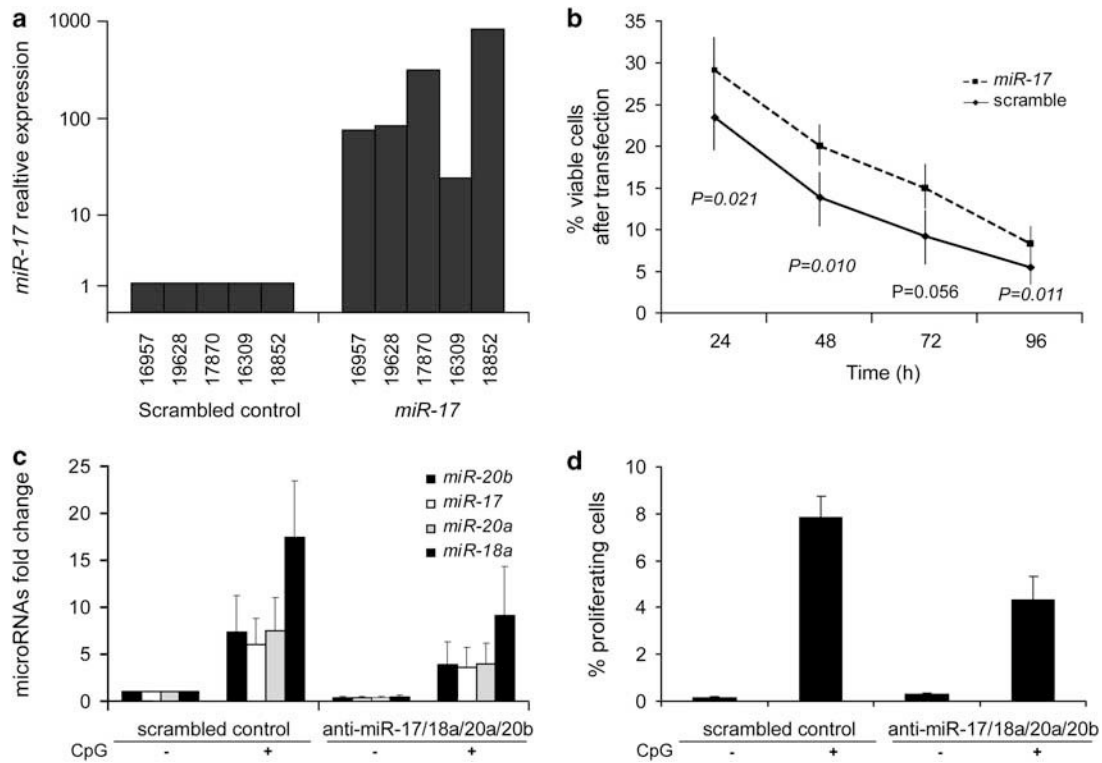


**Figure 5.** MicroRNAs from the *miR-17~92* family control viability and proliferation of primary UM CLL cells. (a) Effective transfection of *miR-17*. Overexpression of *miR-17* in five primary UM CLL cells transfected with pre-*miR-17* compared with the same UM CLL samples transfected with scrambled control. (b) Ectopic expression of *miR-17* and CLL cell viability. Data represent mean  $\pm$  s.e.m. of UM CLL cells from the same five samples transfected in a. Viability was evaluated by AnnexinV and 7-amino-actinomycin-D staining in flow cytometry for different time points (24, 48 and 96 h). *P*-values (Student's *t*-test) for each time point are shown. (c) Effective transfection of antagonomiRs on CpG-induced UM CLL cell. Expression of microRNA from the *miR-17~92* family in UM CLL cells (three cases) transfected with a mixture of scrambled microRNAs (scrambled control), or a mixture of antagonomiR specific for *miR-17*, *miR-18a*, *miR-20a* and *miR-20b* (anti-*miR-17/18a/20a/20b*) is reported (upper panels). Data represent mean  $\pm$  s.e.m. (d) Effect of antagonomiRs on CpG-induced UM CLL cell proliferation. CLL cells were tested for BrdU uptake upon TLR9 triggering. Data represent mean  $\pm$  s.e.m. of UM CLL cells from the same three samples transfected in c.

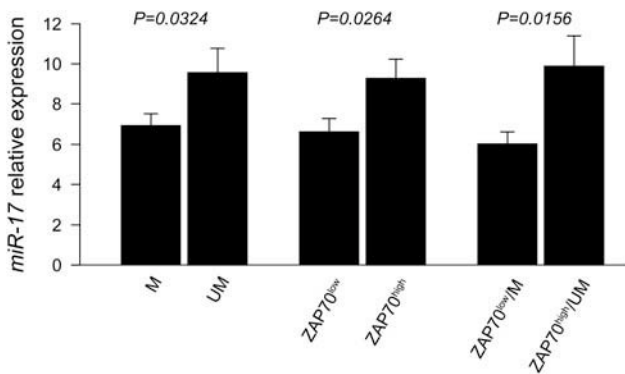


**Figure 6.** Association between *miR-17* expression, *IGHV* gene mutational status and ZAP-70 expression level. *miR-17* relative expression in CLL subgroups defined considering mutational status of *IGHV* genes (M, mutated *IGHV*, 52 cases; UM, unmutated *IGHV*, 31 cases) or ZAP-70 protein expression (ZAP-70<sup>high</sup>, ZAP-70  $\geq$  20% of positive CLL cells, 41 cases; ZAP-70<sup>low</sup>, ZAP-70 < 20% of positive CLL cells, 42 cases), or simultaneously considering ZAP-70 protein expression and mutational status of *IGHV* genes (M and ZAP-70<sup>low</sup>, 33 cases; UM and ZAP-70<sup>high</sup>, 22 cases). Data represent mean  $\pm$  s.e.m.; *P*-values were according to Student's *t*-test.

and/or proliferation when stimulated with a series of exogenous stimuli, including anti-IgM, CpG, CpG/CD40L, IL-4/CD40L, CD40L/IL-2/IL-10/stromal cell co-culture or type I IFNs.<sup>4,40-42</sup> Conversely,

CLL cells from patients with indolent disease usually do not respond or may even respond by undergoing apoptosis.<sup>4,8,43</sup>

In the case of TLR9 signaling, these distinct cellular responses have been associated with differences in intracellular signal transduction.<sup>8,9,20,43</sup> In particular, CpG-stimulated UM CLL cells exhibit greater and prolonged activation of several important downstream signaling molecules, including the transcription factor NF- $\kappa$ B and the kinases Akt, ERK and JNK. Prolonged activation of these downstream signaling molecules has been associated with a greater capacity to traverse the G1/S checkpoint of the cell cycle, as evidenced by [<sup>3</sup>H]thymidine or BrdU incorporation. In contrast, CpG-stimulated M CLL cells show only transient activation of these downstream signaling pathways, usually insufficient for a complete S-phase progression.<sup>8</sup>

Here, we show that differences in the response to TLR9 signaling between UM and M CLL were also demonstrated at GEP and miRome levels. Of the more than 1500 genes that changed expression following CpG stimulation of UM CLL cells and the  $\sim$ 400 genes representing the differential gene expression signature of CpG-stimulated M CLL cells, only a tiny minority (13 genes in our experiments) were shared. More important, the genes that changed expression in UM and M CLL cells belonged to different GO categories, in accordance with the distinct cellular responses induced by TLR9 triggering in these two prognostic subsets.<sup>8,9</sup>

Moreover, a clear-cut miRome signature comprising the differential expression of 24 microRNAs, 21 upregulated, was found to characterize CpG-stimulated UM CLL cells. Conversely, no differences in miRome were obtained by comparing

CpG-stimulated and unstimulated M CLL cells. Despite this, a certain degree of heterogeneity in responses to TLR9 triggering seemed to occur among M CLL, in keeping with literature suggestions,<sup>8,9</sup> although solely revealed by additional cluster analyses carried out utilizing the microRNA signature of UM CLL (Supplementary Figure S1). With the aim to identify the microRNAs whose modulated expression was primarily responsible for GEP changes, *ad-hoc* bioinformatics algorithms were applied to integrate miRome and GEP data.<sup>19</sup> This approach allowed the identification of microRNAs belonging to the *miR-17~92* family as important regulators of the gene expression profile induced by CpG stimulation in UM CLL cells.

The *miR-17~92* family is composed of 15 microRNAs organized in three clusters. The prototypic cluster is the *miR-17~92* polycistronic element (a.k.a. Oncomir-1),<sup>38,44</sup> located at 13q31.3 and composed of six microRNAs (*miR-17*, *miR-18a*, *miR-19a*, *miR-20a*, *miR-19b-1* and *miR-92a-1*), whose transcription is directly transactivated by *c-myc*.<sup>38,44</sup> The two other *miR-17~92* clusters are located on chromosome X and chromosome 7.<sup>21</sup> Notably, a member of one of these paralog clusters, that is, *mir20b*, was also upregulated by CpG stimulation, further emphasizing the involvement of this family in the cascade of events triggered by TLR9 engagement of UM CLL cells. The association of *miR-17~92* with a broad range of cancers underlines the clinical significance of this locus, and suggests its role in many fundamental pathological processes, including tumorigenesis.<sup>38,45-47</sup>

In the present study, as many as 7.5% of the downregulated genes in CpG-stimulated UM CLL cells turned out to be *in-silico* *miR-17~92* targets. These downregulated genes included *ZBTB4* and *TP53INP1*, which regulate apoptosis through *CDKN1A* and *TP53*,<sup>25,26</sup> *E2F5*, necessary for G1 arrest,<sup>24</sup> and *TRIM8*, which is involved in the degradation of *SOCS1*, a well-known regulator of the response to CpG.<sup>23,48</sup> All these genes were identified as direct targets of *miR-17*, as evidenced by their significant downregulation upon ectopic *miR-17* overexpression. In agreement with these results, *miR-17* transfection was also demonstrated to be sufficient to reduce apoptosis induced by serum deprivation in a series of primary UM CLL cells.

The *miR-17~92* locus has also been shown to regulate cell cycle progression by selectively targeting a set of genes involved in the G1/S-phase transition.<sup>38,44,49,50</sup> In this context, ectopic expression of *miR-17* alone was reported to increase the proliferation rate of HEK293 T cells, by suppressing the G1/S-phase checkpoint of the cell cycle.<sup>38,44</sup> Thus, lack of *miR-17~92* upregulation may in part explain the inability of M CLL cells to traverse the G1/S checkpoint following CpG stimulation. In line with this possibility, we show that transfection of primary CLL cells with a mixture of antagomiRs targeting selected *miR-17~92* microRNAs inhibited CpG-induced BrdU incorporation, a marker of DNA synthesis and S-phase progression.

The presence of an UM *IGHV* gene configuration and elevated ZAP-70 levels are both strongly associated with unfavorable prognosis in CLL.<sup>1</sup> Here, we report that expression of *miR-17*, the prototypic member of the *miR-17~92* family, is significantly higher in UM CLL cells expressing high ZAP-70 compared with M CLL cells with a ZAP70<sup>low</sup> phenotype. Interestingly, other microRNAs that we found to be upregulated in UM CLL cells upon CpG stimulation, such as *miR-155*, *miR-221* and *miR-222*, have been also associated with established prognostic factors or with shorter survival in CLL.<sup>12</sup> Overall, the higher expression of microRNAs that are induced by TLR9 triggering in UM/ZAP70<sup>high</sup> CLL cells could suggest that these cells are more frequently subjected to signals capable of activating the TLR9 pathway. Alternatively, UM/ZAP70<sup>high</sup> cells may have a greater capacity to respond to microenvironmental signals, including those delivered through TLR9, as previously elaborated.<sup>51-54</sup>

The GEP analysis performed in this study also showed that *MYC* was substantially upregulated in UM CLL cells upon CpG

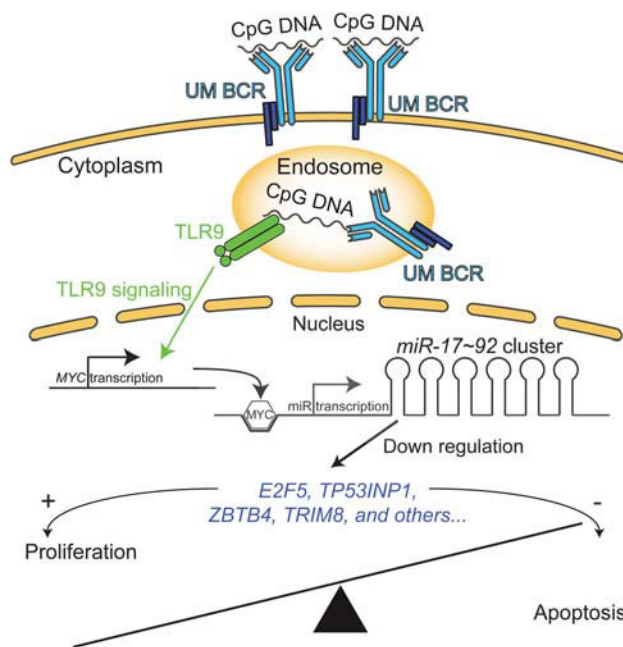


**Figure 7.** Model for pro-survival circuitry operating in CpG-stimulated UM CLL cells. See text for details.

stimulation, but not in M CLL cells. Consistently, the transcriptional activity of *MYC*, defined by the expression of three independent target genes (*CAD*, *TFAM* and *PGK1*), increased in CpG-stimulated UM CLL cells. Pathological activation of *MYC*, which is one of the most common oncogenic events in human cancer, has been shown to result in extensive reprogramming of microRNA expression by tumor cells.<sup>55</sup> In this regard, although *MYC* predominantly induces downregulation of microRNA expression, the *miR-17~92* cluster is known to be directly upregulated by *MYC*.<sup>35-37,44</sup> Results from the present study provide evidence of an associative interaction between *MYC* and *miR-17~92* family also in CLL cells. Despite this, we failed to find a correlation between *miR-17* and *MYC* baseline levels in a relatively wide CLL series (Supplementary Figure S8). This lack of correlation could be explained by considering the different kinetics of *MYC* and *miR-17* modulation upon *in vitro* CpG cell stimulation, as demonstrated here in CLL (Figure 4b), and in other cellular models.<sup>35-37</sup> Alternatively, a *MYC*-independent pathway leading to increased *miR-17* expression has to be also considered.

Induction of microRNAs from the *miR-17~92* family can in turn regulate B-cell proliferation and survival by downregulating a series of genes with anti-proliferative and/or pro-apoptotic activities. A comprehensive scheme of the cascade of events triggered by CpG engagement of TLR9 in UM CLL cells is drawn in Figure 7.

What still remains to be established is the mechanism(s) through which TLR9 signaling leads to enhanced upregulation of *MYC*. In this regard, we can only speculate that an overexpression of *MYC* following TLR9 stimulation may occur by way of the *MyD88*-ERK pathway, as demonstrated in murine models.<sup>6,56</sup> The recent identification of an activating mutation involving the *MyD88* gene in a fraction of CLL with an aggressive clinical behavior<sup>57</sup> suggests to investigate in these cases the constitutive *MYC*/*miR-17* levels or the capability of *MyD88* mutated cells to modulate their expression upon CpG stimulation *in vitro*.

In summary, data from the present report suggest that the TLR9 pathway, through the activity of specific microRNAs, could be an important link between the microenvironment and the

intracellular machinery that regulates CLL cell proliferation and survival. Further support for this possibility comes from the notion that the CLL BCRs, particularly those bearing UM IGHV domains, frequently recognize autoantigens that are either directly associated with DNA or are colocalized in apoptotic blebs with DNA-containing protein complexes.<sup>58,59</sup> The reactivity of the leukemic BCRs could allow efficient delivery of exogenous DNA to endosomes, where TLR9 is located and activated. In line with this possibility, recent GEP analysis showed that CLL cells located in lymph nodes overexpress TLR target genes, indicating that this pathway is frequently activated *in vivo*.<sup>60</sup> Together, these data suggest that the TLR9 pathway may have a role in the pathogenesis of aggressive CLL and, as such, could represent a novel target for therapeutic intervention.

## CONFLICT OF INTEREST

The authors declare no conflict of interest.

## ACKNOWLEDGEMENTS

This work was supported in part by: Ministero della Salute, Ricerca Finalizzata I.R.C.C.S., 'Alleanza Contro il Cancro'; Rete Nazionale Bio-Informatica Oncologica/RN-BIO; Progetto Giovani Ricercatori n. GR-2009-1475467, Rome, Italy; Progetto Giovani Ricercatori n. GR-2008-1138053, Rome, Italy; Fondazione Internazionale di Ricerca in Medicina Sperimentale (FIRMS); Associazione Italiana contro le Leucemie, linfomi e mielomi (AIL), Venezia Section, Prammaggiore Group, Italy; Ricerca Scientifica Applicata, Regione Friuli Venezia Giulia ('Linfonet' Project), Trieste, Italy; the Associazione Italiana Ricerca Cancro (AIRC, Investigator Grant IG-8701, IG-5917 and MFAG-10327), Milan, Italy; '5 × 1000 Intramural Program', Centro di Riferimento Oncologico, Aviano, Italy; and The Leukemia & Lymphoma Society (grant no. R6170-10), White Plains, NY.

## AUTHOR CONTRIBUTIONS

RB performed the research and wrote the manuscript; SG and MDB performed the research and contributed to the writing of the manuscript; ET, AZ and DB performed the research; SV and DM analyzed the miRNA and gene expression data; DR, GDP, GG and LL provided patients' data; and DGE and VG designed the study and wrote the manuscript.

## REFERENCES

- Chiorazzi N, Rai KR, Ferrarini M. Chronic lymphocytic leukemia. *N Engl J Med* 2005; **352**: 804–815.
- Borche L, Lim A, Binet JL, Dighiero G. Evidence that chronic lymphocytic leukemia B lymphocytes are frequently committed to production of natural autoantibodies. *Blood* 1990; **76**: 562–569.
- Stoeger ZM, Wakai M, Tse DB, Vinciguerra VP, Allen SL, Budman DR et al. Production of autoantibodies by CD5-expressing B lymphocytes from patients with chronic lymphocytic leukemia. *J Exp Med* 1989; **169**: 255–268.
- Coscia M, Pantaleoni F, Riganti C, Vitale C, Rigoni M, Peola S et al. IGHV unmutated CLL B cells are more prone to spontaneous apoptosis and subject to environmental prosurvival signals than mutated CLL B cells. *Leukemia* 2011; **25**: 828–837.
- Palacios F, Moreno P, Morande P, Abreu C, Correa A, Porro V et al. High expression of AID and active class switch recombination might account for a more aggressive disease in unmutated CLL patients: link with an activated microenvironment in CLL disease. *Blood* 2010; **115**: 4488–4496.
- Barton GM, Kagan JC. A cell biological view of Toll-like receptor function: regulation through compartmentalization. *Nat Rev Immunol* 2009; **9**: 535–542.
- Clark MR, Tanaka A, Powers SE, Veselits M. Receptors, subcellular compartments and the regulation of peripheral B cell responses: the illuminating state of anergy. *Mol Immunol* 2011; **48**: 1281–1286.
- Longo PG, Laurenti L, Gobessi S, Petlickovski A, Pelosi M, Chiusolo P et al. The Akt signaling pathway determines the different proliferative capacity of chronic lymphocytic leukemia B-cells from patients with progressive and stable disease. *Leukemia* 2007; **21**: 110–120.
- Tarnani M, Laurenti L, Longo PG, Piccirillo N, Gobessi S, Mannocci A et al. The proliferative response to CpG-ODN stimulation predicts PFS, TTT and OS in patients with chronic lymphocytic leukemia. *Leuk Res* 2010; **34**: 1189–1194.
- Lewis BP, Burge CB, Bartel DP. Conserved seed pairing, often flanked by adenosines, indicates that thousands of human genes are microRNA targets. *Cell* 2005; **120**: 15–20.
- Mattick JS. The genetic signatures of noncoding RNAs. *PLoS Genet* 2009; **5**: e1000459.
- Calin GA, Ferracin M, Cimmino A, Di LG, Shimizu M, Wojcik SE et al. A microRNA signature associated with prognosis and progression in chronic lymphocytic leukemia. *N Engl J Med* 2005; **353**: 1793–1801.
- Zenz T, Mohr J, Elderling E, Kater AP, Buhler A, Kienle D et al. miR-34a as part of the resistance network in chronic lymphocytic leukemia. *Blood* 2009; **113**: 3801–3808.
- Bomben R, Dal-Bo M, Benedetti D, Capello D, Forconi F, Marconi D et al. Expression of mutated IGHV3-23 genes in chronic lymphocytic leukemia identifies a disease subset with peculiar clinical and biological features. *Clin Cancer Res* 2010; **16**: 620–628.
- Gattei V, Bulian P, Del Principe MI, Zucchetto A, Maurillo L, Buccisano F et al. Relevance of CD49d protein expression as overall survival and progressive disease prognosticator in chronic lymphocytic leukemia. *Blood* 2008; **111**: 865–873.
- Decker T, Schneller F, Kronschnabl M, Dechow T, Lipford GB, Wagner H et al. Immunostimulatory CpG-oligonucleotides induce functional high affinity IL-2 receptors on B-CLL cells: costimulation with IL-2 results in a highly immunogenic phenotype. *Exp Hematol* 2000; **28**: 558–568.
- Eisen MB, Spellman PT, Brown PO, Botstein D. Cluster analysis and display of genome-wide expression patterns. *Proc Natl Acad Sci USA* 1998; **95**: 14863–14868.
- Draghici S, Khatri P, Martins RP, Ostermeier GC, Krawetz SA. Global functional profiling of gene expression. *Genomics* 2003; **81**: 98–104.
- Volinia S, Visone R, Galasso M, Rossi E, Croce CM. Identification of microRNA activity by Targets' Reverse Expression. *Bioinformatics* 2010; **26**: 91–97.
- Tromp JM, Tonino SH, Elias JA, Jaspers A, Luijckx DM, Kater AP et al. Dichotomy in NF-kappaB signaling and chemoresistance in immunoglobulin variable heavy-chain-mutated versus unmutated CLL cells upon CD40/TLR9 triggering. *Oncogene* 2010; **29**: 5071–5082.
- Ventura A, Young AG, Winslow MM, Lintault L, Meissner A, Erkeland SJ et al. Targeted deletion reveals essential and overlapping functions of the miR-17 through 92 family of miRNA clusters. *Cell* 2008; **132**: 875–886.
- Lee Y, Jeon K, Lee JT, Kim S, Kim VN. MicroRNA maturation: stepwise processing and subcellular localization. *EMBO J* 2002; **21**: 4663–4670.
- Okumura F, Matsunaga Y, Katayama Y, Nakayama KI, Hatakeyama S. TRIM8 modulates STAT3 activity through negative regulation of PIAS3. *J Cell Sci* 2010; **123**: 2238–2245.
- Gaubatz S, Lindeman GJ, Ishida S, Jakoi L, Nevins JR, Livingston DM et al. E2F4 and E2F5 play an essential role in pocket protein-mediated G1 control. *Mol Cell* 2000; **6**: 729–735.
- Weber A, Marquardt J, Elzi D, Forster N, Starke S, Glaum A et al. Zbtb4 represses transcription of P21CIP1 and controls the cellular response to p53 activation. *EMBO J* 2008; **27**: 1563–1574.
- Okamura S, Arakawa H, Tanaka T, Nakanishi H, Ng CC, Taya Y et al. p53DINP1, a p53-inducible gene, regulates p53-dependent apoptosis. *Mol Cell* 2001; **8**: 85–94.
- Chi SW, Zang JB, Mele A, Darnell RB. Argonaute HITS-CLIP decodes microRNA-mRNA interaction maps. *Nature* 2009; **460**: 479–486.
- Emmrich S, Putzer BM. Checks and balances: E2F-microRNA crosstalk in cancer control. *Cell Cycle* 2010; **9**: 2555–2567.
- Kim K, Chadalapaka G, Lee SO, Yamada D, Sastre-Garau X, Defosse PA et al. Identification of oncogenic microRNA-17-92/ZBTB4/specificity protein axis in breast cancer. *Oncogene* 2012; **31**: 1034–1044.
- Kurisetty V, Kovacs K, Luongo T, Erchan J. hsa-miR-20a promotes tumorigenesis in ccRCC cancer cell lines [abstract]. *Proceedings of the 102nd Annual Meeting of the American Association for Cancer Research* 2011, Orlando, FL, USA.
- Tan LP, Seinen E, Duns G, de JD, Sibon OC, Poppema S et al. A high throughput experimental approach to identify miRNA targets in human cells. *Nucleic Acids Res* 2009; **37**: e137.
- Trompeter HI, Abbad H, Iwaniuk KM, Hafner M, Renwick N, Tuschl T et al. MicroRNAs mir-17, mir-20a, and mir-106b act in concert to modulate E2F activity on cell cycle arrest during neuronal lineage differentiation of USSC. *PLoS One* 2011; **6**: e16138.
- Wang Q, Li YC, Wang J, Kong J, Qi Y, Quigg RJ et al. miR-17-92 cluster accelerates adipocyte differentiation by negatively regulating tumor-suppressor Rb2/p130. *Proc Natl Acad Sci USA* 2008; **105**: 2889–2894.
- Yeung ML, Yasunaga J, Bennasser Y, Dusetti N, Harris D, Ahmad N et al. Roles for microRNAs, miR-93 and miR-130b, and tumor protein 53-induced nuclear protein 1 tumor suppressor in cell growth dysregulation by human T-cell lymphotropic virus 1. *Cancer Res* 2008; **68**: 8976–8985.
- Li C, Kim SW, Rai D, Bolla AR, Adhvaray S, Kinney MC et al. Copy number abnormalities, MYC activity, and the genetic fingerprint of normal B cells mechanistically define the microRNA profile of diffuse large B-cell lymphoma. *Blood* 2009; **113**: 6681–6690.

- 36 Chang TC, Yu D, Lee YS, Wentzel EA, Arking DE, West KM *et al*. Widespread microRNA repression by Myc contributes to tumorigenesis. *Nat Genet* 2008; **40**: 43–50.
- 37 O'Donnell KA, Wentzel EA, Zeller KI, Dang CV, Mendell JT. c-Myc-regulated microRNAs modulate E2F1 expression. *Nature* 2005; **435**: 839–843.
- 38 He L, Thomson JM, Hemann MT, Hernando-Monge E, Mu D, Goodson S *et al*. A microRNA polycistron as a potential human oncogene. *Nature* 2005; **435**: 828–833.
- 39 Onnis A, De FG, Antonicelli G, Onorati M, Bellan C, Sherman O *et al*. Alteration of microRNAs regulated by c-Myc in Burkitt lymphoma. *PLoS One* 2010; **5**: pii: e12960.
- 40 Tomic J, Lichty B, Spaner DE. Aberrant interferon-signaling is associated with aggressive chronic lymphocytic leukemia. *Blood* 2011; **117**: 2668–2680.
- 41 Plander M, Seegers S, Ugocsai P, Ermeier-Daucher S, Ivanyi J, Schmitz G *et al*. Different proliferative and survival capacity of CLL-cells in a newly established *in vitro* model for pseudofollicles. *Leukemia* 2009; **23**: 2118–2128.
- 42 Bernasconi NL, Onai N, Lanzavecchia A. A role for Toll-like receptors in acquired immunity: up-regulation of TLR9 by BCR triggering in naive B cells and constitutive expression in memory B cells. *Blood* 2003; **101**: 4500–4504.
- 43 Jahrsdorfer B, Wooldridge JE, Blackwell SE, Taylor CM, Griffith TS, Link BK *et al*. Immunostimulatory oligodeoxynucleotides induce apoptosis of B cell chronic lymphocytic leukemia cells. *J Leukoc Biol* 2005; **77**: 378–387.
- 44 Cloonan N, Brown MK, Steptoe AL, Wani S, Chan WL, Forrest AR *et al*. The miR-17-5p microRNA is a key regulator of the G1/S phase cell cycle transition. *Genome Biol* 2008; **9**: R127.
- 45 Venturini L, Battmer K, Castoldi M, Schultheis B, Hochhaus A, Muckenthaler MU *et al*. Expression of the miR-17-92 polycistron in chronic myeloid leukemia (CML) CD34+ cells. *Blood* 2007; **109**: 4399–4405.
- 46 Hayashita Y, Osada H, Tatematsu Y, Yamada H, Yanagisawa K, Tomida S *et al*. A polycistronic microRNA cluster, miR-17-92, is overexpressed in human lung cancers and enhances cell proliferation. *Cancer Res* 2005; **65**: 9628–9632.
- 47 Volinia S, Calin GA, Liu CG, Ambs S, Cimmino A, Petrocca F *et al*. A microRNA expression signature of human solid tumors defines cancer gene targets. *Proc Natl Acad Sci USA* 2006; **103**: 2257–2261.
- 48 Fujimoto M, Naka T. SOCS1, a negative regulator of cytokine signals and TLR responses, in human liver diseases. *Gastroenterol Res Pract* 2010; **2010**: pii: 470468.
- 49 Cui JW, Li YJ, Sarkar A, Brown J, Tan YH, Premyslova M *et al*. Retroviral insertional activation of the Fli-3 locus in erythroleukemias encoding a cluster of microRNAs that convert Epo-induced differentiation to proliferation. *Blood* 2007; **110**: 2631–2640.
- 50 Frenquelli M, Muzio M, Scielzo C, Fazi C, Scarfo L, Rossi C *et al*. MicroRNA and proliferation control in chronic lymphocytic leukemia: functional relationship between miR-221/222 cluster and p27. *Blood* 2010; **115**: 3949–3959.
- 51 Allsup DJ, Kamiguti AS, Lin K, Sherrington PD, Matrai Z, Slupsky JR *et al*. B-cell receptor translocation to lipid rafts and associated signaling differ between prognostically important subgroups of chronic lymphocytic leukemia. *Cancer Res* 2005; **65**: 7328–7337.
- 52 Chen L, Appgar J, Huynh L, Dicker F, Giago-McGahan T, Rassenti L *et al*. ZAP-70 directly enhances IgM signaling in chronic lymphocytic leukemia. *Blood* 2005; **105**: 2036–2041.
- 53 Gobessi S, Laurenti L, Longo PG, Sica S, Leone G, Efremov DG. ZAP-70 enhances B-cell-receptor signaling despite absent or inefficient tyrosine kinase activation in chronic lymphocytic leukemia and lymphoma B cells. *Blood* 2007; **109**: 2032–2039.
- 54 Mockridge CL, Potter KN, Wheatley I, Neville LA, Packham G, Stevenson FK. Reversible anergy of sIgM-mediated signaling in the two subsets of CLL defined by VH-gene mutational status. *Blood* 2007; **109**: 4424–4431.
- 55 Albiñ A, Johnsen JI, Henriksson MA. MYC in oncogenesis and as a target for cancer therapies. *Adv Cancer Res* 2010; **107**: 163–224.
- 56 Lee SH, Hu LL, Gonzalez-Navajas J, Seo GS, Shen C, Brick J *et al*. ERK activation drives intestinal tumorigenesis in Apc(min/+) mice. *Nat Med* 2010; **16**: 665–670.
- 57 Puente XS, Pinyol M, Quesada V, Conde L, Ordonez GR, Villamor N *et al*. Whole-genome sequencing identifies recurrent mutations in chronic lymphocytic leukaemia. *Nature* 2011; **475**: 101–105.
- 58 Catera R, Silverman GJ, Hatzi K, Seiler T, Didier S, Zhang L *et al*. Chronic lymphocytic leukemia cells recognize conserved epitopes associated with apoptosis and oxidation. *Mol Med* 2008; **14**: 665–674.
- 59 Rosen A, Murray F, Evaldsson C, Rosenquist R. Antigens in chronic lymphocytic leukemia—implications for cell origin and leukemogenesis. *Semin Cancer Biol* 2010; **20**: 400–409.
- 60 Herishanu Y, Perez-Galan P, Liu D, Biancotto A, Pittaluga S, Vire B *et al*. The lymph node microenvironment promotes B-cell receptor signaling, NF-kappaB activation, and tumor proliferation in chronic lymphocytic leukemia. *Blood* 2011; **117**: 563–574.

Supplementary Information accompanies the paper on the Leukemia website (<http://www.nature.com/leu>)

# 13q14 Deletion Size and Number of Deleted Cells Both Influence Prognosis in Chronic Lymphocytic Leukemia

Michele Dal Bo,<sup>1</sup> Francesca Maria Rossi,<sup>1</sup> Davide Rossi,<sup>2</sup> Clara Deambrogi,<sup>2</sup> Francesco Bertoni,<sup>3</sup> Ilaria Del Giudice,<sup>4</sup> Giuseppe Palumbo,<sup>5</sup> Mauro Nanni,<sup>4</sup> Andrea Rinaldi,<sup>3</sup> Ivo Kwee,<sup>3,6</sup> Erika Tissino,<sup>1</sup> Giorgia Corradini,<sup>7</sup> Alessandro Gozzetti,<sup>8</sup> Emanuele Cencini,<sup>8</sup> Marco Ladetto,<sup>9</sup> Angela Maria Coletta,<sup>10</sup> Fabrizio Luciano,<sup>10</sup> Pietro Bulian,<sup>1</sup> Gabriele Pozzato,<sup>11</sup> Luca Laurenti,<sup>12</sup> Francesco Forconi,<sup>8</sup> Francesco Di Raimondo,<sup>5</sup> Roberto Marasca,<sup>7</sup> Giovanni Del Poeta,<sup>10</sup> Gianluca Gaidano,<sup>2</sup> Robin Foà,<sup>4</sup> Anna Guarini,<sup>4</sup> and Valter Gattei<sup>1\*</sup>

<sup>1</sup>Clinical and Experimental Onco-Hematology Unit, Centro di Riferimento Oncologico, I.R.C.C.S., Aviano (PN), Italy

<sup>2</sup>Division of Hematology, Department of Clinical and Experimental Medicine & IRCAD, Amedeo Avogadro University of Eastern Piedmont, Novara, Italy

<sup>3</sup>Laboratory of Experimental Oncology and Lymphoma Unit, Oncology Institute of Southern Switzerland (IOSI), Bellinzona, Switzerland

<sup>4</sup>Division of Hematology, Department of Cellular Biotechnologies and Hematology, Sapienza University, Rome, Italy

<sup>5</sup>Division of Hematology, Ferrarotto Hospital, Catania, Italy

<sup>6</sup>Istituto Dalle Molle di Studi sull'Intelligenza Artificiale (IDSIA), Manno, Switzerland

<sup>7</sup>Division of Hematology, Department of Oncology and Hematology, University of Modena and Reggio Emilia, Modena, Italy

<sup>8</sup>Division of Hematology and Transplant, Department of Clinical Medicine and Immunological Sciences, University of Siena, Siena, Italy

<sup>9</sup>Division of Hematology, Department of Experimental Medicine and Oncology, University of Turin, Italy

<sup>10</sup>Division of Hematology, S.Eugenio Hospital and University of Tor Vergata, Rome, Italy

<sup>11</sup>Department of Internal Medicine and Hematology, Maggiore General Hospital, University of Trieste, Trieste, Italy

<sup>12</sup>Hematology Institute, Catholic University 'Sacro Cuore,' Rome, Italy

Deletion at 13q14 is detected by fluorescence in situ hybridization (FISH) in about 50% of chronic lymphocytic leukemia (CLL). Although CLL with 13q deletion as the sole cytogenetic abnormality (del13q-only) usually have good prognosis, more aggressive clinical courses are documented for del13q-only CLL carrying higher percentages of 13q deleted nuclei. Moreover, deletion at 13q of different sizes have been described, whose prognostic significance is still unknown. In a multi-institutional cohort of 342 del13q-only cases and in a consecutive unselected cohort of 265 CLL, we investigated the prognostic significance of 13q deletion, using the 13q FISH probes locus-specific identifier (LSI)-DI3S319 and LSI-RBI that detect the *DLEU2/MIR15A/MIR16-1* and *RBI* loci, respectively. Results indicated that both percentage of deleted nuclei and presence of larger deletions involving the *RBI* locus cooperated to refine the prognosis of del13q-only cases. In particular, CLL carrying <70% of 13q deleted nuclei with deletions not comprising the *RBI* locus were characterized by particularly long time-to-treatment. Conversely, CLL with 13q deletion in <70% of nuclei but involving the *RBI* locus, or CLL carrying 13q deletion in ≥70% of nuclei, with or without *RBI* deletions, collectively experienced shorter time-to-treatment. A revised flowchart for the prognostic FISH assessment of del13q-only CLL, implying the usage of both 13q probes, is proposed. © 2011 Wiley-Liss, Inc.

Additional Supporting Information may be found in the online version of this article.

Supported by: Ministero della Salute (Ricerca Finalizzata I.R.C.C.S., "Alleanza Contro il Cancro" and Rete Nazionale Bio-Informatica Oncologica/RN-BIO), Rome; Associazione Italiana contro le Leucemie linfomi e mielomi (AIL) Venezia Section, Pramaggiore (VE) Group; Ricerca Scientifica Applicata Regione Friuli Venezia Giulia, Trieste ("Linfonet" Project); Associazione Italiana Ricerca Cancro (AIRC, Investigator Grant IG-8701 and AIRC Special Program Molecular Clinical Oncology, 5 × 1000, No. 10007, Milan, Italy); PRIN 2008, MIUR, Rome, Italy; Helmut Horten Foundation; San Salvatore Foundation;

Fondazione per la Ricerca e la Cura sui Linfomi (Lugano, Switzerland).

\*Correspondence to: Valter Gattei, MD, Clinical and Experimental Onco-Hematology Unit, Centro di Riferimento Oncologico, I.R.C.C.S., Via Franco Gallini 2, Aviano (PN), Italy. E-mail: vgattei@cro.it

Received 13 January 2011; Accepted 27 March 2011

DOI 10.1002/gcc.20885

Published online 11 May 2011 in Wiley Online Library (wileyonlinelibrary.com).

## INTRODUCTION

Chronic lymphocytic leukemia (CLL) is a disease with a highly variable clinical course (Chiorazzi et al., 2005; Dal-Bo et al., 2009), that can be predicted by the presence of specific cytogenetic abnormalities (Dohner et al., 2000; Krober et al., 2002). Among them, deletion at 13q14 represents the most common genomic aberration in CLL, occurring in more than 50% of cases, and being the sole documented cytogenetic abnormality in 36% of CLL (Dohner et al., 2000). Although these latter cases (hereafter indicated as del13q-only CLL) are known to experience a more favorable clinical course (Dohner et al., 2000; Mehes, 2005), recent data suggest a relatively worse clinical behavior for del13q-only CLL carrying higher percentages of 13q14 deleted nuclei (Hernandez et al., 2009; Van Dyke et al., 2010).

Deletion at 13q, as it occurs in CLL, appears to be heterogeneous in size (Ouillet et al., 2008; Mosca et al., 2010), thus suggesting that more than one tumor suppressor gene located in the context of the 13q14 locus may be involved in determining the clinico-biological features of 13q deletion-carrying CLL (Kapanadze et al., 1998; Lagos-Quintana et al., 2001; Calin et al., 2002; Mertens et al., 2002; Baranova et al., 2003; Ivanov et al., 2003; Corcoran et al., 2004; Cimmino et al., 2005; Fulci et al., 2007; Lerner et al., 2007; Linsley et al., 2007; Raveche et al., 2007; Ouillet et al., 2008; Liu et al., 2008; Bandi et al., 2009; Hernandez et al., 2009; Mertens et al., 2009; Klein et al., 2010; Palamarchuk et al., 2010; Mosca et al., 2010; Biredinc et al., 2010). Two anatomical landmarks have been proposed for the characterization of 13q deletion in CLL (Ouillet et al., 2008): (i) the minimal deleted region (MDR) which comprised the *DLEU2* gene, the *MIR15A/MIR16-1* cluster, and the first exon of the *DLEU1* gene (Liu et al., 1997; Lagos-Quintana et al., 2001; Migliazza et al., 2001; Calin et al., 2002); and (ii) the *RB1* gene, localized at chromosomal band 13q14.1–q14.2, that can be considered, when found deleted, as the marker of 13q deletion with larger chromosome losses (Ouillet et al., 2008; Mosca et al., 2010; Parker et al., 2011).

Classically, the pathogenetic role of deletion at 13q in CLL has been related to lack of B-cell proliferation control allegedly determined by deletion of the *DLEU2/MIR15A/MIR16-1* locus, which is known to contain negative regulators of the expression of the *BCL2* gene (Cimmino et al.,

2005; Klein et al., 2010). A role for *RB1* in CLL pathogenesis, although historically excluded (Sakai et al., 1991; Liu et al., 1993), has been also more recently revisited given the involvement of *RB1* in the regulation of cell cycle progression and genomic stability (Hernando et al., 2004; Pickering and Kowalik, 2006). Several genes have been identified as putative tumor suppressor at 13q14 either located in the MDR or lost in larger deletions at 13q14 (Sakai et al., 1991; Kapanadze et al., 1998; Mertens et al., 2002; Baranova et al., 2003; Ivanov et al., 2003; Corcoran et al., 2004; Fulci et al., 2007; Lerner et al., 2007; Ouillet et al., 2008; Hernandez et al., 2009; Mertens et al., 2009; Biredinc et al., 2010; Klein et al., 2010; Mosca et al., 2010; Palamarchuk et al., 2010; Parker et al., 2011), including genes belonging to the *DLEU* family such as *TRIM13* or *DLEU7* (Liu et al., 1997; Kapanadze et al., 1998; Baranova et al., 2003; Corcoran et al., 2004; Lerner et al., 2007; Klein et al., 2010; Palamarchuk et al., 2010), but the pathogenesis of CLL carrying this deletion has still to be completely elucidated.

In this study, by taking advantage of a wide Italian multi-institutional cohort of del13q-only CLL, and a single-institutional unselected consecutive cohort of CLL, we evaluated the prognostic role of 13q deletion of different sizes by a fluorescence in situ hybridization (FISH) approach using the combination of two different locus-specific identifiers (LSI), i.e., LSI-D13S319 and LSI-RB1, respectively detecting the *DLEU2/MIR15A/MIR16-1* and *RB1* loci. Results indicated that deletion at 13q involving the *RB1* locus are characterized by a relatively worse clinical behavior in the context of del13q-only CLL. The combined use of the two LSI for detection of deletion at 13q, if integrated with the percentage of 13q deleted nuclei (Hernandez et al., 2009; Van Dyke et al., 2010), allowed revisiting of the FISH flowchart for the prognostic evaluation of CLL.

## MATERIALS AND METHODS

### Patients

This study was performed on a multi-institutional cohort of 342 CLL carrying a deletion at 13q14 as the sole cytogenetic abnormality; this patient series was used to investigate the prognostic impact of 13q deletion of different sizes in the context of del13q-only CLL. A mono-

institutional consecutive unselected cohort of 265 CLL, which included 97 del13q-only CLL, was also used to compare the prognostic impact of 13q deletion of different sizes with that of the main cytogenic subtypes (Dohner et al., 2000). CLL patients entering the study were diagnosed according to the IWCLL-NCI criteria (Hallek et al., 2008) and had a complete clinical and biological assessment. All patients provided informed consent in accordance with local Institutional Review Board requirements and the Declaration of Helsinki. The main clinical and biological features of the two cohorts are summarized in Supporting Information Tables S1 and S2.

#### Analysis of Cytogenetic Aberrations

Interphase FISH was performed on nuclei preparations of peripheral blood mononuclear cells collected at diagnosis, separated upon Ficoll-Hypaque (Pharmacia, Uppsala, Sweden) density gradient centrifugation, and investigated for deletion at 13q, deletion at 11q, deletion at 17p or presence of trisomy 12. For chromosomes 11 and 17, the two locus specific probes LSI-ATM and LSI-p53, directly labeled with SpectrumGreen (LSI-ATM) or SpectrumOrange (LSI-p53), were used, respectively. An alpha satellite DNA probe CEP12, directly labeled with SpectrumGreen, was used to detect aneuploidy of chromosome 12. For chromosome 13, two locus specific probes LSI-D13S319 and LSI-RB1 were used, directly labeled with SpectrumOrange and SpectrumGreen. All probes were from Vysis (Inc, London, United Kingdom) and FISH analyses were performed according to the manufacturer's protocols and as previously reported (Del Principe et al., 2006). In all of the analyzed CLL cases, at least two hundred interphase round nuclei with well-delineated fluorescent spots were counted; positive cases were defined as having  $\geq 5\%$  of nuclei displaying the investigated abnormality.

#### Identification of Immunoglobulin (IG) Heavy (H) Variable (V) Gene Mutational Status

*IGHV*-diversity(*D*)-joining(*J*) were amplified from either reverse-transcribed total RNA or genomic DNA as previously reported (Capello et al., 2004; Degan et al., 2004; Bomben et al., 2009). Purified amplicons were sequenced either directly or upon subcloning (Capello et al., 2004; Degan et al., 2004). Sequences were aligned to

the ImMunoGeneTics (IMGT) directory for the identification of *IGHV*-D-J rearrangements and for computation of mutational load (Giudicelli et al., 2004; Pommie et al., 2004; Lefranc et al., 2005). *IGHV* sequences were considered mutated or unmutated using the conventional cutoff of 2% mismatch from germline *IGHV* sequences (Damle et al., 1999; Hamblin et al., 1999).

#### Immunophenotypic Analyses

Detection of CD38 and ZAP70 expression was performed as previously reported (Rassenti et al., 2004; Gattei et al., 2008). A cutoff of 30% positive cells was chosen to discriminate CD38<sup>pos</sup> from CD38<sup>neg</sup> CLL, while a cutoff of 20% positive cells was chosen to distinguish ZAP70<sup>pos</sup> from ZAP70<sup>neg</sup> CLL (Crespo et al., 2003; Orchard et al., 2004; Rassenti et al., 2004; Del Principe et al., 2006; Gattei et al., 2008).

#### Beta2-Microglobulin (B2M) Detection

B2M levels, as determined by different laboratories, were standardized by dividing the original mg/L values by the upper limit of normal (ULN) specific for each laboratory, as described (Del Principe et al., 2006; Bulian et al., 2009; Bulian et al., in press).

#### Genome-Wide DNA Analysis

DNA samples were obtained as previously reported (Rossi et al., 2009) in a subgroup of 67 del13q-only cases belonging to the cohort of 342 del13q-only cases (Supporting Information Table S3). DNA integrity was verified by electrophoresis of 50 ng on a 1% agarose gel. Genomic profiles were obtained using Affymetrix Human Mapping GeneChip 6.0 arrays (Affymetrix, Santa Clara, CA). DNA was processed according to the instructions provided in the Affymetrix Genome-Wide Human SNP Nsp/Sty 6.0 Assay Manual. Initial analysis of the array to obtain intensity data were performed using the Affymetrix GeneChip Command Console Software (AGCC). The AGCC probe cell intensity data were then analyzed with the GenotypeConsole 3.01 (GTC3.01) to obtain genotype data and with the circular binary segmentation algorithm (Olshen et al., 2004). A reference dataset of 270 Caucasian HapMap profiles was used to normalize the CLL DNA profiles. Segments were called homozygous deletions with a copy number (CN)  $< -1.0$ , heterozygous deletions with  $-1.0 < CN < -0.092$ , normal with

$-0.092 < CN < 0.092$ , gains if  $0.092 < CN < 1.0$ , and amplifications with  $CN > 1.0$ . The thresholds ( $-0.092, 0.092$ ) were computed as six times the median absolute deviation (MAD), corresponding to a significance of better than  $P < 0.001$  after Bonferroni multiple test correction. The thresholds ( $-1.0, 1.0$ ) for homozygous deletions and amplifications were heuristically established. Comparison of SNP array data and FISH analysis showed agreement in 63 of 67 cases (94%). The four discordant cases revealed low percentages of 13q deleted nuclei (range of percentage of deleted nuclei: 5–10%), and resulted negative in the genome-wide DNA profile. These cases were not considered in the deletion size evaluation.

### Statistical Analysis

Statistical analyses were performed using the R statistical package (<http://www.r-project.org/>) or the MedCalc software (MedCalc Software, Mariakerke, Be). The primary end points were time-to-first-treatment (TTT) and overall survival (OS). TTT data were defined as time from diagnosis to treatment (event) or end of follow-up (censored observation), and were available for all CLL cases entering the study; in our series, 124 events were recorded. In the cohort of CLL cases used for TTT analysis, no CLL cases died before disease progression. For OS analysis, all events were considered as CLL-related, i.e., all deaths were considered as events whatever the cause. OS data were available for 325 out of 342 del13q-only cases, with 32 recorded events. TTT and OS were estimated using the Kaplan-Meier plots and comparisons between groups were made by means of log-rank test. The Cox proportional hazard regression model was chosen to assess the independent effect of covariates, treated as dichotomous, on TTT, with a backward procedure for selecting significant variables. The association between percentage of nuclei carrying a 13q deletion and other variables (Rai stage, CD38, ZAP70, *IGHV* gene mutational status, and B2M) was calculated using the  $\chi^2$  test. Comparison among del13q-only cases was determined using Kruskal-Wallis equality of population rank test.

## RESULTS

### Percentage of Deleted Nuclei has Prognostic Impact in del13q-only CLL

All of the 342 CLL entering this study (del13q-only CLL; Supporting Information Table

S1) were analyzed by FISH for the canonical 13q deletion using the LSI-D13S319 probe. The presence of a biallelic loss was detected in 61 out of 342 cases (17.8%; data not shown). In keeping with previous studies (Van Dyke et al., 2010), no significant difference was observed in TTT between del13q-only cases with monoallelic versus biallelic losses (data not shown).

Recent reports described a relationship between the percentage of nuclei carrying a 13q deletion and the clinical course in CLL. In particular, 80% and 65.5% have been recently proposed as cutoffs capable of separating del13q-only cases into two subgroups with different TTT/OS distributions (Hernandez et al., 2009; Van Dyke et al., 2010). Accordingly, maximally selected log-rank statistics identified the cutoff of 70% of nuclei carrying 13q deletion as the most appropriate cutoff in our series ( $P = 0.0022$ ) (Supporting Information Fig. S1). By using this cutoff, 239/342 del13q-only cases (69.9%) carried a 13q deletion in  $<70\%$  of nuclei. The distribution of biallelic losses between the two subgroups obtained using this cutoff was homogeneous (data not shown), as was the distribution of all of the investigated prognosticators (i.e., Rai stage, *IGHV* gene mutational status, ZAP70 and CD38 expression, B2M levels). Despite higher lymphocyte counts in cases with  $\geq 70\%$  versus  $<70\%$  of 13q deleted nuclei (median of 28.6 vs.  $14.1 \times 10^9/L$ ,  $P < 0.0001$ ), no correlation was found between the percentage of nuclei carrying a 13q deletion and the percentage of neoplastic B cells indicating the deletion load as a biological feature unrelated to the tumor burden ( $r^2 = 0.0119$ ). Clinically, del13q-only CLL with  $\geq 70\%$  of deleted nuclei showed shorter TTT than del13q-only cases with  $<70\%$  of deleted nuclei (median TTT, 77 months vs. 120 months,  $P = 0.0001$ ; Fig. 1). Notably, the presence of a 13q deletion in  $\geq 70\%$  of nuclei also behaved as an independent marker of disease progression for the cohort of del13q-only cases, along with Rai stage and *IGHV* gene mutational status, in a multivariate model testing all of the variables included in this study (Supporting Information Table S4). Similar results, although with lower significance, were obtained using the cutoffs of 80% and 65.5% of deleted nuclei, as previously proposed (Supporting Information Fig. S2), including the independency in additional multivariate models (Supporting Information Table S4) (Hernandez et al., 2009; Van Dyke et al., 2010).

**Deletion Size has Prognostic Impact in del13q-only CLL**

Previous reports described different sizes of 13q deletion in CLL (Ouillette et al., 2008; Mosca et al., 2010; Parker et al., 2011). In our cohort of del13q-only cases, i.e., carrying a 13q deletion in at least 5% of nuclei as detected by the LSI-D13S319 probe, larger 13q deletions were defined by using a LSI-RB1 probe. According to this approach, 135/342 del13q-only cases (39.5%) had 13q deletions that included the *RB1* locus in at least 5% of nuclei.

These larger deletions were always monoallelic (data not shown), and were either present in the

whole 13q deletion cell population (69/135 of cases) or in a subset of the cell population in which a 13q deletion was detected by using the LSI-D13S319 probe (66/135 of cases; Fig. 2A). Overall, FISH results were in keeping with genome-wide DNA analysis carried out in a subset of 67 del13q-only CLL (Supporting Information Table S3). As shown in Figure 2B, larger deletions involving the *RB1* locus in addition to the MDR containing the *DLEU2/MIR15A/MIR16-1* locus occurred in a proportion of del13q-only cases (23 out of 67 cases; 34.3%), and were always monoallelic (light blue in Fig. 2B). Notably, all cases with *RB1* deletion also presented a concomitant deletion at MDR, reaching a deletion median size of 2,380 Kb (range 889–18,728 Kb) versus 1,200 Kb (range 381–2,740 Kb) for cases carrying a 13q deletion not including the *RB1* locus.

A prognostic impact of a larger 13q deletion has been hypothesized (Ouillette et al., 2008). In our series, there was no significant difference in terms of TTT when del13q-only cases were subdivided according to the loss of chromosomal material at the *RB1* locus (*RB1* deleted versus non-*RB1* deleted; hazard ratio (HR) 1.33, 95% confidence interval (CI) 0.94–1.89,  $P = 0.115$ ; Supporting Information Fig. S3A). However, by separately considering TTT intervals according to the percentage of deleted nuclei in the subgroup of del13q-only cases without a concomitant *RB1* deletion (i.e., small 13q deletions, Supporting Information Fig. S3B) or in the subgroup of del13q-only cases with a concomitant *RB1* deletion (i.e., large 13q deletions, Supporting Information Fig. S3C), a relationship between

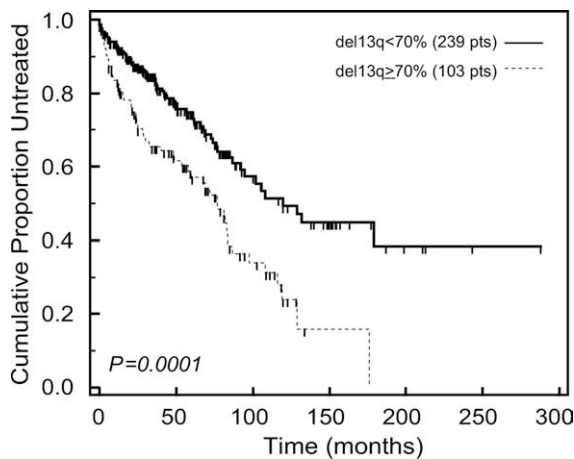


Figure 1. Clinical outcome of del13q-only cases according to the cutoff of 70% of 13q deleted nuclei. Kaplan-Meier curves comparing TTT intervals of del13q-only cases carrying a 13q deletion in  $\geq 70\%$  of nuclei (del13q  $\geq 70\%$  cases) and del13q-only cases carrying a 13q deletion in  $< 70\%$  of nuclei (del13q  $< 70\%$  cases). The number of patients (pts) included in each group is reported in parenthesis; the reported  $P$  value refers to log-rank test.

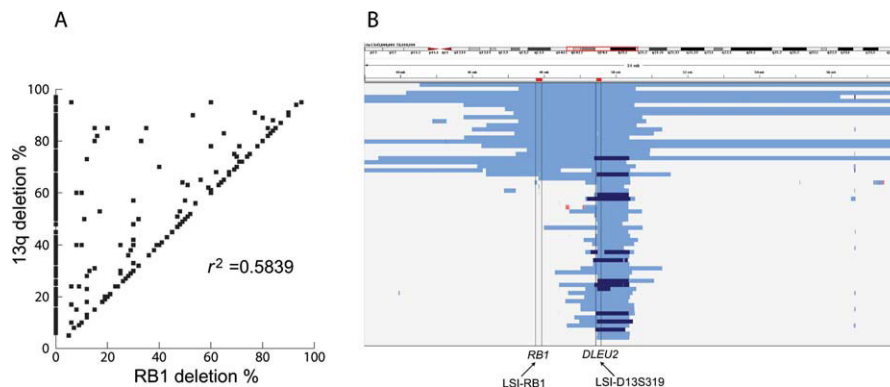


Figure 2. Relationship between 13q deletion and *RB1* deletion. (A) Scatter plot refers to the correlation between the percentage of cells carrying *RB1* deletion (x axis), as investigated by the LSI-RB1 probe, and the percentage of cells carrying a 13q deletion (y axis), as investigated by the LSI-D13S319 probe. (B) Heat map showing the

distribution of 67 del13q-only cases according to the size of deletion at 13q defined by array-CGH. Monoallelic deletions are represented in light blue; the presence of a biallelic deletion (in 12 out of 67 cases) is represented in dark blue.

percentage of deleted nuclei and clinical course was maintained only for those cases in which a small deletion 13q was present (Supporting Information Fig. S3B), thus suggesting a role of deletion size in refining CLL prognosis in the context of del13q-only cases.

Therefore, we classified del13q-only cases in four subtypes by combining both deletion load and deletion size: (i) del13q-only cases carrying a 13q deletion in <70% of nuclei without a concomitant *RB1* deletion (del13q < 70% cases), 144 cases (42.1%); (ii) del13q-only cases carrying a 13q deletion in <70% of nuclei with a concomitant *RB1* deletion (del13q < 70%+delRB1 cases), 96 cases (27.8%); (iii) del13q-only cases carrying a 13q deletion in ≥70% of nuclei without a concomitant *RB1* deletion (del13q ≥ 70% cases), 64 cases (18.7%); (iv) del13q-only cases carrying a

13q deletion in ≥70% of nuclei with a concomitant *RB1* deletion (del13q ≥70%+delRB1 cases), 39 cases (11.4%). As shown in Figure 3, the median TTT of del13q <70% cases (not reached) was significantly longer than the median TTT of del13q <70% + delRB1 cases (92 months,  $P = 0.012$ ), del13q ≥70% cases (68 months,  $P < 0.0001$ ) and del13q ≥70% + delRB1 cases (82 months,  $P = 0.0025$ ). Moreover, del13q < 70% cases showed longer TTT than the other three categories also in the context of subgroups of cases with good prognosis as defined by the other prognosticators (i.e., Rai stage 0 cases, mutated *IGHV* cases, *ZAP70* negative cases, *CD38* negative cases or B2M negative cases, Supporting Information Fig. S4). Notably, the distribution of all of the investigated prognosticators was not different among cases belonging to the four categories (Supporting Information Table S5).

Because of the differences in the prognostic relevance of *RB1* deletion in del13q-only cases carrying a 13q deletion in <70% of nuclei versus ≥70% of nuclei, as emerged by the trend of TTT curves (Supporting Information Fig. S3 and Fig. 3), the possibility of an interaction between 13q deletion size and deletion load was considered and first assessed by a bivariate Cox proportional hazard model. According to this analysis, the presence of *RB1* deletion in del13q <70% CLL was associated with a HR for progressive disease of 1.91 (95% CI = 1.18–3.08;  $P = 0.008$ ). Conversely, no additional prognostic information was provided when the presence of *RB1* deletion was tested in the context of del13q ≥ 70% cases (HR = 0.87, 95% CI = 0.50–1.51;  $P = 0.63$ ). To evaluate the independent prognostic value of *RB1* deletion in del13q-only cases, these combinations were incorporated in a multivariate model along with all of the other significant prognosticators for this CLL subset. As shown in Table 1, the presence of *RB1* deletion was confirmed to increase the risk of progressive diseases of del13q-only cases carrying <70% of deleted

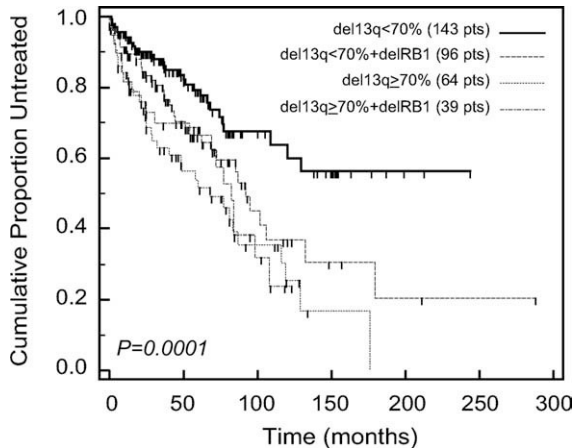


Figure 3. Clinical outcome of del13q-only cases according to the cutoff of 70% of 13q deleted nuclei and the presence of a concomitant *RB1* deletion. Kaplan-Meier curves comparing TTT intervals of del13q-only cases carrying a 13q deletion in <70% of nuclei without a concomitant *RB1* deletion (del13q < 70% cases), del13q-only cases carrying a 13q deletion in <70% of nuclei with a concomitant *RB1* deletion (del13q < 70% + delRB1 cases), del13q-only cases carrying a 13q deletion in ≥70% of nuclei without a concomitant *RB1* deletion (del13q ≥ 70% cases) and del13q-only cases carrying a 13q deletion in ≥70% of nuclei with a concomitant *RB1* deletion (del13q ≥ 70% + delRB1 cases). The number of patients (pts) included in each group is reported in parenthesis; the reported  $P$  value refers to log-rank test.

TABLE 1. Multivariate Cox Regression Analysis of TTT in del13q-only Cases (Model with Interactions)<sup>a</sup>

	Sample size	HR (95% CI) <sup>b</sup>	$P$ value
Rai stage (I, II, III, IV vs. 0)	311	1.74 (1.20–2.54)	0.003
<i>IGHV</i> mutational status (UM vs. M)		1.92 (1.28–2.87)	0.001
13q deletion and <i>RB1</i> deletion (del13q < 70% + delRB1 vs. del13q < 70%)		1.69 (1.03–2.77)	0.036
13q deletion and <i>RB1</i> deletion (del13q > 70% + delRB1 vs. del13q > 70%)		0.76 (0.43–1.33)	0.338

<sup>a</sup>Multivariate Cox regression analysis of TTT was performed by including the following covariates: Rai stage, *IGHV* gene mutational status, interaction between 13q deletion groups and *RB1* deletion (i.e., del13q < 70% + delRB1, del13q ≥ 70% + delRB1). For each variable, the selected cut-points or the compared categories are indicated. TTT, time-to-first-treatment.

<sup>b</sup>Based on the final model after backward selection of covariates. HR, hazard ratio; CI, confidence interval.

nuclei (HR = 1.69,  $P = 0.036$ ), such an increased risk being independent of Rai staging and *IGHV* gene mutational status. The independent prognostic value provided by the additional information regarding 13q deletion size and load was further demonstrated by a significant likelihood test obtained comparing models including or not this interaction ( $P = 0.006$ ).

The four FISH subtypes of del13q-only cases, as emerged by combining both deletion load and deletion size, were also analyzed by genome-wide DNA profiles. In particular, among the 67 del13q-only cases that were investigated, FISH analysis defined 23 cases as del13q < 70% cases, 19 cases as del13q < 70% + delRB1 cases, 16 cases as del13q ≥ 70% cases and 9 cases as del13q ≥ 70% + delRB1 cases. As shown in Supporting Information Fig. S5, with the only exclusion of rare cases in which *RB1* deletion was detected in as few as 5–10% of nuclei by FISH, genome-wide DNA analysis confirmed smaller deletions for del13q < 70% (median size 904 Kb, range 694–2,740 Kb) or del13q ≥ 70% cases (median size 954 Kb, range 381–1,788 Kb), compared with CLL carrying concomitant *RB1* deletion (del13q < 70% + delRB1 cases, median size 4,386 Kb, range 889–18,598 Kb; del13q ≥ 70% + delRB1 cases, median size 3,727 Kb, range 936–18,728 Kb). A total of 10 out of 28 cases with extremely large deletions (median 13,785 Kb, range 982–18,728 Kb, vs. median 2,627 Kb, range 859–4,974 Kb for the remaining *RB1* deleted cases) were identified by genome-wide DNA analysis both among del13q < 70% + delRB1 and del13q ≥ 70% + delRB1 subgroups. Notably, these cases showed shorter TTT than the remaining *RB1* deleted cases (median TTT, 8 months vs. 98 months,  $P = 0.0182$ ) without a skewing in the distribution of all of the investigated prognosticators (data not shown).

#### Prognostic Significance of the Percentage of 13q Deleted Nuclei and 13q Deletion Size in an Unselected Consecutive Mono-Institutional CLL Cohort

To further characterize the clinical heterogeneity related to deletion at 13q, also in relationship with the main chromosomal abnormalities with prognostic relevance in CLL, we evaluated the clinical course of 265 CLL cases belonging to a consecutive unselected mono-institutional CLL cohort, in which FISH analyses at diagnosis were performed for 13q deletion (LSI-D13S319 and

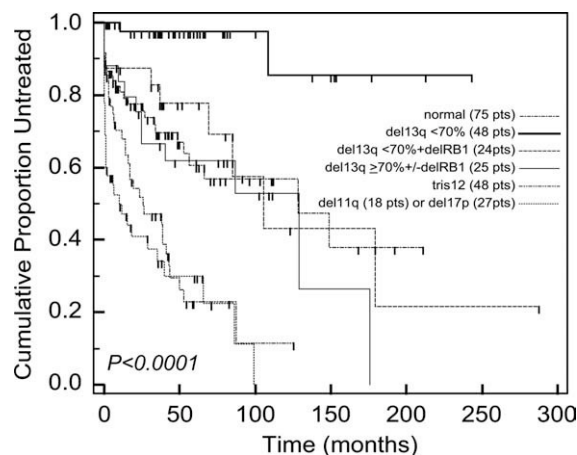


Figure 4. Prognostic significance of the percentage of 13q deleted nuclei and 13q deletion size in an unselected consecutive mono-institutional CLL cohort. Kaplan-Meier curves obtained by comparing TTT intervals of CLL cases with normal karyotype (normal), trisomy 12 (tris12), deletion at 11q (del11q), deletion at 17p (del17p), and deletion at 13q. The latter cases were split in three groups according to the percentage of nuclei carrying a 13q deletion and the presence or the absence of a concomitant *RB1* deletion: (i) 13q deletion in <70% of nuclei in the absence of a *RB1* deletion (del13q < 70% cases); (ii) 13q deletion in <70% of nuclei with the presence of a concomitant *RB1* deletion (del13q < 70% + delRB1 cases); (iii) 13q deletion in ≥70% of nuclei in the absence of a *RB1* deletion and cases carrying a 13q deletion in ≥70% of nuclei in the presence of a *RB1* deletion (del13q ≥ 70% ± delRB1 cases). The number of patients (pts) included in each group is reported in parenthesis; the reported  $P$  value refer to log-rank test.

LSI-*RB1* probes), trisomy 12, 11q deletion, and 17p deletion (Supporting Information Table S2). This cohort presented 136 cases with a 13q deletion, of which 97 were del13q-only cases, while 14 (out of 48), 11 (out of 18), and 14 (out of 27) cases had a concomitant trisomy 12, 11q deletion or 17p deletion, respectively. No difference was detected in terms of TTT by comparing cases with a concomitant 13q deletion versus cases without a concomitant 13q deletion in the context of these chromosomal aberrations (data not shown). Moreover, a significant association was found between the previously described cytogenetic groups (i.e., normal karyotype, 13q deleted, trisomy 12, 11q deleted and 17p deleted cases) (Dohner et al., 2000; Mehes, 2005) and duration of TTT intervals also in the present series (data not shown).

In this consecutive unselected cohort, maximally selected log-rank statistics confirmed a cut-off close to 70% of nuclei carrying 13q deletion as appropriate for discriminating del13q-only cases into two subgroups with different TTT distributions ( $P = 0.0198$ , data not shown). As summarized in Figure 4, the presence of 13q deletion in <70% of cells in the absence of *RB1* deletion

identified a patient subset with a particularly stable and benign clinical course (48 cases; median TTT not reached). Conversely, patients characterized by 13q deletion in <70% of cells but with a larger deletion, as determined by concomitant *RB1* deletion (24 cases), or 13q deletion in  $\geq 70\%$  of cells (with or without *RB1* deletion, 25 cases) or a normal karyotype (75 cases) had shorter median TTT intervals (ranging from 105 to 129 months,  $P < 0.01$  in all of the comparisons). Finally, patients carrying trisomy 12 (48 cases) and 11q deleted or 17p deleted (45 cases) experienced the worst clinical course ( $P < 0.0001$ ).

#### Survival According to Percentage of 13q Deleted Nuclei and 13q Deletion Size

OS data were available in 325 out of 342 del13q-only cases. Although the number of events in this series was relatively low (32/325, 9.8%), both the deletion load, using the 70% cutoff, and the deletion size, reaching or not the *RB1* locus, turned out to have prognostic relevance as OS predictors (Supporting Information Fig. S6,  $P < 0.05$  in both cases). Despite this, in multivariate analysis, both the percentage of nuclei carrying a 13q deletion and the presence of larger deletion involving the *RB1* locus failed to be selected as independently related to OS (data not shown).

### DISCUSSION

Two recent studies (Hernandez et al., 2009; Van Dyke et al., 2010) described a relationship between the number of CLL nuclei carrying 13q deletion, expressed as percentage of deleted nuclei, and disease outcome. Specifically, Hernandez et al., (2009) reported that del13q-only cases carrying a del13 in  $\geq 80\%$  of nuclei had a shorter TTT and OS than those with <80% of deleted nuclei. Van Dyke et al., (2010), using a cutoff of 65.5% of deleted nuclei, obtained the same result comparing the TTT of the two categories, whereas no difference in OS was observed. In this study, by taking advantage of a wider cohort of del13q-only cases than those previously investigated (Hernandez et al., 2009; Van Dyke et al., 2010), we were able to confirm this relationship for both TTT and OS. Although in our series we chose to use the value of 70% of deleted nuclei as the optimal cutoff, significant differences were maintained, also when the previously proposed cutoffs (Hernandez et al., 2009;

Van Dyke et al., 2010) were applied. These results concordantly confirm the notion that del13q-only cases represent a clinically non-homogeneous CLL subgroup, and that a 13q deletion load, when involving the vast majority of the neoplastic clone, has a negative prognostic impact for del13q-only CLL (Hernandez et al., 2009; Van Dyke et al., 2010). Additional metaanalysis studies or studies in the context of wide, randomized clinical trials are needed to definitely identify the cutoff of 13q deleted nuclei to be used to separate del13q-only CLL in subgroups with different prognosis. Finally, biallelic 13q deletion failed to have a prognostic impact both in our and previous studies (Hernandez et al., 2009; Van Dyke et al., 2010), suggesting the existence of additional factors (e.g., deletion of different sizes) in defining del13q-only CLL prognosis.

Beside the deletion load, another matter of heterogeneity among 13q deleted CLL is represented by the size of 13q deletion (Ouillette et al., 2008; Mosca et al., 2010; Parker et al., 2011). In this context, recent studies proposed to classify del13q-only CLL based on genomic maps, and indicated the *RB1* gene as size landmark. In particular, the existence of at least two subtypes of 13q deletion, different in size and discernible by investigating losses at the *RB1* locus, has been proposed (Ouillette et al., 2008; Mosca et al., 2010). These studies, however, failed to correlate the size of 13q deletion with the clinical behavior of CLL patients carrying these chromosomal abnormalities.

In this study, by investigating for deletion involving the *RB1* locus in nuclei from 342 del13q-only CLL, we clearly demonstrated that the relationship between percentage of 13q deleted nuclei and prognosis can be refined by adding information regarding the deletion size. In particular, small 13q deletions, i.e., not comprising the *RB1* locus, appeared to characterize a subgroup of del13q-only cases with a particularly indolent clinical course, whereas the presence of larger 13q deletions, i.e., involving the *RB1* locus, increased the risk of progressive disease in del13q-only cases with <70% of deleted nuclei. This group of patients as well as all those with 13q deletions detectable in more than 70% of nuclei, irrespective of the presence of a 13q deletion involving the *RB1* locus, had a clinical course similar to that of the so-called CLL with “normal karyotypes.” Thus, our results from TTT demonstrate a contribution of deletion size in refining the prognostic significance of deletion load in the

### The del13q prognostic flow chart

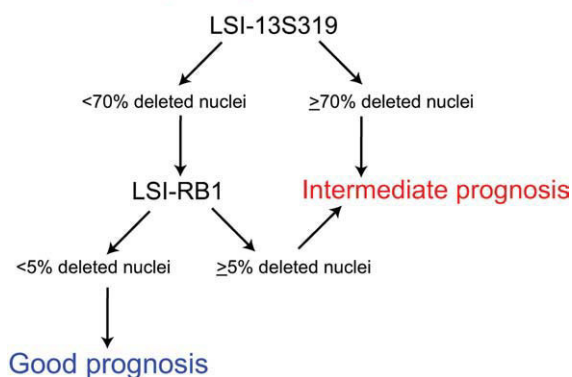


Figure 5. FISH diagnostic flowchart for CLL cases harboring 13q deletion.

context of del13q-only CLL. Of note, this contribution appears evident also by analyzing OS data, although with a necessary word of caution due to a low number of events in our CLL series.

Thus, the knowledge of the 13q deletion load, measured as percentage of deleted nuclei, and of the 13q deletion size, measured by using two 13q-specific probes (i.e., LSI-D13S319 and LSI-RB1), closely cooperate to better define the prognostic cytogenetic classification of del13q-only CLL (Dohner et al., 2000; Mehes, 2005). According to these data, we propose a novel FISH flowchart for an accurate prognostic evaluation of del13q-only cases that specifically keep in consideration the interaction between 13q deletion size and deletion load in the context of del13q-only cases with less than 70% of deleted nuclei. As summarized in Figure 5, cases in which a 13q deletion, as investigated by using the LSI-D13S319 probe, is detected in more than 70% of nuclei should be directly considered as having an intermediate prognosis. Conversely, cases in which a 13q deletion is detected in less than 70% of nuclei should be tested with an *RB1*-specific probe to investigate for the 13q deletion size. This additional FISH analysis allows classifying a given del13q-only CLL as belonging to a group of either good or intermediate prognosis (Fig. 5).

The reason(s) explaining the clinical course of the different CLL categories identified by 13q deletion size/load remain to be elucidated. In this regard, in a subset of 44 del13q-only cases, representative of all of the four 13q deletion categories here reported, we were not able to find any correlation between the expression levels of *RB1*, as determined by quantitative real-time PCR, and

the presence of *RB1* deletion by FISH (unpublished data). Similarly, variable levels of *MIR15A/MIR16-1* were also detected in the same cases, the lowest levels being found in the few cases with documented biallelic deletions, in agreement with previous reports (Calin et al., 2005; Cimmino et al., 2005; Fulci et al., 2007; Bomben et al., 2010).

Another possible explanation could be that del13q-only cases with worse prognosis have also larger 13q deletions, reaching or not the *RB1* gene, but involving additional chromosomal loci usually located centromeric to the *DLEU2/MIR15A/MIR16-1* locus, representing the canonical MDR of 13q deleted CLL (Liu et al., 1997; Lagos-Quintana et al., 2001; Migliazza et al., 2001; Calin et al., 2002). According to this line of reasoning, genome-wide DNA analysis carried out in this study actually detected slightly larger deletions, centromerically located to the *DLEU2/MIR15A/MIR16-1* locus, in the vast majority (13/16) of cases classified by FISH as having more than 70% of deleted nuclei. Conversely, only 13 out of 23 del13q-only CLL belonging to the good prognosis category with less than 70% of deleted nuclei presented comparably large 13q deletions (unpublished data). Notably, deletion of the *DLEU2/MIR15A/MIR16-1* locus in mice determines the development of a lymphoproliferative disorder with the phenotype of aggressive CLL (Klein et al., 2010). Such an aggressive phenotype was thought to be due to the involvement of other genetic elements, such as *TRIM13*, which partially overlaps the *DLEU2/MIR15A/MIR16-1* cluster in mice, but is centromerically located in humans (Ivanov et al., 2003; Klein et al., 2010). Whether CLL with more than 70% of 13q deleted nuclei and larger 13q deletions might have deletions of additional genetic elements located in a chromosomal region just centromeric to the *DLEU2/MIR15A/MIR16-1* locus, including the *TRIM13* gene, remains to be demonstrated.

In summary, the analysis of a large series of CLL allowed to demonstrate the prognostic heterogeneity that occurs in the context of del13q-only cases, which can be revealed by FISH analysis of both deletion load and deletion size. A novel prognostic flowchart is thus proposed that involves sequential hybridization with the LSI-D13S319 and LSI-RB1 probes. Further studies are needed to confirm these findings and to identify the putative tumor suppressor genes involved in the pathogenesis of 13q deleted CLL.

## REFERENCES

- Bandi N, Zbinden S, Gugger M, Arnold M, Kocher V, Hasan L, Kappeler A, Brunner T, Vassella E. 2009. miR-15a and miR-16 are implicated in cell cycle regulation in a Rb-dependent manner and are frequently deleted or down-regulated in non-small cell lung cancer. *Cancer Res* 69:5553–5559.
- Baranova A, Hammarsund M, Ivanov D, Skoblov M, Sangfelt O, Corcoran M, Borodina T, Makeeva N, Pestova A, Tyazhelova T, Nazarenko S, Gorreta F, Alsheddi T, Schlauch K, Nikitin E, Kapanadze B, Shagin D, Poltarau A, Ivanovich VA, Zabarovsky E, Lukianov S, Chandhoke V, Ibbotson R, Oscier D, Einhorn S, Grandt D, Yankovsky N. 2003. Distinct organization of the candidate tumor suppressor gene RFP2 in human and mouse: Multiple mRNA isoforms in both species- and human-specific antisense transcript RFP2OS. *Gene* 321:103–112.
- Birerdinc A, Nohelty E, Marakhonov A, Manyam G, Panov I, Coon S, Nikitin E, Skoblov M, Chandhoke V, Baranova A. 2010. Pro-apoptotic and antiproliferative activity of human KCNRG, a putative tumor suppressor in 13q14 region. *Tumour Biol* 31:33–45.
- Bomben R, Dal BM, Capello D, Forconi F, Maffei R, Laurenti L, Rossi D, Del Principe MI, Zucchetto A, Bertoni F, Rossi FM, Bulian P, Cattarossi I, Ilariucci F, Sozzi E, Spina V, Zucca E, Degan M, Lauria F, Del PG, Efremov DG, Marasca R, Gaidano G, Gattei V. 2009. Molecular and clinical features of chronic lymphocytic leukaemia with stereotyped B cell receptors: Results from an Italian multicentre study. *Br J Haematol* 144:492–506.
- Bomben R, Dal-Bo M, Benedetti D, Capello D, Forconi F, Marconi D, Bertoni F, Maffei R, Laurenti L, Rossi D, Del Principe MI, Luciano F, Sozzi E, Cattarossi I, Zucchetto A, Rossi FM, Bulian P, Zucca E, Nicoloso MS, Degan M, Marasca R, Efremov DG, Del PG, Gaidano G, Gattei V. 2010. Expression of mutated IGHV3-23 genes in chronic lymphocytic leukemia identifies a disease subset with peculiar clinical and biological features. *Clin Cancer Res* 16:620–628.
- Bulian P, Del PG, Gattei V. 2009. How would I manage a sample submitted for flow cytometry analysis for suspicious chronic lymphocytic leukaemia. *Hematol Oncol* 27:186–189.
- Bulian P, Tarnani M, Rossi D, Forconi F, Del PG, Bertoni F, Zucca E, Montillo M, Pozzato G, Deaglio S, D'Arena G, Efremov D, Marasca R, Lauria F, Gattei V, Gaidano G, Laurenti L. Multicentre validation of a prognostic index for overall survival in chronic lymphocytic leukaemia. *Hematol Oncol* 2010 Jul 28 (Epub ahead of print).
- Calin GA, Dumitru CD, Shimizu M, Bichi R, Zupo S, Noch E, Alder H, Rattan S, Keating M, Rai K, Rassenti L, Kipps T, Negrini M, Bullrich F, Croce CM. 2002. Frequent deletions and down-regulation of micro-RNA genes miR15 and miR16 at 13q14 in chronic lymphocytic leukemia. *Proc Natl Acad Sci USA* 99:15524–15529.
- Calin GA, Ferracin M, Cimmino A, Di LG, Shimizu M, Wojcik SE, Iorio MV, Visone R, Sever NI, Fabbri M, Iuliano R, Palumbo T, Pichiorri F, Roldo C, Garzon R, Sevignani C, Rassenti L, Alder H, Volinia S, Liu CG, Kipps TJ, Negrini M, Croce CM. 2005. A MicroRNA signature associated with prognosis and progression in chronic lymphocytic leukemia. *N Engl J Med* 353:1793–1801.
- Capello D, Guarini A, Berra E, Mauro FR, Rossi D, Ghia E, Cerri M, Logan J, Foa R, Gaidano G. 2004. Evidence of biased immunoglobulin variable gene usage in highly stable B-cell chronic lymphocytic leukemia. *Leukemia* 18:1941–1947.
- Chiorazzi N, Rai KR, Ferrarini M. 2005. Chronic Lymphocytic Leukemia. *N Engl J Med* 352:804–815.
- Cimmino A, Calin GA, Fabbri M, Iorio MV, Ferracin M, Shimizu M, Wojcik SE, Aqeilan RI, Zupo S, Dono M, Rassenti L, Alder H, Volinia S, Liu CG, Kipps TJ, Negrini M, Croce CM. 2005. miR-15 and miR-16 induce apoptosis by targeting BCL2. *Proc Natl Acad Sci USA* 102:13944–13949.
- Corcoran MM, Hammarsund M, Zhu C, Lerner M, Kapanadze B, Wilson B, Larsson C, Forsberg L, Ibbotson RE, Einhorn S, Oscier DG, Grandt D, Sangfelt O. 2004. DLEU2 encodes an antisense RNA for the putative bicistronic RFP2/LEU5 gene in humans and mouse. *Genes Chromosomes Cancer* 40:285–297.
- Crespo M, Bosch F, Villamor N, Bellosillo B, Colomer D, Rozman M, Marce S, Lopez-Guillermo A, Campo E, Montserrat E. 2003. ZAP-70 expression as a surrogate for immunoglobulin-variable-region mutations in chronic lymphocytic leukemia. *N Engl J Med* 348:1764–1775.
- Dal-Bo M, Bertoni F, Forconi F, Zucchetto A, Bomben R, Marasca R, Deaglio S, Laurenti L, Efremov DG, Gaidano G, Del PG, Gattei V. 2009. Intrinsic and extrinsic factors influencing the clinical course of B-cell chronic lymphocytic leukemia: Prognostic markers with pathogenetic relevance. *J Transl Med* 7:76.
- Damle RN, Wasi T, Fais F, Ghiotto F, Valetto A, Allen SL, Buchbinder A, Budman D, Dittmar K, Kolitz J, Lichtman SM, Schulman P, Vinciguerra VP, Rai KR, Ferrarini M, Chiorazzi N. 1999. IgV gene mutation status and CD38 expression as novel prognostic indicators in chronic lymphocytic leukemia. *Blood* 94:1840–1847.
- Degan M, Bomben R, Dal Bo M, Zucchetto A, Nanni P, Rupolo M, Steffan A, Attadia V, Ballerini PF, Damiani D, Pucillo C, Del Poeta G, Colombatti A, Gattei V. 2004. Analysis of IgV gene mutations in B cell chronic lymphocytic leukaemia according to antigen-driven selection identifies subgroups with different prognosis and usage of the canonical somatic hypermutation machinery. *Br J Haematol* 126:29–42.
- Del Principe MI, Del Poeta G, Buccisano F, Maurillo L, Venditti A, Zucchetto A, Marini R, Niscola P, Consalvo MA, Mazzone C, Ottaviani L, Panetta P, Bruno A, Bomben R, Suppo G, Degan M, Gattei V, de Fabritiis P, Cantonetti M, Lo Coco F, Del Principe D, Amadori S. 2006. Clinical significance of ZAP-70 protein expression in B-cell chronic lymphocytic leukemia. *Blood* 108:853–861.
- Dohner H, Stilgenbauer S, Benner A, Leupolt E, Krober A, Bullinger L, Dohner K, Bentz M, Lichter P. 2000. Genomic aberrations and survival in chronic lymphocytic leukemia. *N Engl J Med* 343:1910–1916.
- Fulci V, Chiaretti S, Goldoni M, Azzalin G, Carucci N, Tavolaro S, Castellano L, Magrelli A, Citarella F, Messina M, Maggio R, Peragine N, Santangelo S, Mauro FR, Landgraf P, Tuschl T, Weir DB, Chien M, Russo JJ, Ju J, Sheridan R, Sander C, Zavolan M, Guarini A, Foa R, Macino G. 2007. Quantitative technologies establish a novel microRNA profile of chronic lymphocytic leukemia. *Blood* 109:4944–4951.
- Gattei V, Bulian P, Del Principe MI, Zucchetto A, Maurillo L, Buccisano F, Bomben R, Dal-Bo M, Luciano F, Rossi FM, Degan M, Amadori S, Del PG. 2008. Relevance of CD49d protein expression as overall survival and progressive disease prognosticator in chronic lymphocytic leukemia. *Blood* 111:865–873.
- Giudicelli V, Chaume D, Lefranc MP. 2004. IMGT/V-QUEST, an integrated software program for immunoglobulin and T cell receptor V-J and V-D-J rearrangement analysis. *Nucleic Acids Res* 32:W435–W440.
- Hallek M, Cheson BD, Catovsky D, Caligaris-Cappio F, Dighiero G, Dohner H, Hillmen P, Keating MJ, Montserrat E, Rai KR, Kipps TJ. 2008. Guidelines for the diagnosis and treatment of chronic lymphocytic leukemia: A report from the International Workshop on Chronic Lymphocytic Leukemia updating the National Cancer Institute-Working Group 1996 guidelines. *Blood* 111:5446–5456.
- Hamblin TJ, Davis Z, Gardiner A, Oscier DG, Stevenson FK. 1999. Unmutated Ig V(H) genes are associated with a more aggressive form of chronic lymphocytic leukemia. *Blood* 94:1848–1854.
- Hernandez JA, Rodriguez AE, Gonzalez M, Benito R, Fontanillo C, Sandoval V, Romero M, Martin-Nunez G, de Coca AG, Fisac R, Galende J, Recio I, Ortuno F, Garcia JL, de las RJ, Gutierrez NC, San Miguel JF, Hernandez JM. 2009. A high number of losses in 13q14 chromosome band is associated with a worse outcome and biological differences in patients with B-cell chronic lymphoid leukemia. *Haematologica* 94:364–371.
- Hernando E, Nahle Z, Juan G, az-Rodriguez E, Alaminos M, Hemann M, Michel L, Mittal V, Gerald W, Benzra R, Lowe SW, Cordon-Cardo C. 2004. Rb inactivation promotes genomic instability by uncoupling cell cycle progression from mitotic control. *Nature* 430:797–802.
- Ivanov DV, Tyazhelova TV, Lemonnier L, Kononenko N, Pestova AA, Nikitin EA, Prevarskaya N, Skryma N, Panchin YV, Yankovsky NK, Baranova AV. 2003. A new human gene KCNRG encoding potassium channel regulating protein is a cancer suppressor gene candidate located in 13q14.3. *FEBS Lett* 539:156–160.
- Kapanadze B, Kashuba V, Baranova A, Rasool O, van EW, Liu Y, Syomov A, Corcoran M, Poltarau A, Brodyansky V, Syomova N, Kazakov A, Ibbotson R, van den BA, Gizatullin R, Fedorova L, Sulimova G, Zelenin A, Deaven L, Lehrach H, Grandt D, Buys C, Oscier D, Zabarovsky ER, Einhorn S, Yankovsky N.

1998. A cosmid and cDNA fine physical map of a human chromosome 13q14 region frequently lost in B-cell chronic lymphocytic leukemia and identification of a new putative tumor suppressor gene, *Leu5*. *FEBS Lett* 426:266–270.
- Klein U, Lia M, Crespo M, Siegel R, Shen Q, Mo T, Ambesi-Impiomato A, Califano A, Migliazza A, Bhagat G, Dalla-Favera R. 2010. The DLEU2/miR-15a/16-1 cluster controls B cell proliferation and its deletion leads to chronic lymphocytic leukemia. *Cancer Cell* 17:28–40.
- Krober A, Seiler T, Benner A, Bullinger L, Brückle E, Lichter P, Döhner H, Stilgenbauer S. 2002. V(H) mutation status, CD38 expression level, genomic aberrations, and survival in chronic lymphocytic leukemia. *Blood* 100:1410–1416.
- Lagos-Quintana M, Rauhut R, Lendeckel W, Tuschl T. 2001. Identification of novel genes coding for small expressed RNAs. *Science* 294:853–858.
- Lefranc MP, Giudicelli V, Kaas Q, Duprat E, Jabado-Michaloud J, Scaviner D, Ginestoux C, Clement O, Chaume D, Lefranc G. 2005. IMGT, the international ImMunoGeneTics information system. *Nucleic Acids Res* 33:D593–D597.
- Lerner M, Corcoran M, Cepeda D, Nielsen ML, Zubarev R, Ponten F, Uhlen M, Hober S, Grandér D, Sangfelt O. 2007. The RBCC gene *RFP2* (*Leu5*) encodes a novel transmembrane E3 ubiquitin ligase involved in ERAD. *Mol Biol Cell* 18:1670–1682.
- Linsley PS, Schelter J, Burchard J, Kibukawa M, Martin MM, Bartz SR, Johnson JM, Cummins JM, Raymond CK, Dai H, Chau N, Cleary M, Jackson AL, Carleton M, Lim L. 2007. Transcripts targeted by the microRNA-16 family cooperatively regulate cell cycle progression. *Mol Cell Biol* 27:2240–2252.
- Liu Q, Fu H, Sun F, Zhang H, Tie Y, Zhu J, Xing R, Sun Z, Zheng X. 2008. miR-16 family induces cell cycle arrest by regulating multiple cell cycle genes. *Nucleic Acids Res* 36:5391–5404.
- Liu Y, Szekely L, Grandér D, Soderhall S, Juliusson G, Gahrton G, Linder S, Einhorn S. 1993. Chronic lymphocytic leukemia cells with allelic deletions at 13q14 commonly have one intact *RB1* gene: Evidence for a role of an adjacent locus. *Proc Natl Acad Sci USA* 90:8697–8701.
- Liu Y, Corcoran M, Rasool O, Ivanova G, Ibbotson R, Grandér D, Iyengar A, Baranova A, Kashuba V, Merup M, Wu X, Gardiner A, Mullenbach R, Poltaraua A, Hultstrom AL, Juliusson G, Chapman R, Tiller M, Cotter F, Gahrton G, Yankovsky N, Zabarovsky E, Einhorn S, Oscier D. 1997. Cloning of two candidate tumor suppressor genes within a 10 kb region on chromosome 13q14, frequently deleted in chronic lymphocytic leukemia. *Oncogene* 15:2463–2473.
- Mehes G. 2005. Chromosome abnormalities with prognostic impact in B-cell chronic lymphocytic leukemia. *Pathol Oncol Res* 11:205–210.
- Mertens D, Wolf S, Schroeter P, Schaffner C, Döhner H, Stilgenbauer S, Lichter P. 2002. Down-regulation of candidate tumor suppressor genes within chromosome band 13q14.3 is independent of the DNA methylation pattern in B-cell chronic lymphocytic leukemia. *Blood* 99:4116–4121.
- Mertens D, Philippen A, Ruppel M, Allegra D, Bhattacharya N, Tschuch C, Wolf S, Idler I, Zenz T, Stilgenbauer S. 2009. Chronic lymphocytic leukemia and 13q14: miRs and more. *Leuk Lymphoma* 50:502–505.
- Migliazza A, Bosch F, Komatsu H, Cayanis E, Martinotti S, Toniato E, Guccione E, Qu X, Chien M, Murty VV, Gaidano G, Inghirami G, Zhang P, Fischer S, Kalachikov SM, Russo J, Edelman I, Efstratiadis A, la-Favera R. 2001. Nucleotide sequence, transcription map, and mutation analysis of the 13q14 chromosomal region deleted in B-cell chronic lymphocytic leukemia. *Blood* 97:2098–2104.
- Mosca L, Fabris S, Lionetti M, Todoerti K, Agnelli L, Morabito F, Cutrona G, Andronache A, Matis S, Ferrari F, Gentile M, Spriano M, Callea V, Festini G, Molica S, Lambertenghi DG, Biciotto S, Ferrarini M, Neri A. 2010. Integrative genomics analyses reveal molecularly distinct subgroups of B-cell chronic lymphocytic leukemia patients with 13q14 deletion. *Clin Cancer Res* 16:5641–5653.
- Olshen AB, Venkatraman ES, Lucito R, Wigler M. 2004. Circular binary segmentation for the analysis of array-based DNA copy number data. *Biostatistics* 5:557–572.
- Orchard JA, Ibbotson RE, Davis Z, Wiestner A, Rosenwald A, Thomas PW, Hamblin TJ, Staudt LM, Oscier DG. 2004. ZAP-70 expression and prognosis in chronic lymphocytic leukaemia. *Lancet* 363:105–111.
- Ouillette P, Erba H, Kujawski L, Kaminski M, Shedden K, Malek SN. 2008. Integrated genomic profiling of chronic lymphocytic leukemia identifies subtypes of deletion 13q14. *Cancer Res* 68:1012–1021.
- Palamarchuk A, Efanov A, Nazaryan N, Santanam U, Alder H, Rassenti L, Kipps T, Croce CM, Pekarsky Y. 2010. 13q14 deletions in CLL involve cooperating tumor suppressors. *Blood* 115:3916–3922.
- Parker H, Rose-Zerilli MJ, Parker A, Chaplin T, Wade R, Gardiner A, Griffiths M, Collins A, Young BD, Oscier DG, Strefford JC. 2011. 13q deletion anatomy and disease progression in patients with chronic lymphocytic leukemia. *Leukemia* 25:489–497.
- Pickering MT, Kowalik TF. 2006. Rb inactivation leads to E2F1-mediated DNA double-strand break accumulation. *Oncogene* 25:746–755.
- Pommie C, Levadoux S, Sabatier R, Lefranc G, Lefranc MP. 2004. IMGT standardized criteria for statistical analysis of immunoglobulin V-REGION amino acid properties. *J Mol Recognit* 17:17–32.
- Rassenti LZ, Huynh L, Toy TL, Chen L, Keating MJ, Gribben JG, Neuberg DS, Flinn IW, Rai KR, Byrd JC, Kay NE, Greaves A, Weiss A, Kipps TJ. 2004. ZAP-70 compared with immunoglobulin heavy-chain gene mutation status as a predictor of disease progression in chronic lymphocytic leukemia. *N Engl J Med* 351:893–901.
- Raveche ES, Salerno E, Scaglione BJ, Manohar V, Abbasi F, Lin YC, Fredrickson T, Landgraf P, Ramachandra S, Huppi K, Toro JR, Zenger VE, Metcalf RA, Marti GE. 2007. Abnormal microRNA-16 locus with synteny to human 13q14 linked to CLL in NZB mice. *Blood* 109:5079–5086.
- Rossi D, Cerri M, Deambroggi C, Sozzi E, Cresta S, Rasi S, De PL, Spina V, Gattei V, Capello D, Forconi F, Lauria F, Gaidano G. 2009. The prognostic value of TP53 mutations in chronic lymphocytic leukemia is independent of Del17p13: Implications for overall survival and chemorefractoriness. *Clin Cancer Res* 15:995–1004.
- Sakai T, Toguchida J, Ohtani N, Yandell DW, Rapaport JM, Dryja TP. 1991. Allele-specific hypermethylation of the retinoblastoma tumor-suppressor gene. *Am J Hum Genet* 48:880–888.
- Van Dyke DL, Shanafelt TD, Call TG, Zent CS, Smoley SA, Rabe KG, Schwager SM, Sonbert JC, Slager SL, Kay NE. 2010. A comprehensive evaluation of the prognostic significance of 13q deletions in patients with B-cell chronic lymphocytic leukaemia. *Br J Haematol* 148:544–550.

*I would like to thank all the colleagues belonging to the Clinical and Experimental Onco-Hematology Unit of CRO Aviano National Cancer Institute for their helpful suggestions and advise throughout the development of the present study.*